Syntheses, Characterization, Physical and Biological Properties of Long-chain, Water-soluble, Dendritic Amphiphiles

André Arvin Williams

Dissertation submitted to the Faculty of Virginia Polytechnic Institute and State University in partial fulfillment of the requirements for the degree of

DOCTOR OF PHILOSOPHY

in

Chemistry

Richard D. Gandour, Chairman
Godson Nwokogu
John R. Morris
David G.I. Kingston
James M. Tanko

February 15th 2008
Blacksburg, VA

Keywords: multi-headed, tri-carboxylato, dendritic amphiphile, aqueous solubility, microorganism, antimicrobial activity, surface chemistry

Syntheses, Characterization, Physical and Biological Properties of Long-chain, Water-soluble, Dendritic Amphiphiles

André Arvin Williams

ABSTRACT

In this project, we have designed and synthesized a new series of long-chain, water-soluble, dendritic, anionic amphiphiles [**3CAmn**, $RCONHC(CH_2CH_2COOH)_3$, R= C_nH_{2n+1}] to alleviate the low aqueous solubility of fatty acids. The dendritic-tricarboxlyato headgroup improves aqueous solubility and allows us to measure the intrinsic biological activity of our amphiphiles without the potential hindrance of low aqueous solubility. The aqueous solubilities of the anionic amphiphiles have been measured and were vastly higher than that of fatty acids. For example, **3CAm17** (1700 μM at pH 7.2) has much better aqueous solubility than the C_{18} fatty acid analog (<<1 micromol at pH 7.4).

Following the determination of aqueous solubility, both anionic and nonionic amphiphiles were tested against a wide variety of microorganisms. The anionic amphiphiles were mostly active against *Candida albicans* (4.4 microgram/mL), *Saccharomyces cerevisiae* (4.4 μg/mL), and *Mycobacterium smegmatis* (18 microgram/mL) and exhibited modest activity against both Gram-negative (71–280 microgram/mL) and Gram-positive bacteria (36– >6300 microgram/mL). With the exception of *Neisseria gonorrhoeae* (9.8 microgram/mL), the nonionic amphiphiles were mostly minimally active or inactive against Gram-negative bacteria (630–5000

microgram/mL). The nonionic amphiphiles were similarly inactive against fungi (625–5000 microgram/mL). However, the nonionic amphiphiles exhibited good activity against *M. smegmatis* (20 microgram/mL) and exhibited the best activity against Gram-positive bacteria, such as MRSA (22 microgram/mL), *Staphylococcus aureus* (20 microgram/mL), and *Micrococcus luteus* (20 microgram/mL).

The anionic and nonionic amphiphiles were also tested for possible spermicidal and anti-human immunodefiency virus (HIV) activity. The anionic amphiphiles exhibited anti-HIV activity (EC_{50}, 73–340 microgram/mL), but lacked spermicidal activity. The series had comparable anti-HIV activity to the commercial product N-9 (80 microgram/mL). Except **3CAm13**, all anionic amphiphiles (1.4–4) had better selectivity indices than that of N-9 (0.9). The nonionic amphiphiles exhibited both anti-HIV (44–67 microgram/mL) and spermicidal activity (226–2000 microgram/mL). The nonionic amphiphile were more spermicidal and antiviral than Nonoxynol-9.

In addition to biological activity, we determined whether the anionic amphiphiles could be utilized as corrosion inhibitors or ore flotation enhancers. The anionic amphiphiles formed stable thin films on silver oxide that were resistant to ethanol washings. We also measured the water contact angles of the anionic amphiphiles on mineral surfaces [apatite (95°), calcite (92°)].

Acknowledgements

I would like to thank my parents (Roma and Stanford Williams) for their undying support and encouragement throughout my doctoral studies. I would also like to thank my sisters, Carolyn Lynch and Tiffany Williams, for their unconditional support.

I would like to enthusiastically thank my advisor Dr. Richard Gandour. I greatly appreciate his guidance, support, and most importantly patience. From the very beginning, Dr. Gandour has taken a keen interest in not only my experimental results but my academic studies as well. For his efforts, I am extremely grateful.

I am also grateful to the past and present members of the Gandour group. My lab mates have helped me with my research and created a fun atmosphere that I enjoyed. I am especially grateful to Dr. Brett Kite, who helped me tremendously throughout the years. I would also like to thank Dr. Winny Sugandhi, Richard Macri, Shauntrece Hardrict, Tu Sheng, Dr. Jennifer Kile, Marcelo Actis, and Aaron Commons.

Additionally, I would like to thank Dr. Joseph Falkinham III for opening his lab to me. The time I spent in Dr. Falkinham's lab was rewarding and fun. I am also appreciative to Thomas Wall for showing me how to perform microbial assays and to Myra Williams for her patience and answering my many questions.

I would like thank my doctoral committee (Dr. Godson Nwokogu, Dr. David Kingston, Dr. James Tanko, and Dr. John Morris) for their guidance. I would also like to thank other individuals who have assisted me in my research (Dr. Carla Slebodnick, Dr. Alan Esker, Dr. Roe–Hoan Yoon, Jinhong Zhang, Ruijia Wang, Scott Day, Melinda Ferguson, Dr. Janka Karlovská, Dr. Daníelá Uhrková, Dr. Pavol Balgavý, Amadeu Sum, and Qiongdan Xie).

Finally, I would like to thank Shelby Schuler for helping me get acclimated to VA Tech and Blacksburg. I would also like to thank long time roommate Wesley Gordon because we shared many similar moments such as preliminary exam, literature review, etc. I am also grateful to Afia Karikari for her friendship and keeping each other sane during our times in Blacksburg. I am immensely grateful to Dr. Winny Sugandhi for reviewing and improving the quality of this document.

Dedication

I dedicate this document in the loving memory of my grandparents (Edith Lynch, John Lynch, and Nellie Maynard) and to my parents (Roma and Stanford Williams).

Table of Contents

List of Figures

List of Tables

List of Schemes

Chapter I. Antimicrobial Activity and Surface Chemistry of Amphiphiles

1.1 Introduction and Goals of Project

The purpose of this research project is to synthesize new multi-headed, long-chain, anionic (**3CAmn**), and nonionic (**3DMAUrn** and **3MorUrn**) amphiphiles (Figure 1.1), which are commonly referred to as surfactants (surface active agents). Ionic and nonionic surfactants find many uses in a variety of applications[1]—detergents, phase transfer catalysts, corrosion inhibitors, ore flotation agents, fabric softeners, shampoos, crude oil recovery enhancers, cosmetics, chelating agents[2], and antimicrobial agents.[1, 3, 4] In this dissertation, we will mainly focus on the biological activity of these surfactants based on the use of ionic and nonionic amphiphiles in the antimicrobial field.[5]

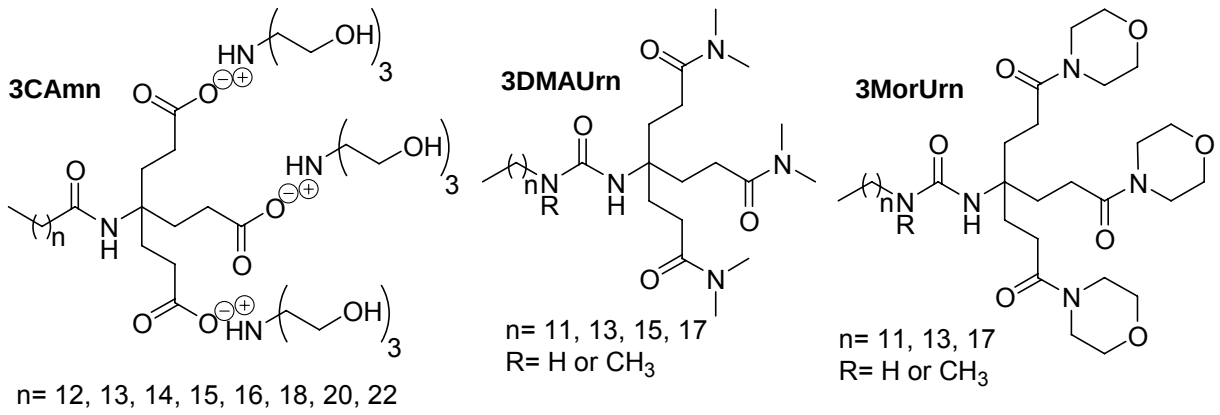

Figure 1.1 Anionic and Nonionic Dendritic Amphiphiles

In this study, we emphasize the term amphiphile instead of surfactant because researchers expect surfactants to be detergents. We do not want these dendritic amphiphiles to be detergents, because detergents are associated with cytotoxicity, inflammation, and irritation. Amphiphiles become detergents at or near the critical

micelle concentration (cmc).[6, 7] We aim to synthesize amphiphiles that have high cmcs to minimize the chance of detergency, and therefore irritation.

Typically, antimicrobial properties of amphiphiles tend to increase with hydrocarbon chain length.[8, 9] However, the increased chain length decreases the solubility of amphiphiles in aqueous systems.[10] Biological activity, in this case antimicrobial activity, does not have a linear relationship with chain length. Biological activity within a homologous series of amphiphiles increases with chain length up to a specific chain length, after which it decreases with longer chain lengths. A "cutoff effect" (Figure 1.2),[8] formerly known as the parabolic case,[6] limits the biological activity of long-chain amphiphiles. This effect occurs in all types of amphiphiles; it is a general phenomenon. One reason given for the cutoff effect is decreased amphiphile concentration at the site of action, due to limited amphiphile solubility.

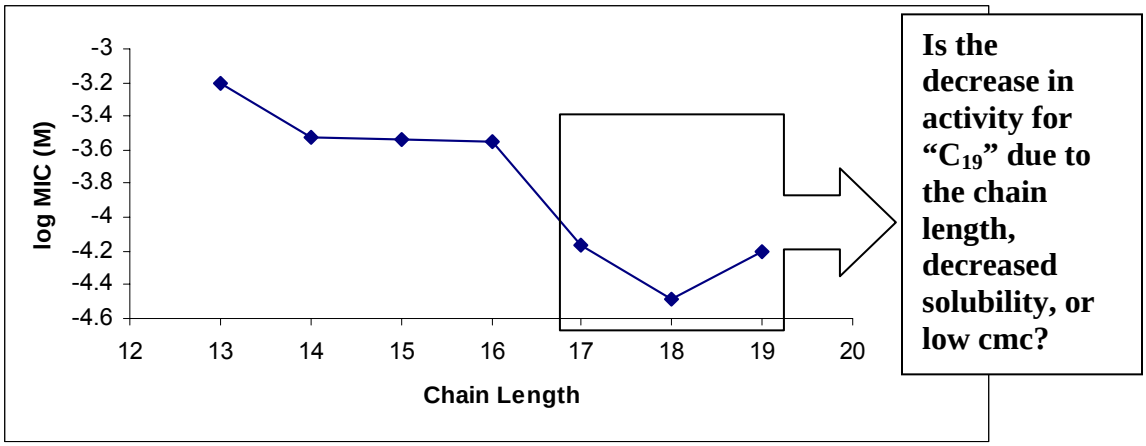

Figure 1.2 Cutoff Effect: Changes in Antimicrobial Activity with Respect to Chain Length. MIC is minimal inhibitory concentration**.**

We plan to remove solubility as a possible cause of the cutoff effect. We will begin by synthesizing long-chain, multi-headed, anionic amphiphiles (**3CAmn**). Multi-headed, ionic, amphiphiles have higher solubilities than single-headed amphiphiles in

aqueous systems.[11] Therefore, we expect multi-headed amphiphiles to improve the solubility of longer hydrocarbon chains.

The ultimate goal of this project is to synthesize topical microbicides, especially those active against the human immunodefiency virus (HIV). These microbicides should be spermicidal, antibacterial, antifungal, and antiviral. To accomplish this goal, a homologous series of amphiphiles have been designed. The goals of this research project (Figure 1.3) include (1) the design, synthesis, and characterization of amphiphiles, (2) measurement of antimicrobial activity, and (3) measurement of cytotoxicity (measured by Dr. Gustavo Doncel, Eastern Virginia Medical School). Additional goals for the **3CAmn** series include; (4) the assessment of the amphiphiles as possible coating agents for metal surfaces to avoid surface oxidation (rusting), (5) measurement of the aqueous solubility, and (6) measurement of cmc (measured by my Richard Macri, Chemistry Department of Virginia Tech).

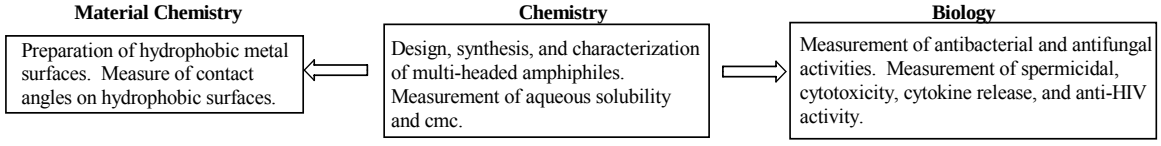

Figure 1.3 Overall Goals of Projects

1.2 Introduction to Amphiphiles

Amphiphiles (Figure 1.4) have unique properties because of their structure, which has two separate parts: the hydrophilic (water-loving) group is referred to as the head and the hydrophobic (water- hating) group is referred to as the tail. Variables—temperature, chain length, number of headgroups, addition of salts and alcohols, and counterions—affect the solubility, activity, and cmc.

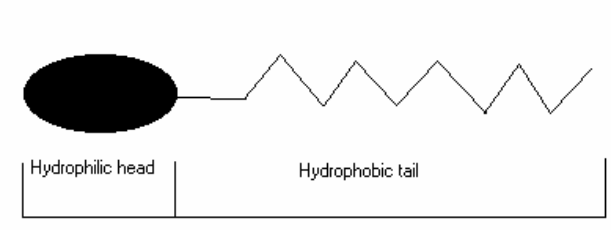

Figure 1.4 General Structure of an Amphiphile

Because of their unique structure, amphiphiles naturally adsorb at interfaces, which are the boundaries between at least two immiscible phases. Typically, the headgroup is polar or charged; however, it is part of an organic molecule that has little attraction for water. Subsequently, a compromise must be reached. The hydrophobic tail will enter any phase—air, oil, or solid—that is nonpolar. However, when no other surfaces are present the amphiphiles will form phases for themselves. The hydrocarbon chain will self assemble to form aggregates (Figure 1.5). The hydrophobic tails cluster together away from water, with the head projecting toward the surrounding water. Amphiphiles can form small aggregates called micelles or large layer structures called bilayers. Amphiphiles with two hydrophobic alkyl tails tend to form bilayers.

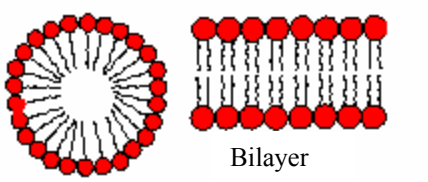

Figure 1.5 Aggregates of Amphiphiles

The opposing affinity for water gives amphiphiles their peculiar properties. Because of their love–hate relationship with water, amphiphiles can be used as

emulsifying, foaming, and cleaning agents.[12] While individual water molecules unquestionably repel the hydrocarbon chain, there is no strong attraction of hydrocarbon chains for each other. The water–water interactions are much stronger than the hydrocarbon chain–hydrocarbon chain and hydrophilic head–water interactions. The powerful water–water interactions are optimized by allowing the hydrocarbon chains to form micelles.[12, 13] A single hydrocarbon chain displaces a large number of water molecules about 5 Å apart.[12] Ironically, micelle formation of amphiphiles can actually be regarded as the aggregation of water.[12] Consequently, due to the preferred water–water interactions, amphiphiles form micelles to lower the total number of separated water molecules. The interior of the micelle has properties of a liquid hydrocarbon that enables micelles to solubilize hydrophobic organic molecules that are insoluble in water.

Hydrophobic groups can be long, straight-chain alkyl ($>C_8$), branched-chain alkyl, alkylbenzenes, alkylnaphalenes, polydimethylsiloxanes, fluoroalkyl, etc.[14] With respect to the toxicity of hydrophobic groups, fatty acid hydrophobic groups are preferred because amphiphiles containing aromatic groups are relatively more toxic toward humans.[15]

The hydrophilic headgroup makes the amphiphiles soluble in water. The headgroup must be ionic or polar to induce solubility. The ionic character of the headgroup determines the classification of the amphiphile (Table 1.1).[16, 17] There are four main types—anionic, cationic, nonionic, and amphoteric (zwitterionic)—of amphiphiles. Anionic amphiphiles have negatively charged headgroups; cationic amphiphiles, positively charged headgroups. Nonionic amphiphiles have uncharged, polar groups that make hydrogen bonds with the aqueous solvent. Amphoteric

amphiphiles have a combination of anionic and cationic headgroups. Zwitterionic amphiphiles fall under this category. Consequently, they are anionic, cationic, or neutral depending on the pH of the system. Some zwitterionic amphiphiles (due to quaternary ammonium groups) have a permanent charge on the cationic group at all pHs.

Table 1.1 Examples of Anionic, Cationic, Nonionic, and Zwitterionic Amphiphiles

Anionic Headgroups	**General Structure R= hydrophobic tail**	**Cationic Headgroups**	**General Structure R= hydrophobic tail**
Sulfonate	$R\text{-}SO_3^-M^+$	Ammonium salts	$R_xH_yN^+X^-$
Sulfate	$R\text{-}OSO_3^-M^+$	Quaternary Ammonium Salts	$R_4N^+X^-$
Carboxylate	$R\text{-}COO^-M^+$		
Phosphate	$R\text{-}OPO_3^-M^+$		
Zwitterionic Amphiphiles		**Nonionic headgroups**	
Betaines	$R\text{-}N^+(CH_3)_2CH_2CH_2COO^-$	Polyoxyethlene (POE)	$R\text{-}CH_2CH_2(OCH_2CH_2)_nOH$
Sulfobetaines	$R\text{-}N^+(CH_3)_2CH_2CH_2SO_3^-$		

The solubility of amphiphiles in water depends on the nature of the headgroup. Ionic groups do a much better job of making long hydrocarbons chains soluble than nonionic groups.[18] One sulfate or quaternary group can solubilize a C_{12} hydrocarbon chain. Ten ethylene oxide groups are as water soluble as an ionic group.[18]

The solubility of nonionic, zwitterionic, cationic, and anionic amphiphiles varies with pH (Table 1.2).[18] Nonionic amphiphiles solubilize over a wide pH range. Hydrogen bonding gives these amphiphiles their solubility. Having both anionic and cationic groups give zwitterionic amphiphiles aqueous solubility over a wide pH range. Ammonium salts dissolve in acidic solutions. They are weak cationic groups because their positive charge is due to protonation. However, quaternary ammonium groups, because they have a permanent positive charge are soluble over the entire pH range in a

variety of solvents (aqueous and organic). Anionic amphiphiles are soluble in slightly acidic to basic conditions.

Table 1.2 pH Solubility of Amphiphiles

Surfactant Type	pH Solubility
Anionic	5–14
Nonionic	3–12
Ammonium Salts	1–8
Quaternary Ammonium Salts	1–14
Zwitterionic	1–6, 8–14

1.3 Cutoff Effect

In this study, solubility will be removed as the primary cause of the cutoff effect. If an amphiphile is not soluble in the same aqueous media as the microorganism, then the antimicrobial activity is poorly defined. Therefore, if our amphiphiles are highly water soluble, solubility cannot be the cause for any observed cutoff effect.

Antimicrobial properties of amphiphiles tend to increase with hydrocarbon chain length.[8, 9] However, the increased hydrocarbon length decreases the solubility of amphiphiles in aqueous systems.[10] Past research done by the Gandour group has shown a direct correlation between hydrocarbon chain length and both spermicidal and anti-HIV activities.[19, 20] However, both spermicidal and anti-HIV activity drop off after a certain chain length, e.g. $>C_{16}$. This phenomenon is known as the cutoff effect.[8] In those examples, larger homologues are insoluble in water.

Balgavý and Devinský suggested four reasons for the cutoff effect: (1) size discrimination, (2) limited aqueous solubility of amphiphiles, (3) kinetic effects, (4) and free volume. [8] The first explanation, size discrimination, a microorganism has a receptor with a fixed volume. As chain length increases, a drug fills the volume of the receptor and becomes more active. Activity increases until the receptor's volume is

completely filled with a specific chain length. This chain length is the optimal chain length. As chain length further increases, the drug becomes too big for the receptor's volume and cannot fit into the receptor as tightly as before; consequently, activity decreases.

The second explanation, limited aqueous solubility of amphiphiles, is that as the chain length increases, the hydrophobicity of the amphiphile increases. This increase leads to decreased aqueous solubility. Balgavý and Devinský theorized that the decrease in activity of long-chain amphiphiles is due to the decreased aqueous solubility of amphiphiles with longer chains.[8] Specifically, the decreased activity is due to low amphiphile concentration at the site of action.

For the third explanation, kinetic effects, Balgavý and Devinský theorized that antimicrobial activity is based on time-dependent drug concentration at the site of action (receptor).[8] This explanation assumes the location where the drug enters the cell is located at a distance from the receptor behind a series of lipid bilayers. The drug is separated from the receptor by sequential compartments of lipid bilayers and water (Figure 1.6). Antimicrobial activity depends on the concentration at the receptor, which is based on the hydrophobicity of the amphiphiles, as well as the time that it takes for the drug to reach the receptor.

Based on this explanation, short-chain amphiphiles would not exhibit antimicrobial activity because they are not sufficiently hydrophobic to pass through the hydrophobic lipid bilayers during a given time. Long-chain amphiphiles would not exhibit antimicrobial activity because they cannot cross the aqueous compartments between the bilayers and the receptor during a given time. The amphiphiles that possess

the best antimicrobial activity must have the optimal balance between hydrophobicity and hydrophilicity. The amphiphile must be hydrophobic enough to pass through the lipid bilayer but not too hydrophobic to prevent travel across the aqueous compartments.

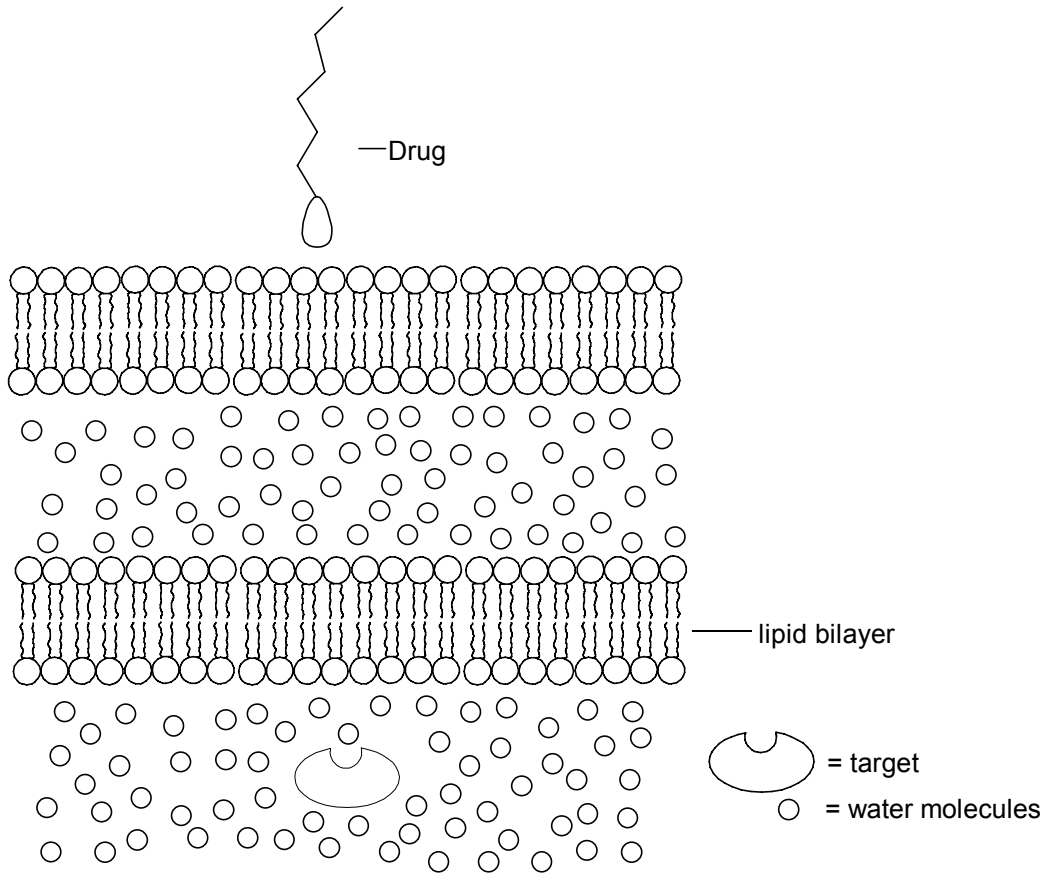

Figure 1.6 Cutoff Effects: Kinetics

For the fourth explanation, free volume, Balgavý and Devinský proposed that chain length can affect the amount of free volume that is created when an amphiphile incorporates its alkyl chain into the bilayer membrane of a cell.[8] This argument is also based on partition coefficients of the amphiphiles. In this model, when an amphiphile's tail is inserted into the bilayer membrane, volume (space) is created due to the differing chain lengths of the amphiphile and phospholipids of the membrane. The phospholipids rearrange their tails to fill the volume. This rearrangement leads to changes in bilayer

thickness, which can affect the activity of proteins associated with the membranes, as well as membrane fragmentation or leakage.

The free-volume model proposes that short-chain amphiphiles would not exhibit antimicrobial activity. If the amphiphile's alkyl chain length is much shorter than that of the phospholipids, a large free volume would be created (Figure 1.7A). However, there would be a low concentration of the amphiphile in the membrane because of weak hydrophobic interactions with the phospholipids. Consequently, the partition coefficient would favor the amphiphile being in the media and not in the bilayer. Therefore, overall, the free volume that is created would be small because there would be a low concentration of the amphiphile in the bilayer. As the chain length of the amphiphile increases, the free volume increases because there would be a larger concentration of the amphiphile in the bilayer membrane due to an increasingly favorable partition coefficient (Figure 1.7B). As the chain length of the amphiphile approaches the chain length of the phospholipids, the partition coefficient increases, but the free volume is decreased to zero because of the reduced differences in chain lengths (Figure 1.7C). High amphiphile concentration in the bilayer, coupled with adequate free volume, results in decreased lipid bilayer thickness. These circumstances lead to changes in the activity of membrane-bound proteins, cell membrane fragmentation, or cell leakage of vital components, resulting in cell death.

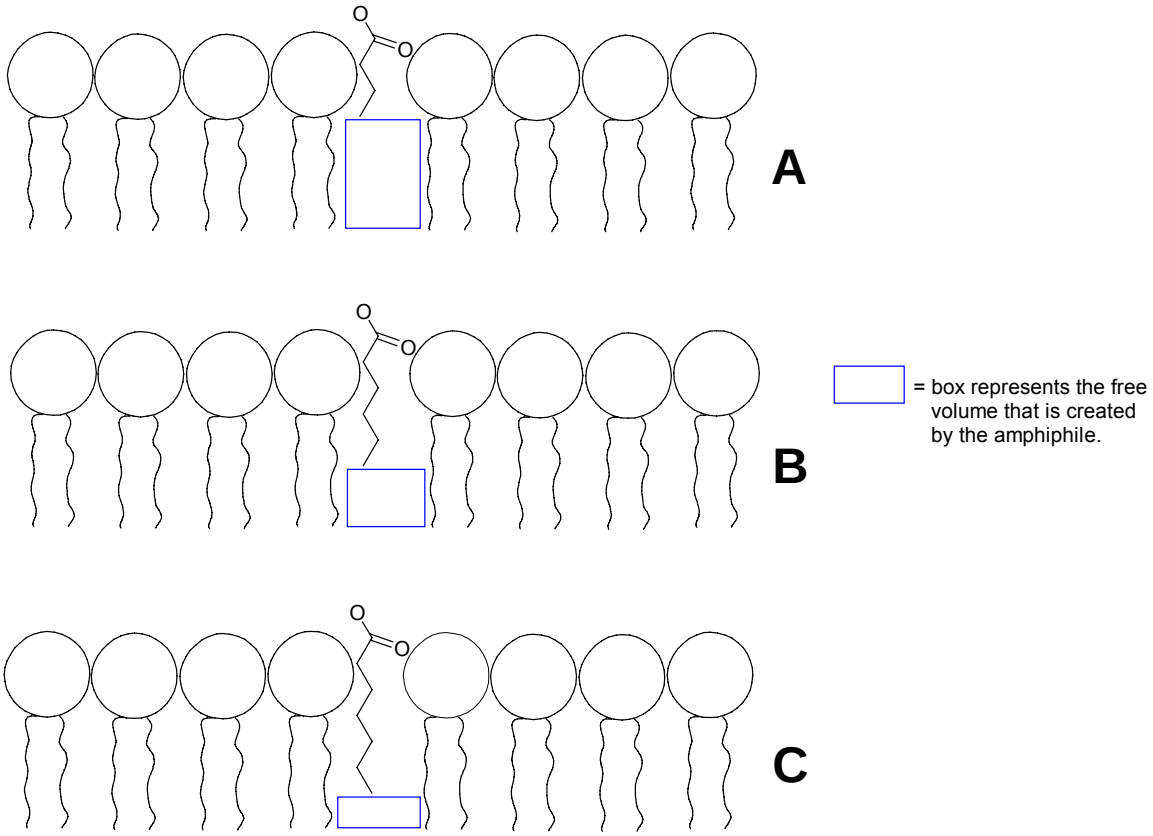

Figure 1.7 Cutoff Effects: Free Volume. **A** show a short-chain FA with a large free volume; **B** shows the optimal FA; **C** shows a long-chain FA with a small free volume.

1.4 Aqueous Solubility of Saturated Fatty Acids

The most effective saturated fatty acids (FAs) tend to have medium, C_8–C_{14}, chain lengths. The long-chain FAs, C_{16}–C_{20}, are either not as active or inactive against a wide range of microorganisms. One reason given why long-chain FAs are not antimicrobial is low aqueous solubility. Long-chain FAs simply are not very water soluble, especially compared to their short-chain counterparts. Vorum et al. reported that short to medium chain FAs are more water soluble than long-chain FAs.[21] As the chain length increases, the hydrophobicity of the FAs increases, leading to lower aqueous solubility.

Vorum et al.'s experiments were designed to determine the aqueous solubility of saturated, long-chain FAs at pH 7.4.[21] The aqueous solubility of C_{16} (~1 μM) was dramatically lower compared to C_{14} (20–30 μM). The aqueous solubility for C_{18} was <<1 μM, while the solubilities for C_{20} and C_{22} were too low to be measured.

Robb measured the solubility of FAs in water at pH 5.7.[22] His measurements were different than Vorum et al.'s due to differences in pH. The solubility for C_{14} was similar as both measurements are in the 20 μM range. Robb's measurements displayed a similar dramatic drop off in solubility as the chain length increased from C_{14} to C_{16}. The solubility for C_{16} (3.71 μM) was somewhat similar to Vorum et al.'s measurement (~1 μM). However, after C_{16}, the measurements of the two publications were dramatically different. Robb's solubility for C_{18} was 2.68 μM, while Vorum's value was much less than 1 μM. While Rob could not measure the solubility for C_{22}, Robb reported the solubility for C_{20} was 1.97 μM; Vorum et al. could not measure C_{20}.

The **3CAmn** series (Figure 1.1) was designed to overcome the low aqueous solubility of long-chain FAs by incorporating three dendritic carboxylic acid groups in the headgroup of the amphiphile. We hypothesize that increasing the number of anionic carboxylate groups in the headgroup of the amphiphile will lead to enhanced aqueous solubility relative to FAs. As mentioned previously, it is the hydrophilic headgroup of an amphiphile which imparts aqueous solubility. Consequently, additional headgroups should impart greater aqueous solubility than one or two headgroups. Removing solubility as a possible cause of the cutoff effect will lead to a greater understanding of chain length effects in antimicrobial measurements.

1.5 Cmcs of Multi-headed, Anionic Amphiphiles

Along with our desire that the **3CAmn** series be highly soluble in aqueous media, we also want the series to have high cmcs. It is believed that the non-detergent antimicrobial activity of FAs is caused by monomers and not micelles.[23] Therefore, for the **3CAmn** series to be effective microbicides, it must have high cmcs. The multi-headed, dendritic headgroup will aid in the aqueous solubility of the series. We hypothesize that an amphiphile with a trianionic headgroup will have a higher cmc than the corresponding amphiphile with a single headgroup. Without the limitations of low aqueous solubility and low cmcs, we can measure the intrinsic effect that chain length has on antimicrobial activity.

Properties, such as solubility and cmc of amphiphiles, are directly related to the number of headgroups. Shinoda[24, 25], Haldar et al.[26, 27], and Linderman[11] have demonstrated that the number of headgroups directly affects the cmc of amphiphiles. The Shinoda group studied how the number of headgroups and the length of hydrophobic chain affect the cmc of the amphiphile (Figure 1.8).[24, 28] They observed that the cmc values for **1** and **2** were 3.5–15 times higher than those of the corresponding FA. They attributed this observation to the two or three carboxylate groups on the alkyl malonates.

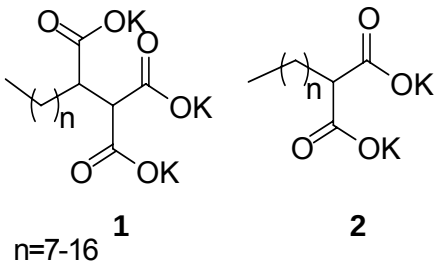

Figure 1.8 Multi-headed Amphiphiles Studied by Shinoda

An increase in the number of headgroups led to an increase in headgroup repulsion in the micelle.

The Shinoda group also compared the cmc values for a homologous series of dicarboxyl potassium alkyl malonates, **2**, with different chain lengths.[28] The results showed that cmc decreased as the length of the hydrophobic tail increased. They observed that the logarithm of the cmc fits Eqn. 1.1, where *m* is the number of carbon atoms in the chain plus one, and K_1 is the experimental constant given as 0.51. The Shinoda group work verified that the slope is not constant, but varies with the number and types of polar groups.

$$\log \text{cmc} = -K_1 m + \text{const.} \qquad \text{Eqn. 1.1}$$

The Shinoda group followed this work with a study of potassium alkane tricarboxylates. They studied the relationship of log cmc for a series of potassium alkane tricarboxylates, **1**, as the chain length was increased. Like their previous work with **2**, the results indicated that the slope of log cmc versus *m* varies with the number and type of groups present. The Shinoda group compared the cmc values of di-and tri- carboxyl alkane malonates (Figure 1.9).[29] Within a homologous series of carboxylates (mono, di, tri), the cmc decreased as chain length increased. When the cmc values of mono-, di-, and tri-carboxylates of equal chain length were compared, the cmc increased with the number of headgroups. These observations support our hypothesis that an increased number of headgroups would lead to increased cmcs for longer chains.

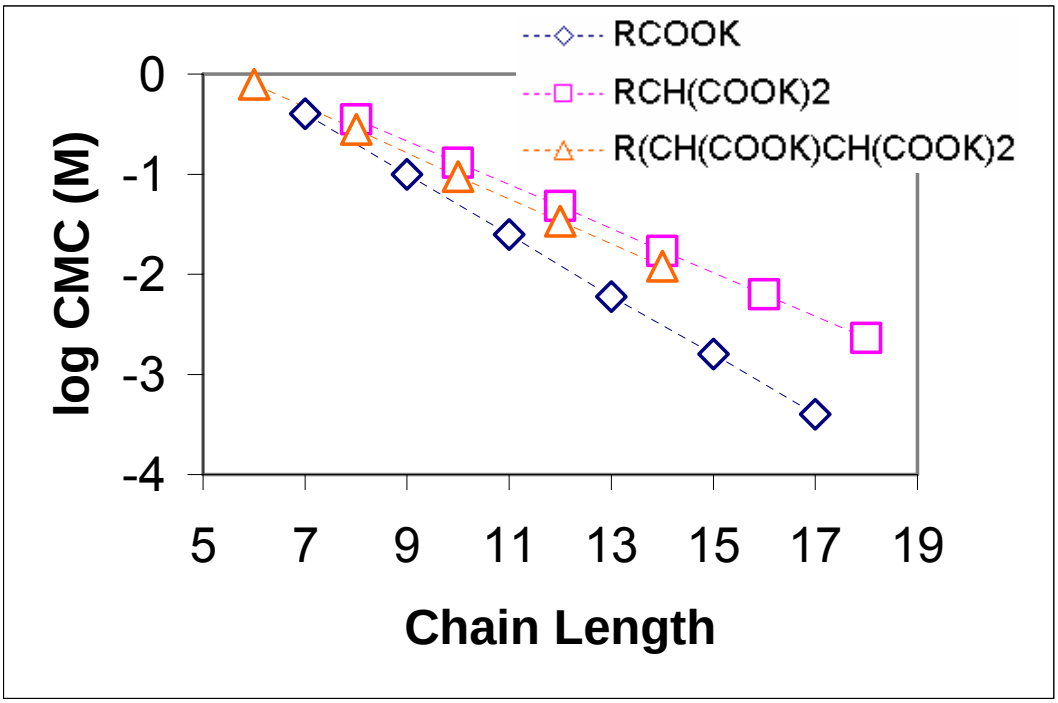

Figure 1.9 The Effect of the Number of Headgroups on cmc

Although cmc is not a direct measure of water solubility, Shinoda has shown that multi-headed anionic amphiphiles have higher cmcs than their single headed and double headed counterparts. While the cmc for the tri-headed amphiphile is not much higher than the double headed amphiphile, the two headed amphiphile displays a much higher cmc than a single headed amphiphile. As monomers are needed to determine the intrinsic antimicrobial activity of the chain length, our goal is to make amphiphiles with high cmcs.

The concept of why additional headgroups increase the cmc of amphiphiles can be summed up in the following sentences. Hydrophilic repulsion between ionic headgroups has a profound effect on cmc. If the ionic repulsion between the headgroups

is small compared to the hydrophobic attractions between the tails, the cmc will be low. This means amphiphiles will aggregate and form micelles at low concentrations. Conversely, if the ionic repulsion between the headgroups is large, compared to the hydrophobic attraction between the tails, the cmc will be high. Amphiphiles will only form micelles when forced by high concentrations of amphiphile.[30] Any increase of the hydrophilic repulsion between the headgroups relative to the hydrophobic attraction between the tails will result in an increase of the cmc. However, any decrease of hydrophilic repulsion between the headgroups relative to the hydrophobic attraction between the tails, will result in a decrease of the cmc. Therefore, making the headgroup(s) more hydrophilic will result in an increase of the cmc.[31]

1.6 Cell Walls of Microorganisms

The main functions of cell walls of microorganisms are to: prevent osmotic lysis, allow the selective passage of nutrients, exclude harmful antimicrobial agents, act as a scaffold for proteins, and maintain cell shape.[32]

Cell walls are the protectors of the inner cytoplasmic membrane and can differ from one microorganism to another microorganism. These differences are probably the cause of their differing susceptibility to FAs. There are major differences among bacteria due to their different cell walls. For example, the cell walls of Gram-positive bacteria are thicker than Gram-negative bacteria, but thinner than mycobacteria. The following review will highlight the differences in the cell walls of microorganisms.

1.6.1 Cell Wall of Gram-negative Bacteria

The cell wall of Gram-negative bacteria is more complex than that of Gram-positive bacteria (Figure 1.10). The surface of the cell wall of Gram-negative bacteria is

considered hydrophilic because of the hydrophilic lipopolysaccharide (LPS). Neither Gram-positive bacteria nor mycobacteria possess LPS. Additionally, the Gram-negative bacteria also possess an outer bilayer membrane that is unique to Gram-negative bacteria. However, Gram-positive, Gram-negative, and mycobacteria do share the inclusion of peptidoglycan in their cell walls. Peptidoglycan is a polymer composed of *N*-acetyl glucosamine, *N*-acetyl muramic acid, and amino acids.[33] The peptidoglycan layer, which is unique to bacteria, is relatively thinner than that of Gram-positive bacteria. The LPS and outer bilayer membrane give Gram-negative added protection against membrane perturbers that destabilize the inner cytoplasmic membrane.

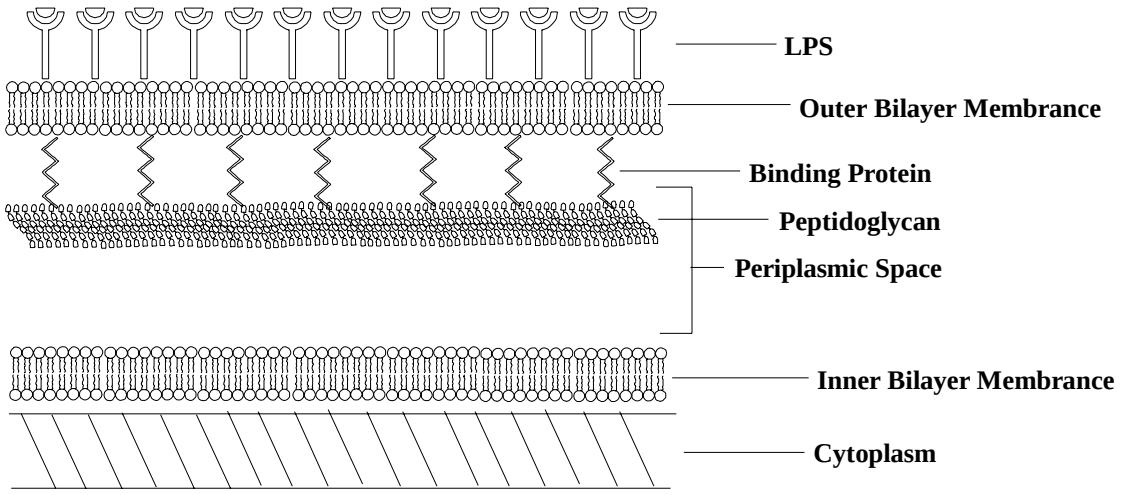

Figure 1.10 Cell Wall of Gram-negative Bacteria

1.6.2 Cell Wall of Gram-positive Bacteria

Gram-positive bacteria have a less complex cell wall than Gram-negative bacteria and mycobacteria (Figure 1.11). The cell wall of Gram-positive bacteria consists only of a very thick peptidoglycan layer. In Gram-positive bacteria, peptidoglycan accounts for 50% of the entire cell and 90% of the cell wall. In Gram-negative bacteria, peptidoglycan only accounts for 15–20% of the cell wall.[33] The cell wall of Gram-

positive bacteria is 20–80 nm, while the cell wall of Gram-negative bacteria is 10 nm.[33] Gram-negative and Gram-positive bacteria also differ in the amount of cross-linking in the peptidoglycan layer. The physical arrangement of peptidoglycan in the cell walls of Gram-positive and Gram-negative bacteria is different because of cross-linking. In Gram-positive bacteria, the peptidoglycan has a heavily cross-linked structure with multiple layers.[33] However, for Gram-negative bacteria, the peptidoglycan layer is only intermittently cross-linked.[33]

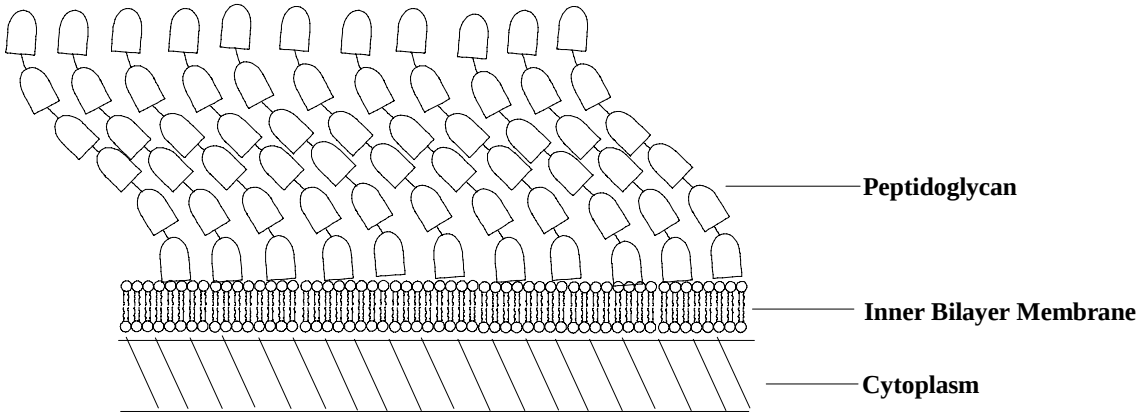

Figure 1.11 Cell Wall of Gram-positive Bacteria

1.6.3 Cell Wall of Mycobacteria

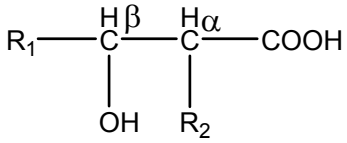

Figure 1.12 Mycolic Acid Structure

The cell wall of mycobacteria is thicker and more hydrophobic than both Gram-negative and Gram-positive bacteria (Figure 1.13). The cell wall also contains peptidoglycan, mycolic acids, lipoarabinomannan (LAM), and arabinogalactan (D-arabinose and D-galactose). The thickness and hydrophobicity are both due to mycolates.

Mycolic acids are very long, hydrophobic, molecules (Figure 1.12) where the R groups add up to C_{70}–C_{90} depending on the genus.[34] The mycolic acids are bonded to other components of the cell wall. Peptidoglycan is bonded to arabinogalactan, which is bonded to mycolic acids. The thick, hydrophobic cell wall makes mycobacteria resilient to a large number of antimicrobial agents.

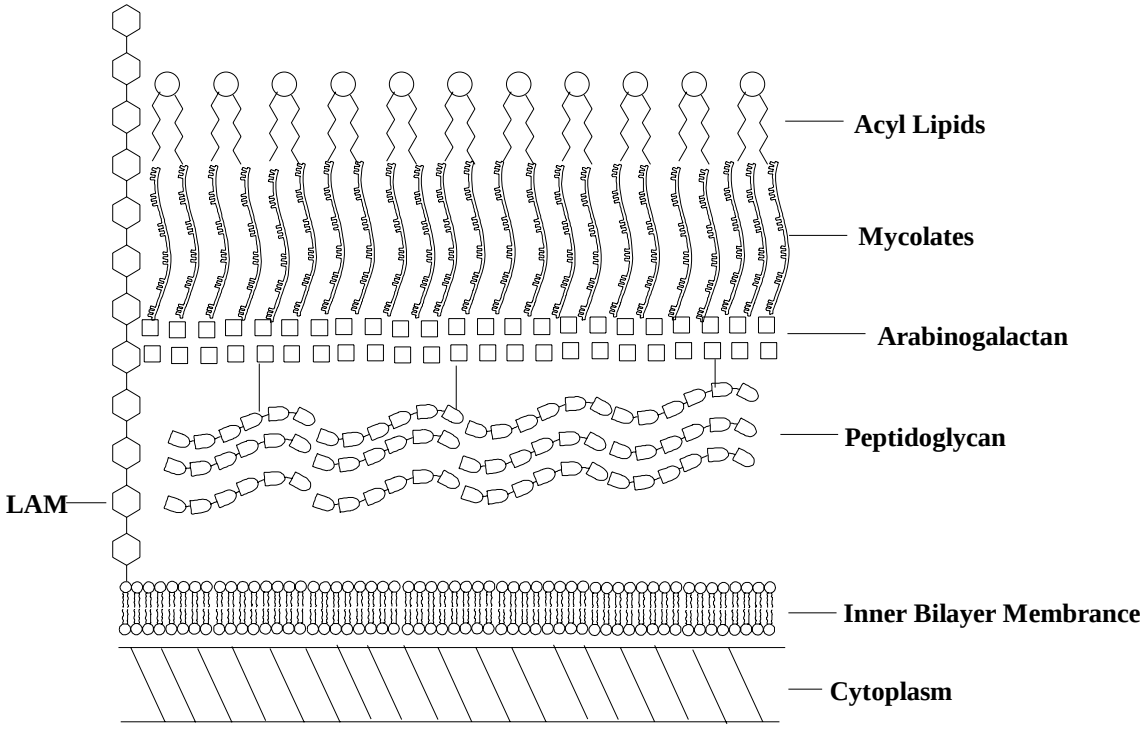

Figure 1.13 Cell Wall of Mycobacteria

1.6.4 Cell Wall of Yeasts

The yeast cell wall is completely different from that of bacteria (Figure 1.14). It completely lacks peptidoglycan. Chitin, a (β 1-4)-linked polymer of *N*-acetyl-D-glucosamine, is one component that differentiates yeast from bacteria. Chitin is a linear polymer that forms microfibrils held to by hydrogen bonding. The cell wall is comprised of chitin (polymers of glucosamine), β-glucan (polymers of galactose), and

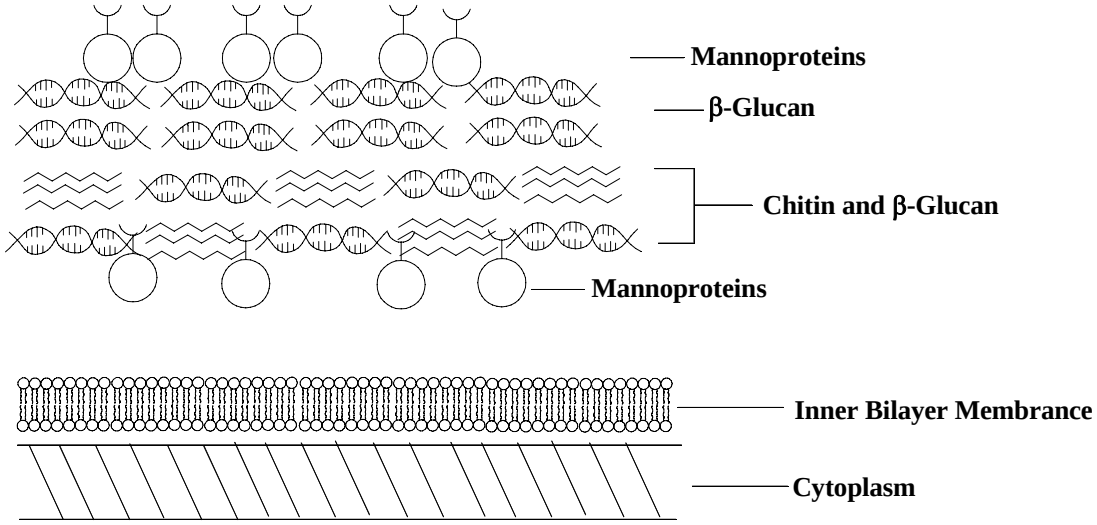

Figure 1.14 Cell Wall of Yeast

mannoproteins (polymers of mannose). The various components of the cell wall are present in varying amounts in different microorganisms. β-1,6-Glucan polymer of *Candida albicans* has more β-1,6-glucan than *Saccharomyces cerevisiae.*[35] Collectively, mannoproteins form yeast mannon, which form the outer layer of the cell wall.[35]

Yeast can also have a combination of β-glucan (most common) and α-glucan in varying amounts. There are also variations in the types of β-glucan. For example, yeast can have β-1,6-glucans and β-1,3-glucans. *C. albicans* has more linear β-1,6-glucan polymer and more β-1,6-glucan than *S. cerevisiae*.[35]

1.7 Antimicrobial Activity of Fatty Acids

1.7.1 Introduction of Antibacterial and Antifungal Activities of Fatty Acids

FAs have been known to display antimicrobial activity since the 1920s.[36, 37] As more microorganisms become resistant to current antibiotics, there is a great need for new antimicrobial agents. For example, *Staphylococcus aureus* is a bacterium that has become increasingly resistant to a numbers of drugs, e.g. methicillin, which is commonly

used to treat microbial infections.[38] Methicillin-resistant *S. aureus* (MRSA) is more resilient than *S. aureus* because MRSA produces a binding protein, PBP2′, that has less affinity for β-lactam antibiotics than *S. aureus*.[38]

FAs inhibit the growth of a wide variety of microorganisms, for example, Gram-negative bacteria, Gram-positive bacteria, mycobacteria, and fungi.[15, 23, 39-46] FAs tend to have better antimicrobial activity against Gram-positive bacteria than against Gram-negative bacteria.[46, 47] One reason for differing activities is that Gram-negative bacteria have two bilayer membranes (Figure 1.10) while Gram-positive bacteria have one bilayer membrane (Figure 1.11). Additionally, Gram-negative bacteria have a LPS layer embedded in the outer bilayer membrane, providing additional protection against antimicrobial agents by preventing entry into the bilayer.[47, 48] Even with these generalizations, there are always exceptions. For example, long-chain FAs are active against *Neisseria gonorrhoeae*, a Gram-negative bacterium.[23]

In the following review, we will review the antimicrobial activity of FAs against a wide varity of microorganisms. This review will be limited to those microorganisms that the **3CAmn** series will be tested against. We will attempt to determine (1) which chain length gives maximum activityagainst a particular microorganism and (2) chain length (cutoff effects). Multiple reviews of the antimicrobial activity of FAs against a particular microorganism will be included to get well rounded account of the antimicrobial activity.

1.7.2 Antibacterial Activity of Fatty Acids against *Staphylococcus aureus*

Walker reported the antibacterial activity of Na^+ and K^+ salts of even numbered FAs from C_8–C_{18} against *S. aureus*.[36] However, no carboxylate salt inhibited the growth of *S. aureus*. Walker noted that the sodium salts of the C_{14}, C_{16}, and C_{18} acids

could not be tested at high concentration due to gelation. He also reported the same problem for the potassium salt of C_{18} acid. Seventy years later, Vorum et al. reported that the alkali salts of FAs, especially for long-chains, have low solubility in aqueous media.[21] (This author concludes that low aqueous solubility probably caused the inactivity of the carboxylate salts in Walker's study.)

Bayliss studied the antibacterial properties of FAs against *S. aureus* using a plate count method.[49] For the plate count method, following incubation of the microorganism with the FAs, the media was grown on agar plates to determine how many colonies of the microorganism survived. Bayliss discovered that the shortest FA tested, $Na^{+-}C_{12}$ acid, was the most active (plate count 4,000). Longer chain FAs (C_{14}–C_{18}) FAs were inactive (plate count 10,000+).

Wyss et al. examined the antimicrobial activity of FAs against *S. aureus*.[50] They observed that odd chain FAs did not exhibit any enhanced antimicrobial activity relative to their even chain homologues. Chain length and cutoff effects were observed. The investigators believed that solubility limited the activity of the longer chains against some of the other organisms that they tested (e.g. *Aspergillus niger*). The insolubility of the longer chains was less of a problem with *S. aureus* because it was more susceptible to FAs. Activity increased with chain length, reached a maximum at C_{10} acid, and then decreased with longer chain lengths. *S. aureus* was inhibited by 0.015% of C_{10}, 0.05% of C_{12}, and >0.08 % of C_{14} and C_{16} acids.

Kabara et al. measured the minimum inhibitory concentrations (MIC) against *S. aureus*.[41] A chain length effect was observed as the activity initially increased from

C_{11} (1000 μg/mL) to C_{12} (500 μg/mL) while all of the longer chains (C_{13}, C_{16}, and C_{18}) were inactive.

In additional studies, Kabara et al. measured the antimicrobial activity of short and long-chain FAs (C_6–C_{18}) against *S. aureus*.[40, 51, 52] Unlike the previous study, because short-chain FAs were tested, definitive chain length and cutoff effects were observed. The shorter acids (C_6 and C_8) were inactive. Activity then increased with chain length, reached a maximum at C_{12} (499 μg/mL); after which, the activity then decreased ($C_{14,}$ 998 μg/mL), then ceased with the longest acids (C_{16} and C_{18}). The MIC values were higher in this study, which could be explained by different test conditions or different strains of microorganisms.

Jossifova et al. tested the antibacterial activity, in DMF, of long-chain FAs (C_{10}–C_{18}) against *S. aureus*.[53] Chain length and cutoff effects were observed for *S. aureus*. Activity increased from 2500 μg/mL for the C_{10} acid to a maximum of 1300 μg/mL for the C_{14} acid. The activity then decreased to 2100 μg/mL and 2500 μg/mL for C_{16} and C_{18}, respectively.

Ohta et al. reported the antibacterial activity of both saturated and unsaturated FAs against *S. aureus*.[54] The authors observed that the number of double bonds in the FAs had a profound effect on the antimicrobial activity. The saturated FAs that were tested, C_{14} and C_{18}, were inactive. Only FAs with two or more double bonds in the alkyl chain were active against *S. aureus*. The activity against *S. aureus* increased with the number of double bonds. Oleic acid ($C_{18:1}$) was inactive, while linolenic acid ($C_{18:3}$) was active at 10 μg/mL.

Bergsson et al. also studied the antibacterial activity of even chain, unsaturated ($C_{16:1}$ and $C_{18:1}$) and saturated (C_8–C_{14}) FAs against three strains of *S. aureus*.[55] The C_8, C_{14}, and $C_{18:1}$ acids caused minimal inhibition of *S. aureus*. At 10 mM, C_{14} and $C_{16:1}$ acids caused a modest inhibition (1 to 2.8 $\log_{10}$ reduction) of the bacteria. At 10 mM, C_{10} acid (5 to ≥ 7 $\log_{10}$ reduction) had the best activity. At 5 mM, C_{10} acid lost almost all activity.

Kitahara et al. studied the antibacterial activity of saturated FAs against *S. aureus*.[38] The authors acknowledged the difficulty in studying lipids because lipids become turbid and insoluble. The authors had to use disposable oxygen electrode sensors (DOX-96) instead of the usual microdilution method to measure MIC because of the turbidity caused by the insolubility of FAs. Antimicrobial activity increased with chain length, to a maximum at C_{14} (400 μg/mL); after which, the activity decreased with increasing chain length (C_{18} >1600 μg/mL).

Gutiérrez studied the antibacterial activity of FAs against *S. aureus*.[56] Contrary to other studies, this long chain amphiphiles (C_{17} and C_{18}) inhibited the growth of *S. aureus*. The shortest FA was the most active (C_{12}, 1500 μg/mL), the activity then decreased with a longer chain (C_{17}, 4200 μg/mL), then increased again (C_{18}, 2800 μg/mL).

Kilic et al. reported the antimicrobial activity of C_{18} acid against *S. aureus*. The C_{18} acid did not inhibit the growth of *S. aureus*.[57] These results were expected because most studies have shown that *S. aureus* was not susceptible to C_{18} acid.

Sivasamy et al. studied the antimicrobial activity of *N*-octadecyl amino acid derivatives (Figure 1.15) against *S. aureus* using the zone of inhibition method.[58] Both

C_{18}-*N*-glutamic acid and C_{18}-*N*-aspartic acid derivatives inhibited the growth of *S. aureus*. C_{18}-*N*-aspartic acid's activity is the same as C_{18} acid's activity; however, **4** was more active than **3** and C_{18} acid. This result showed the attachment of multi-headed anionic group can enhance the antimicrobial activity of a single-headed amphiphile. Unlike other studies that showed no activity of C_{18} FA[36, 38, 41, 52], this study illustrated that a C_{18} amphiphile can inhibit *S. aureus*.

1.7.3 Antibacterial Activity of Fatty Acids against MRSA

Ohta et al. reported the antibacterial activity of both saturated and unsaturated FAs against MRSA.[54] The authors observed that the number of double bonds had a profound effect on the antibacterial activity. Both saturated FAs that were tested, C_{14} and C_{18}, were inactive against MRSA. Only FAs with two or more double bonds in the alkyl chain were active against MRSA. The activity against MRSA increased with the number of double bonds. Oleic acid ($C_{18:1}$) was inactive, while linolenic acid ($C_{18:3}$) was active at 20 μg/mL.

Kitahara et al. studied the antibacterial activity of saturated FAs against five strains of MRSA.[38] In all cases, antimicrobial activity increased with chain length, from C_8 (>1600 μg/mL) to a maximum at C_{12} (400 μg/mL). In four of the five strains, the longer chain FAs (C_{14} to C_{18}) were mostly inactive (≥1600 μg/mL).

1.7.4 Antibacterial Activity of Fatty Acids against *Micrococcus luteus*

Sivasamy et al. studied the antimicrobial activity of C_{18}-*N*-amino acid derivatives against *M. luteus* using the zone of inhibition method (Figure 1.15).[58] The C_{18} FA was inactive against *M. luteus*; however, both **3** and **4** inhibited the growth of *M. luteus*. The glutamic derivative was more active than the aspartic derivative. The dicarboxylate

anionic group enhanced the antimicrobial activity relative to the monocarboxylate anionic headgroup of the FA.

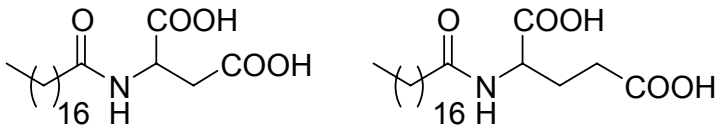

3 **4**

Aspartic Acid Derivative **Glutamic Acid Derivative**

Figure 1.15 Amino Acid Derivatives of C_{18} Acid

1.7.5 Antibacterial Activity of Fatty Acids against *Escherichia coli*

Bayliss studied the antibacterial properties of FAs against *E. coli* using a plate count method.[49] Bayliss observed the same solubility problems that Walker reported, stating that the inactivity of sodium C_{18} was likely due to the insolubility of the salt. He reported that a 1% solution of sodium C_{18} resulted in a semi-rigid gel. He discovered that the shortest FAs tested, sodium C_{12}, was the most active against *E. coli* (plate count 100+). The C_{14}–C_1 FAs were inactive (plate count 10,000+).

Hassinen et al. measured the antibacterial activity of FAs against *E. coli*.[59] The data showed the typical antimicrobial pattern that is normally displayed against Gram-negative bacteria. Short to medium chain FAs are the most active and long-chain FAs displaying no activity. At 96 h, C_4, C_{14}, C_{16}, and C_{18} acids did not inhibit the growth of *E. coli*. The C_6 (330 µg/mL) and C_{10} (95 µg/mL) acids were the most active FAs. At 500 µg/mL, C_{10} and C_{12} acids caused 38% and 5% reduction of growth, respectively.

Kabara et al. measured the antimicrobial activity against *E. coli*. All FAs tested (C_{11}–C_{18}) were inactive.[41] This fits with most reports that long-chain FAs are inactive against *E. coli*.

Jossifova et al. studied the activity, in DMF, of medium to long-chain FAs (C_{10}–C_{18}) against *E. coli*.[53] The authors reported that C_{18} (1300 μg/mL) was the most active FA tested. The activity initially increased from C_{12} (2500 μg/mL) to C_{14} (1700 μg/mL); however, the activity then decreased for C_{16} (3300 μg/mL) before it increased again for C_{18} (1300 μg/mL).

Marounek et al. measured the susceptibility of *E. coli* to C_2–C_{18} saturated FAs.[60] The results suggest that the medium chains FAs (C_8 and C_{10}) are better inhibitors of *E. coli* than either short or long-chain FAs. These results agree with Sheu and Freese's results that short and medium chains FAs (C_6 and C_{10}) inhibit *E. coli*.[48] Some short chain FAs (C_2–C_6), medium chain FAs (C_{10}), and long chain FAs (C_{14}–C_{18}) did not inhibit the growth of *E. coli*.[60] FAs, C_8 and C_{10}, had an IC_{50} (concentration required to inhibit the growth of a microorganism by 50%) of 450 μg/mL and 2000 μg/mL, respectively.

Gutiérrez studied the antibacterial activity of FAs against *E. coli*.[56] The most active FA had the shortest alkyl chain (C_{12}, 1700 μg/mL), followed by C_{17} at 2100 μg/mL, and finally C_{18} at 1800 μg/mL.

Kilic et al. reported the antimicrobial activity of C_{18} against *E. coli*.[57] The C_{18} acid did not inhibit the growth *E. coli*. These results were expected because most studies have shown that *E. coli* were not susceptible to C_{18} acid.

Gaur and Shauhan tested multi-headed derivatives of FAs (**5** and **6**) for antibacterial activity (Figure 1.16).[61] The multi-headed derivatives were not active against *E. coli* at the maximum concentration tested (2500 μg/mL).

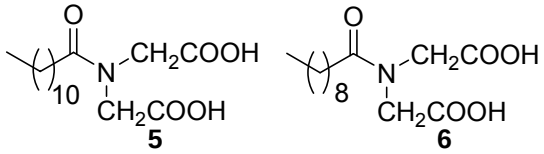

Figure 1.16 Multi-headed Amphiphile Derivatives of Fatty Acids

Sivasamy et al. studied the antimicrobial activity of C_{18}-*N*-amino acid derivatives (Figure 1.15) against *E. coli* using a zone of inhibition study.[58] The C_{18}-*N*-glutamic acid derivative, **4**, inhibited the growth of *E. coli*. However, the C_{18}-*N*-aspartic acid derivative, **3**, was inactive. MICs were not reported in this study, however, this study did show that attaching a multi-anionic headgroup on a long chain FA acid, that was previously inactive, can enhance activity.

1.7.6 Antibacterial Activity of Fatty Acids against *Klebsiella pneumoniae*

Jossifova et al. studied the antibacterial activity of long-chain FAs against *K. pneumoniae*.[53] The results do not follow a chain length trend. The activity increased from C_{10} (2500 μg/mL) to C_{12} (1200 μg/mL) acid. The activity decreased for C_{14} acid (2100 μg/mL), then increased for C_{16} (1700 μg/mL) and C_{18} (1300 μg/mL) acids.

Gutiérrez reported that long chain amphiphiles inhibited the growth of *K. pneumoniae*.[56] The shortest FA (C_{12}) inhibited *K. pneumoniae* at 3900 μg/mL, the activity increased slightly with a longer chain (C_{17}, 3400 μg/mL), then increased again for C_{18} (1500 μg/mL) acid.

1.7.7 Antibacterial Activity of Fatty Acids against *Neisseria gonorrhoeae*

Miller et al. reported the antibacterial activity (IC_{50}) of FAs against *N. gonorrhoeae*.[23] Cutoff and chain length effects were observed. With the exception of C3 (670 μg/mL), the activity increased with chain length. Starting with C_1 (4100 μg/mL),

the activity increased with chain length with a maximum at C_{16} (1.54 μg/mL); at which point, the activity decreased for C_{17} (21.6 μg/mL), then ceased for the longest chains (C_{18}–C_{20}). The authors hypothesized that FAs with ≥ C_{18} alkyl chains could be too large to pass through the outer bilayer membrane. They stated that α, ω-dicarboxylic acids were inactive because the placement of a second polar carboxylic acid group at the end of the hydrocarbon chain would prevent the binding of the diacid to the hydrophobic regions of the membrane.

Bergsson et al. measured the susceptibilities of *N. gonorrhoeae* to even numbered FAs (C_8–C_{14}).[62] Chain length and cutoff effects were observed. Activity initially increased with chain length, and then decreased. The optimum chain length, against all strains, was C_{12} acid. The activity increased with chain length up to C_{12}, then decreased. The C_8 acid was minimally active against three out of five strains ($10^{0.1–0.5}$ inhibition). The inhibition due to C_{10} acid varied with the strain used. For strains I–III, inhibitions of $10^{0.3–1.2}$ were recorded. For strains IV and V inhibitions of 10^4 and 10^6, respectively, were reported. The C_{12} acid exhibited 10^6 inhibition against all strains. The C_{14} acid exhibited modest activities against four out of five strains ($10^{1.5–2.2}$).

1.7.8 Antifungal Activity of Fatty Acids against *Candida albicans*

Kabara et al. measured the antifungal activity of FAs against *C. albicans*.[41] The most active FA had the shortest chain (C_{10}, 100 μg/mL). All longer chains displayed decreased activity. The C_{11} and C_{12} acids inhibited at 1000 μg/mL, while the longer chains (C_{13}, C_{16}, and C_{18}) were inactive.

In additional studies, Kabara et al. measured the antifungal activity of short to long chain FAs (C_6–C_{18}) against *C. albicans*.[40, 51, 52] Unlike the previous study that did not include short-chain FAs, this study included a wide range of chain lengths so definitive chain length and cutoff effects could be observed. The shorter acids (C_6 and C_8) were inactive. The activity then increased with chain length, reached a maximum at C_{12} (500 μg/mL); after which, the activity decreased (C_{14}, 1000 μg/mL), then ceased for the longest acids (C_{16} and C_{18}). The MIC values were higher in this study, which could be explained by different test conditions or different strains of microorganisms.

Parang et al. studied the antifungal activities of C_{14} analogs against *C. albicans*.[63] The terminal halo and α-halo analogs were very active against *C. albicans*. 2-Bromo-C_{14} acid (12.3 μg/mL) was the best antifungal agent, while 11-iodo-C_{14} acid had minimal activity (670 μg/mL). However, C_{14} acid was inactive.

Bergsson et al. measured the antifungal activity of both saturated and unsaturated even chain FAs against three strains of *C. albicans*.[45] The authors observed that chain length, not unsaturation, affected the antifungal activity. The activity initially increased with chain length, then decreased. The optimum chain length for antifungal activity was C_{10} acid. FAs, C_8 and C_{14}, were inactive. At 10 mM, C_{10} acid caused the greatest reduction of colony forming unit (≥ log 6.75), while C_{12} acid caused a reduction of log 5.25. At 5 mM, C_{10} acid lost almost all activity, while C_{12} acid was moderately less active (log 2.28 reduction). The saturated FAs were more antifungal, while the unsaturated FAs ($C_{16:1}$ and $C_{18:1}$) were inactive.

Kilic et al. reported the antimicrobial activity of C_{18} acid against *C. albicans*. The C_{18} acid did not inhibit the growth of *C. albicans*.[57] This result was expected because most studies have shown *C. albicans* was not susceptible to C_{18} acid.

Sivasamy et al. studied the antimicrobial activity of C_{18}-*N*-amino acid derivatives against *C. albicans.*[58] Unfortunately, neither C_{18} acid, nor **3** and **4,** inhibited the growth of *C. albicans*.

1.7.9 Antifungal Activity of Fatty Acids against *Saccharomyces cerevisiae*

Kabara et al. measured the antifungal activity of FAs against *S. cerevisiae*. The shortest acid (C_{11}, 500 μg/mL) was the most active. The C_{12} and C_{13} acids (1000 μg/mL) were less active than C_{11} acid, while C_{16} and C_{18} acids were inactive.

Parang et al. studied the antifungal activities of C_{14} analogs against *S. cerevisiae*.[63] The terminal halo and α-halo analogs were very active against *S. cerevisiae*. 2-Bromo-C_{14} acid (3.10 μg/mL) was the best antifungal agent, while 11-iodo-C_{14} acid was mildly antifungal (430 μg/mL). However, C_{14} acid was inactive.

1.7.10 Antifungal Activity of Fatty Acids against *Cryptococcus neoformans*

Parang et al. studied the antifungal activities of C_{14} analogs against *C. neoformans*.[63] The terminal halo and α-halo analogs were very active against *C. neoformans*. 2-Bromo-C_{14} acid (6.20 μg/mL) was the best antifungal agent, while 11-iodo-C_{14} acid had modest antifungal activity (42.5 μg/mL). However, C_{14} acid was inactive.

1.7.11 Antifungal Activity of Fatty Acids against *Aspergillus niger*

Wyss et al. examined the antimicrobial activity of FAs against *A. niger*.[50] They observed that odd chain FAs did not exhibit any enhanced antifungal activity relative to

their even chain homologues. Chain length and cut-off effects were observed. Against *A. niger*, the antifungal activity increased with chain length up to C_{11} acid, and then decreased. The investigators believed that solubility limited the activity of the longer chains. The authors theorized that C_{12} acid should inhibit *A. niger* at 0.03%; however, as C_{12} acid does not dissolve to that extent, no inhibition is exhibited. *A. niger* was inhibited by 3%, 0.06% of C_{11}, and >0.08% of C_{12}, C_{13}, C_{14}, and C_{16} acids, respectively.

Parang et al. studied the antifungal activities of C_{14} analogs against *A. niger*.[63] The terminal halo and α-halo analogs were very active against *A. niger*. 11-Iodo-C_{14} acid (<10.6 μg/mL) was the best antifungal agent, while 2-Bromo-C_{14} acid (<12.3 μg/mL) was the second best antifungal agent. However, C_{14} (620 μg/mL) acid was relatively inactive.

1.7.12 Antimicrobial Activity of Fatty Acids against *Mycobacterium smegmatis*

Kondo and Kanai measured the antibacterial of even-chain FAs (C_8–C_{18}) against *M. smegmatis*.[43] Chain length and cut-off effects were observed as activity increased with chain length, reached a maximum, then ceased. The C_{10} acid caused a 99.96% reduction in growth, while C_{12} caused a 99.98% reduction in growth. All the other even chain FAs (C_8–C_{12} and C_{16}–C_{18}) were inactive against *M. smegmatis*. All acids were tested at 20 μg/mL. (Some of the other FAs might have been active if they were tested at a higher concentration.)

Saito et al. studied the susceptibility of *M. smegmatis* to FAs (C_2–C_{20}).[44] Only C_{10} inhibited the growth of *M. smegmatis* (100 μg/mL). All other FAs (C_2–C_8 and C_{12}–C_{20}) did not inhibit the growth of *M. smegmatis* at the maximum concentration (400 μg/mL).

1.7.13 Summary

Overall, FAs exhibit a wide range of antimicrobial activity against several microorganisms. FAs have shown activity against Gram-positive bacteria, fungi (including yeasts), and mycobacteria. FAs are generally are not active against Gram-negative bacteria but there are exceptions, such as *N. gonorrhoeae.*

Medium-chain FAs (C_8-C_{14}) tend to be the most active. Long-chain FAs are not as water soluble as medium-chain FAs; the relative insolubility of long-chain FAs could explain their relative inactivity. We expect the addition of a dendritic headgroup will "drag" longer alkyl tails into aqueous solution. The increased aqueous solubility of these longer chains should then lead to a better assessment of the effect of chain length on the antimicrobial activity.

1.8 Possible Antimicrobial Mechanisms of Action for Fatty Acids

1.8.1 Introduction to Possible Antimicrobial Mechanisms of Action

Although FAs have a long history[36, 49] of inhibiting the growth of microorganisms, the mechanism(s) of how FAs inhibit the growth of microorganisms is not widely understood. Researchers typically give a wide variety of mechanisms of action.[39] For example, in a 1979 review, Kondo and Kanai have presented multiple examples of how FAs inhibit the growth of bacteria.[46] One example is that the attack of the cytoplasmic membrane by FAs can lead to loss of membrane structure. Another stated mechanism is the interaction of FAs with the enzymes of the bacterial membrane; this interaction leads to reduced enzymatic activities.[46] Enzymatic activities that are said to be inhibited are oxygen consumption, amino acid uptake, electron-transport chain, $NADH_2$ (nicotinamide adenine dinucleotide) oxidase, and tetrazollium-reducing

activity.[46] (The mechanisms of action probably vary from microorganism to microorganism, and they are probably related. The inhibition of growth of microorganisms is probably due to a combination of mechanisms.)

There are many theories about the antimicrobial activity of FAs.[8, 23, 39, 44, 64-68] The most prevalent possible mechanisms of action are (1) destabilization of the cell membrane, (2) inhibition of enzymatic activities, (3) inhibition of oxygen uptake, (4) uncoupling of the electron transport chain and oxidative phosphorylation, (5) changes in turgor (osmotic) pressure, (6) changes in lipid bilayer thickness, (7) inhibition of cell wall synthesis, and (8) inhibition of protein myristoylation.

1.8.2 Overview of Fatty Acid Antimicrobial Activity

Inhibition of microorganisms via membrane destabilization is probably the most popular mechanism. The membranes of cells are highly organized barriers that protect the inner components of a cell from the outside environment.[33] This protection is essential because it allows the cell to selectively interact with the outside environment.[33] FAs are believed to insert their hydrophobic chains into the phospholipid bilayers of the microorganisms' cell membranes.[44, 67] This insertion can cause different consequences. One consequence would be the change in membrane permeability.[44] This change could lead to a loss of membrane integrity (disintegration, lysis) or change in the porosity of the membrane.[46] Other consequences include inhibiting essential membrane proteins responsible for cellular maintenance and uncoupling oxidative phosphorylation.[67]

Saito and Tomioka further theorized that FAs incorporate their alkyl chains into the cell membrane, and this incorporation causes; (1) changes in the porosity of the cell

membrane, (2) uncoupling of the oxidative phosphorylation system, and (3) the inhibition or change in the functionality of vital membrane proteins for cellular maintenance.[44] Speculation that FAs must go through the cell surface and cell wall led the authors to theorize that a change in porosity was probably the predominant cause of antimycotic activity.

Another consequence of FA insertion into the cytoplasmic membrane would be a change in membrane bound proteins, causing the inactivation or change in functions of vital membrane bound proteins.[44] Inhibited acid-sensitive proteins and nucleic acids could lead to the uncoupling of the oxidative phosphorylation and electron transport chain, which is used to provide the cell with energy.[60]

In an exhaustive review in 1954, Nieman theorizes that FAs adsorb and become integrated into the cell membrane causing changes in cell permeability.[37] These changes in cell permeability could lead to blocking the entry of essential nutrients or causing the release of vital cellular components.[37]

1.8.3 Specific Examples of Fatty Acid Antimicrobial Activity

Kitahara et al. speculated that the cytoplasmic membrane was a site of attack for FAs in *S. aureus* and MRSA.[38] They theorized that FAs accumulate in the phospholipid bilayer of the cytoplasmic membrane, which caused the membrane to become destabilized. The outer membrane of Gram-negative bacteria blocks FA entry into the inner membrane, conversely; the cell wall of Gram-positive bacteria facilitates the adsorption and transport of FAs into the inner membrane.[38]

Saito and Tomioka measured the antimycotic activity of C_{10} and C_{12} acids against colonial variants of *Mycobacterium avium*.[67] The authors stated that fast-growing

mycobacteria (i.e., *M. smegmatis*)[44] are susceptible to FAs because FAs can easily incorporate into the highly hydrophobic cell surface of mycobacteria and be transported to the target sites in the cell membrane.

Kondo and Kanai also stated that mycobacteria are sensitive to long-chain FAs due to their highly hydrophobic surfaces. Additionally, the highly hydrophobic interior or their cell walls facilitated the integration of FAs into the cell membrane.[69] Kondo and Kanai tested the antimycotic activity of long-chain FAs against *Mycobacterium bovis* (BCG).[69] They concluded that the cell wall of BCG assisted in the antimycotic activity by absorbing FAs, which were later brought into contact with the active site (cytoplasmic membrane). They observed that the antimycotic activity of long-chain FAs decreased when the heat-killed whole cell (or cell wall) of BCG was added to suspensions of active mycobacteria. This result indicated that the cell walls of BCG absorbed the long-chain FAs; this absorption prevented the FAs from exhibiting antimycotic activity. Despite the authors assertion that the cytoplasmic membrane was the site of attack for FAs, the authors did not observe any increased leakage using a spectrophotometric assay.[69]

In a later study, Kondo and Kanai tested the antimycotic activity of FAs against BCG and *Mycobacterium tuberculosis*.[70] They theorized that FAs inhibited mycobacteria by inserting their alkyl tails into the cytoplasmic membrane, which led to an increased negative charge in the membrane, resulting in an increased porosity of the membrane.[70]

Bergsson et al. hypothesized that the antibacterial activity of FAs against five strains of *N. gonorrhoeae* was due to the disruption of the cell membrane of *N.*

gonorrhoeae.[62] Due to the disruption, the authors did not believe that resistant strains will emerge.

Although there are many theories regarding the antimicrobial mechanism of action of FAs, researchers have rarely tested their theories. However, some researchers have tried to validate their theories. For example, Galbraith and Miller used a radiochemical assay to observe whether protoplasts and whole cell of *Bacillus megaterium* absorbed FAs.[65] (A protoplast is a bacterial or plant cell that has the cell wall removed but still retains the protoplasm and plasma membrane.)[71] The authors noted that the absorption of FAs increased with chain length and FA adsorption to the cell membrane was dependent on FA solubility. At pH 6, C_{12} acid was more bactericidal than the longer FAs; however, when the pH was raised to pH 8, the longer FAs (C_{14}, C_{15}, and C_{16} acids) were more bactericidal due to the increased solubility of these FAs in aqueous media. They also theorized that the site of action was the cytoplasmic membrane. This assertion was supported by the observation that adsorption of FAs in the protoplast was greater than the adsorption in the whole cell.

1.8.4 Inhibition of Enzymatic Activities

Miller et al. stated that the growth of *N. gonorrhoeae* was inhibited by inhibiting $NADH_2$ oxidase activity.[23] The authors assumed that the loss of $NADH_2$ oxidase activity was at least partially caused by blocking electron transport.

Ferdinandus and Clark reported that FAs inhibited bacterial enzymes that are involved in lipogenesis in *Arthrobacter crystallopoietes* (Table 1.3).[72] Lipogenesis, the synthesis of bacterial lipids, is important because lipids are involved in bacterial morphogenesis. FAs inhibited both glucose-6-phosphate dehydrogenase and malic

enzyme, both of which produce reduced nicotinamide adenine dinucleotide phosphate (NADPH). NADPH is vital for many cellular functions. FAs inhibit fumarase, the enzyme which is needed in the Krebs cycle.[72] The Krebs cycle produces ATP, a molecule used as cellular energy. Medium-chain FAs (C_{12} and C_{14} acids) inhibited the activities of the enzymes at a much lower concentration than that of the shorter chain FAs (C_8 acid).

Table 1.3 Percent Inhibition of Enzyme Activity of *A. crystallopoietes* by Fatty Acids. Table recreated from Reference [72].

Enzymes	Sodium Salts of Fatty Acids		
	C_8	C_{12}	C_{14}
Phosphofructokinase	45	-	-
Glucose-6-phosphate dehydrogenase	58	-	-
Malic enzyme	30	-	-
Pyruvate kinase	100	-	-
Lactate dehydrogenase	58	100	-
Fumarase	60	45	68

3.3×10^4 μM of sodium C_8, 2.5×10^4 μM of sodium C_{12}, and 0.67×10^4 μM of sodium C_{14} were used in this experiment.

Eisler and Heckly studied the antibacterial activity of FAs on *Pasteurella pestis* (Table 1.4).[73] Using a spectrophotometric assay, they observed that FAs did not cause the lysis of the cell, or leakage of proteins and nucleic acids. However, FAs did inhibit the growth of *P. pestis* by interfering with enzymatic functions.[73] The FAs did not inhibit β-D-glucose. In fact, C_{14}–C_{18} acids promoted the growth of *P. pestis*. The FAs showed minimal activity of glucose-6-phosphate but good activity against 6-phosphogluconate. 6-Phosphogluconate is important because it used in the production of NADPH. Activity, initially, increased with chain length, leveled off, and then decreased.

Table 1.4 Effects of Fatty Acids on Metabolism of some Carbohydrates

FAs	Percent Inhibition of Dehydrogenases of		
	β-D-Glucose	6-Phosphogluconate	Glucose-6-phosphate
C_8	3	52	25
C_{10}	6	82	19
C_{12}	3	100	32
C_{14}	-20	100	32
C_{16}	-31	88	16
C_{18}	-15	74	26

Final concentration of FAs tested was 330 μmoles/mL

1.8.5 Inhibition of Oxygen Uptake

Levine and Novak studied the effect of FAs on oxygen uptake of the pathogenic *Blastomyces dermatitidis*.[74] Initially, the short-chain FAs (C_2–C_8) stimulated oxygen intake (21%–73%). FAs did not begin to inhibit oxygen uptake until C_9 (54%). The longer chains (C_{10}–C_{12}) FAs completely inhibited oxygen uptake.

Bernheim studied the ability of FAs to control the respiration of *B. dermatitidis*. Similar to Levine and Novak, Bernheim noted that the short-chain FAs did not inhibit oxygen uptake; however, long-chain FAs (C_{16} and C_{18}) inhibited oxygen uptake. Bernheim reported that 1000 μg sodium C_{16} acid inhibited 93% of oxygen uptake. Sodium C_{18} acid (2000 μg) inhibited 62% of oxygen uptake. Bernheim theorized that the FAs cover the cell surface of the microorganism, thereby preventing the penetration of oxygen and substrates through the cell surface.

1.8.6 Uncoupling of the Electron Transport Chain and Oxidative Phosphorylation

Marounek et al. theorized that "fatty acids facilitate the transport of protons across the bacterial membrane and thus collapse the proton gradient. The collapse of the proton gradient results in depletion of cellular energy, which leads to the denaturation of acid-sensitive proteins and nucleic acids."[60]

Miller et al. proposed FAs inhibited *N. gonorrhoeae* by inhibiting oxygen uptake and $NADH_2$ oxidase activity. They proposed that the inhibition of oxygen consumption and $NADH_2$ oxidase activity were due to the uncoupling of oxidative phosphorylation and blocking electron transport. The uncoupling of oxidative phosphorylation led to the inhibition of electron transport.[23] Uncoupling of oxidative phosphorylation is thought to occur by the insertion of FAs into the membrane and the FAs functioning as "circulating carriers, conducting protons across the membrane barrier."[23] Uncoupling can also occur by FA binding to membrane proteins, causing "conformational changes in the protein structure and loss of biological activity."[23, 75]

1.8.7 Changes in Turgor (Osmotic) Pressure

To further investigate the effect of FAs on protoplast and discern the antibacterial activity, using a spectrophotometric assay, Galbraith and Miller studied the lysis ability of FAs on protoplast.[66] Based on the data, one cannot draw any conclusion as to whether lysis of the protoplast was the mechanism of action because of pH dependency. At lower pH (pH=6), the lysis concentration was above the bactericidal concentration. At higher pH (pH=8), the lysis concentration was below the bactericidal concentration. However, at an intermediate pH (pH=7.4), the lysis and bactericidal concentrations were similar. At pH 8, a cutoff effect was observed. Lysis increased from C_{12}–C_{15}, then decreased from C_{15}–C_{18}.

Bergsson et al. studied a possible mechanism of C_{10} acid against *C. albicans*.[45] The authors used transmission electron microscopy (TEM) to study cells of *C. albicans* that were treated with 10 mM of C_{10} acid. No visible changes in the cell wall were observed. However, the images did show a disorganization of the cytoplasm in the cell,

which the authors attributed to the change in hydrostatic turgor (osmotic) pressure within the cell.

1.8.8 Changes in Lipid Bilayer Thickness

In a review, Balgavý and Devinský proposed that amphiphiles inhibit microorganisms through their integration into the phospholipid bilayers of biological membranes.[8] They proposed that amphiphiles inserted their alkyl chains into the phospholipid bilayer. This insertion of the alkyl chain into the phospholipid bilayer created a free volume in the bilayer membranes due to the mismatch between the alkyl chains of the amphiphiles and phospholipids (Figure 1.7). As the phospholipids rearranged their alkyl chains to fill the free volume that was created, a change in bilayer thickness, or a destabilization of the phospholipid bilayer, resulted. A change in the bilayer thickness exposed membrane proteins to a new environment, which resulted in the inactivation of these proteins. Protein functionality was based on bilayer thickness; consequently, changes in bilayer thickness could inactive proteins, which could be the cause of bactericidal activity. A destabilization of the cell membrane could also lead to the collapse of the bilayer membrane.

1.8.9 Inhibition of Cell Wall Synthesis

Niwano et al. studied the effect of FAs as inhibitors of microbial cell wall synthesis (Table 1.5).[68] The investigators studied whether FAs inhibited the growth of vital components of bacterial (peptidoglycan) and fungi (chitin and β-1,3-glucan) cell walls. Saturated FAs were not as active as the unsaturated FAs. Saturated FAs exhibited minimal to modest inhibition of β-1,3-glucan but no inhibition of chitin or peptidoglycan.

Table 1.5 Effects of Fatty Acids on Cell Wall Synthesis. Table recreated from Reference [68].

Fatty acids	ID_{50} (μg/mL)		
	β-1,3-Glucan	Peptidoglycan	Chitin
C_{12}	1200	NA	NA
C_{18}	450	NA	NA
$C_{18:1}$	6	32	90

NA= not active. β-1,3-Glucan comes from *S. cerevisiae*, Peptidoglycan came from *E. coli*, Chitin from *Piricularia oryzae*

1.8.10 Inhibition of Protein Myristoylation

Parang et al. theorized that the C_{14} (myristic) acid analogs inhibited the growth of fungi by inhibiting protein synthesis via blocking *N*-myristoylation.[76, 77] This resulted in the perturbation of fungal protein functions. *N*-Myristoylation is a process in which the NH_2-terminal group of glycine residues, of various fungal and viral proteins, is acylated by myristic acid to form an amide bond.[77] The modification of viral and cellular proteins is crucial for association with membranes and proteins.[77]

1.9 Possible Antiviral Mechanisms of Action for Fatty Acids

FAs, especially unsaturated FAs, have been shown to inhibit enveloped viruses.[78-80] Typically, FAs do not inhibit viruses that lack viral envelopes.[79] This observation indicates that the viral envelope is the site of attack for FAs.[79, 81] We want our amphiphiles (anionic and nonionic) to inhibit HIV. Unfortunately, to our knowledge, saturated FAs have not been tested against HIV. In this review, we will show that FAs do inhibit other enveloped viruses.

Stock and Francis reported the activity of various organic acids—even chain saturated ($C_{10–20}$ and C_{26}) and various unsaturated ($C_{11:1}$, $C_{18:1E}$, $C_{18:1Z}$, $C_{18:2}$, $C_{18:3(9, 11, 13)}$, $C_{18:3(9, 12, 15)}$ FAs—against the PR8 strain of the influenza virus.[78] Additionally, a tri-headed acid (aconitic) as well as di-headed acids (sebacic, mucic, maleic) were also

tested but were inactive. The C_{14} acid (1 mM) caused a slight inactivation; however, other saturated FAs were inactive (at 1 mM). The C_{12} and C_{16} acids did slightly inactivate the virus at a higher concentration (10 mM). The number of double bonds did not affect activity as $C_{18:1E}$, $C_{18:1Z}$, $C_{18:2}$, and $C_{18:3(9, 12, 15)}$ acids all inactivated the virus at 1 mM. Double bonds did not always lead to activity as the C_{18} conjugated isomer ($C_{18:3(9, 11, 13)}$), as well as $C_{11:1}$, were inactive. The authors did report that higher concentrations of some acids could not be prepared because of the insolubility of some FAs. This suggests that the cutoff effect could have been due to the lack of solubility of those FAs. Based on their results, the authors concluded that neither chain length nor number of double bonds were the sole factors responsible for virus inactivation.

Kohn et al. reported the antiviral activity of C_{18} acid, as well as $C_{18:1}$, $C_{18:2}$, $C_{20:4}$ acids, against enveloped viruses.[82] The authors reported that nonenveloped viruses were not affected by FAs. The C_{18} acid exhibited minimal activity (log 0–0.5 reduction) against Influenza and Sindbis viruses, while the unsaturated FAs ($C_{18:1}$, $C_{18:2}$, $C_{20:4}$) showed good activity (log 3.8–6.1 reduction).

Thormar et al. reported the antiviral effect of FAs on enveloped and nonenveloped viruses.[79] The activity of these acids were tested against enveloped viruses, such as vesicular stomatitis virus (VSV), herpes simplex virus (HSV), visa virus (VV), as well as an nonenveloped virus (poliovirus). A cutoff effect was observed for VSV. Initially, the shorter chain FAs (C_4–C_6) were inactive or relatively inactive (C_8), while the medium-chain FAs (C_{10}–C_{14}) were the most active. The longer chain FAs (C_{16} and C_{18}) exhibited minimal to no activity. The antiviral activities for HSV-1 and VV were similar to that for VSV. The short- and long-chain FAs exhibited minimal to no

activity, while the medium-chain FAs were the most active. As a group, unsaturation appeared to have a major effect on the activity. Unsaturated FAs ($C_{16:1,}$ $C_{18:1}$, $C_{18:2}$, $C_{18:3}$, $C_{20:4}$) completely inhibited VSV and HSV-1. They also exhibited very good activity (≥ 3.2 $\log_{10}$ reduction) against VV. While the medium-chain saturated FAs and long-chain unsaturated FAs both exhibited the maximal activity (≥4.0 $\log_{10}$ reduction) against HSV and very good activity (≥3.2 $\log_{10}$ reduction) against VV, the unsaturated FAs displayed this activity at much lower concentrations. With the unsaturated FAs, there also was a chain length effect. While $C_{16:1}$ acid exhibited minimal activity (0.7–1 $\log_{10}$ reduction) the longer chain unsaturated acids were more active (3.2–4 $\log_{10}$ reduction). Activity also increased with the number of double bonds within a given chain length. $C_{18:1(Z\text{ and }E)}$ (7 mM), $C_{18:2}$ (3.5 mM), and $C_{18:3}$ (3.6 mM) were less active than $C_{20:4}$ (1.6 mM). None of the FAs, saturated or unsaturated, inhibited the nonenveloped virus (poliovirus).

Harper et al. reported the antiviral activity (IC_{50}) of 2-hydroxy-C_{14} and C_{16} acids against HSV (type 1 and 2), HIV-1, vesicular stomatitis virus (VZV), cytomegalovirus (CMV), and poliovirus. Neither acid deactivated the HSV virus (type 1 or 2). Both C_{14} (5.8×10^{-3} mM) and C_{16} (7.3×10^{-3} mM) acids were equally active against poliovirus. The C_{14} (9×10^{-3} mM) acid was more active than C_{16} (5×10^{-2} mM) acid against HIV-1. While the C_{14} acid did not deactivate CMV at the maximum concentration (2×10^{-1} mM) tested, the C_{16} acid (1.8×10^{-1} mM) exhibited minimal activity.

Hilmarsson et al. studied the antiviral activities of even chain FAs (C_8–C_{12}) and unsaturated FAs (C_{14}–C_{18}) against HSV-2.[81] Except for C_8 acid, which exhibited minimal activity, all FAs fully inhibited the growth of HSV-2. In further tests against HSV-2, C_{12} acid exhibited the best antiviral activity. Additionally, $C_{16:1}$ and $C_{18:1}$ acids

completely inhibited the growth of HSV-2. The antiviral activity appeared independent of chain length or unsaturation.

Bryant et al. reported the anti-HIV-1 activity of C_{10} acid and ether- and sulfide-C_{14} acid analogs (at 0.1 mM).[83] They reported that the C_{10} acid only reduced HIV-1 replication by 20%. The other analogs (13-oxa-C_{14}, 11-oxa-C_{14}, 6-oxa-C_{14}, 12-thia-C_{14} acids) were far better inhibitors of HIV-1 (82–90%).

1.10 Antiviral Mechanism of Action for Fatty Acids

The antiviral mechanism of action of FAs is mostly unknown. However, researchers have many, mostly untested, theories about how FAs inhibit enveloped viruses. Mostly, virucidal activity is believed to be due to the disruption of the viral envelope and cell membranes leading to the disintegration of the viral envelope. The mechanism for the disintegration of the viral envelope has not been clearly identified; however, the antiviral activity of FAs is usually dependent on the length of the alkyl chain[78, 79] as well as the degree of unsaturation[78, 79, 82] in the alkyl chain. Both chain length and unsaturation probably affect the degree at which FAs can penetrate the viral envelope.[79] Mostly, FAs are believed to inhibit viruses by: (1) destabilizing the viral envelope, (2) prevention of myristolylation and (3) destabilizing viral proteins.

1.10.1 Destabilization of Viral Envelope

Kohn et al. reported that C_{18} acid, unlike $C_{18:1}$, $C_{18:2}$, $C_{20:4}$ acids, did not disintegrate the viral envelope of Sendai and Sindbis viruses.[82] The authors attributed the inactivity of C_{18} acid to the inability to remove the viral envelope of the viruses.

Thormar et al. reported that FAs caused the leakage and total disintegration of the viral envelope and the viral particles of enveloped viruses.[79] The viral envelope is

comprised of the cell's plasma membrane. The authors seem to agree with a proposed theory, by Cullis and Hope[84], which states that FAs accumulate into the lipid membrane, which leads to destabilization of the membrane.

1.10.2 Prevention of Myristoylation

Harper et al. theorized that 2-hydroxy-C_{14} (2-hydroxymyristic) acid inhibited myristoylation.[85] Myristolyation is required for the assembly of some retroviruses (e.g. HIV).[83] 2-Hyroxy-C_{14} acid is an inhibitor of myristoylation.[85, 86]

1.10.3 Destabilization of Viral Proteins

In their study of FA effectiveness against the influenza virus, Stock and Francis suggested that acids can cause the denaturation of viral proteins as well as form tight complexes with viral proteins.[78] Another hypothesis given by the authors (attributed to Rideal[87]) is that proteins form a monolayer, which compose the surface of the virus. The monolayer is held together by the mutual attraction of the individual molecules. This monolayer can be dispersed if another molecule, e.g. FAs, forms a stronger association with the proteins, which make up the monolayer.[87]

Bryant et al. reported the anti-HIV activity of ether- and sulfide-C_{14} acid analogs.[83] Bryant et al. theorized that the analogs exhibited antiviral activity by selectively incorporating into the viral or cellular proteins, leading to the interruption of interactions between the viral proteins and the cell.

1.11 Antiviral Activity of Polyanionic Amphiphiles

Polyanionic compounds have received a lot of attention because of their antiviral activity against a variety of enveloped viruses.[88-91] Examples include HSV, CMV, ortho- and paramyxoviruses [influenza A, respiratory syncytial virus (RSV)], toga-, flavi-

, arena-, bunya-, and rhabdoviruses. Specifically, De Clercq has reviewed the literature of polyanionic compounds—polysulfates, polysulfonates, polyphosphates, polycarboxylates (Figure 1.17), polyoxometalates, and polyphosphonates—that inhibit HIV replication by blocking binding of the viruses to cell surfaces.[88-91] Of the classes of polycarboxylate antiviral amphiphiles (**7**)[92] have anti-HIV activity by binding to the positively charged sites in the V3 loop of the viral envelope glycoprotein (gp120).[88-91] This binding blocks virus attachment to a primary binding site, CD4, of the cell. Therefore, the viral particles cannot enter the cell and replicate.

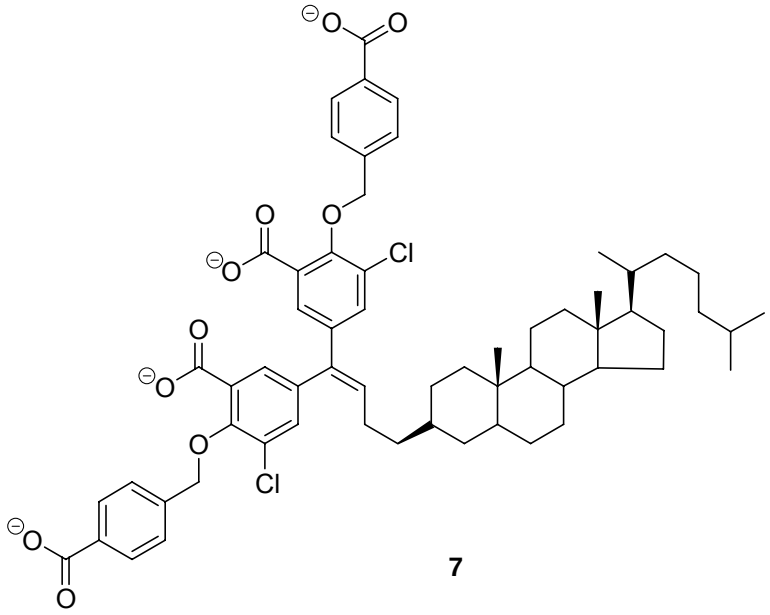

7

Figure 1.17. Example of a Cosalane Analogue

Leydet et al. published a series of articles that dealt with the antiviral activities of a series of polyanionic compounds.[93-99] Some of these polyanionic compounds were polymerized and some were not polymers. These compounds had a variety of hydrophobic moieties. Some of these compounds are not amphiphiles but these compounds did show that polyanionic compounds could be potent inhibitors of

enveloped viruses, including HIV. In this review, we will only focus on the anti-HIV activity of these polyanions.

Leydet et al. studied the anti-HIV activity of a series of anionic amphiphiles; these monomers had multi-charged headgroups derived from malonic acid, L-aspartic acid, L-glutamic acid, cysteinic acid and L-serine.[95] They also synthesized amphiphiles with three and four anionic headgroups to determine whether density and distribution of anionic groups had an e ffect on antiviral activity. None of the monomers inhibited the growth of any of the viruses tested. (This author believes the chain lengths were too short for the monomers to exhibit anti-HIV activity.) The polyanions were tested to determine if they inhibited HIV in the T4-lymphocyte cell line CEM-4 and MT-4 (Table 1.6). The introduction of a second, third, or fourth anionic headgroup to the polymerized amphiphiles did not significantly change anti-HIV-1 activity. Consequently, Leydet et al. concluded that anti-HIV-1 activity was not influenced by the local charge density or charge distribution.

Table 1.6 Anti-HIV Activity of Polyanions in CEM-4 and MT-4 Cells. Table recreated from Reference [95].

Monomers of Polyanions	Antiviral Activity (μg/mL)		
	RT	MTT (CEM-4)	MTT (MT-4)
	IC_{50}	IC_{50}	IC_{50}
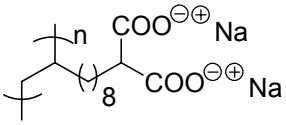	1.7	ND	4.9
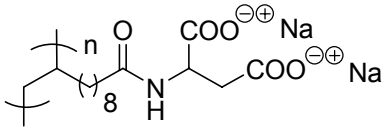	8	ND	0.8
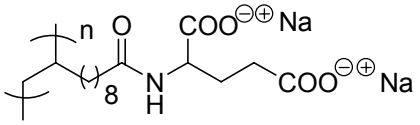	0.2	0.8	ND
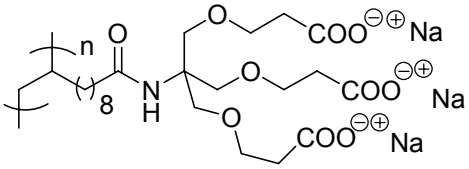	3	3	ND
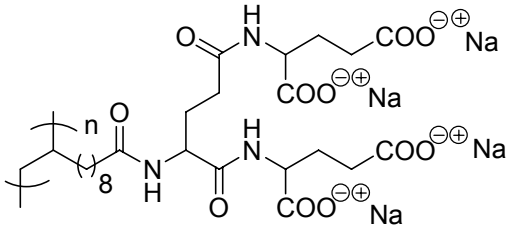	30	24	1.1
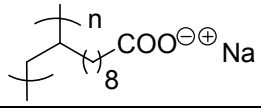	3.5	ND	3.6

IC_{50}= compound concentration required to reduce by 50% HIV-1 induced cytopathicity, based on the Reverse Transcriptase (RT) activity or on the MTT assay. ND= not determined

Leydet et al. studied the antiviral activity of telomerized, polyanionic amphiphiles derived from amino acids (**8**).[93] The authors investigated whether the number of carboxylic acids groups affected anti-HIV activity (Table 1.7). Also, they investigated: (1) whether the amide group's proximity to the carboxylic acid groups affected anti-HIV activity, (2) whether a primary, secondary, or whether tertiary amides would lead to better anti-HIV activity. The data showed that tertiary amides were the better inhibitors,

and ethyl substituents were better than methyl substituents. As a group, the polymers were not very active but the most active compounds had a large number of carboxylate groups (16 and 25), which indicated that the number of carboxylate groups affected anti-HIV activity. Ultimately, the authors concluded that the polyanions must contain more than ten carboxylate groups to be effective. The data also suggested that HIV-2 was more resistant than HIV-1 toward the polyanions.

Table 1.7 Anti-HIV Activity of Telomers in MT-4 Cells. Table recreated from Reference [93].

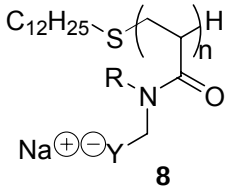

8

Telomer Structure			IC_{50} (μg/mL)	
			Cytopathicity	
Y	**R**	**N**	HIV-1	HIV-2
	H	6	20	47
	H	11.2	55	69
$-CO_2$	H	20	5	1.3
	Me	5.3	28	70
	Et	16	>16	>29
	Et	5.5	13	30
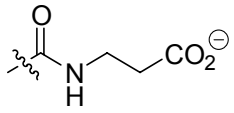	H	2.3	6	27
	H	6.5	3	12
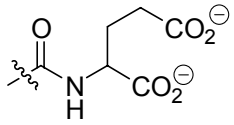	Et	25	0.1	7

IC_{50}= compound concentration required to inhibit HIV-induced cytopathicity by 50% (based on MTT assay).

Leydet et al. tested the antiviral activity of polyanionic compounds that had a carbohydrate core (Table 1.8).[98] Based on the data, for significant anti-HIV activity, a minimum of sixteen carboxylic acid groups were necessary for maximum inhibition

against CEM-4 cells. Compounds with ≤ sixteen carboxylic acid groups were much less active. HIV-2 was also again more resistant than HIV-1.

Table 1.8 Anti-HIV Activity of Carbohydrate Polyanions in MT-4 Cells. Table recreated from Reference [98].

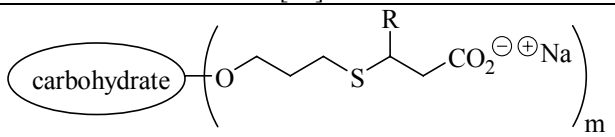

CMPD	Cabohydrate	R	m
15	D-glucose	H	5
16	D-glucose	CO_2Na	5
17	Sucrose	H	8
18	Sucrose	CO_2Na	8
19	Cellobiose	CO_2Na	8
20	Lactose	CO_2Na	8
21	Maltose	CO_2Na	8

Polyanions	Charge Number	IC_{50} (μM) Cytopathicity	
		HIV-1	HIV-2
16	10	85.9	>185
17	8	29	>148
18	16	0.18	2.89
19(α+β)	16	0.04	4.17
19β	16	0.37	4.47
20	16	1.85	>56.4
21	16	0.67	>56.4

IC_{50}= compound concentration required to inhibit HIV-induced cytopathicity by 50%

Leydet et al. measured the antiviral activities of polymerized anionic amphiphiles (Table 1.9).[94] The authors investigated whether linkers (ester or amides) affected the antiviral activity. Initially, some monomers had poor aqueous solubility. These monomers were converted into more water soluble tertiary amides. Monomers lacked antiviral activity. The antiviral activities of polymers, with ester and amide linkers, were not significantly different. In some cases, entries **27** and **28**, an increase in the distance between the amide and carboxylate group led to increased activity. HIV-2 was more resistant to the polyanions than HIV-1.

Table 1.9 Anti-HIV-1 and Anti-HIV-2 Activity of Polymerized Polyanions. Table recreated from Reference [94]

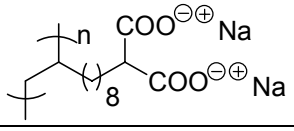

Compound	X^-	IC_{50} (μg/mL)	
		HIV-1	HIV-2
22	$-CO_2^-$	3.6	13.4
23	$-OCO(CH_2)_3CO_2^-$	1.3	ND
24	$-CONHCH_2CO_2^-$	ND	4.6
25	$-CON(CH_3)CH_2CO_2^-$	2.8	12.8
26	$-CONH(CH_2)_2CO_2^-$	0.2	7.2
27	$-CON(CH_3)(CH_2)_2CO_2^-$	0.6	4.2
28	$-CON(CH_3)(CH_2)_5CO_2^-$	0.8	4.5

IC_{50}= compound concentration required to inhibit HIV-induced cytopathicity in MT-4 cells by 50%. ND= Not Done

Leydet et al. studied the antiviral activity of polymerized anionic amphiphiles derived from amino acids and dipeptides (**29**).[96] The monomers were not antiviral. The data in Table 1.10 showed that all compounds were very active against HIV-1 (CEM-4 cells). Anti-HIV activity decreased as the hydrophobicity of the alkyl or aryl side chain increased (Phenylalanine and Leucine analogs). Overall, the diacid analog (Proline-Glutamic acid) was the most active against HIV-1 and HIV-2. The other diacid analog (Phenylalanine -βAlanine) was also very active against both HIV-1 and HIV-2. The Thr analog was the most active compound against HIV-1, while the Serine analog was the second most active compound against HIV-1. HIV-2 was again more resistant against the polyanions than HIV-1.

Table 1.10 Anti-HIV-1 and Anti-HIV-2 Activity of Amino Acid Polyanions in MT-4 Cells. Table recreated from Reference [96].

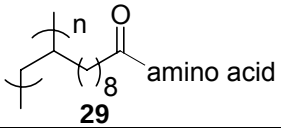

29

Compound or Amino Acid	IC_{50} (μg/mL)	
	HIV-1	HIV-2
Ala	0.37	4.11
Val	0.7	2.00
Ile	0.83	2.43
Leu	2.20	3.86
Phe	2.41	7.52
Thr	0.10	3.41
Ser	0.40	1.31
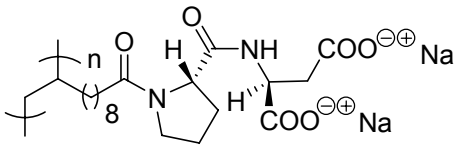 Pro-Glu	0.19	0.51
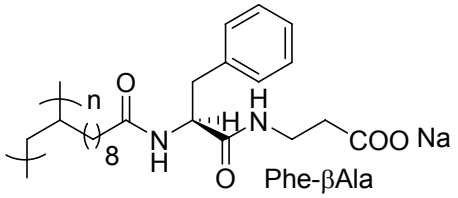 Phe-βAla	0.67	1.40

IC_{50}= compound concentration required to inhibit HIV-induced cytopathicity by 50%

Leydet et al. studied the antiviral activity of polyanions derived from cyclodextrins (Table 1.11).[99] These polyanions were more active than the other polyanions studied by Leydet et al. (Tables 5-8). The polyanions with the most carboxylate groups (36–48) exhibited the best anti-HIV activity.

Table 1.11 Anti-HIV-1 and Anti-HIV-2 Activity of Cyclodextrin-Polyanionic Compounds. Table recreated from Reference [99].

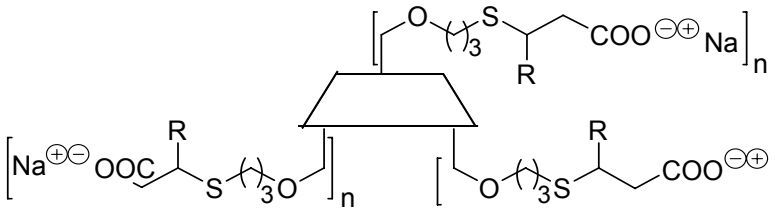

CMPD	n	R
31	6	H
32	7	H
33	8	H
34	6	CO ONa
35	7	CO ONa
36	8	CO ONa

Compound	Charge number	IC_{50} (μM)	
		HIV-1	HIV-2
		MT-4	MT-4
31	18	0.7	>31
32	21	2.9	21.1
33	24	1.4	12.4
34	36	0.3	14.8
35	42	0.3	>21
36	48	0.1	>18

IC_{50}= compound concentration required to inhibit HIV-induced cytopathicity by 50%

Enveloped viruses, such as HSV, Orthomyxovirus, and Rhabdovirus, were tested by Poli et al. to determine the antiviral activity of organic acids (Table 1.12).[100] Their study investigated whether the number of carboxylic acids groups affected enveloped viruses. None of the acids tested had medium or long carbon chains. However, this study exhibited the effect of the number of headgroups on antiviral activity. All of the acids with two or three carboxylic acid groups showed equal or better activity than the single-headed counterparts. The author concluded that virucidal activity was directly proportional to molecular polarity.

Table 1.12 Effect of the Number of Acid Groups on Antiviral Activity. Table recreated from Reference [100]

Name	Structure	Virucidal Activity		
		HSV	Orthomyxovirus	Rhabdovirus
Citric	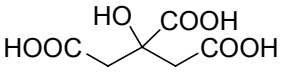	++	++	++
Malic	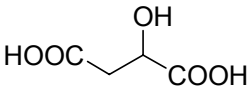	++	++	++
Fumaric	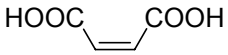	++	++	++
Malonic	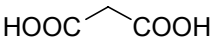	++	++	++
Succinic	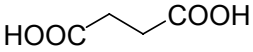	++	++	++
Lactic	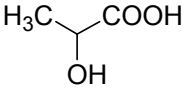	+	++	++
Acetic	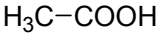	+	++	-
Propionic	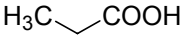	+	+	-
ε-Amino caproic	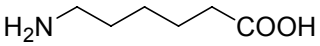	-	-	-
Sorbic	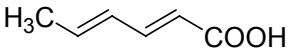	-	-	-
Benzoic	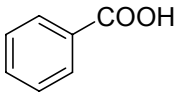	±	±	-

++ = complete inhibition of the virus, + = inactivation of more than 99.9% of the virus,
± = inactivation of 99–99.9% of virus, - = inactive

1.12 Surface Chemistry of Fatty Acids

1.12.1 Introduction of Fatty Acids on Metal Surfaces

Besides the potential biological aspects detailed in the previous chapters, we envision that the **3CAmn** series can form thin films on metal oxide surfaces. The **3CAmn** series would be applied to metal surfaces providing a hydrophobic barrier, which would prevent water droplets from reaching the metal surface, thereby, eliminating one source of corrosion. Water will wet a metal surface completely if the metal surface is

not protected by a film or monolayer.[101] FAs have been known for a long time[101] to bond to the surface of metals, thereby, creating a hydrophobic surface.

The dendritic headgroup should enhance the adsorption of the **3CAmn** series, relative to FAs.[102, 103] The headgroup of the **3CAmn** series has three carboxylic acid groups that could potentially bind to metal surfaces, while FAs only have one carboxylic acid group. Additionally, when the carboxylic acid groups of FAs detach from the metal surface, that molecule is desorbed and removed from the metal surface (Figure 1.18A). Hypothetically, if all three headgroups of the **3CAmn** series bind to the metal surface, the detachment of one carboxylate group will not lead to the removal of the molecule from the metal surface because the **3CAmn** series would still have two additional carboxylate groups anchored to the surface (Figure 1.18B). Additionally, as the molecule would still be anchored to the surface, the detached carboxylate group could potentially reattach to the surface because the detached group would still be in close proximity to the surface (Figure 1.18B).

Dendrons and dendrimers are used to attach molecules to surfaces. The strategy employs the dendron as a tripod or multi-pod,[103] which is attached to a large, bulky molecule. Rigid tripodal ligands have been used to attach dyes to semiconductor nanoparticles.[102] Newkome-type dendrons[104-106] (first, second, and third generation) that terminate with carboxylates have been used to attach a ferrocene in close proximity to a gold electrode that is coated with ammonio-terminated thiols.[107]

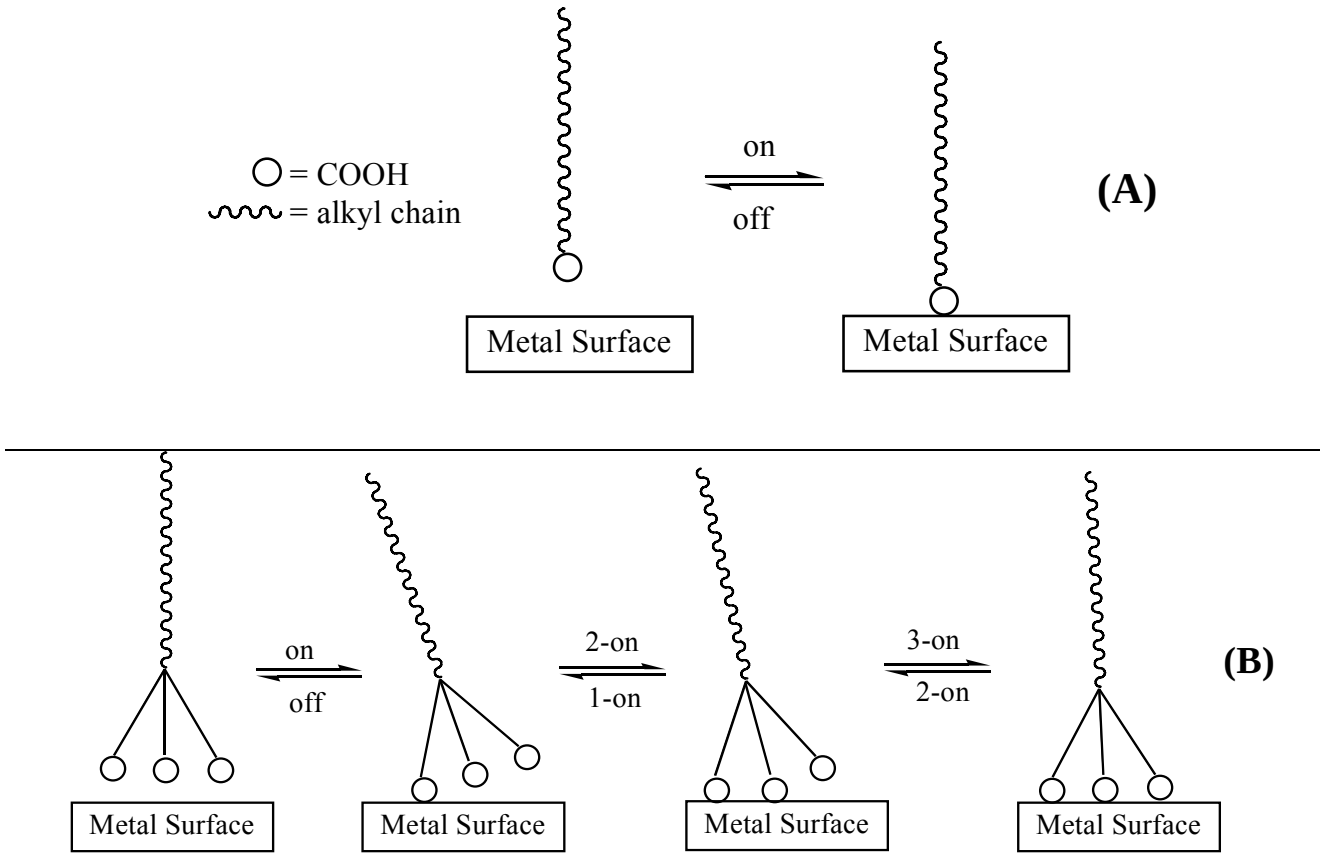

Figure 1.18 Comparison of Fatty Acid (A) and Possible **3CAmn** (B) Adsorption on a Metal Surface

1.12.2 Surface Chemistry, Literature Review of Fatty Acids on Metal Surfaces

Mostly, this review will discuss contact angles as a measure of the surface wettability of thin films formed by FAs. The change in surface wettability of a metal surface, before and after FA adsorption, demonstrates the hydrophobizing ability of the FA. Contact angles cannot provide structural information about a thin film; however, contact angles can provide an indication of the quality of the film.[108] A film that gives a small contact angle is assumed to be disordered or has a low coverage of molecules on the metal surface. Large contact angles indicate the formation of a hydrophobic metal–substrate surface. A film, with a large contact angle, could be considered as a self-

assembled monolayer (SAM). A SAM that gives a very high contact angle (>100°) is assumed to be highly ordered and has a highly covered surface.

In a growing trend, organic molecules are being used to protect metals from oxidation (rusting) by coating the metals with a hydrophobic film (barrier). Researchers have used long-chain alkyl thiols, carboxylic acids, and phosphonic acids to attach to various metal surfaces.[108] These films can be either Langmuir–Blodgett films or SAMs. For several decades, initially reported by Bigelow et al. in 1946, carboxylic acids have been known to provide hydrophobic surfaces on metals such as Pt.[101] Carboxylates (hard bases) adsorb on oxidized metal surfaces and form stable hard acid–hard base interactions with hard acid, multivalent cations such as Al^{3+} and Fe^{3+}.[109]

During the formation of SAMs by a carboxylic acid, the polar carboxylate group is bound to the metal surface and then additional acid molecules organize on the surface due to intermolecular interactions. The organization and alignment of the hydrophobic alkyl chains is due to van der Waals interactions.[110] Both film thickness and organization of alkyl chains increase with the chain length.[111]

For a film to be considered a SAM, the surface must be comprised of a single layer of molecules and the hydrophobic ends (tails) of the molecules must be highly organized (Figure 1.19A). The molecules that make up the film must fully cover the metal surface (Figure 1.19A) and have few defects, such as gaps (Figure 1.19B). The alkyl chains of these molecules must not lie across the surface (Figure 1.19C). A "good" SAM should have few gaps and be well ordered; the alkyl chains should be well organized (Figure 1.19A). Poor coverage, large number of gaps, and disorganization of

the metal surface will lead to unwanted agents (e.g., water) getting to the surface and causing corrosion.

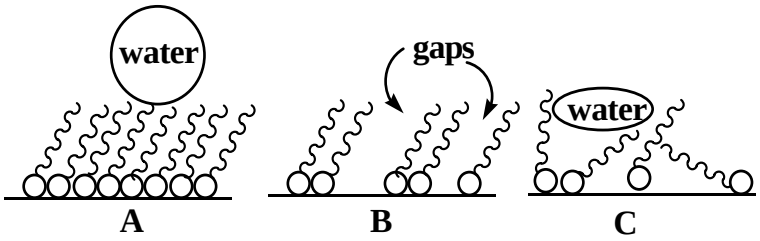

Figure 1.19 Examples of Organic Films on Metal Surfaces. (A) SAM); (B) SAM with gaps; (C) Disorganized FA–Metal surface

The density and orientation of the alkyl chains contribute to the quality of the SAM. Pertays et al. reported that a disordered SAM will have methylene groups that are exposed.[112] This exposure will cause a reduction in the water contact angle. The alkyl chains must be closely packed and be in the correct orientation to create a sufficiently high density of methyl groups to create a high quality SAM.[101] If a SAM is tightly packed and well organized, the surface is predominantly composed of methyl groups. A methyl-terminated surface has lower surface wettability. Conversely, if a SAM is loosely packed and disorganized, the surface is predominantly, or substantially, composed of methylene groups. A SAM with exposed methylenes would have relatively higher surface wettability and a lower contact angle.[113]

Alkyl chain length strongly influences both the formation and quality of SAMs. Both the density and rigidity of SAMs increase with chain length. Each methylene group of the alkyl chain has a highly localized force associated with it.[101] These forces, which attract methylenes to each other, lead to the packing of the alkyl chains. Therefore, as the chain length increases, so do the total attractive forces. As the chain length and attractive forces increase, the alkyl chains begin to pack "straight up".[111]

Chen et al. reported that film thicknesses of Al SAMs, formed by FAs on Al, increased with chain length from C_{14} acid (19.5 ± 2 Å) to C_{22} acid (29.6 ± 2 Å).[110] The authors reported that H_2O contact angles of (97° ± 2) were obtained for FAs.[110] Tao has reported that short chain carboxylic acids form disordered and liquid-like surface on Cu and Al.[111]

Carboxylates can bind to metal surfaces in two different orientations. They can bind to the metal surface in a bidentate orientation, approximately equal attachment of the two oxygen atoms via a delocalized double bond (Figure 1.19).[114] Alternatively, they can bind through a monodentate orientation, where one oxygen atom attaches to the surface (Figure 1.20). The binding orientation of carboxylates depends on the type of metal. Carboxylates bind to Ag in a bidentate orientation[111], but bind to Al and Cu oxides in a monodentate orientation.[111]

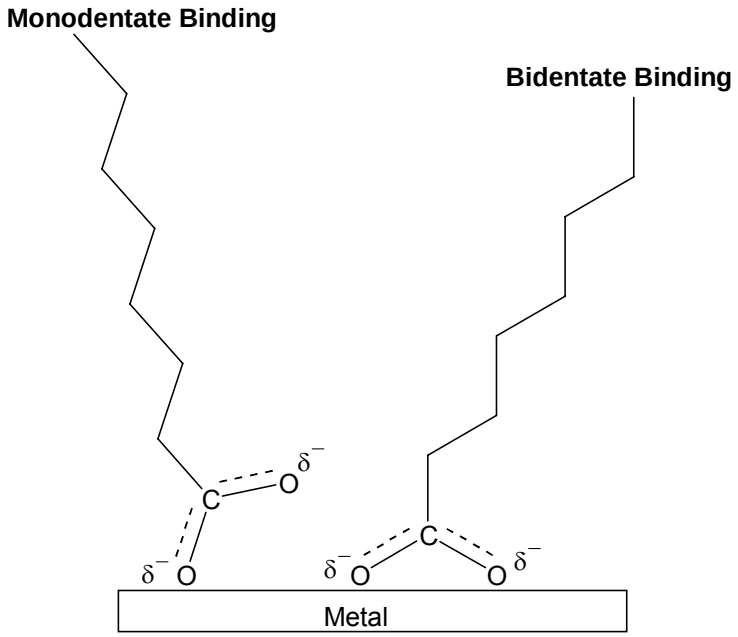

Figure 1.20 Examples of Monodentate and Bidentate Binding on a Metal Surface from Reference [114]

In addition to binding orientation, carboxylic acids adsorb on metal surfaces differently. Carboxylic acids bind to oxidized metal surfaces through chemisorption, while carboxylic acids bind to oxide-free metal surfaces through physisorption.[115] In chemisorption, the acid bonds as a carboxylate salt through dissociation of the acidic hydrogen or transferring a proton to a lattice oxygen atom.[115] In contrast, physisorption does not involve a carboxylate salt.[115] Binding involves metal–acid interactions through the hydroxyl or carbonyl group.[115] The acid group can also interact with neighboring molecules. Carboxylic acids chemisorb on Ag, Cu, and Al metal surfaces.[116]

Presently, there is a need for additional hydrophobizing agents on metal–oxide surfaces, although SAMs of alkylthiolates on Au and Ag surfaces are stable and useful in scientific applications. Alkanethiols do not strongly adsorb on many metal–oxide surfaces[117] because those metals are covered by a hydrophobic native oxide layer.[118] The interaction between carboxylic acids and metal oxides is relatively weak compared to thiol–Au interaction because carboxylic acids form ionic bonds with the metal surface, while alkylthiols form covalent bonds with the metal surface.[119] Although the thiol–metal binding is stronger than the metal binding, we theorize that three carboxylate–metal bonds will equal one thiol–metal bond. Alternatives to alkanethiols are needed due to the toxicity and foul odor of alkanethiols, as well as their low affinity to engineering metals such as steel, stainless steel, and Al.[113]

1.12.3 Carboxylic Acid SAMs on Metal Surfaces

As stated previously, carboxylic acids attach in different orientations (Figure 19, monodentate and bidentate binding) depending on the metal surface. The quality of the

different acid–metal surfaces also varies. For example, carboxylic acids form more stable SAMs on Ag than those on Cu, Au, or Al.[111] The stability seems to parallel the basicity order as $AgO>Cu_2O>Al_2O_3$.[111] There is less strain or twisting of the molecular chains on a FA–Ag surface than there is on a FA–Cu or FA–Al surfaces.[111] Due to carboxylic acids' low adsorption on some metals (e.g., Au); researchers have modified the surface to enhance acid–metal adsorption. The following review will cover many studies of carboxylate-bound metal surfaces.

Paik et al. studied the adsorption of carboxylates on Au via electrochemical experiments.[120] Carboxylic acids do not adsorb on Au as well as they do on other metals such as Ag. Most carboxylates only adsorb on Au when high positive potentials are applied to the metal, which suggests an anodic reaction. The authors observed that carboxylic acids required a relatively higher anodic potential, compared to thiols, to bind to Au. They reported less binding if the potential was not high enough, which demonstrated that carboxylates lack the strong interactions that thiols have with Au. The authors suggested that carboxylates adsorb readily on Ag and Cu because these metals are readily oxidized at lower potentials. Surface oxidation of the substrate metal must take place for the adsorption of thiols and carboxylic acids. However, the reaction will not take place with Au without manipulation of the potential. The authors speculated that the carboxylate–metal bond was partially ionic, while the sulfur–metal bond was mostly covalent (Eqn 1.2).[120]

$$RCOOH + M \rightarrow RCOOM + H^+ + e^- \text{ (M= Au, Ag, Cu)} \qquad \text{Eqn 1.2}$$

To counteract the low affinity of carboxylic acids for Au, some researchers have modified the Au surface, enhancing the acid–Au affinity. Lin et al. studied SAMs of

carboxylic acids on Ag and Cu modified Au surfaces.[121] The surfaces initially did not appear to benefit from the adlayer. Initially, the bulk Ag– and Cu–FA SAMs gave better contact angles. However, this changed as the bulk Cu–acid and Ag–acid showed degradation of contact angles over time, while the modified surfaces' contact angles were preserved (Table 1.13).[121]

Table 1.13 Stability of C_{19} Acid on Metal Surfaces. Table recreated from Reference [121].

Surfaces	Average Contact Angles (°)	
	Fresh Surface	24 h surface
Ag(bulk)	115.6	105.5
Ag/Au	114.6	115.6
Cu(bulk)	119	115.8
Cu/Au	115.2	114.2

Lin et al. studied the adsorption of FAs on Au-modified surfaces.[117] Due to the softness of Au, only soft bases such as alkanethiols form SAMs. Lin et al. modified Au surfaces by adding adlayers of Ag and Cu, which raised the hardness of the surface and promoted the adsorption of carboxylates.[117] An adlayer is a material added to a surface, in this case metal surface, that enhances the adsorption of other materials (e.g., fatty acids) to the metal surface. If the adlayer of Ag and Cu were not utilized, FAs did not chemisorp on bare Au surfaces. For Au/Ag surfaces, contact angles increased with the chain length of the carboxylic acid. Initially, contact angles started at 104–105° for C_7 and C_8 acids, increased to 114° for C_{13} acid, then leveled off at 117° for acids $\geq C_{19}$. The Cu/Au surface gave slightly better contact angles. The trend was the same for the Cu/Au SAMs, except the contact angles leveled off for acids $\geq C_{20}$ at a contact angle of 121°. Both Cu and Ag modified surfaces exhibited bidentate binding.

Smith and Porter reported the adsorption of carboxylic acids (C_2–C_{11}) on Ag via the gas phase.[122] The experiment was performed in the gas phase because of corrosion

of metal surfaces caused by ethanolic solution of carboxylic acids. The use of a nonpolar solvent can impede the corrosion process caused by longer carboxylic acids and facilitate the formation of densely packed alkyl chains surfaces. Because the use of a nonpolar solvent would not remove corrosion concerns for short-chain acids, the gas-phase was used. They reported that all acids chemisorbed on the Ag surface through bidendate binding. The authors reported that all acids, C_3–C_{11}, formed monomolecular films of the corresponding carboxylate salts. The authors noted that gas-phase monolayers had a larger coverage area than the corresponding solution-phase monolayers. Greater coverage leads to increased packing density of alkyl chains. Water contact angles increased with chain length starting at 80° for C_3 acid, then leveled off at 117° for C_{10} and C_{11}.

Tao did an exhaustive study on the differences of SAMs on the native oxide layer of Ag, Cu, and Al with short- and long-chain carboxylic acids.[111] Tao observed that carboxylic acids were bound to Ag in a bidentate orientation, while bound to Cu and Al in a monodentate orientation. All acids were bound to the metal surface as carboxylates. For the Ag surface, the alkyl chains, for all chain lengths, were extended and had zigzag (all anti) conformations. Conversely, for Cu and Al surfaces, the short chain acids were disordered and liquid-like. As the chain length increased and, consequently, the van der Waals interactions increased, the packing of the alkyl chains became denser and chains adopted a near vertical alignment.[111]

On Ag surfaces, SAMs were formed for chain lengths >C_5.[111] For chain lengths <C_5, no films were observed; however, film thicknesses increased with chain length for acids >C_5. Water contact angles increased with chain length but leveled off, at

113–115°, for chain lengths >C_{12}. Odd–even effects—odd chains gave smaller contact angles than even chain homologues—were observed but were more pronounced for shorter chain lengths (C_2–C_6).

Unlike Ag surfaces, for Cu surfaces, only longer chain carboxylic acid > C_{10} formed monolayers.[111] Additionally, only C_{14}–C_{24} carboxylic acids formed ordered monolayers. Film thickness was not linear for shorter chains, possibly, because of low packing density. For chain lengths ≥C_{14}, film thickness increased with chain length. The contact angles for the long-chain acids leveled off at 116 ± 1° for ≥C_{14}.

On Al surfaces, film thickness and contact angles increased with chain length for acids > C_5.[111] Contact angles increased with chain length and leveled off at 113 ± 1° for acids that were ≥C_{14}. Similar to the Cu surfaces, the short-chain carboxylic acids led to films that were disordered and liquid-like.

Tao explained the odd–even effect by discussing the orientation of the terminal methyl group (Figure 1.21).[111] For even numbered carboxylic acids, the terminal methyl was perpendicular to the surface. For odd numbered acids, the terminal methyl group was oriented at a ~30° angle relatively parallel to the surface, which exposes the adjacent methylene group. This exposure led to smaller contact angles. Conversely, for even numbered chains, the methyl groups were perpendicular to the surface, which led to the optimal methyl terminated chain. This led to high contact angles. For acid bound Cu and Al surfaces, odd–even effects were not observed. Because the carboxylic acids were bound to the Cu and Al surfaces through a monodentate orientation (thus, the terminal methyl groups had similar orientations) both odd and even chains were unaffected.[111]

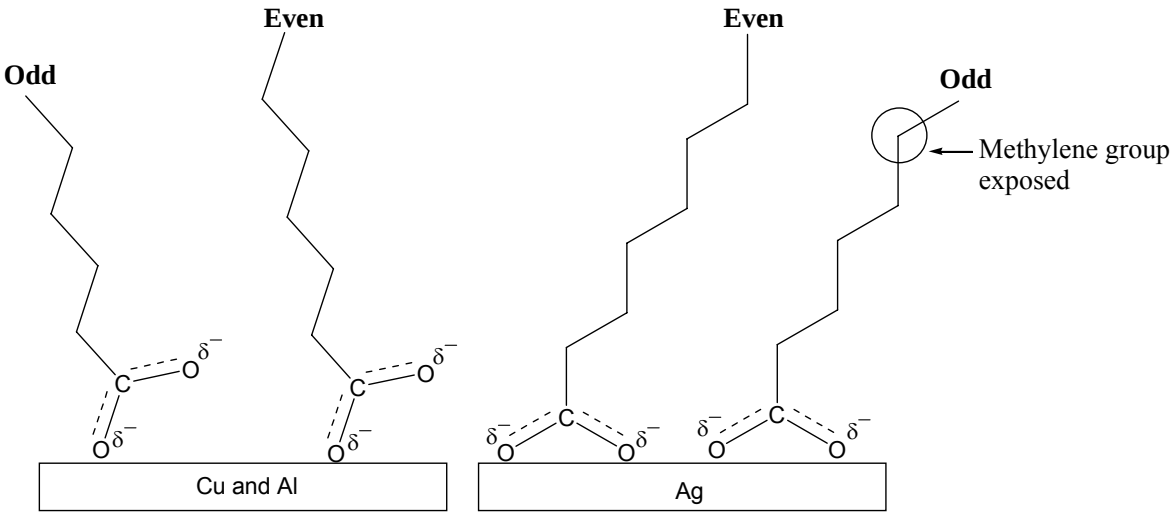

Figure 1.21 Odd-Even Effects Illustrated for Monodentate and Bidentate Orientations from Reference [111]

Tao also compared the relative order and stability of the SAMs formed on the different surfaces.[111] The acid–Ag surface was thought to be more stable because it remained intact following a solvent rinse; however, the acid–Al surface was disrupted. He explained that the acid–Ag surface was more ordered than the acid–Cu and acid–Al surfaces. The higher order of the acid–Ag surface was most likely due to the twisting or strain of the alkyl chains on the acid–Al surface.

Touwslager and Sonday studied the effects of chain length on the order of carboxylic acid SAMs on Al oxide.[123] The authors reported the relative number of gauche torsion angles relative to the preferred anti torsion angles decreased with increasing chain length. Additionally, they proposed that the packing density was larger for long chains relative to short chains, with a phase transition occurring between C_{10} and C_{14}. The cause of this phase transition was the attractive energy between alkyl chains, which resulted in densely packed surfaces. The authors estimated that the packing density for smaller alkyl chains was 70% less than the packing density for longer alkyl chains.

Allara and Nuzzo studied the formation of carboxylic acid (C_6–C_{24}) SAMs on Al oxide.[124] Multilayers were observed for acids with chain lengths $<C_{12}$. Acids that were $\geq C_{12}$ led to the formation of SAMs. Water contact angles increased with chain length; they started at 78° for C_6, and then leveled off at 115° for acids $\geq C_{18}$. Acids $>C_{11}$ were required for well ordered, dense SAMs.

Thompson and Pemberton compared the adsorption of C_{18} acid on Al oxide and Ag surfaces.[114] The authors suggested that acids bind to the Lewis acid sites of both metals (Figure 1.22).[114] The C_{18} acid was bound to an Ag oxide-free surface in a monodentate fashion, but bound to Ag oxide in a bidentate orientation.

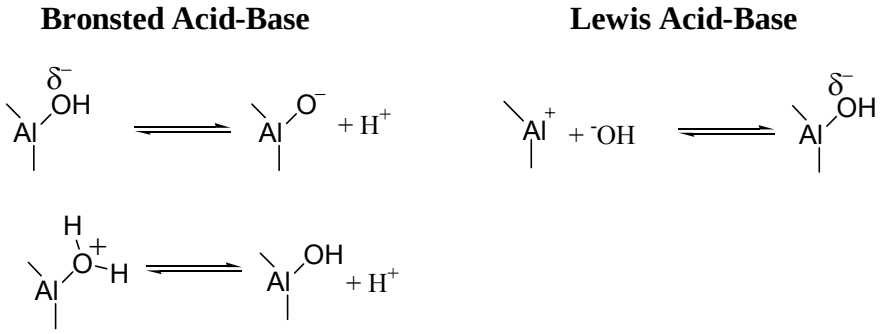

Figure 1.22 Lewis Acid-Base Sites on Al from Reference [114]

Arnoff et al. enhanced the weak binding of carboxylic acids to the native oxide surface of Al by treating the oxide surface with Zr alkoxide (Scheme 1.1).[118] Further treatment with C_8 acid led to strong acid absorption, due to strong Zr–C_8 acid binding. The carboxylate purportedly bound to the surface in a bidentate fashion but the alkyl chains were disordered on the metal surface. Although Zr enhanced the binding of acids to Al, 80% of the films were removed after being in water for 15 h.

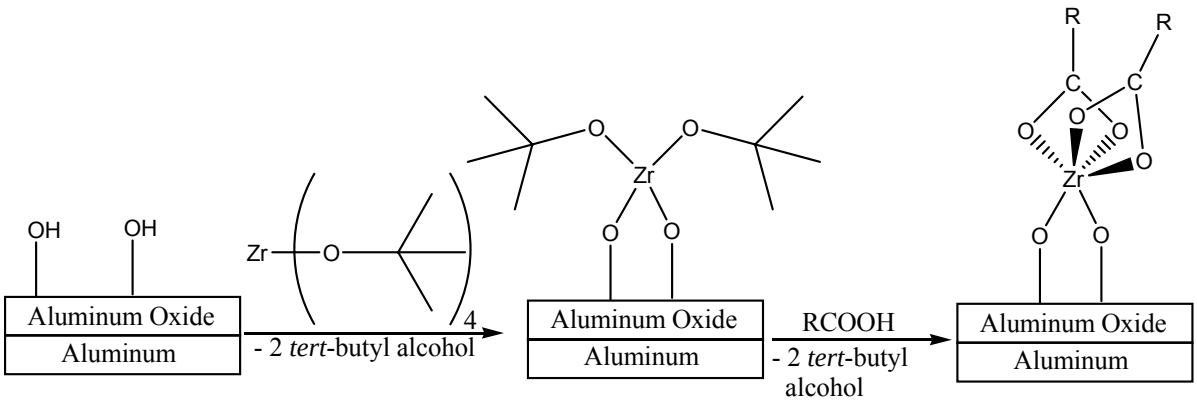

Scheme 1.1 Formation of Zirconium Modified Al SAMs

Folkers et al. measured the contact angles of C_{18} SAMs prepared on Cu, Ag, Ti, Al, Zr, and Fe surfaces with both isooctane and ethanol.[108] In all cases, the contact angles for SAMs prepared from the nonpolar solvent (isooctane) gave better contact angles than those prepared from ethanol. The authors theorized that SAMs prepared from isooctane were stable because solvent molecules would not compete with the carboxylates for the polar metal surface sites. The polar ethanol molecules could compete for those sites.

Pertays et al. reported that the solvents used to prepare the SAMs contribute to the quality of surfaces obtained on Al.[112] Like Folkers et al., the authors noticed a strong link between the solvent used to prepare the SAMs and contact angles. The C_{18} SAMs prepared from toluene and hexadecane gave water contact angles of 119° and 118°, respectively, while SAMs prepared in ethanol gave contact angles of 90°. Like Folkers, they attributed these observations to ethanol molecules competing with C_{18} to adsorb on the hydroxyl groups on the surface of Al.

Wang et al. studied the superhydrophobicity (contact angle >150°) produced by carboxylic acids, C_3–C_{19}, on Cu films.[125] They measured the contact angles of

carboxylic acids on rough and smooth Cu surfaces. A chain length effect was observed for both surfaces. For the rough surfaces, the C_3 acid produced a contact angle of 0°; however, contact angles increased with chain length until leveling off at 160° for acids $>C_{11}$. For smooth surfaces, a chain length effect was also observed, although the contact angles were smaller. Contact angles started at 68.3° for the C_3 acid then leveled off at 113° for acids $>C_{11}$. The authors explained that smaller chain lengths led to a disorganized surface, which led to the native Cu surface being exposed. Consequently, these surfaces were hydrophilic, leading to low contact angles. As the chain length of the carboxylic acid increased, the surface became more ordered and denser. The native Cu surface was no longer exposed; no exposure led to a hydrophobic surface and higher contact angles. The differences between the rough and smooth films were attributed to the relatively more hydrophobic, rough film surface, which is a model for the rough surface found on lotus leaves.

Aramaki and Shimura studied the ability of carboxylic acids to prevent the breakdown of Fe films.[109] Carboxylic acids should bind to the Fe oxide surface via a substitution reaction (Eqn 1.3). The formation of densely packed long-chain SAMs would prevent Cl^- from reaching and accumulating on the metal surface; Cl^- accumulation would lead to film breakdown. Protection initially increased with chain length (C_{12}–C_{14}), then decreased with chain length (C_{16}–C_{18}). The authors suggested that the decreased protection of the longer acids was due to low solubility of the longer acids. Water contact angles increased with chain length reaching a maximum of 112° for C_{16} before decreasing to 110° for C_{18}. Due to the relatively lower contact angles compared to acid–Cu surfaces, the authors suggested a disordered acid–Fe SAM.

$(FeO)X + C_{n-1}H_{2n-1}CO_2^- \rightarrow (FeO)O_2CC_{n-1}H_{2n-1} + OH^-$ (X= OH or H_2O) Eqn 1.3

Timmons and Zisman studied the adsorption of C_1–C_{26} carboxylic acids on Pt and NiO substrates.[126] On the Pt surface, the packing and orientation of absorbed molecules did not change for acids that were $\geq C_{14}$. Similarly, for the NiO substrates, the packing and orientation did not change for acids $\geq C_{10}$. The authors concluded that when the alkyl chains get to a certain length, the interactions between the alkyl chains becomes sufficient for close, organized packing. Based on methylene iodide contact angles, the NiO films appeared more organized and densely packed than the Pt films. They theorized that FAs were chemisorbed on NiO surfaces, but physisorbed on the Pt surfaces.

Pawsey et al. reported that carboxylic acids formed SAMs on ZrO_2 surfaces.[119] The strong binding was due to strong carboxylate–Zr linkage. The acids were bound to the surface in both monodentate and bidentate orientations; however, the bidentate state dominated. A chain length effect was observed, only carboxylic acids with chain lengths $> C_{17}$ formed conformationally ordered monolayers.

Raman and Gawalt studied surface wettability of carboxylic acid SAMs on the native oxide layer of stainless steel.[113] Carboxylic acids were bound to the surface in a bidentate orientation. The SAMs were very stable and remained following ethanol rinsing and sonication. The C_{18} SAM had a contact angle of 104°. Atomic force microscopy (AFM) confirmed that the C_{18} SAM had a complete and uniform monolayer.

Shustak et al. studied the SAMs of C_{10}–C_{18} FAs on 316L stainless steel.[127] They reported that C_{10} acid formed a disordered monolayer on stainless steel, while C_{14}–C_{18} acids formed a highly-ordered, closed-packed monolayer. The carboxylates were

bound to the metal oxide surface mainly though ionic interactions. Contact angles increased with chain length. The bare stainless steel surface gave a water contact angle of 59°. The C_{10}, C_{14}, and C_{16} acid monolayers gave water contact angles of 87°, 97°, and 109°, respectively. The contact angle for the C_{18} acid monolayer was not reported. The authors speculated that the carboxylate groups were mostly bound to the surface in a bidentate orientation; however, small fractions of the headgroups were bound as a carboxylic acid species. Both organization and binding to the surface through a bidentate orientation increased with increasing alkyl chain length.

Liu et al. reported the formation of even chain FA (C_{12}, C_{16}, C_{18}) SAMs on Mg alloy surfaces.[128] SAMs, on Mg, can help improve the poor corrosion resistance of Mg. Contact angles increased with chain length, from C_{12} (115°) to C_{18} (131°). Film thickness also increased with chain length, from C_{12} (12.8 Å) to C_{18} (21.7 Å). The authors attributed the increase in contact angles and film thickness to the increased hydrophobicity of the longer alkyl chains. The authors reported monodentate binding to the metal surface. The barrier properties (anticorrosion) of the prepared SAMs retarded the transfer of ionic species to the metal surface. The anticorrosion properties of the SAMs directly correlated with increasing chain length.

Karsi et al. compared the SAMs formed from alkanethiols and carboxylic acids on tin-doped indium oxide (ITO) surfaces.[129] The alkanethiols formed more organized SAMs due to the relatively higher reversible binding of acids to the ITO surface. The C_{20} acid gave a contact angle of 111°, while C_{16} acid gave a contact angle of 109°. The acid–ITO films were relatively weak; the FA SAMs could be removed by ultrasound rinsing while the thiol SAMs remained intact.

Zharnikov et al. studied C_{18}– and C_{20}– ITO SAMs.[130] They reported that both water contact angles and film thickness increased with chain length. Both C_{18} and C_{20} acids gave a contact angle of 118°. The C_{18} and C_{20} acid films had thicknesses of 20 and 22 Å, respectively. Both acids formed stable and well ordered SAMs on the ITO surface.

1.12.4 Conclusions

In summary, FAs can bind to metal surfaces and hydrophobize the metal surface. FAs can bind to a wide assortment of surfaces. However, FAs are clearly bound to some surfaces (Ag, Cu, Al, ITO, Mg, stainless steel, Zr, Ni, Fe) more strongly than other surfaces (Au and Pt). Long chain lengths (>C_{12}–C_{14}) are needed to form dense, well-ordered SAMs, which give good contact angles (>100°). To overcome the weak attachment of FAs to some surfaces, researchers are beginning to enhance the attachment of carboxylates to surfaces that they typically weakly bind to, by adding an adlayer. The addition of adlayers has enhanced the attachment of FAs to Au and Cu.

1.12.5 Multi-headed Amphiphiles on Metal Surfaces

An important assumption is that the three carboxylate groups of the **3CAmn** series will bind to the metal surface. Even if the three carboxylate groups do not bind to the surface, we at least anticipate two of the three carboxylate groups will bind to the surface. Unfortunately, in the literature, multi-headed compounds have not always shown multi-carboxylate metal binding.

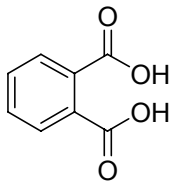

10

Figure 1.23. Structure of Phthalic Acid

Joo et al. reported the binding of a dicarboxylate compound, phthalic acid (**10)**, to a Ag surface (Figure 1.23).[131] They observed that phthalic acid was easily displaced by mono-carboxylic acids. They attributed this easy displacement to the steric hindrance and electrostatic repulsion of the two carboxylate groups of phthalic acid. Phthalic acid was bound to Ag as a dicarboxylate; however, both carboxylate groups were bound to Ag in a monodentate state.

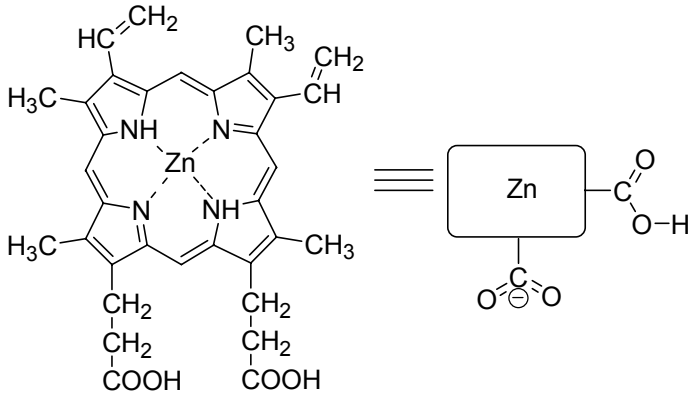

Figure 1.24 Structure of Protoporphyrin IX Zinc

Noting the absence of stable carboxylic acids SAMs on Au due to the weak interactions between carboxylic acids and Au, Zhang and Imae reported the formation of Au– protoporphyrin IX zinc SAMs (Figure 1.24).[132] The authors reported that only one carboxylate group was bound to the Au surface in a bidentate state. The other COOH group was not bound to the surface; however, it was hydrogen bonded to another unbound COOH group of an adjacent porphyrin molecule (Figure 1.25). Although one COOH group was unbound to the surface, the authors argued that the hydrogen bonding of the second COOH group enhanced binding to the Au surface.

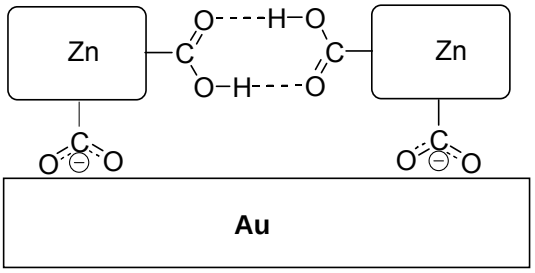

Figure 1.25 Protoporphyrin IX Zinc on Au Surfaces

Allara et al. studied the formation of monolayers on α,ω alkanedioic acids on Ag.[133] The authors noted that 1,32-dotricontanedioic acid formed a monolayer on Ag oxide surface through a looped-folded structure. The folded portion of the molecule consisted of six methylene groups. A water contact angle of 103° was obtained. The authors reported that only one carboxylate group was bound to the surface. One carboxylate group was chemisorbed onto the surface, while the other COOH group was physisorbed to the metal surface.

1.12.6 Conclusions

In summary, diacids do bind to metal surfaces. However, the results were mixed. Mostly, the diacids were chemisorbed to the metal through one carboxylate group. The other carboxylate group was physisorbed to the metal surface or involved in intermolecular interactions. In the case of phthalic acid, both groups were weakly bound to the metal surface because of steric hindrance or ionic repulsion.

1.13 Antimicrobial Activity of Mono, Di, and Tertiary Amides

1.13.1 Overview of Long-Chain Fatty Amides

In this review, the antimicrobial activity of long-chain, nonionic amphiphiles will be investigated. Unlike FAs, there have been few systematic studies of unsubstituted, long-chain, saturated amides. Most studies have involved long-chain amides with

substituents on the alkyl chain. Unfortunately, most literature articles report the antimicrobial activity via zone of inhibition studies; consequently, MIC values are not widely available in the open literature. Unlike the review of FAs, this review will include microorganisms that our amphiphiles will not be tested against. This change is due to fatty amides not being as widely tested as FAs.

Although nonionic amphiphiles are generally not as active as anionic and cationic amphiphiles, nonionic amphiphiles also exhibit antimicrobial activity. Fatty alcohols, amines, amides, and ester have activity against a wide variety of microorganisms. Nonionic amphiphiles, like FAs, tend to be more active against Gram-positive bacteria than they do against Gram-negative bacteria.[42, 134] Long-chain amides exhibit a similar spectrum of antimicrobial activity to that of FAs.[42, 134] However, nonionic amphiphiles offer narrower antimicrobial activities than that of anionic and cationic amphiphiles.[134] Although long-chain amides are generally not as active as FAs, they have displayed a wide spectrum of antimicrobial activity against bacteria, yeasts, and fungi.[42, 134-139]

Two important factors—chain length and *N*-alkylation—affect the antimicrobial activity of long-chain amides.[134, 139, 140] Similar to FAs, fatty amides also exhibit a cutoff effect.[134, 138, 140] For substituted amides, generally, the most active chain length varies with structure. Substituents, in some cases, improve the antimicrobial activity. There are conflicting reports concerning the effect of unsaturation in the alkyl chain. Kabara et al.[134] reported that unsaturation did not noticeably affect antimicrobial activity; however, Ōmura et al.[139] reported that unsaturation improved

antimicrobial activity. (Whether unsaturation increases antimicrobial activity is probably due to the structure of the amide and cell of the particular organism.)

1.13.2 Review of the Antimicrobial Activity of Fatty Amides

The alkylation of the amide nitrogen has a pronounced effect on the antimicrobial activity of long-chain amides.[134, 139] *N*-Alkylated amides display better antimicrobial activity than non *N*-alkylated amides.[134, 139] Generally, monoalkylated amides are more active than nonalkylated amides[139], while dialkylated amides are more active than monoalkylated amides.[139] Generally, the dimethylamide group is the best amide headgroup.[134, 139]

Ōmura et al. reported the systematic study of structure-activity relationships of dodecanoyl, amide derivates of the antibiotic cerulenin (**11**).[139] Cerulenin is an antibiotic that displays antimicrobial activity against bacteria and yeast. Cerulenin is thought to inhibit these microbes by inhibiting cellular lipid biosynthesis.[141] Initial changes to the headgroup portion of the molecule, C1–C4, led to the compete loss of activity (dihydro cerulenin and hexahydro cerulenin) or decreased activity (tetrahydro cerulenin), Table 1.14.

Table 1.14 Antimicrobial Activity of Cerulenin Derivatives. Table recreated from Reference **[139]**

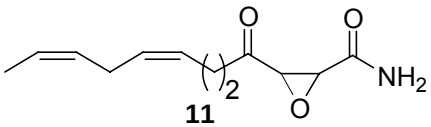

11

Compound	MIC (μg/mL) Microorganisms						
	B. s.	S. a.	M.	E. c.	P. a.	C.a.	P. o.
Cerulenin	1.56	100	1.56	12.5	>100	1.56	3.12
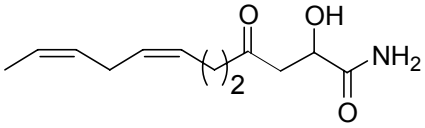 **Dihydro cerulenin**	>100	>100	>100	>100	>100	>100	>100
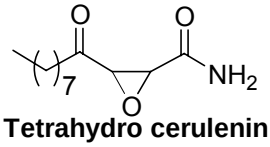 **Tetrahydro cerulenin**	>100	>100	>100	>100	>100	50	6.25
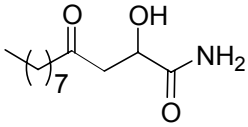 **Hexahydro cerulenin**	>100	>100	>100	>100	>100	>100	>100

B. s., *Bacillus subtilis*; S. a., *S. aureus*; M., *M. smegmatis*; E. c., *E. coli*; P. a., *Pseudomonas aeruginosa*; C. a., *C. albicans*; P. o., *Piricularia oryzae*

The authors also examined the effect of *N*-alkylation on antimicrobial activity (Table 1.15).[139] Relative to C_{12} acid, the mono-*N*-alkylated and non-*N*-alkylated unsubstituted C_{12} amide derivatives displayed similar inactivity against the microorganisms tested. However, the *N*,*N*-dimethylamide derivatives displayed better activity than the FA, and other amides (non-*N*-alkylated and mono-*N*-alkylated). However, the antimicrobial activity of the dimethyl derivative was not as good as cerulenin. The activity was much better than dihydro, tetrahydro, and hexahydro cerulenin. The data showed that the *N*,*N*-dialkylatedamides were more active than the mono-*N*-alkylatedamides and the mono-*N*-alkylatedamide was more active than the non-*N*-alkylatedamide.

Table 1.15. Effect of Different Headgroups on Antimicrobial Activity. Table recreated from Reference [139].

Compounds	MIC (μg/mL)						
	Microorganisms						
	B. s.	S. a.	M.	E. c.	P. a.	C.a.	P. o.
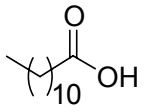	>100	>100	>100	>100	>100	>100	>100
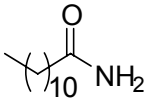	>100	>100	>100	>100	>100	>100	>100
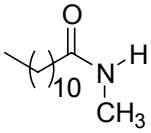	>100	>100	>100	>100	>100	>100	>100
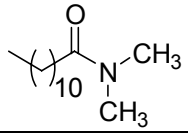	15.6	15.6	31.2	31.2	>100	62.5	31.2

B. s., *B. subtilis*; S. a., *S. aureus*; M., *M. smegmatis*; E. c., *E. coli*;
P. a., *P. aeruginosa*; C. a., *C. albicans*; P. o., *P. oryzae*

The authors then investigated whether the alkene (C2 and C3) and carbonyl (C4) groups of cerulenin were necessary for antimicrobial activity (Table 1.16).[139] The epoxide group of cerulenin was nonessential for antimicrobial activity. The unsaturated and saturated derivates were both better that the epoxide derivative. However, the saturated and unsaturated derivates were not as active as cerulenin. Arguably, the unsaturated dimethylamide, with two C=O groups had the best overall activity. This derivative had similar antimicrobial activity to that of cerulenin. Against some microorganisms, *S. aureus* and *E. coli*, this derivative was more active than cerulenin. The *N*,*N*-dimethylamide headgroup again showed the best antimicrobial activity. The carboxylic acid derivative was not as active as the amide derivatives. Like the previous table, generally, *N*-alkylation led to more active compounds. The hydroxylamide derivative led to a dramatic decrease in activity, which suggested that a relatively hydrophobic atom or group led to increased activity.

Table 1.16 Effect of Headgroup and Hydrophobic Backbone on Antimicrobial Activity. Table recreated from Reference [139].

Structures	MIC (μg/mL)							
	Microorganisms							
	B. s.	S. a.	M.	E. c.	P. a.	C.a.	P. o.	T. i.
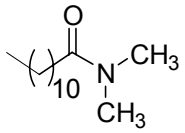	15.6	15.6	31.2	31.2	>100	62.5	31.2	X
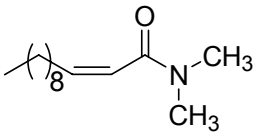	31.2	31.2	7.8	62.5	>100	>100	15.6	X
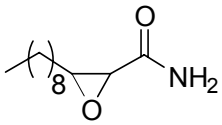	62.5	>100	31.2	>100	>100	>100	>100	X
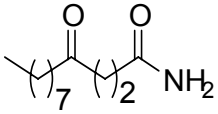	15.6	15.6	31.2	31.2	>100	62.5	31.2	>100
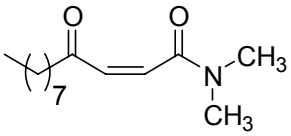	6.25	3.12	6.25	3.12	>100	12.5	6.25	6.25
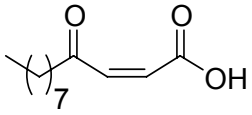	25	50	>100	50	>100	100	>100	50
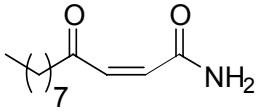	50	50	25	12.5	>100	>100	25	12.5
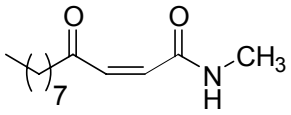	50	12.5	12.5	25	>100	>100	>100	<3.12
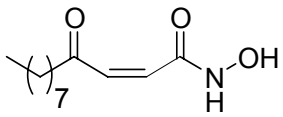	>100	>100	>100	>100	>100	>100	100	25

B. s., *B. subtilis*; S. a., *S. aureus*; M., *M. smegmatis*; E. c., *E. coli*;
P. a., *P. aeruginosa*; C. a., *C. albicans*; P. o., *P. oryzae*; T.i., *Trihophyton rubrum*

The authors further modified the amide headgroup to determine which headgroup would lead to optimal activity (Table 1.17).[139] Of the uncyclized headgroups, the *N*,*N*-dimethylamide headgroup displayed the best overall antimicrobial activity. Increasing the hydrophobicity, greater than a methyl group, generally led to decreased activity (dimethyl vs. diethyl analog). The mono-2-hydroxyethyl derivative had very good activity against *S. aureus* and *E. coli*; but overall, this headgroup was not as active as the dimethylamide headgroup.

Table 1.17 Effect of Headgroups on Antimicrobial Activity. Table recreated from Reference [139].

Compound R= —$CO(CH_2)_7CH_3$	MIC (μg/mL)							
	B. a	S. a.	M.	E. c.	P.a.	C.a.	P. o.	T. i.
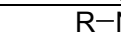	50	50	25	12.5	>100	>100	25	12.5
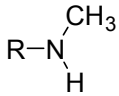	50	12.5	12.5	25	>100	>100	>100	<3.12
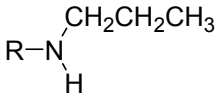	100	1.56	25	1.56	>100	>100	X	100
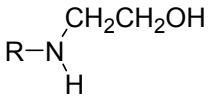	12.5	0.8	25	0.8	>100	>100	12.5	12.5
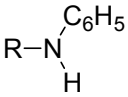	>100	>100	>100	>100	>100	>100	>100	>100
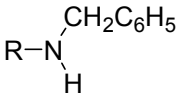	>100	>100	>100	>100	>100	>100	>100	>100
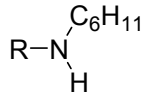	>100	>100	>100	>100	>100	>100	>100	>100
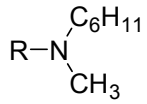	12.5	3.12	12.5	6.25	>100	>100	6.25	12.5
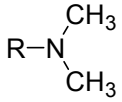	6.25	3.12	6.25	3.12	>100	12.5	6.25	6.25
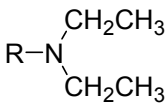	12.5	3.12	12.5	3.12	>100	100	12.5	6.25
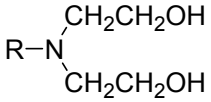	100	50	100	50	>100	>100	X	50
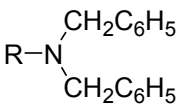	>100	>100	>100	>100	>100	>100	3.12	6.25

B. s., *B. subtilis*; S. a., *S. aureus*; M., *M. smegmatis*; E. c., *E. coli*;
P. a., *P. aeruginosa*; C. a., *C. albicans*; P. o., *P. oryzae*; T.i., *Trihophyton rubrum*

The effect that chain length on antimicrobial activity was also investigated (Table 1.18).[139] Chain length had a significant effect on activity. Antimicrobial activity increased with chain length and reached a maximum activity at C_{12}. The derivative with

a C_{15} alkyl chain led to decreased activity against almost all microorganisms. However, it is possible that the C_{13} and C_{14} amides would be more active than the C_{12} amide; however, those amides were not tested.

Table 1.18 Effect of Chain Length on Antimicrobial Activity. Table recreated from Reference [139].

R'= 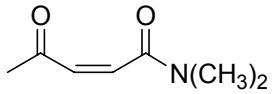

Compound	MIC (μg/mL)							
	B. a	S. a.	M.	E. c.	P.a.	C.a.	P. o.	T. i.
$CH_3(CH_2)_2R'$	>100	100	>100	25	>100	>100	3.12	25
$CH_3(CH_2)_3R'$	100	25	100	6.25	>100	>100	0.8	12.5
$CH_3(CH_2)_4R'$	50	50	100	12.5	>100	50	6.25	6.25
$CH_3(CH_2)_5R'$	50	25	100	12.5	>100	50	3.12	6.25
$CH_3(CH_2)_6R'$	25	6.25	6.25	6.25	>100	12.5	1.56	12.5
$CH_3(CH_2)_7R'$	6.25	3.12	6.25	3.12	>100	12.5	6.25	6.25
$CH_3(CH_2)_{10}R'$	25	12.5	25	12.5	>100	25	3.12	6.25

B. s., *Bacillus subtilis*; S. a., *S. aureus*; M., *M. smegmatis*; E. c., *E. coli*; P. a., *Pseudomonas aeruginosa*; C. a., *C. albicans*; P. o., *Piricularia oryzae*; T.i., *Trihophyton rubrum*

Bailey et al. tested long-chain amides against Gram-positive, Gram-negative, yeasts, and fungi (Table 1.19).[142] In addition to the amide moiety, the compounds also contained an ester moiety. No compound inhibited every organism. Only two compounds with saturated alkyl chains were tested, consequently, a definite chain length effect cannot be determined from this study. Chain length, the ester group, and the space between the ester and amide group appeared to affect activity. The C_{16} analogs were less active than the C_{12} analogs. However, in one case against *S. aureus*, the C_{16} analog (8) had better activity than (1). (The increased activity may have been due to a longer spacer.) The amides exhibited the best activity against *S. aureus* and the *Torula* species. With a few exceptions, most of the compounds were inactive against *C. albicans*, the *Aspergillus* species, *Aspergillus flavus*, and *E. coli*. The longer spacer of samples 5 and 7

exhibited better activity than their short-chain analogs (2 and 4). Longer spacers also improved activity against the *Torula* species (5 and 7 vs. 2 and 3). Overall, the most active sample appeared to be sample 5 because it exhibited maximum activity against three microorganisms (*S. aureus* and the *Torula* and *Aspergillus* species).

Table 1.19 Antimicrobial Activity of Long-Chain Amide-Esters. Table recreated from Reference [142].

Sample No.	Amide Acyl	Ester Acyl, R_1	Antimicrobial Activity					
			Microorganisms					
			A	B	C	D	E	F
1	C_{12}	Benzoyl	00	+	0	-	-	00
2	C_{12}	Furoyl	+	0	0	-	-	00
3	C_{12}	Trimethylacetyl	0	+	-	0	-	00
4	C_{12}	Benzoyl	0	00	0	-	-	0
5	C_{12}	Furoyl	++	00	++	-	-	++
6	C_{12}	*p*-Toluoyl	+	00	0	-	-	++
7	C_{12}	Trimethylacetyl	++	0	-	+	-	++
8	C_{16}	Benzoyl	+	00	00	-	00	-
9	C_{16}	Furoyl	0	00	00	-	00	-

Structure for Nos. 1-3, $RCON(CH_2CH_2OR)_2$; structure for No. 4-9, $RCON(CH_3)CH_2CH_2OR_1$.

++ = Zone of inhibition was at least 0.5 cm beyond disc or cylinder area at 120 h; + = Zone of inhibition was less than 0.5 cm beyond disc or cylinder area at 120 h; 00 = Organism failed to grow on disc or cylinder area at 120 h; 0 = slight growth on the saturated disc or cylinder area at 120 h.

A = *S. aureus*; B = *E. coli*; C = *Aspergillus* species; D = *Aspergillus flavus*; E = *C. albicans*; F = *Torula* species.

Novak et al. reported the antimicrobial activity of various *N*-mono and *N*,*N*-disubstitutedamides against a wide spectrum of bacteria, yeast, and molds (Table 1.20).[138] Amide (2) was either as active as or more active than the acid (1) in all cases. Unsaturation in the alkyl chain yielded mixed results. Some unsaturated derivatives displayed enhanced activities while others displayed decreased activity. Unsaturation alone did not appear to lead to enhanced activity. Unsaturation, coupled with changes in the headgroup, led to enhanced activity. Unsaturation and a substituted chain (6 and 2)

did not enhance activity compared to their unsaturated and unsubstituted analog (2). The unsaturated compounds (6–13) did not enhance the overall activity compared to the saturated chains (2 and 4). Increased unsaturation (6 vs. 13) led to enhanced activity against some microorganisms (I, X, and Y) but reduced activity against other microorganisms (V and S). Similar to the Ōmura et al. study, *N*-alkyl groups longer than methyl led to reduced activity (2 vs. 3). Unlike the Ōmura et al. study, the *N*,*N*-bis(2-hydroxyethyl) headgroup was equally active as the *N*,*N*-dimethyl headgroup. However, the *N*,*N*-bis(2-hydroxyethyl) did not enhance the activity of the $C_{18:1}$ chain. While the epoxy analogs (14–18) were active against a wide variety of microorganisms, overall, they were not as active as the saturated chain analogs (2 and 4). However, the most active epoxy analogs (16–18) were more active than the most active unsaturated analogs (10 and 11).

Table 1.20 Antimicrobial Activity of Long-Chain Amides. Table recreated from Reference [138]

Compounds	Microorganisms																			
	A	**B**	**C**	**D**	**E**	**F**	**G**	**H**	**I**	**J**	**K**	**L**	**M**	**N**	**O**	**P**	**Q**	**R**	**S**	**T**
1 C_{12} acid	X	X	++	++	+	+	++	+	+	+	++	+	+	+	++	+	++	+	++	+
2. C_{12}-*N*,*N*-dimethylamide	X	X	++	++	++	+	++	+	++	+	++	++	++	++	++	++	++	++	++	++
3. neoC_{12}-*N*,*N*-dibutylamide	X	X	-	X	X	X	X	X	∞	X	X	X	X	X	X	X	X	X	-	X
4. C_{12}-*N*,*N*-bis(2-hydroxyethyl)amide	+	++	++	++	+	++	++	++	++	+	++	++	++	++	++	++	++	+	++	+
5. C_{12}-*N*,*N*-bis(2-lauroyloxyethyl)amide	0	0	∞	∞	0	0	∞	∞	0	+	∞	∞	0	0	-	0	∞	0	∞	∞
6. $C_{18:1}$-*N*,*N*-dimethylamide	X	X	-	X	X	X	X	X	∞	X	X	X	X	X	X	X	X	X	+	X
7. $C_{18:1}$-*N*,*N*-di-*sec*-butylamide	X	X	-	X	X	X	X	X	∞	X	X	X	X	X	X	X	X	X	-	X
8. $C_{18:1}$-*N*-(*tert*-butyl)amide	X	-	-	0	∞	∞	∞	∞	0	0	0	∞	++	∞	+	0	-	-	∞	0
9. $C_{18:1}$-*N*,*N*-bis(2-hydroxyethyl)amide	X	X	∞	-	∞	0	+	0	-	-	∞	∞	+	∞	++	0	∞	0	∞	++
10. $C_{18:1}$-*N*,*N*-bis(2-acetoxyethyl)amide	X	X	∞	+	+	+	+	∞	+	∞	+	+	+	∞	+	∞	+	∞	+	+
11. $C_{18:1}$-*N*,*N*-bis(2-benzoyloxyethyl)amide	X	X	∞	++	+	+	++	+	+	+	∞	++	∞	+	++	∞	++	+	++	++
12. $C_{18:1}$-*N*-(2-piperidinoethyl)amide	X	X	∞	X	X	X	X	X	X	X	X	X	X	X	X	X	X	X	X	X
13. $C_{18:2}$-*N*,*N*-dimethylamide	X	X	-	X	X	X	X	X	+	X	X	X	X	X	X	X	X	X	-	-
14. C_{18}-*N*-(1,2-dibromopropyl) -9, 10-epoxyamide	X	X	∞	X	X	X	X	X	X	X	X	X	X	X	X	X	X	X	X	X
15. C_{18}-*N*,*N*-bis(2-hydroxyethyl) -9, 10-epoxyamide	X	X	∞	X	X	X	X	X	X	X	X	X	X	X	X	X	X	X	X	X
16. C_{18}-*N*,*N*-bis(2-acetoxyethyl) -9, 10-epoxyamide	X	X	-	0	+	+	++	++	+	++	+	∞	+	∞	+	∞	++	++	∞	+
17. C_{18}-*N*,*N*-bis(2-acetoxyethyl)-9, 10 (12,13)-epoxyamide	X	X	∞	0	∞	+	++	∞	+	+	+	+	++	+	+	+	++	++	+	+
18. C_{18}-*N*,*N*-bis(2-acetoxyethyl) -9, 10-12), 13-diepoxyamide	X	X	∞	0	++	+	++	+	++	+	+	++	+	+	++	+	++	++	+	+

X= not tested. ++ = the zone of inhibition was at least one-half centimeter, + = the zone of inhibition was less than one-half centimeter, ∞ = organism failed to grow on saturated disc or solid. 0 = slight growth of organism on saturated disc or solid, - = no inhibition detectable, gf = promoted growth of organism. A, *E. coli*; B, *Micrococcus pyogenes*; C = *C. albicans*; D, *Candida wernwcki*; E, *Epidermmophyton floccosum*; F, *Keratinomyces ajelloi*; G, *Microsporum canis*; H, *Microsporum cookii*; I, *Microsporum gypseum*; J, *Microsporum hanum*; K, *Trichophyton concentricum*; L, *Trichophyton epilans*; M, *Trichophyton eqinum*; N, *Trichophyton ferrugineum*; O, *Trichophyton gallinae*; P, *Trichophyton megnini*; Q, *Trichophyton mentagrophytes* various interdigitales; R, *Trichophyton mentagrophytes* various *granulare*; S, *Trichophyton rubrum*; T, *Trichophyton sabouraudi*; U, *Trichophyton schoenleini*; V, *Trichophyton sulfurium*; W, *Trichophyton tonsurans*; X, *Trichophyton violaceum*; Y, *Cladosporium Wernecki*; Z, *Aspergillus flavus*

Table 1.20 Continued

Compound	Microorganisms					
	U	**V**	**W**	**X**	**Y**	**Z**
1 C_{12} acid	+	+	++	+	X	X
2. C_{12}-*N*, *N*-dimethylamide	++	++	++	++	X	X
3. neoC_{12}-*N*,*N*-dibutylamide	-	-	-	-	-	-
4. C_{12}-*N*,*N*-bis(2-hydroxyethyl)amide	+	++	++	++	X	X
5. C_{12}-*N*,*N*-bis(2-lauroyloxyethyl)amide	0	∞	∞	0	X	X
6. $C_{18:1}$-*N*,*N*-dimethylamide	-	+	+	-	-	-
7. $C_{18:1}$-*N*,*N*-di-*sec*-butylamide	-	-	-	-	-	-
8. $C_{18:1}$-*N*-(*tert*-butyl)amide	0	∞	+	∞	X	X
9. $C_{18:1}$-*N*,*N*-bis(2-hydroxyethyl)amide	∞	∞	+	+	X	X
10. $C_{18:1}$-*N*,*N*-bis(2-acetoxyethyl)amide	+	+	+	+	X	X
11. $C_{18:1}$-*N*,*N*-bis(2-benzoyloxyethyl)amide	+	++	++	+	X	X
12. $C_{18:1}$-*N*-(2-piperidinoethyl)amide	X	X	X	∞	X	∞
13. $C_{18:2}$-*N*,*N*-dimethylamide	X	-	+	++	-	-
14. C_{18}-*N*-(1,2-dibromopropyl)-9, 10-epoxyamide	X	X	X	∞	+	∞
15. C_{18}-*N*,*N*-bis(2-hydroxyethyl)-9, 10-epoxyamide	X	X	X	+	X	++
16. C_{18}-*N*,*N*-bis(2-acetoxyethyl)-9, 10-epoxyamide	∞	+	+	+	X	X
17. C_{18}-*N*,*N*-bis(2-acetoxyethyl)-9, 10(12,13)-epoxyamide	+	++	+	+	X	X
18. C_{18}-*N*,*N*-bis(2-acetoxyethyl)-9, 10-12), 13-diepoxyamide	+	∞	+	+	X	X

Gershon et al. studied the antifungal activity of short- and medium-chain fatty amides and 2-fluorofatty amides (Table 1.21).[140] With a few exceptions, the antimicrobial activity of both series increased until C_6 or C_7, at which point, the antifungal activity began to decrease. The incorporation of a fluoro substituent at the α carbon did not enhance the antifungal activity. The short-chains (C_6 and C_7) compounds were as active, mostly more active, than the medium- to long-chain ($\geq C_9$) compounds.

Table 1.21 Comparison of Antifungal Activity of Unsubstituted and α–Fluoro Fatty Acids. Table recreated from Reference [140].

R	RCH_2CONH_2			
	A. Niger	*Trichoderma viride*	*Myrothecium verrucaria*	*Trichophyton mentagrophytes*
C_2H_5	0	0	1	ND
C_3H_7	1	1	1	ND
C_4H_9	1	1	1	1
C_5H_{11}	1	1	2	2
C_6H_{13}	2	2	2	2
C_7H_{15}	2	2	3	3
C_8H_{17}	0	0	1	3
C_9H_{19}	0	0	0	ND
$C_{10}H_{21}$	0	0	2	3
$C_{12}H_{25}$	ND	ND	ND	2
			$RCHFCONH_2$	
C_2H_5	0	0	1	ND
C_3H_7	1	1	1	ND
C_4H_9	1	1	1	2
C_5H_{11}	1	2	2	3
C_6H_{13}	1	2	2	3
C_7H_{15}	1	1	3	2
C_8H_{17}	0	1	1	2
C_9H_{19}	0	1	1	ND
$C_{10}H_{21}$	0	1	1	2
$C_{12}H_{25}$	0	1	2	3
$C_{14}H_{29}$	0	0	1	ND
$C_{16}H_{33}$	0	0	1	ND

ND= not done. Compounds incorporated in test medium at 10^4, 10^3, and 10^2 μg/mL; 3= inhibition at all levels of compound; 2= inhibition at 2 levels, 1= inhibition at highest level only.

Kabara et al. compared the antibacterial activity of various amides versus C_{12} acid (Table 1.22).[134] They observed that neither C_{12} acid nor C_{12}-*N*,*N*-dimethylamide inhibited the growth of any Gram-negative bacteria tested (data not shown). However, C_{12} acid and various amides did inhibit the growth of various Gram-positive bacteria. Except against *Diplococcus*

pneumoniae, C_{12}-*N*,*N*-dimethylamide was more active against Gram-positive bacteria than C_{12} acid. The inclusion of unsaturation did enhance the antimicrobial activity against a few microorganisms. The *N*,*N*-dialkylated derivatives were consistently more active than non-*N*-alkylated amides. Besides C_{12}-*N*,*N*-dimethylamide, the other members of the amide series were mostly inactive. The increased chain length of C_{12}, C_{14}, and C_{16} amides reduced the antibacterial activity. Based on the activity of C_{12}-*N*,*N*-dimethylamide, C_{12} amide, $C_{18:1}$ amide and $C_{18:1}$-*N*,*N*-dimethylamide, it seemed that the headgroup had a more profound effect than the chain length or unsaturation in the alkyl chain of the amide.

Table 1.22 Gram-Positive Antibacterial Activity of Long-Chain Amides (μmol/mL). Table recreated from Reference [134].

Compounds	Gram-positive Bacteria											
	A	B	C	D	E	F	G	H	I	J	K	L
C_{12} Acid	4.9	0.24	0.24	0.62	0.06	2.49	1.24	1.24	2.49	0.62	0.82	2.49
C_{12}-*N*,*N*-dimethyl amide	0.2	0.05	0.05	0.1	0.1	0.2	0.2	0.2	0.2	0.67	0.1	0.1
C_{12}amide	NI	0.05	0.05	NI	NI	NI	NI	NI	NI	2.5	2.5	NI
C_{14}amide	NI	NI	NI	NI	4.4	NI	NI	NI	NI	NI	NI	NI
$C_{18:1}$amide	NI	0.08	0.35	NI	0.88	NI	NI	NI	NI	NI	NI	NI
$C_{18:1}$ N,N-dimethyl-amide	0.4	0.04	0.04	0.4	0.02	0.08	0.32	0.16	0.16	0.04	3.2	ND
N,*N*-Dimethyl methyl isovalerylamide	NI	1.08	1.08	NI	2.17	4.2	NI	NI	NI	1.08	1.08	4.3

NI= not inhibitory. Microorganisms: A, *Streptococcus faecalis*; B, *S. pyogenes* (group A); C, *S. pyogenes* (nongroup A); D, *Streptococcus* (Viridans group); E, *Diplococcus pneumoniae*; F, *Micrococcus* sp.; G, *Sarcina* sp.; H, *S. aureus*; I, *S. epidermidis*; J, *Corynbacterium* sp.; K, *Nocardia* asteroids; L, *Candida purapsilosis*. The following compounds had no affect on any of the microorganisms tested; *N*-methyl, *N*-valerylamide, *N*-dimethyl, *t*-valerylamide: *N* -dimethyl, *sec*-valerylamide: and n-hexadecanamide.

In another study, Kabara et al. studied the antimicrobial activity of derivatives of C_{12} acid (Table 1.23).[42] The dimethylamide headgroup exhibited the best antimicrobial against all microorganisms. The amide displayed activity against Gram-positive bacteria and fungi. Only the amine analogs (data not shown) had better activity than the amides.

Table 1.23 Antimicrobial Activity of Dodecyl Derivatives. Table recreated from Reference [42].

Microorganisms	MIC μmol/mL					
	Dodecyl Derivatives					
	C_{12} acid	C_{12} alcohol	C_{12} aldehyde	Methyl Dodecanoate	C_{12}-N, N-dimethylamide	1-Dodecane-thiol
Pneumococci	0.062	0.067	0.136	X	0.054	NI
Streptococcus group A	0.124	0.067	0.136	4.6	0.054	NI
Streptococcus beta-hemolytic non-A	0.249	0.271	0.136	NI	0.109	NI
Corynebacteria	0.124	0.135	0.136	4.6	0.054	NI
N. asteroides	0.124	0.135	0.136	4.6	0.054	NI
Micrococci	0.624	0.135	2.3	2.3	0.109	NI
C. albicans	2.49	0.135	4.6	4.6	0.109	NI
S. aureus	2.49	0.271	NI	NI	0.109	NI
S. epidermidis	2.49	0.135	NI	NI	0.109	NI
Streptococcus group D	2.49	5.4	4.6	4.6	0.109	NI

NI= not inhibitory. X= not done.

Novak et al. tested the antimicrobial activity of mono and C_{10}-*N*,*N*-disubstituted amides against a wide spectrum of bacteria, yeasts, and fungi (Table 1.24).[138] Overall, the mono-*N*-substituted amides performed just as well as the disubstituted amides. While C_{12}-*N*,*N*-bis(2-hydroxyethyl)amide was the most active compound, the dialkylated amides and monoalkylated amides were mostly inactive.

Table 1.24 Antimicrobial Activity of Secondary and Tertiary Amides. Table recreated from Reference [138].

Microorganisms	Compounds						
	C_{12}-*N*-butyl-amide	C_{12}-*N*-isoamyl-mide	C_{12}-*N*-cyclohexyl-amide	C_{12}-*N*,*N*-Bis(2-ethoxyethyl) Amide	C_{12}-*N*,*N*-Bis(2-decanoyloxy-ethyl)amide	C_{12}-*N*,*N*-Bis(2-hydroxyethyl) amide	C_{12}-*N*,*N*-Bis(2-decanoyl-oxyethyl) amide
A	X	X	X	X	X	+	00
B	+	00	X	X	-	++	-
C	-	-	-	-	0	++	00
D	0	0	0	X	0	++	0
E	+	+	00	X	0	+	00
F	0	00	00	X	+	++	00
G	++	++	00	X	00	++	00
H	00	++	00	X	0	++	00
I	+	++	-	++	0	++	0
J	++	++	00	X	0	+	+
K	+	+	00	X	0	++	0
L	00	+	++	X	00	++	00
M	00	00	00	X	00	++	00
N	+	+	0	X	0	++	00
O	+	+	+	X	00	++	0
P	00	+	0	X	-	++	0
Q	00	++	-	X	-	++	-
R	00	++	-	++	0	+	-
S	00	X	0	X	-	++	00
T	+	++	-	X	0	+	00
U	0	+	0	+	00	+	0
V	+	00	0	-	0	++	-
W	00	++	0	++	00	++	00
X	+	+	-	++	0	++	00
Y	X	X	X	00	X	X	X
Z	X	X	X	00	X	X	X

X= not tested. ++= The zone of inhibition was at least 0.5 cm beyond disc or cylinder area at 120 hrs, += The zone of inhibition was less than 0.5 cm beyond disc or cylinder area at 120 hrs, 00= organism failed to grow on the disc or cylinder area at 120 hrs, 0= slight growth on the disc or cylinder area at 120 hrs., -= no inhibition detectable. A, *E. coli*; B, *M. pyogenes*; C = *C. Albicans*; D, *C. wernwcki*; E, *E. floccosum*; F, *K. ajelloi*; G, *M. canis*; H, *M. cookii*; I, *M. gypseum*; J, *M. hanum*; K, *T. concentricum*; L, *T. epilans*; M, *T. eqinum*; N, *T. ferrugineum*; O, *T. gallinae*; P, *T. megnini*; Q, *T. mentagrophytes* various interdigitales; R, *T. mentagrophytes* various *granulare*; S, *T. rubrum*; T, *T. sabouraudi*; U, *T. schoenleini*; V, *T. sulfurium*; W, *T. tonsurans*; X, *T. violaceum*; Y, *C. Wernecki*; Z, *A. flavus*

1.14 Antiviral Amide Activity

Sands et al. compared the antiviral activity of FAs and amides against bacteriophage ϕ6 as a model system for enveloped mammalian viruses, such as Herpes simplex virus (Table 1.25).[143] The *N*,*N*-dimethylamides displayed equal or better activity than the corresponding FA.

Table 1.25 Amide Inactivation of Bacteriophage ϕ6. Table recreated from Reference [143].

Derivative	Alkyl chain concn (μg/mL) that reduces survival to 1%		
	Alkyl Chain Lengths		
	C_{10}	C_{14}	$C_{18:1}$
Acids	NA	NA	3
Dimethylamides	10	4	3

NA= not active

Asculai et al. compared the ability of nonionic amphiphiles to inhibit HSV (Table 1.26).[144] Ethers and amides were clearly better anti-HSV agents than the esters and ether-esters amphiphiles that were tested. The authors observed that C_{14} bis(2-hydroxyethyl)amide

Table 1.26 Inactivation of HSV by Nonionic Surface-Active Agents. Table recreated from Reference [144].

Surfactant	Linkage	Virus titer (PFU/mL)	
		HSV-1	HSV-2
None (control virus)		1×10^7	1×10^6
5% Nonoxynol-9 (Nonylphenoxypolyethoxyethanol)	Ether	<500	<500
1% Triton-X-100 (*p*-diisobutylphenoxy polyethoxyethanol)	Ether	<500	<500
1% Brij-97 [polyoxyethylene (10) oleyl ether)	Ether	<500	<500
Span-20 (sorbitan monolaurate)	Ester	8.8×10^6	6.1×10^5
Span-80 (sorbitan monooleate)	Ester	8.0×10^6	5.1×10^6
Tween-20 (polysorbate-20)	Ether-Ester	4.3×10^6	5.4×10^6
Tween-80 (polysorbate-80)	Ether-Ester	9.2×10^6	6.5×10^6
Onyxol 345 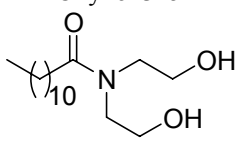	Amide	<500	<500

PFU, Plaque-forming units

equaled the anti-HSV ability of the common microbicide (N-9).

1.15 Antimicrobial Activity of Morpholine Amides

Similar to the dimethylamide headgroup, the morpholinoamide headgroup has exhibited a wide spectrum of activity against Gram-negative, Gram-positive, mycobacteria, and fungi (including yeasts).[136, 137, 139] Morpholine (**12)** is known to inhibit the growth of pathogenic yeast and molds.[137]

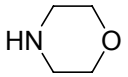

12

Figure 1.26 Structure of Morpholine

Novak et al. reported the antimicrobial activity of morpholinoamides (Table 1.27).[138] Generally, the antimicrobial activity increased with chain length. The morpholinoamide had equal activity to that of C_{12}-*N*,*N*-dimethylamide and exhibited enhanced activity relative to C_{12} acid. The effect of unsaturation was mixed. While $C_{18:1}$ acid exhibited enhanced activity, relative to C_{18}, against G, K, Q, and L, it exhibited reduced activity against I and N. The effect of the number of double bonds was also mixed. The $C_{18:2}$ amide, relative to $C_{18:1}$ amide, exhibited enhanced activity against some microorganisms (D, H, M, N, P, S, U, V, and X) but reduced activity against some microorganisms (G, K, L, Q, and T). Substitution on the unsaturated chain led to inactivity against most microorganisms. The terminal unsaturated analog was active against every microorganism. The epoxy analogs, especially *N*-[9,10(12,13)-epoxyoctadec-9(12)-enoyl]morpholine, were active against almost all microorganisms. A cutoff effect was observed as the activity increased for C_9–C_{12} and then decreased for C_{16}–C_{18}.

Table 1.27 Antimycotic Activity of Morpholine Amides. Table recreated from Reference [138].

Compounds	Microorganisms																			
	A	**B**	**C**	**D**	**E**	**F**	**G**	**H**	**I**	**J**	**K**	**L**	**M**	**N**	**O**	**P**	**Q**	**R**	**S**	**T**
C_{12} Acid	X	X	++	++	+	+	++	+	+	+	++	+	+	+	++	+	++	+	++	+
N,*N*-dimethylC_{12}amide	X	X	++	++	++	+	++	+	++	+	++	++	++	++	++	++	++	++	++	++
Sorbic Acid	++	++	++	++	++	++	++	+	++	++	++	++	++	++	++	+	++	++	++	++
N-sorboylmorpholine	X	X	++	++	++	++	++	++	++	++	++	++	++	++	++	++	++	++	++	++
N-C_9morpholine	∞	∞	++	++	+	++	++	++	++	++	+	++	++	+	+	+	++	++	+	+
N-C_{12}morpholine	X	X	++	++	++	+	++	+	++	+	++	++	++	++	++	++	++	++	++	++
N-C_{16}morpholine	0	0	-	-	++	+	+	∞	-	0	+	+	+	∞	∞	+	∞	∞	∞	∞
N-C_{18}morpholine	+	-	∞	∞	+	+	∞	∞	+	+	+	+	∞	+	+	∞	0	+	∞	+
N-$C_{18:1}$morpholine	X	X	∞	-	+	+	++	∞	0	+	++	++	0	∞	+	∞	+	+	∞	+
N-$C_{18:1}$-2,6-dimethylmorpholine	∞	X	-	-	0	∞	X	∞	0	-	∞	∞	+	∞	+	0	-	-	∞	∞
N-(11-$C_{11:1}$)morpholine	+	+	++	++	++	+	++	++	++	+	++	++	++	+	++	+	++	++	++	+
N-$C_{18:2}$morpholine	X	X	∞	+	+	+	+	+	-	+	+	+	+	+	+	+	∞	+	++	∞
N-(9,10-epoxy C_{18})morpholine	X	X	∞	+	+	∞	+	∞	+	+	+	∞	+	+	∞	+	+	+	+	+
N-[9,10(12,13)-epoxyC_{18}-9(12)-Enoyl] morpholine	X	X	+	++	+	+	++	+	++	+	+	++	+	+	++	+	++	+	++	++

X= not tested. ++= The zone of inhibition was at least 0.5 cm beyond disc or cylinder area at 120 hrs, += The zone of inhibition was less than 0.5 cm beyond disc or cylinder area at 120 hrs, ∞= organism failed to grow on the disc or cylinder area at 120 hrs, 0= slight growth on the disc or cylinder area at 120 hrs., -= no inhibition detectable. A, *E. coli*; B, *M. pyogenes*; C = *C. albicans*; D, *C. wernwcki*; E, *E. floccosum*; F, *K. ajelloi*; G, *M. canis*; H, *M. cookii*; I, *M gypseum*; J, *M. hanum*; K, *T. concentricum*; L, *T. epilans*; M, *T. eqinum*; N, *T. ferrugineum*; O, *T. gallinae*; P, *T. megnini*; Q, *T. mentagrophytes* various interdigitales; R, *T. mentagrophytes* various *granulare*; S, *T. rubrum*; T, *T. sabouraudi*; U, *T.schoenleini*; V, *T. sulfurium*; W, *T. tonsurans*; X, *T. violaceum*; Y, *C. Wernecki*; Z, *A. flavus*

Table 1.27 Continued

Compound	Microorganisms					
	U	**V**	**W**	**X**	**Y**	**Z**
C_{12} Acid	+	+	++	+	X	X
N,*N*-dimethylC_{12}amide	++	++	++	++	X	X
Sorbic Acid	++	++	++	++	X	X
N-sorboylmorpholine	++	++	++	++	X	X
N-C_9morpholine	+	+	++	+	X	X
N-C_{12}morpholine	++	++	++	++	X	X
N-C_{16}morpholine	+	++	∞	++	X	X
N-C_{18}morpholine	0	+	∞	∞	X	X
N-$C_{18:1}$morpholine	0	∞	∞	0	X	X
N-$C_{18:1}$-2,6-dimethylmorpholine	0	∞	0	∞	X	X
N-(11- $C_{11:1}$)morpholine	++	+	++	+	X	X
N- $C_{18:2}$morpholine	+	+	∞	+	X	X
N-(9,10-epoxy C_{18})morpholine	+	+	∞	∞	X	X
N-[9,10(12,13)-epoxyC_{18}-9(12)-Enoyl] morpholine	+	+	++	+	X	X

Novak et al. compared the antimicrobial activity of saturated and unsaturated acids versus their morpholinoamide analogs (Table 1.28).[136] While amidization improved the activity of some acids, the results varied. The amide of $C_{18:1trans}$ acid yielded the exact same activity as the acid. The amidization of ricinelaidic, 12-hydroxy-C_{18}, and $C_{18:1cis}$ acids enhanced activity. The amidization of C_{18} and ricinoleic acids led to both enhanced and reduced activity. Except for (12-β-cyanoethoxyoleoyl)morpholine, ether and ester substituents did not enhance activity relative to the other morpholinoamides. Overall, most morpholinoamides were not active against a wide variety of microorganisms.

Table 1.28 Antimicrobial Activity of Morpholinoamide-Fatty Acid Derivatives. Table recreated from Reference [136].

Compound	Structure	Antimicrobial Activity										
		A	B	C	D	E	F	G	H	I	J	K
Ricinoleic Acid	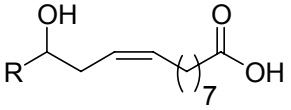	++	-	-	-	-	+	++	0	+	+	++
4-Ricinoleoyl-morpholine	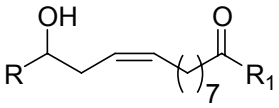	++	+	-	-	0	++	-	++	+	+	00
Ricinelaidic Acid	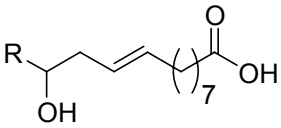	+	-	-	-	-	+	-	-	0	-	0
4-Ricinelaidoyl-morpholine	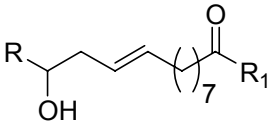	+	+	-	-	-	++	++	-	0	+	0
12-Hydroxy-C_{18} Acid	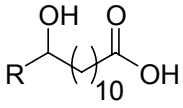	-	-	-	-	-	-	-	-	-	-	0
4-(12-hydroxyoctadecyl) Morpholine	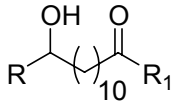	+	+	+	-	-	+	-	-	-	-	-
$C_{18:1cis}$ Acid	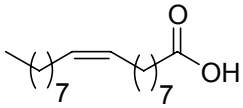	+	-	-	-	-	-	-	-	-	-	-
4-Oleoylmorpholine	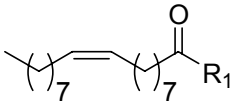	+	-	-	-	0	+	-	-	-	-	++
$C_{18:1trans}$ Acid	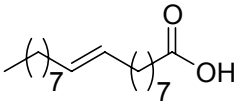	+	-	-	-	-	-	-	0	-	-	-
4-Elaidoylmorpholine	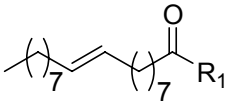	+	-	-	-	-	-	-	0	-	-	-
C_{18} Acid	$CH_3(CH_2)_{16}COOH$	+	-	-	-	-	-	-	-	-	0	0
(4-Octadecyl) morpholine	$CH_3(CH_2)_{16}COR_1$	-	+	-	-	-	+	-	0	0	+	0

R = $CH_3(CH_2)_5$ R_2= CH_2CH_2CN R_1 = 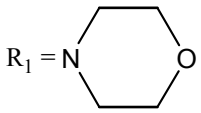 R_3 = CH_3CO R_4 = CH_3CH_2CO

++ = good, + = fair, 00 =organism failed to grow over organism, 0 = very slight growth over the compound, - = no inhibition A = *Micrococcus pyogenes*, B = *E. coli*, C = *S. cerevisiae*, D = *Candida stellatoidea*, E = *Torulopsis* sp., F = *Nuerospora* sp., G = *Alternaria* sp., H = *Mucor* sp., I = *Hormodenfrum* sp., J = *Geotrichum* sp., K = *Penicillium* sp.

Table 1.28 Continued

Compound	Structure	Antimicrobial Activity										
		A	B	C	D	E	F	G	H	I	J	K
4-(12-β-Cyanoethoxyoleoyl) morpholine	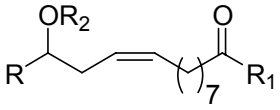	+	+	-	-	0	+	-	++	0	+	+
4-(12-β-Cyanoethoxyelaidoyl) morpholine	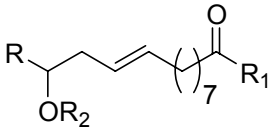	+	-	-	-	-	-	-	+	-	-	-
4-(12-β-Cyanoethoxy octadecyl) morpholine	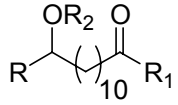	-	-	-	-	-	+	-	0	-	-	-
4-(12-Acetoxyoleoyl) morpholine	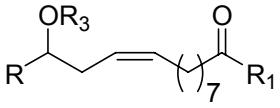	-	-	-	-	-	-	-	-	-	-	-
4-(12-Acetoxy octadecyl) morpholine	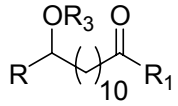	+	-	-	-	-	+	-	-	-	-	-
4-(12-Propionoxyoleoyl) morpholine	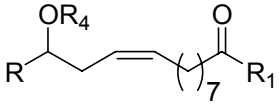	+	+	-	-	-	++	-	-	-	-	-

Novak et al. reported the antimycotic activity of morpholinoamides (Table 1.29).[137] Direct comparisons between the amides and the corresponding carboxylic acids yielded mixed results. The formation of morpholinoamides improved the overall antimicrobial activity of petroselinic and ricinoleic acids. However, morpholinoamides of 6(7)-hydroxy-C_{18} acid and 12-hydroxy-C_{18} acid were less active than the corresponding carboxylic acids.

Table 1.29 Antimycotic Activity of Morpholinoamide-Fatty Acid Derivatives. Table recreated from Reference [137].

Sample #	Structure	Antimycotic activity Microorganisms																				
		A	**B**	**C**	**D**	**E**	**F**	**G**	**H**	**I**	**J**	**K**	**L**	**M**	**N**	**O**	**P**	**Q**	**R**	**S**	**T**	**U**	**V**
1	$HO(CH_2)_4COOH$	+	++	+	∞	++	+	++	+	+	++	∞	+	++	+	++	∞	++	+	+	++	++	+
2	$HO(CH_2)_4COOR$	0	0	∞	+	++	∞	++	+	++	+	+	+	++	+	++	+	++	+	+	+	++	+
3	$R'CH_2CHOH(CH_2)_5COOH$	0	0	∞	0	∞	0	∞	∞	0	∞	-	0	∞	-	-	0	∞	0	0	0	-	-
4	$R'CH_2CHOH(CH_2)_5COOR$	0	0	+	∞	+	+	0	+	+	∞	+	+	+	++	++	+	++	+	∞	+	+	+
5	C_{18}-12-Hydroxy Acid	-	∞	∞	0	∞	∞	-	∞	0	∞	∞	0	∞	0	+	∞	∞	∞	∞	-	-	0
6	4-(12-hydroxyoctadecyl) morpholine	-	+	+	+	+	+	+	+	∞	++	+	∞	++	+	-	∞	∞	+	+	++	-	∞
7	Ricinoleic acid	gf	+	+	+	+	+	0	+	+	++	+	+	++	+	+	+	++	+	+	+	++	+
8	4-Ricinoleoylmorpholine	+	++	++	++	++	+	+	++	++	++	+	++	++	+	+	++	++	++	+	++	++	+
9	4-(12-Propionoxyoleoyl) morpholine	+	∞	∞	∞	++	+	∞	∞	∞	∞	+	∞	∞	∞	+	∞	∞	+	∞	∞	++	0
10	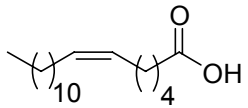	gf	++	+	∞	+	+	+	+	∞	++	∞	+	++	+	+	∞	∞	+	∞	++	+	+
11	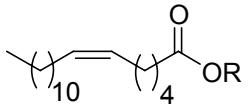	∞	0	∞	+	∞	0	∞	0	0	+	∞	0	∞	∞	∞	∞	∞	+	++	+	∞	∞
12	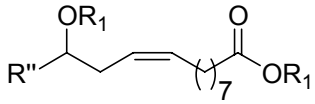	+	∞	∞	∞	++	+	∞	∞	∞	∞	∞	+	∞	∞	+	∞	∞	+	∞	∞	++	0
13	Morpholine	+	++	+	+	++	+	++	++	+	++	++	+	++	++	++	++	++	++	+	++	++	++

++ = the zone of inhibition was at least one-half centimeter, + = the zone of inhibition was less than one-half centimeter, ∞ = organism failed to grow on saturated disc or solid, 0 = slight growth of organism on saturated disc or solid, - = no inhibition detectable. gf = promoted growth of organism. A = *C. albicans*; B, *C. wernwcki*; C, *E. floccosum*; D, *K. ajelloi*; E, *M. canis*; F, *M. cookii*; G, *M. gypseum*; H, *M. nanum*; I, *T. concentricum*; J, *T. epilans*; K, *T. equinum*; L, *T. ferrugineum*; M, *T. gallinae*; N, *T. megnini*; O, *T. mentagrophytes* various interdigitales; P, *T. mentagrophytes* various *granulare*; Q, *T. rubrum*; R, *T. sabouraudi*; S, *T. schoenleini*; T, *T. sulfurium*; U, *T. tonsurans*; V, *T. violaceum*.

Ōmura et al. compared various fatty acid-amide derivatives of cerulenin.[139] Besides the *N*,*N*-dialkyl headgroups that were tested (Table 14–17); the authors also tested cyclic headgroups (Table 1.30).[139] The pyrrolidine derivative was just as active as the *N*,*N*-dimethyl derivative. The antimicrobial activity decreased as the size of the ring increased. The morpholino headgroup was the least active of the cyclic headgroups and displayed relatively poor activity against all microorganisms.

Table 1.30 Antimicrobial Activity of Cyclic-Cerulenin Derivatives. Table recreated from Reference [139].

Compound R= —$CO(CH_2)_7CH_3$	MIC (μg/mL)							
	B. s	S. a.	M.	E. c.	P.a.	C.a.	P. o.	T. i.
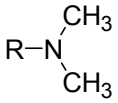	6.25	3.12	6.25	3.12	>100	12.5	6.25	6.25
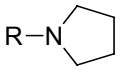	6.25	1.56	12.5	1.56	>100	25	X	1.56
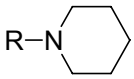	12.5	3.12	25	1.56	>100	100	X	6.25
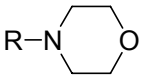	100	50	25	25	>100	>100	50	50

B. s., *B. subtilis*; S. a., *S. aureus*; M., *M. smegmatis*; E. c., *E. coli*; P. a., *P. aeruginosa*; C. a., *C. albicans*; P. o., *P. oryzae*; T.i., *Trihophyton rubrum*

Novak et al. tested a vide variety of *N*,*N*-disubstituted decanamides against a wide spectrum of bacteria, yeast, and molds (Table 1.31).[145] The morpholine derivates inhibited a wide array of bacteria, yeasts, and molds. The morpholine derivatives displayed better activity than piperidine derivatives (data not shown). They attributed the better activity to the morpholine headgroups' relatively better hydrophilic and amphiphilic character. Derivative C_{10}-*N*-morpholine was less active than morpholine and C_{12} acid. Derivative C_{10}-*N*-decanoyl-2,6-dimethylmorpholine exhibited enhanced activity relative to both morpholine and C_{12} acid.

Table 1.31 Antimicrobial Activity of Decanoylmorpholinoamides. Table recreated from Reference [145].

Microorganisms	MIC			
	Compounds			
	Morpholine	C_{10} Acid	*N*-Decanoyl-Morpholine	*N*-Decanoyl-2,6-Dimethylmorpholine
A	X	+	+	XX
B	X	+	+	++
C	+	++	++	+
D	++	++	++	++
E	+	++	+	++
F	+	+	+	++
G	++	++	++	++
H	+	+	+	++
I	++	+	++	++
J	++	+	+	++
K	+	+	+	++
L	++	++	++	++
M	++	+	+	++
N	+	+	+	++
O	++	++	++	++
P	++	+	+	++
Q	++	++	++	++
R	++	+	+	++
S	++	++	++	++
T	++	++	++	++
U	+	+	+	++
V	++	++	+	++
W	++	++	+	++
X	++	++	+	++

++= The zone of inhibition was at least 0.5 cm beyond disc or cylinder area at 120 hrs, += The zone of inhibition was less than 0.5 cm beyond disc or cylinder area at 120 hrs, XX= organism failed to grow on the disc or cylinder area at 120 hrs, X= slight growth on the disc or cylinder area at 120 hrs., -= no inhibition detectable. A, *E. coli*; B, *M. pyogenes*; C = *C. Albicans*; D, *C. wernwcki*; E, *E. floccosum*; F, *K. ajelloi*; G, *M. canis*; H, *M. cookii*; I, *M. gypseum*; J, *M. hanum*; K, *T. concentricum*; L, *T. epilans*; M, *T. eqinum*; N, *T. ferrugineum*; O, T. gallinae; P, *T. megnini*; Q, *T. mentagrophytes* various interdigitales; R, *T. mentagrophytes* various *granulare*; S, *T. rubrum*; T, *T. sabouraudi*; U, *T. schoenleini*; V, *T. sulfurium*; W, *T. tonsurans*; X, *T. violaceum*; Y, *C. Wernecki*.

Novak et al. reported the antimicrobial activity of long-chain morpholinoamides against a wide array of bacteria and fungi (Table 1.32).[138] They reported the effects that chain length, unsaturation, and alkyl chain substituents had on the antimicrobial activity. With respect to chain length, a cutoff effect was observed. The overall activity increased as the chain length increased from C_9–C_{14}, and then the overall activity decreased from C_{14}–C_{16}. The C_{16} and C_{18} morpholinoamides had somewhat similar overall activity. It appeared that increasing the number of double bonds led to increased activity. The C_{18} amide was active against a larger number of

Table 1.32 Study of the Antimycotic Activity of Morpholinoamide-Fatty Acid Derivatives. Table recreated from Reference [138].

Compounds	Antimycotic activity Microorganisms																				
	A	**B**	**C**	**D**	**E**	**F**	**G**	**H**	**I**	**J**	**K**	**L**	**M**	**N**	**O**	**P**	**Q**	**R**	**S**	**T**	**U**	**V**
1. C_{12} acid	+	++	+	∞	++	+	++	+	+	++	∞	+	++	+	++	∞	++	+	+	++	++	+
2. 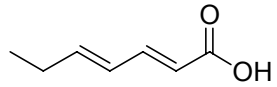	0	0	∞	+	++	∞	++	+	++	+	+	+	++	+	++	+	++	+	+	+	++	+
3. 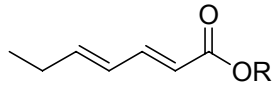	X	X	++	++	++	++	++	++	++	++	++	++	++	++	++	++	++	++	++	++	++	++
4. 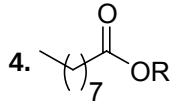	∞	∞	++	++	+	++	++	++	++	++	+	++	++	+	+	+	++	++	+	+	+	+
5. 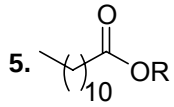	X	X	++	++	++	+	++	++	++	+	++	++	++	++	++	++	++	++	++	++	++	++
6. 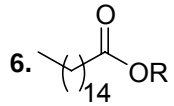	0	0	-	-	++	+	+	∞	-	0	+	+	+	∞	∞	+	∞	∞	∞	∞	+	++
7. 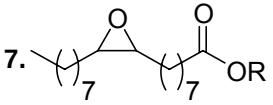	X	X	∞	+	+	∞	+	∞	+	+	+	∞	+	+	∞	+	+	+	+	+	+	+
8. 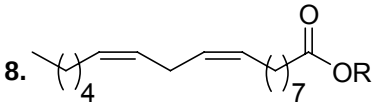	X	X	∞	+	+	+	+	+	-	+	+	+	+	+	+	+	∞	+	++	∞	+	+

++ = the zone of inhibition was at least one-half centimeter, + = the zone of inhibition was less than one-half centimeter, ∞ = organism failed to grow on saturated disc or solid, 0 = slight growth of organism on saturated disc or solid, - = no inhibition detectable. gf = promoted growth of organism. A = *C. Albicans*; B, *C. wernwcki*; C, *E. floccosum*; D, *K. ajelloi*; E, *M. canis*; F, *M. cookii*; G, *M. gypseum*; H, *M. nanum*; I, *T. concentricum*; J, *T. epilans*; K, *T. equinum*; L, *T. ferrugineum*; M, *T. gallinae*; N, *T. megnini*; O, *T. mentagrophytes* various interdigitales; P, *T. mentagrophytes* various *granulare*; Q, *T. rubrum*; R, *T. sabouraudi*; S, *T. schoenleini*; T, *T. sulfurium*; U, *T tonsurans*; V, *T. violaceum*;

Table 1.32 Continued

Microorganisms	Compounds		
	9. 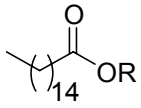	**10.** 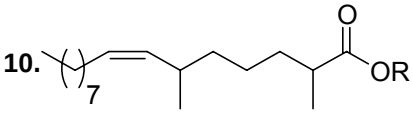	**10.** 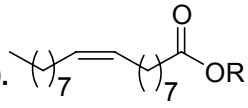
A	+	∞	X
B	-	X	X
C	∞	-	∞
D	∞	-	-
E	+	0	+
F	+	∞	+
G	∞	X	++
H	∞	∞	∞
I	+	0	0
J	+	-	+
K	+	∞	++
L	+	∞	++
M	∞	+	0
N	+	∞	∞
O	+	+	+
P	∞	0	∞
Q	0	-	+
R	+	-	+
S	∞	∞	∞
T	+	∞	+
U	0	0	0
V	+	∞	∞

organisms than the $C_{18:1}$ amide; however, the $C_{18:2}$ amide was more active than the C_{18} amide. Adding a substituent to the alkyl chain increased the activity as the epoxy derivative was more active than the unsubstituted C_{18} amide analog.

1.16 References for Chapter 1

1. Cross, J., *Surfactant Science*, ed. J. Cross, Singer, E. J. Vol. p. 53. 1994, New York: Marcel Dekker, Inc. 7-14.
2. Urizzi, P., Souchhard, J. P., Nepveu, F., *EDTA and DTPA analogs of dipalmitoylphosphatidylethanolamine as lipophilic chelating agents for metal labeling of LDL.* Tetrahedron Lett., 1996. **37**: p. 4685-4688.
3. Lawrence, C.A., *Surfactant Science*, ed. E. Jungermann. Vol. 4. 1970, New York: Marcel Dekker, Inc. 491-495.
4. Myers, D., *Surfactant Science and Technology*. 1988, VCH: New York, N.Y. p. 65.
5. Singer, E.J.E., *Cationic Surfactants*, ed. J. Cross, Singer, E. J. 1994, New York: Marcel Dekker, Inc. p. 29.
6. Hansch, C., Clayton, J. M., *Lipophilic character and biological activity of drugs. II. The parabolic case.* J. Pharm. Sci., 1973. **62**: p. 1-21.

7. Lichtenberg, D., *Characterization of the solubilization of lipid bilayers by surfactants.* Biochim. Biophys. Acta, 1985. **821**: p. 470-478.
8. Balgavy, P., Devinsky, F., *Cut-off effects in biological activities of surfactants.* Adv. Colloid Interface Sci., 1996. **66**: p. 23-63.
9. Devinsky F., A., K.-L., Sersen, F., Balgavy, P., *Interaction of surfactants with model and biological membranes. Part VIII. Cut-off effect in antimicrobial activity and in membrane perturbation efficiency of the homologous series of N,N-dimethylalkylamine oxides.* J. Pharm. Pharmacol., 1990. **42**(11): p. 790-794.
10. Klevens, H.B., *Solubilization.* Chem. Rev., 1950. **47**: p. 1-74.
11. Lindman, B., Wennerström, H., M., *Topics in current chemistry*. Vol. 87. 1980, New York: Springer-Verlag, Berlin Heidelberg. 10.
12. Hartley, G.S., *Aqueous solutions of paraffin-chain salts; a study in micelle formation*. 1936, Paris: Paris, Hermann & C^{ie}. 42-45s.
13. Ottewill, R.H., *Surfactants*, ed. T.F. Tadros. 1984, Orlando, Fla.: Academic Press: London. p. 1.
14. Myers, D., *Surfactant Science and Technology*. 1988, New York, N.Y.: VCH. p. 34-65.
15. Kabara, J.J., *Structure-Function-Relationships of Surfactants as Anti-Microbial Agents.* J. Soc. Cosmet Chem., 1978. **29**(11): p. 733-741.
16. Clint, J.H., *Surfactant Aggregation*. 1991, New York: Chapman and Hall. p. 5.
17. Myers, D., *Surfactant Science and Technology*. 1988, New York, N.Y.: VCH. p. 33.
18. Lomax, E.G., *Amphoteric Surfactants*. 2nd ed, ed. E.G. Lomax. Vol. 59. 1996, New York: Marcel Dekker, Inc. 3.
19. Wong, Y.-L., Hubieki, M. P., Curfman, C. L., Doncel, G. F., Dudding, T. C., Savle, P. S., Gandour, R. D., *A structure-activity study of spermicidal and anti-HIV properties of hydroxylated cationic surfactants.* Bioorg. Med. Chem., 2002. **10**: p. 3599-3608.
20. Wong, Y.-L., Curfman, C. L., Doncel, G. F., Hubieki, M. P., Dudding, T. C., Savle, P. S., Gandour, R. D., *Spermicidal, anti-HIV, and micellar properties of di- and trihydroxylated cationic surfactants.* Tetrahedron, 2002. **58**(1): p. 45-54.
21. Vorum, H., Brodersen, R., Kragh-Hansen, U., Pedersen, A. O., *Solubility of long-chain fatty acids in phosphate buffer at pH 7.4.* . Biochim. Biophyis. Acta., 1992. **1126**(2): p. 135-142.
22. Robb, I.D., *Determination of the aqueous solubility of fatty acids and alcohols.* Aust. J. Chem., 1966. **19**(12): p. 2281-2284.
23. Miller, R.D., Brown, K. E., Morse, S. A., *Inhibitory action of fatty-acids on growth of Neisseria-Gonorrhoeae.* Infect. Immun., 1977. **17**(2): p. 303-312.
24. Shinoda, K., *The critical micelle concentrations in aqueous solutions of potassium alkyl malonates.* J. Phys. Chem., 1955. **59**: p. 432-435.
25. Shinoda, K., *The critical micelle concentrations in aqueous solutions of potassium alkane tricarboxylates.* J. Phys. Chem., 1956. **60**: p. 1439-1441.
26. Haldar, J., Aswal, V. K., Goyal, P. S., Bhattacharya, S. , *Molecular modulation of surfactant aggregation in water. Effect of the incorportation of multiple headgroups on micellar properties.* Angrew. Chem. Int. Ed., 2001. **40**: p. 1228-1232.
27. Bhattacharya, S., Haldar, J., *Molecular design of surfactants to tailor its aggregation properties.* Colloids Surf., A, 2002. **205**: p. 119-126.

28. Shinoda, K., *The effect of alcohols on the critical micelle concentrations of fatty acid soaps and the critical micelle concentration of soap mixtures.* J. Phys. Chem., 1954. **58**: p. 1136-1141.
29. Shinoda, K., *Colloidal surfactants: some physicochemical properties*. 1963, New York: Academic Press. p. 44-45.
30. Lomax, E.G., *Cationic Surfactants*, ed. E.G. Lomax. Vol. 59. 1996, New York: Marcel Drekker, Inc. 11.
31. Lomax, E.G., *Cationic Surfactants*, ed. E.G. Lomax. Vol. 59. 1996, New York: Marcel Dekker, Inc. p. 13.
32. Todar, K., *Bacterial Struture in Relationship to Pathogenicity* http://textbookofbacteriology.net/BSRP.html, Accessed July 16, 2007
33. Paustian, T., Roberts, G., *Through the microscope: A look at all things small*, http://www.microbiologytext.com/index.php?module=Book&func=displayarticle&art_id=47, Accessed July 16, 2007
34. Brennan, P.J., Nikaido, H., *The envelope of mycobacteria.* Annu. Rev. Biochem., 1995. **64**: p. 29-63.
35. Lesage, G., Bussey, H., *Cell wall assembly in Saccharomyces cerevisiae.* Microbiol. Mol. Biol. Rev., 2006. **70**(2): p. 317-343.
36. Walker, J.E., *The germicidal properties of chemically pure soaps.* J. Infect. Dis., 1924. **35**: p. 557-566.
37. Nieman, C., *Influence of trace amounts of fatty acids on the growth of microorganisms.* Bacteriol. Rev., 1954. **18**: p. 147-63.
38. Kitahara, T., Koyama, N., Matsuda, J., Aoyama, Y., Hirakata, Y., Kamihira, S., Kohno, S., Nakashima, M., Sasaki, H., *Antimicrobial activity of saturated fatty acids and fatty amines against Methicillin-Resistant Staphylococcus aureus.* Biol. Pharm. Bull., 2004. **27**(9): p. 1321-1326.
39. McGaw, L.J., Jager, A. K., van Staden, J., *Antibacterial effects of fatty acids and related compounds from plants.* South African J. Botany, 2002. **68**: p. 417-423.
40. Kabara, J.J., *Lipids as host-resistance factors of human-milk.* Nutr. Rev., 1980. **38**(2): p. 65-73.
41. Kabara, J.J., Vrable, R., Liekenjie, M. S. F., *Antimicrobial lipids-natural and synthetic fatty-acids and monoglycerides.* Lipids, 1977. **12**(9): p. 753-759.
42. Kabara, J.J., Swieczkowski, D. M., Conley, A. J., Truant, J. P., *Fatty acids and derivatives as antimicrobial agents.* Antimicrob. Agents Chemother., 1972. **2**(1): p. 23-28.
43. Kondo, E., Kanai, K., *Lethal effect of long-chain fatty acids on mycobacteria.* Jpn J. Med. Sci. Biol., 1972. **25**(1): p. 1-13.
44. Saito, H., Tomioka, H., Yoneyama, T., *Growth of Group-IV mycobacteria on medium containing various saturated and unsaturated fatty-acids.* Antimicrob. Agents Chemother., 1984. **26**(2): p. 164-169.
45. Bergsson, G., Arnfinnsson, J., Steingrimsson, O., Thormar, H., *In vitro killing of Candida albicans by fatty acids and monoglycerides.* Antimicrob. Agents Chemother., 2001. **45**(11): p. 3209-3212.
46. Kanai, K., Kondo, E., *Antibacterial and cytotoxic aspects of long-chain fatty-acids as cell-surface events-selected topics.* Jpn. J. Med. Sci. Biol., 1979. **32**(3): p. 135-174.

47. Thormar, H., Bergsson, G., *Antimicrobial effects of lipids.* Recent Dev. Antiviral Res., 2001. **1**: p. 157-173.
48. Sheu, C.W., Freese, E., *Lipopolysaccharide layer protection of Gram-negative bacteria against inhibition by long-chain fatty acids.* J. Bacteriol., 1973. **115**(3): p. 869-875.
49. Bayliss, M., *The effect of the chemical constitution of soaps upon their germicidal properties.* J. Bacteriol., 1936. **31**: p. 489-504.
50. Wyss, O., Ludwig, B. J., Joiner, R. R., *The fungistatic and fungicidal action of fatty acids and related compounds.* Arch. Biochem., 1945. **7**: p. 415-425.
51. Kabara, J.J., *Structure-function relationship of anti-microbial lipids - Review.* J. Am. Oil Chem. Soc., 1978. **55**(3): p. A235-A235.
52. Kabara, J.J., *Toxicological, bacteriocidal and fungicidal properties of fatty acids and some derivatives.* J. Am. Oil Chem. Soc., 1979. **56**(11): p. 760A-767A.
53. Jossifova, L.T., Manolov, I., Golovinsky, E. V., *Antibacterial action of some saturated and unsaturated long-chain carboxylic acids and their bis(2-chloroethyl)aminoethyl esters in vitro.* Die Pharmazie 1989. **44**(12): p. 854-856.
54. Ohta, S., Shiomi, Y., Kawashima, A., Aozasa, O., Nakao, T., Nagate, T., Kitamura, K., Miyata, H., *Antibiotic effect of linolenic acid from chlorococcum Strain Hs-101 and Dunaliella-Primolecta on Methicillin-Resistant Staphylococcus-Aureus.* J. Appl. Phycol., 1995. **7**(2): p. 121-127.
55. Bergsson, G., et al., *Killing of Gram-positive cocci by fatty acids and monoglycerides.* Apmis, 2001. **109**(10): p. 670-678.
56. Perez Gutierrez, R.M., *Antimicrobial activity of fatty acids isolated from Tubifex tubifex.* Revista Mexicana de Ciencias Farmaceuticas, 2005. **36**(1): p. 5-10.
57. Kilic, T., Dirmenci, T., Satil, F., Bilsel, G., Kocagoz, T., Altun, M., Goren, A. C., *Fatty acid compositions of seed oils of three Turkish salvia species and biological activities.* Chem. Nat. Compd., 2005. **41**(3): p. 276-279.
58. Sivasamy, A., Krishnaveni, M., Rao, P. G., *Preparation, characterization, and surface and biological properties of N-stearoyl amino acids.* J. Am. Oil Chem. Soc., 2001. **78**(9): p. 897-902.
59. Hassinen, J.B., Durbin, G. T., Bernhart, F. W., *The bacteriostatic effects of saturated fatty acids.* Arch. Biochem. and Biophys., 1951. **31**: p. 183-189.
60. Marounek, M., Skrivanova, E., Rada, V., *Susceptibility of Escherichia coli to C_2-C_{18} fatty acids.* Folia Microbiol., 2003. **48**(6): p. 731-735.
61. Gaur, R.K., Chauhan, V. S., *Fatty-acid derivatives of acidic amino-acids as potential antibiotics.* Indian. J. Chem. B, 1988. **27**(5): p. 405-408.
62. Bergsson, G., Steingrimsson, O., Thormar, H., *In vitro susceptibilities of Neisseria gonorrhoeae to fatty acids and monoglycerides.* Antimicrob. Agents Chemother., 1999. **43**(11): p. 2790-2792.
63. Parang, K., Knaus, E. E., Wiebe, L. I., Sardari, S., Daneshtalab, M., Csizmadia, F., *Synthesis and antifungal activities of myristic acid analogs.* Arch. Pharm., 1996. **329**(11): p. 475-482.
64. Bergsson, G., Arnfinnsson, J., Steingrimsson, O., Thormar, H., *Killing of Gram-positive cocci by fatty acids and monoglycerides.* Apmis, 2001. **109**(10): p. 670-678.
65. Galbraith H., M.T.B., *Effect of metal cations and pH on the antibacterial activity and uptake of long chain fatty acids.* J. Appl. Bacteriol., 1973. **36**: p. 635-646.

66. Galbraith H., M.T.B., *Physicochemical effects of long chain fatty acids on bacterial cells and their protoplasts.* J. Appl. Bacteriol., 1973. **36**: p. 647-658.
67. Saito, H., Tomioka, H., *Susceptibilities of transparent, opaque, and rough colonial variants of Mycobacterium-Avium complex to various fatty-acids.* Antimicrob. Agents Chemother., 1988. **32**(3): p. 400-402.
68. Niwano, M., Mirumachi, E., Uramoto, M., Isono, K., *Fatty-acids as inhibitors of microbial cell-wall synthesis.* Agric. Biol. Chem., 1984. **48**(5): p. 1359-1360.
69. Kondo, E., Kanai, K., *Further-studies on lethal effect of long-chain fatty-acids on mycobacteria.* Japan. J. Med. Sci. Biol., 1976. **29**(1): p. 25-37.
70. Kondo, E., Kanai, K., *Relationship between chemical-structure of fatty-acids and their mycobactericidal activity.* Jpn. J. Med. Sci. Biol., 1977. **30**(4): p. 171-178.
71. Voet, D., Voet, J. G., *Biochemistry*. Second Edition ed. 1995, Somerset, NJ: John Wiley & Sons.
72. Ferdinandus, J., Clark, J. B., *Selective inhibition of bacterial enzymes by free fatty acids.* J. Bacteriol., 1969. **98**: p. 1109-1113.
73. Eisler D. M.; Heckly, R.J., *Possible mechanisms of action of an anti-Pasteurella pestis factor.* . J. Bacteriol., 1968. **96**: p. 1977-1981.
74. Levine, S., Novak, M., *The effect of fatty acids on the oxygen uptake of Blastomyces dermatitidis.* J. Bacteriol., 1949. **57**: p. 93-94.
75. Weinbach, E.C., Garbus, J., *Mechanism of action of reagents that uncouple oxidative phosphorylation.* Nature (London, United Kingdom) 1969. **221**: p. 1016-1018.
76. Parang, K., Knaus, E. E., Wiebe, L. I., Sardari, S., Daneshtalab, M., Csizmadia, F., *Synthesis and antifungal activities of myristic acid analogs.* Archiv Der Pharmazie, 1996. **329**(11): p. 475-482.
77. Heuckeroth, R.O., Glaser, L., Gordon, J. I., *Heteroatom-substituted fatty-acid analogs as substrates for N-myristoyltransferase - an approach for studying both the enzymology and function of protein acylation.* Proc. Natl. Acad. Sci. U.S.A., 1988. **85**(23): p. 8795-8799.
78. Stock, C.C., Francis, T., *Inactivation of the virus of epidemic influenza by soaps.* J. Exp. Med., 1940. **71**: p. 661-681.
79. Thormar, H., Isaacs, C. E., Brown, H. R., Barshatzky, M. R., Pessolano, T., *Inactivation of enveloped viruses and killing of cells by fatty-acids and monoglycerides.* Antimicrob. Agents Chemother., 1987. **31**(1): p. 27-31.
80. Horowitz, B., Piet, M. P. J., Prince, A. M., Edwards, C. A., Lippin, A., Walakovits, L. A., *Inactivation of lipid-enveloped viruses in labile blood derivatives by unsaturated fatty-acids.* Vox Sanguinis, 1988. **54**(1): p. 14-20.
81. Hilmarsson, H., Kristmundsdottir, T., Thormar, H., *Virucidal activities of medium- and long-chain fatty alcohols, fatty acids and monoglycerides against herpes simplex virus types 1 and 2: comparison at different pH levels.* Apmis, 2005. **113**(1): p. 58-65.
82. Kohn, A., Gitelman, J., Inbar, M. , *Interaction of polyunsaturated fatty acids with animal cells and enveloped viruses.* Antimicrob. Agents Chemother., 1980. **18**(6): p. 962-968.
83. Bryant, M.L., Heuckeroth, R. O., Kimata, J. T., Ratner, L., Gordon, J. I., *Replication of Human Immunodeficiency Virus-1 and Moloney Murine Leukemia-Virus is inhibited by different heteroatom-containing analogs of myristic acid.* Proc. Natl. Acad. Sci. U.S.A., 1989. **86**(22): p. 8655-8659.

84. Cullis, P.R., Hope, M. J., *Effects of fusogenic agent on membrane structure of erythrocyte-ghosts and mechanism of membrane-fusion.* Nature, 1978. **271**(5646): p. 672-674.
85. Harper, D.R., Gilbert, R. L., OConnor, T. J., Kinchington, D., Mahmood, N., McIlhinney, R. A. J., Jeffries, D. J., *Antiviral activity of 2-hydroxy fatty acids.* Antiviral Chem. Chemother., 1996. **7**(3): p. 138-141.
86. Paige, L.A., Zheng, G. Q., Defrees, S. A., Cassady, J. M., Geahlen, R. L., *Metabolic-activation of 2-substituted derivatives of myristic acid to form potent inhibitors of myristoyl Coa-Protein N-Myristoyltransferase.* Biochemistry, 1990. **29**(46): p. 10566-10573.
87. Rideal, E.K., *Film reactions as a new approach to biology.* Science, 1939. **90**: p. 217-225.
88. Declercq, E., *Chemotherapeutic approaches to the treatment of the Acquired-Immune-Deficiency-Syndrome (Aids).* J. Med. Chem., 1986. **29**(9): p. 1561-1569.
89. Declercq, E., *Toward improved Anti-Hiv chemotherapy - Therapeutic strategies for intervention with HIV-Infections.* J. Med. Chem., 1995. **38**(14): p. 2491-2517.
90. DeClercq, E., *New developments in anti-HIV chemotherapy.* Curr. Med. Chem., 2001 **8**: p. 1543-1572.
91. DeClercq, E., *New developments in anti-HIV chemotherapy.* Biochim. Biophys. Acta 2002. **1587**: p. 258-275.
92. Kuchimanchi, K.R., Gandhi, M. D., Sheta, R. R., Johnston, T. P., Santhosh, K. C., Cushman, M., Mitra, A. K., *Intestinal absorption and biodistribution of cosalane and its amino acid conjugates: novel anti-HIV agents.* Int. J. Pharm., 2002. **231**(2): p. 197-211.
93. Leydet, A., Barragan, V., Boyer, B., Montero, J. L., Roque, J. P., Witvrouw, M., Este, J., Snoeck, R., Andrei, G., DeClercq, E., *Polyanion inhibitors of human immunodeficiency virus and other viruses .5. Telomerized anionic surfactants derived from amino acids.* J. Med. Chem., 1997. **40**(3): p. 342-349.
94. Leydet, A., Barthelemy, P., Boyer, B., Lamaty, G., Roque, J. P., Bousseau, A., Evers, M., Henin, Y., Snoeck, R., Andrei, G., Ikeda, S., Reymen, D., Declercq, E., *Polyanion inhibitors of Human-Immunodeficiency-Virus and other viruses .1. Polymerized anionic surfactants.* J. Med. Chem., 1995. **38**(13): p. 2433-2440.
95. Leydet, A., Barthelemy, P., Boyer, B., Lamaty, G., Roque, J. P., Witvrouw, M., DeClercq, E., *Polyanion inhibitors of human immunodeficiency virus .4. Polymerized anionic surfactants: Influence of the density and distribution of anionic groups on the antiviral activity.* Bioorg. Med. Chem. Lett., 1996. **6**(4): p. 397-402.
96. Leydet, A., ElHachemi, H., Boyer, B., Lamaty, G., Roque, J. P., Schols, D., Snoeck, R., Andrei, G., Ikeda, S., Neyts, J., Reymen, D., Este, J., Witvrouw, M., DeClercq, E., *Polyanion inhibitors of human immunodeficiency virus and other viruses .2. Polymerized anionic surfactants derived from amino acids and dipeptides.* J. Med. Chem., 1996. **39**(8): p. 1626-1634.
97. Leydet, A., JeantetSegonds, C., Barthelemy, P., Boyer, B., Roque, J. P., *Polyanion inhibitors of Human Immunodeficiency Virus .3. Polymerized anionic surfactants derived from D-glucose.* Recueil Des Travaux Chimiques Des Pays-Bas-J. Royal Netherlands Chem. Soc., 1996. **115**(10): p. 421-426.
98. Leydet, A., JeantetSegonds, C., Bouchitte, C., Moullet, C., Boyer, B., Roque, J. P., Witvrouw, M., Este, J., Snoeck, R., Andrei, G., DeClercq, E., *Polyanion inhibitors of*

Human Immunodeficiency Virus and other viruses .6. Micelle-like anti-HIV polyanionic compounds based on a carbohydrate core. J. Med. Chem., 1997. **40**(3): p. 350-356.
99. Leydet, A., Moullet, C., Roque, J. P., Witvrouw, M., Pannecouque, C., Andrei, G., Snoeck, R., Neyts, J., Schols, D., De Clercq, E., *Polyanion inhibitors of HIV and other viruses. 7. Polyanionic compounds and polyzwitterionic compounds derived from cyclodextrins as inhibitors of HIV transmission.* J. Med. Chem., 1998. **41**(25): p. 4927-4932.
100. Poli, G., Biondi, P. A., Uberti, F., Ponti, W., Balsari, A., Cantoni, C., *Virucidal activity of organic-acids.* Food Chem., 1979. **4**(4): p. 251-258.
101. Bigelow, W.C., Pickett, D. L., Zisman, W. A., *Oleophobic monolayers. I. films adsorbed from solution in non-polar liquids.* J. Colloid Sci., 1946. **1**: p. 513-538.
102. Galoppini, E., *Linkers for anchoring sensitizers to semiconductor nanoparticles.* Coord. Chem. Rev., 2004. **248**(13-14): p. 1283-1297.
103. Whitesell, J.K., Chang, H. K., *Directionally aligned helical peptides on surfaces.* Science, 1993. **261**(5117): p. 73-76.
104. Newkome, G.R., Behera, R. K., Moorefield, C. N., Baker, G. R., *Chemistry of micelles series .18. Cascade polymers - syntheses and characterization of one-directional arborols based on adamantane.* J. Org. Chem., 1991. **56**(25): p. 7162-7167.
105. Newkome, G.R., Weis, C. D., Moorefield, C. N., Baker, G. R., Childs, B. J., Epperson, J., *Isocyanate-based dendritic building blocks: Combinatorial tier construction and macromolecular-property modification.* Angew. Chem., Int. Ed. Engl., 1998. **37**(3): p. 307-310.
106. Newkome, G.R., He, E. F., Moorefield, C. N., *Suprasupermolecules with novel properties: Metallodendrimers.* Chem. Rev., 1999. **99**(7): p. 1689-1746.
107. Ong, W., Kaifer, A. E., *Unusual electrochemical properties of unsymmetric viologen dendrimers.* J. Am. Chem. Soc., 2002. **124**(32): p. 9358-9359.
108. Folkers, J.P., Gorman, C. B., Laibinis, P. E., Buchholz, S., Whitesides, G. M., Nuzzo, R. G., *Self-assembled monolayers of long-chain hydroxamic acids on the native oxides of metals.* Langmuir, 1995. **11**(3): p. 813-824.
109. Aramaki, K., Shimura, T., *Self-assembled monolayers of carboxylate ions on passivated iron for preventing passive film breakdown.* Corros. Sci., 2004. **46**(2): p. 313-328.
110. Chen, S.H., Frank, C. W., *Infrared and fluorescence spectroscopic studies of self-assembled N-alkanoic acid monolayers.* Langmuir, 1989. **5**(4): p. 978-987.
111. Tao, Y.T., *Structural comparison of self-assembled monolayers of N-alkanoic acids on the surfaces of silver, copper, and aluminum.* J. Am. Chem. Soc., 1993. **115**(10): p. 4350-4358.
112. Pertays, K.M., Thompson, G. E., Alexander, M. R., *Self-assembly of stearic acid on aluminium: the importance of oxide surface chemistry.* Surf. Interface Anal., 2004. **36**(10): p. 1361-1366.
113. Raman, A., Gawalt, E. S., *Self-assembled monolayers of alkanoic acids on the native oxide surface of SS316L by solution deposition.* Langmuir, 2007. **23**(5): p. 2284-2288.
114. Thompson, W.R., Pemberton, J. E., *Characterization of octadecylsilane and stearic-acid layers on Al_2O_3 surfaces by Raman-spectroscopy.* Langmuir, 1995. **11**(5): p. 1720-1725.
115. Dote, J.L., Mowery, R. L., *Infrared reflectance absorption-spectra of Langmuir-blodgett stearic-acid monolayers on gold and aluminum-influence of substrate.* J. Phys. Chem., 1988. **92**(6): p. 1571-1575.

116. Oberg, K., Persson, P., Shchukarev, A., Eliasson, B., *Comparison of monolayer films of stearic acid and methyl stearate on an Al_2O_3 surface.* Thin Solid Films, 2001. **397**(1-2): p. 102-108.
117. Lin, S.Y., Tsai, T. K., Lin, C. M., Chen, C. H., Chan, Y. C., Chen, H. W., *Structures of self-assembled monolayers of n-alkanoic acids on gold surfaces modified by underpotential deposition of silver and copper: Odd-even effect.* Langmuir, 2002. **18**(14): p. 5473-5478.
118. Aronoff, Y.G., Chen, B., Lu, G., Seto, C., Schwartz, J., Bernasek, S., *Stabilization of self-assembled monolayers of carboxylic acids on native oxides of metals.* J. Am. Chem. Soc., 1997. **119**(2): p. 259-262.
119. Pawsey, S., Yach, K., Halla, J., Reven, L., *Self-assembled monolayers of alkanoic acids: A solid-state NMR study.* Langmuir, 2000. **16**(7): p. 3294-3303.
120. Paik, W.K., Han, S. B., Shin, W., Kim, Y. S., *Adsorption of carboxylic acids on gold by anodic reaction.* Langmuir, 2003. **19**(10): p. 4211-4216.
121. Lin, S.Y., Chen, C. H., Chan, Y. C., Lin, C. M., Chen, H. W., *Self-assembly of alkanoic acids on gold surfaces modified by underpotential deposition.* J. Phys. Chem. B, 2001. **105**(21): p. 4951-4955.
122. Smith, E.L., Porter, M. D., *Structure of monolayers of short-chain N-alkanoic acids ($CH_3(CH_2)_nCOOH$, n = 0-9) spontaneously adsorbed from the gas-phase at silver as probed by infrared reflection spectroscopy.* J. Phys. Chem., 1993. **97**(30): p. 8032-8038.
123. Touwslager, F.J., Sondag, A. H. M., *Order and disorder in N-alkylcarboxylic acid monolayers-chain-length dependence and lateral interaction effects.* Langmuir, 1994. **10**(4): p. 1028-1033.
124. Allara, D.L., Nuzzo, R. G., *Spontaneously organized molecular assemblies .1. Formation, dynamics, and physical-properties of normal-alkanoic acids adsorbed from solution on an oxidized aluminum surface.* Langmuir, 1985. **1**(1): p. 45-52.
125. Wang, S.T., Feng, L., Liu, H., Sun, T. L., Zhang, X., Jiang, L., Zhu, D. B., *Manipulation of surface wettability between superhydrophobicity and superhydrophilicity on copper films.* ChemPhysChem, 2005. **6**(8): p. 1475-1478.
126. Timmons, C.O., Zisman, W. A., *Investigation of fatty acid monolayers on metals by contact potential measurements.* J. Phys. Chem., 1965. **69**(3): p. 984-990.
127. Shustak, G., Domb, A. J., Mandler, D., *Preparation and characterization of n-alkanoic acid self-assembled monolayers adsorbed on 316L stainless steel.* Langmuir, 2004. **20**(18): p. 7499-7506.
128. Liu, Y.L., Yu, Z. F., Zhou, S. X., Wu, L. M., *Self-assembled monolayers on magnesium alloy surfaces from carboxylate ions.* Appl. Surf. Sci., 2006. **252**(10): p. 3818-3827.
129. Karsi, N., Lang, P., Chehimi, M., Delamar, M., Horowitz, G., *Modification of indium tin oxide films by alkanethiol and fatty acid self-assembled monolayers: A comparative study.* Langmuir, 2006. **22**(7): p. 3118-3124.
130. Yan, C., Zharnikov, M., Golzhauser, A., Grunze, M., *Preparation and characterization of self-assembled monolayers on indium tin oxide.* Langmuir, 2000. **16**(15): p. 6208-6215.
131. Joo, S.W., Han, S. W., Han, H. S., Kim, K., *Adsorption and stability of phthalic acid on a colloidal silver surface: surface-enhanced Raman scattering study.* J. Raman Spectrosc., 2000. **31**(3): p. 145-150.

132. Zhang, Z.J., Imae, T., *Hydrogen-bonding stabilized self-assembled monolayer film of a functionalized diacid, protoporphyrin IX zinc(II), onto a gold surface.* Nano Lett., 2001. **1**(5): p. 241-243.
133. Allara, D.L., Atre, S. V., Elliger, C. A., Snyder, R. G., *Formation of a crystalline monolayer of folded molecules by solution self-assembly of alpha,omega-alkanedioic acids on silver.* J. Am. Chem. Soc., 1991. **113**(5): p. 1852-1854.
134. Kabara, J.J., Conley, A. J., Truant, J. P., *Relationship of chemical structure and antimicrobial activity of alkyl amides and amines.* Antimicrob. Agents and Chemother., 1972. **2**(6): p. 492-498.
135. Mod, R.R., Magne, F. C., Sumrell, G., Novak, A. F., *Sulfur derivatives of N,N-disubstituted amides of long-chain fatty-acids and their antimicrobial activities.* J. Am. Oil Chem. Soc., 1975. **52**(11): p. 455-456.
136. Novak, A.F., Clark, G. C., Dupuy, H. P., *Antimicrobial activity of some ricinoleic and oleic acid derivatives.* J. Am. Oil Chem. Soc., 1961. **38**: p. 321-324.
137. Novak, A.F., Fisher, M. J., Fore, Sara, P., Dupuy, H. P., *Antimycotic activity of some fatty acid derivatives.* J. Am. Oil Chem. Soc., 1964. **41**(7): p. 503-505.
138. Novak, A.F., Solar, J. M., Mod, R. R., Magne, F. C., Skau, E. L., *Antimicrobial activity of some N-substituted amides of long-chain fatty acids.* Appl. Microbiol., 1969. **18**(6): p. 1050-1056.
139. Omura, S., Katagiri, M., Awaya, J., Furukawa, T., Umezawa, I., Oi, N., Mizoguchi, M., Aoki, B., Shindo, M., *Relation between the structures of fatty acid amide derivatives and their antimicrobial activities.* Antimicrob. Agents Chemother., 1974. **6**(2): p. 207-215.
140. Gershon, H., Rodin, R. L., Parmegiani, R., Godfrey, P. K., *Organic fluorine compounds. IV. Synthesis and antifungal properties of 2-fluoro fatty acid amides.* J. of Med. Chem., 1970. **13**(6): p. 1237-1239.
141. Vance, D., Goldberg, I., Mitsuhashi, O., Bloch, K., Omura, S., Nomura, S., *Inhibition of fatty acid synthetases by the antibiotic cerulenin.* Biochem. Biophys. Res. Commun., 1972. **48**: p. 649-656.
142. Bailey, A.V., Boudreaux, G. J., Sumrell, G., Novak, A. F., *Anti-Microbial properties of some fatty ester-amides.* J. Am. Oil Chem. Soc., 1978. **55**: p. 835-836.
143. Sands, J.A., Landin, P., Auperin, D., Reinhardt, A., *Enveloped virus inactivation by fatty-acid derivatives.* Antimicrob. Agents Chemother., 1979. **15**(1): p. 134-136.
144. Asculai, S.S., Weis, M. T., Rancourt, M. W., Kupferberg, A. B., *Inactivation of Herpes-Simplex Viruses by non-ionic surfactants.* Antimicrob. Agents Chemother., 1978. **13**(4): p. 686-690.
145. Novak, A.F., Solar, J. M., Mod, R. R., Magne, F. C., Skau, E. L., *Antimicrobial activity and physical characteristics of some N,N-disubstituted decanamides.* J. Am. Oil Chem. Soc., 1969. **46**: p. 249-251.

Chapter 2: Synthesis, Solubility, and Cmc of the 3CAmn Series

2.1 Introduction to Synthesis of the 3CAmn Series

The synthesis of the **3CAmn** series is accomplished in two steps (Scheme 2.1). The first step involves attaching the dendritic headgroup to hydrophobic chains by combining Behera's amine (**13)** with either long-chain acid halides or carboxylic acids (**3EAmn**). Scheme 2.1 shows the attachment of the hydrophobic moiety to **13** by utilizing either an acid halide via condensation or carboxylic acid via dicyclohexylcarbodiimide (DCC) coupling reaction. The resulting compounds are abbreviated as **3EAmn**, where "**3E**" represents three *tert*-butyl groups, "**Am**" represents the amido linker, and "**n**" represents the number of carbons in the hydrophobic tail. The final step is the removal of the *tert*-butyl protecting groups, yielding the carboxyl groups. This homologous series is abbreviated as **3CAmn**, where "**3C**" represents three carboxylic acid or carboxylate headgroups, "**Am**" represents the amido linker, and "**n**" represents the number of carbons in the hydrophobic tail.

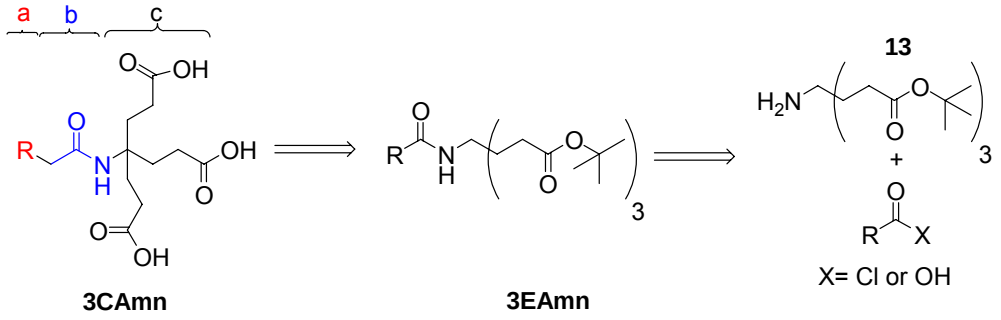

a. hydrophobic moiety; b. amido linker; c. hydrophilic moiety

Scheme 2.1 Retrosynthesis of the **3CAmn** Series

2.2 Formation of Behera's Amine

Formation of **13** is accomplished via a heterogeneous metal reduction starting with a nitrotriester precursor (Scheme 2.2).[1] Newkome stated that a *tert*-butylester is needed, instead of a less bulky alkyl group (e.g., methyl group) to prevent intramolecular cyclization, i.e. the

formation of a cyclic lactam **14**. Typically, the reaction is run in an alcoholic solvent. However, a recent report[2] states that running the reaction in heptane avoids formation of **14**.

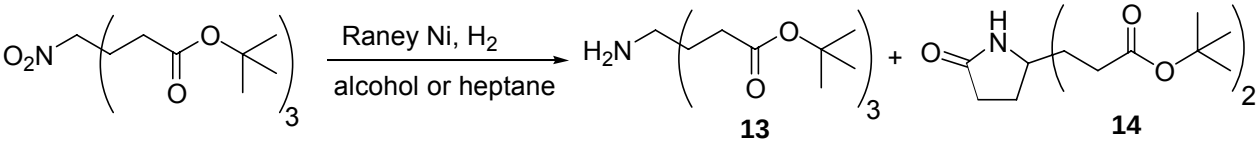

13 **14**

Scheme 2.2 Formation of Behera's Amine

2.3 Formation of an Amide Bond Utilizing Behera's Amine

To obtain the **3CAmn** series, an amide bond must be made, via an attachment of the hydrophobic moiety to the hydrophilic moiety (Scheme 2.1). To achieve this, two different strategies were employed. Behera's amine (hydrophilic moiety) was attached to long-chain compounds (hydrophobic moiety) via two synthetic strategies (Scheme 2.3). Strategy one utilized long-chain acid halides, while strategy two utilized long-chain FAs. Both strategies were slightly modified from reactions employed by Newkome et al. in which Behera's amine was allowed to react with dendritic carboxylic acids promoted by DCC or with adamantanecarbonyl chloride.[1]

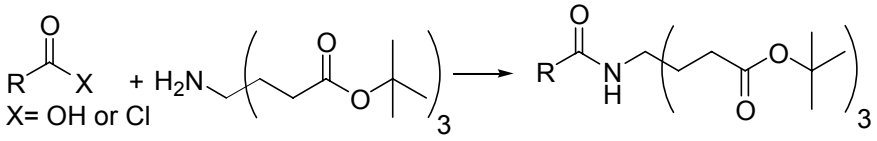

Scheme 2.3 Synthetic Strategies for the Formation of an Amide Bond

2.4 Synthesis of Long-Chain Acid Halides

Acid halides were prepared according to a published procedure[3] by combining the appropriate FA with thionyl chloride and catalytic amounts of DMF at refluxing temperatures (Scheme 2.4).[3] This procedure consistently produced orange or reddish orange products. The liquids were purified via multiple bulb-to-bulb distillations until clear–colorless liquids were obtained.

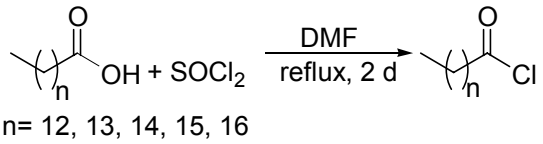

Scheme 2.4 Thionyl Chloride Preparation of Long-Chain Acid Halides

2.5 Attachment of Behera's Amine via Acid Halide Condensation

There are multiple examples of Behera's amine reacting with acid halides (Table 2.1);[1, 4-6] however, there are no examples of reactions with medium- or long-chain acid halides. The only differences between our procedures and the procedures in the literature were solvents and reaction times.

Table 2.1 Attachment of Behera's Amine to Acid Halides

Acid Halides	Reaction Conditions	Ref
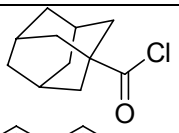	NEt_3, Benzene, 20 h, rt, 71%	[1]
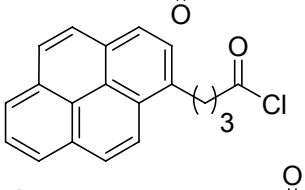	NEt_3, THF, N_2, 4 d, 20 °C, 78%	[4]
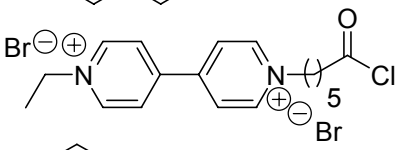	DMF, 12 h n-HATU, N_2 Proton Sponge®, 81%	[5]
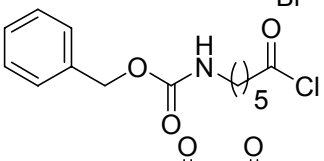	NEt_3, DCM, 1 h, 70%	[6]
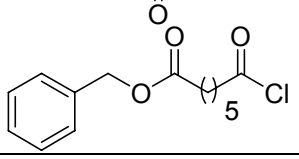	NEt_3, DCM, 1 h, 86%	[6]

2.6 Attachment of Behera's Amine via DCC Coupling

Table 2.2 Attachment of Behera's Amine to Carboxylic Acids

Carboxylic Acids	Reaction Conditions	Ref
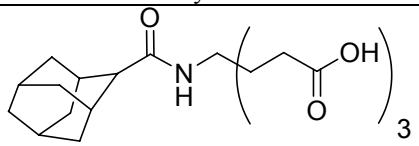	DCC, HOBt, DMF, 48 h, 25 °C, 61%	[1]
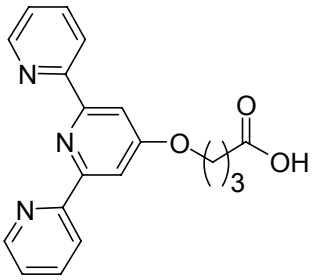	DCC, HOBt, DMF, 48 h, 25 °C, 72%	[7]
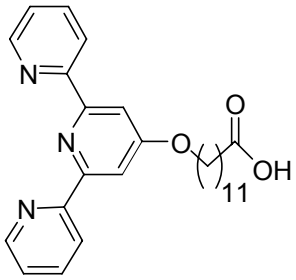	DCC, HOBt, DMF, 24 h rt, 58%,	[8]
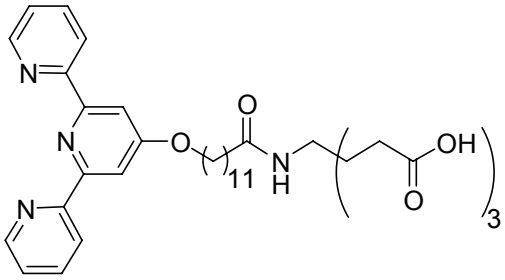	DCC, HOBt, DMF, 1 h, % yield not reported	[8]
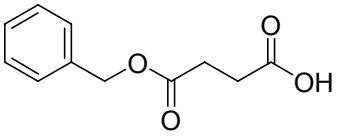	DCC, HOBt. THF, % yield not reported	[9]
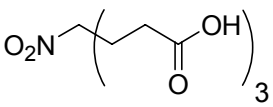	1. DCC, HOBt, THF, 6 d 20 °C.	[10]
	2. DCC, HOBt, THF, N_2, 6 d 23 °C, % yield not reported	[11]
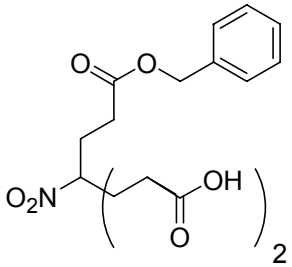	DCC, HOBt, DMF, 24 h, 25 °C, % yield not reported	[12]

There are multiple examples of Behera's amine reacting with various carboxylic acids[1, 7, 10-12] via DCC/1-hydroxybenzotriazole (HOBt) coupling (Table 2.2); however, there are no examples of Behera's amine reacting with long-chain FAs. Behera's amine was usually coupled to the carboxylic acid functional groups of dendritic polymers or dendrons.[1] The published procedures that involved DCC coupling of Behera's amine were very similar, mostly differing in the choice of solvent (DMF or THF).

2.7 Formation of Amide Linker via Weisocyanate™

Another possible method that would lead to the formation of an amide functional group is the reaction between Weisocyanate™ **15** and various carboxylic acids (Scheme 2.5).[13, 14] Ideally, this reaction can be run neat and the only byproduct should be CO_2. Newkome et al. reported the coupling of Weisocyanate™ with acetic and propanoic acids.[13]

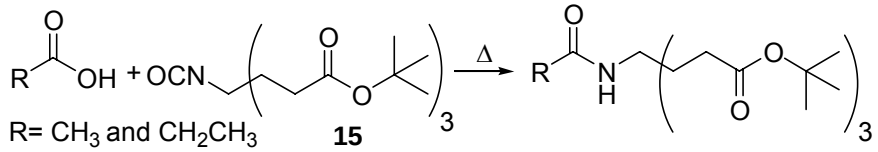

Scheme 2.5 Direct Coupling of Weisocyanate™ with Short-Chain Carboxylic Acids

2.8 Removal of the *tert*-Butyl Group via Formic Acid Formolysis

tert-Butyl groups are routinely removed under acidic conditions with formic acid.[1, 15] Newkome et al. routinely utilized formic acid to remove the *tert*-butyl groups of various dendritic polymers or dendrons.[1, 16-18]

Typically, the *tert*-butyl group of Behera's amine is removed with formic acid. However, Adamczyk et al. successfully used trifluoroacetic acid (TFA) to remove the bulky *tert*-butyl group (Scheme 2.6).[6] The advantage seems to be shorter reaction times and a more accommodating solvent (DCM vs. formic acid).

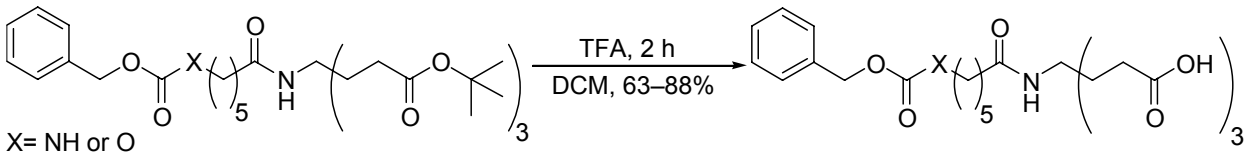

Scheme 2.6 Removal of the *tert*-Butyl Group with TFA

2.9 Overall Synthesis of the 3CAmn Series

Only two steps are needed to form the **3CAmn** series (Scheme 2.7). The first step is formation of the amide bond via either acid halide condensation or DCC coupling. The final step is removal of the *tert*-butyl group via formolysis.

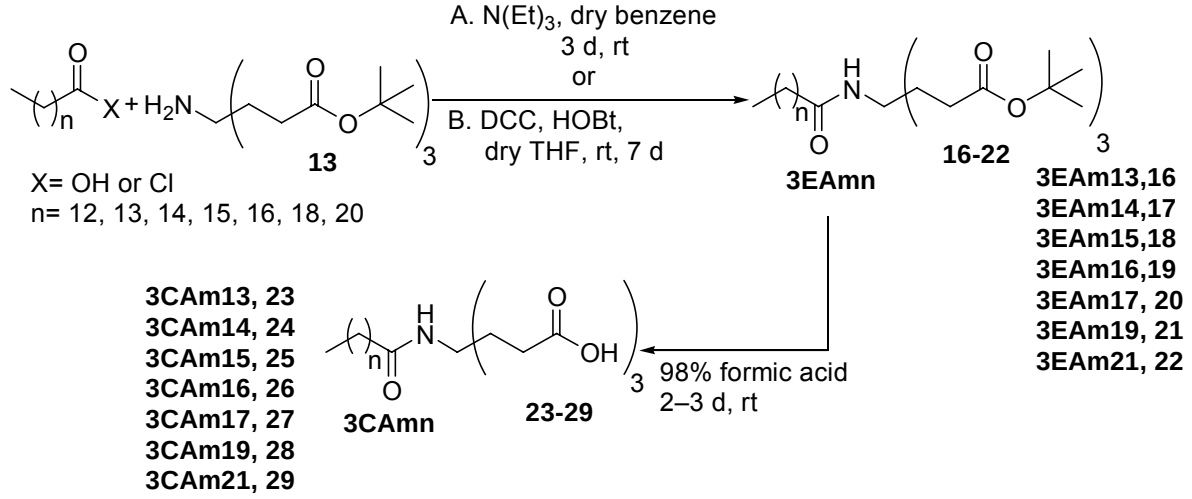

Scheme 2.7 Synthetic Scheme for the **3CAmn** Series

2.10 Challenges in the Formation of Behera's Amine

Behera's amine was prepared according to published procedures—hydrogenation of the preceding nitrotriester with Raney Ni.[1] Special care was taken to stop the reaction when the uptake of H_2 ceased. If the reaction was not stopped in a timely manner, the cyclic lactam (**14**) was observed in the ^{1}H NMR spectrum of the reaction product (Scheme 2.8). Attempts to remove the lactam impurity via recrystallization with hexane and column chromatography (silica) with ethyl acetate[1] were unsuccessful. Recrystallization led to increased **14** formation.

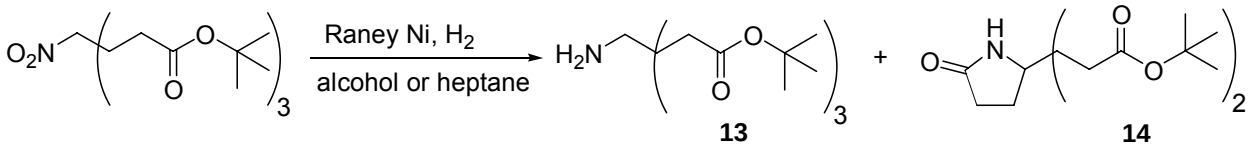

Scheme 2.8 Formation of Behera's Amine and Lactam

2.11 Preparation of Long-Chain Alkyl Halides

FAs or acid halides were attached to **13** via two separate methods (A or B). The shorter hydrophobic chains (C_{14}–C_{18}) were attached to **13** via condensation reactions using acid halides. The longer hydrophobic moieties, C_{18} and C_{20}, were attached via DCC coupling. Even though the FAs were commercially available, the shorter chain FAs, C_{14}–C_{18}, were converted into the corresponding acid halides with $SOCl_2$ (Scheme 2.9).[3]

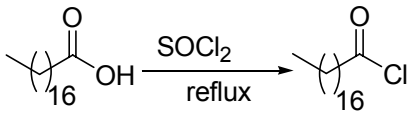

Scheme 2.9 Formation of Long-Chain Acid Halides

Initially, the longer chain FAs, C_{20} and C_{22} were converted into acid halides; however, the resulting orange or yellow solids were impure. Attempts to purify the acid halides, which were solids at room temperature, were unsuccessful. The high reactivity of the acid halide functional group prevented the use of purification techniques (i.e. column chromatography) and use of various solvents (protic and nucleophilic) for possible recrystallizations. The acid halides of the shorter chain FAs, C_{14}–C_{18}, were liquids at room temperature; therefore, they were purified via bulb-to-bulb distillations; however, due to the low prices of the even chain C_{14}–C_{18} FAs, multiple distillations and low yields were acceptable. Contrarily, C_{20} and C_{22} acids are much more expensive. Consequently, due to purification and cost concerns, DCC couplings with C_{20} and C_{22} acids were preferred.

Other methods of preparing acid halides were investigated by Moriyama et al.[19] and Hiramatsu et al.[20] They reported the conversion of the sodium salt of C_{18} acid into the corresponding C_{18} acid halide utilizing thionyl chloride at room temperature (Scheme 2.10). This procedure would have been beneficial because the side product would be NaCl (precipitate), instead of HCl that is produced in the thionyl chloride reactions.

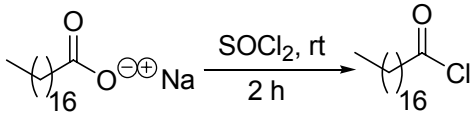

Scheme 2.10 Synthesis of C_{18} Acid Halide via Sodium Carboxylate

Attempts utilizing this procedure yielded mixed results. The sodium salt was prepared from the corresponding FA by adding the FA to an aqueous NaOH solution. The sodium salt was dried and then added to thionyl chloride. Unfortunately, according to the ^{1}H NMR spectrum, the reaction did not go to completion because unreacted fatty acid was present at the end of the reaction. The incomplete reaction was most likely due to the incomplete formation of the sodium salt, which was probably due to the low aqueous solubility of alkaline FA salts in aqueous media.[21]

2.12 Formation of the 3EAmn Series

The preparation of the **3EAmn** series followed either Methods A or B (Scheme 2.11). Acid halides were preferred over the use of FAs (DCC coupling), due to ease of synthesis. Method A had the advantage of not producing difficult emulsions, during extractions with saturated sodium bicarbonate, observed during the DCC coupling procedures. Additionally, the DCC coupling procedure produced dicyclohexylurea (DCU), which was often difficult to separate from other products. Overall, both DCC and condensation reactions led to similar yields (61–82%).

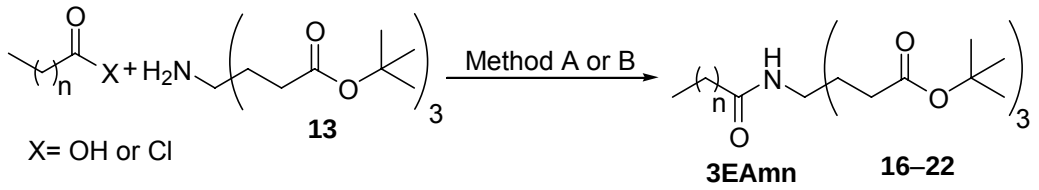

Scheme 2.11 Formation of the **3EAmn** Series

2.13 X-ray Crystal Structure of 3EAm15

The X-ray crystal structure of **3EAm15** shows that the alkyl tails are packed in parallel and antiparallel orientations, where anti-parallel chains pack more closely than parallel chains (Figure 2.1). For anti-parallel chains, every other carbon lies close to a corresponding carbon in the neighboring chain; C…C distances range from 3.91–4.34 Å. For parallel chains, all the carbons lie approximately the same distance apart; C…C distances range from 4.48–4.72 Å. An intermolecular hydrogen bond between the amide N–H (blue sphere) on one molecule and an ester carbonyl oxygen (red sphere) on a parallel neighboring molecule is indicated by a dashed line. The N…O distance is 2.970 Å.

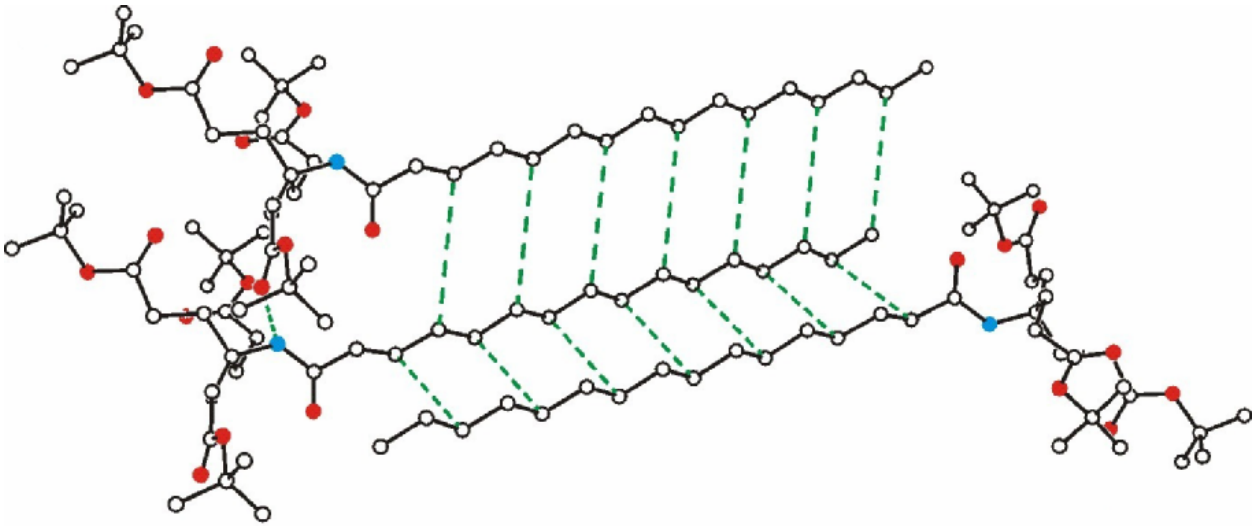

Figure 2.1 X-ray Crystal Structure of **3EAm15**. Picture obtained from Dr. Carla Slebodnick.

2.14 X-ray Crystal Structure of 3EAm16

Although the packing of **3EAm15** and **3EAm16** appear similar there are some differences. In both cases, there are parallel and antiparallel packing. However, the molecules are packed tighter in the crystal lattice of **3CAm16**. For **3CAm15**, the antiparallel chains are closer than the parallel chains. Contrarily, for **3CAm16**, the parallel chains (3.94–4.09 Å) are packed closer than the antiparallel chains (4.05–4.08 Å). With respect to **3CAm16**, within the unit cell, the four closest molecules include both antiparallel and parallel. With respect to **3CAm15**, the four closest molecules are exclusively antiparallel, the parallel chains are farther away from each other than the antiparallel chains. The X-ray crystal structure of **3EAm15** and **3CAm16** both have an H-bond between a carbonyl oxygen (red sphere) and the NH amide (blue sphere). The H-bond distance in **3CAm16** (2.969 Å) is almost identical to that of **3CAm15** (2.970 Å).

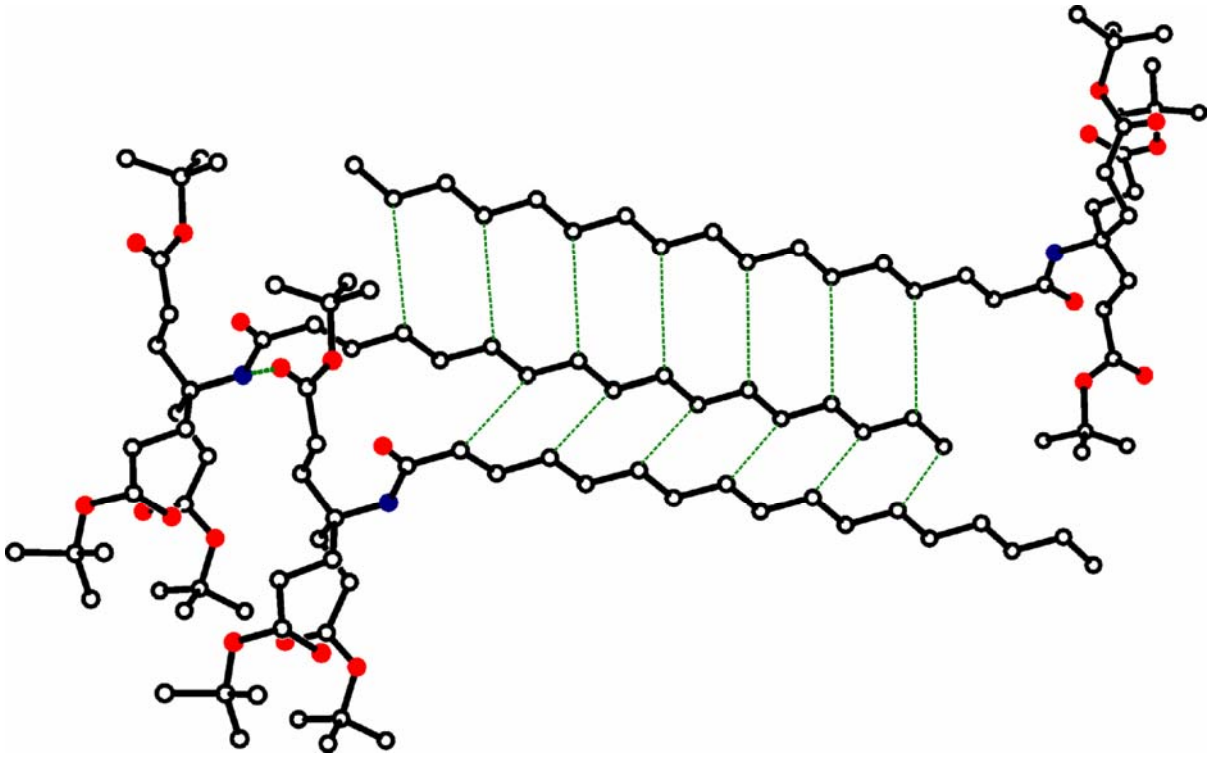

Figure 2.2 X-ray Crystal Structure of **3EAm16**. Picture obtained from Dr. Carla Slebodnick.

2.15 Attempted Synthesis of 3EAmn Series via Condensation of Carboxylic Acid and Weisocyanate™

Multiple attempts were made to replicate Scheme 2.5 by combining **15** and C_{18} acid at elevated temperatures (Scheme 2.12). The IR spectrum showed the formation of an amide bond. However, ^{1}H NMR spectra showed the presence of multiple side products.

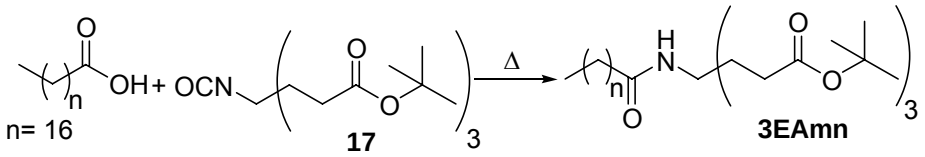

Scheme 2.12 Attempted Coupling of Weisocyanate with Long-Chain Fatty Acids

2.16 Formation of the 3CAmn Series

The formation of the **3CAmn** series from **3EAmn** proceeded with relative ease (Scheme 2.13). Following the reaction, a white mixture was concentrated. The resulting solid was recrystallized in either ethyl acetate or acetic acid/hexane, resulting in moderate-good yields (65–86%).

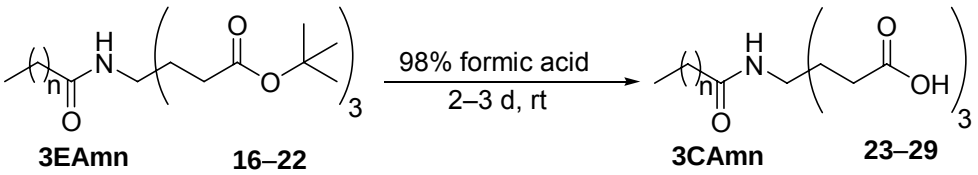

Scheme 2.13 Formolysis of the **3CAmn** Series

2.17 X-ray Crystal Structure of 3CAm13

The X-ray crystal structure of **3CAm13** has some similarities to the crystal structures of **3EAm15** and **3EAm16**. The X-ray crystal structure of **3CAm13** has parallel and antiparallel alkyl chain packing. However, there is extensive H-bonding of the carboxylic acid groups. Antiparallel chains pack significantly closer than parallel chains (Figure 2.3). For anti-parallel chains, every other carbon lies close to a corresponding carbon in the neighboring chain, dashed

green lines indicate the C…C distance (3.88–4.12 Å). Six strong intermolecular hydrogen bonds form with four neighboring molecules. There are four acid–acid (O…O distances, 2.636–2.656 Å and two acid–amide (O…O distances, 2.676 Å and 2.660 Å hydrogen bonds (not shown). In the latter, the acid O–H is the donor and the amide carbonyl oxygen is the acceptor.

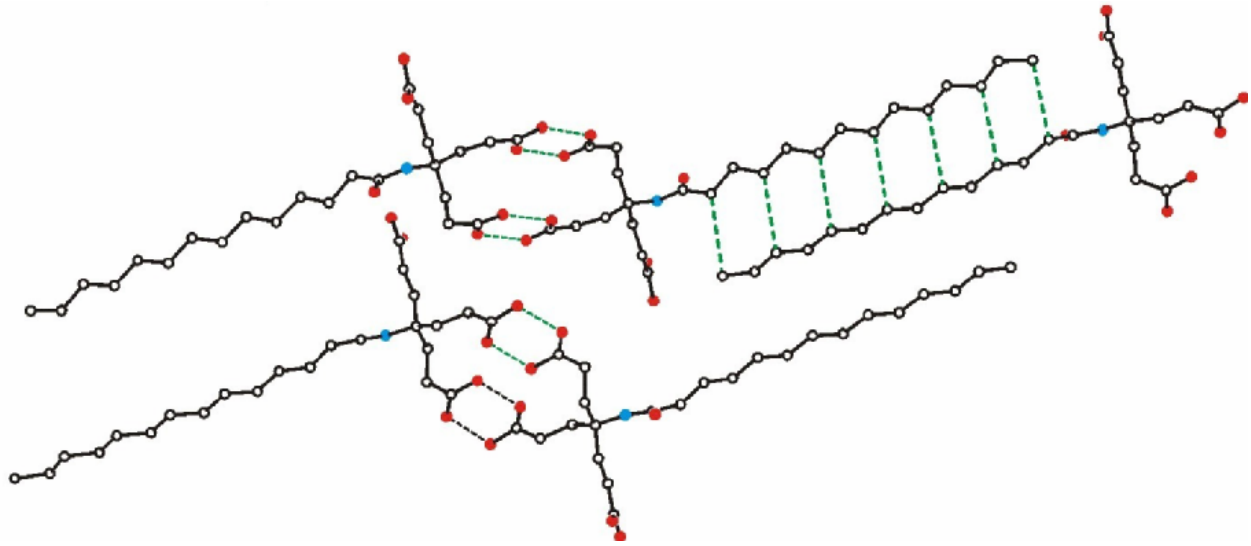

Figure 2.3 X-ray Crystal Structure of **3CAm13**. Picture obtained from Dr. Carla Slebodnick.

2.18 Solubility Studies of the 3CAmn Series

Triethanolamine, which is found in several cosmetic and health care products, is a weak base (pK_a = 7.76). (Stock solutions of the amphiphiles in aqueous triethanolamine had a pH of 8–9). Comparable solubility data for FAs in triethanolamine are not in the open literature.

A micromolar comparison of the solubilities in phosphate buffer of the **3CAmn** series and saturated FAs[21] show that the solubilities fell as the chain length increased (Table 2.3). For FAs, the drop-off in solubility was substantial with each addition of two carbons. In the **3CAmn** series, a slight decrease in solubility occurred for **3CAm13** to **3CAm17**, followed by a dramatic decrease in solubility for **3CAm19,** then a modest decrease for **3CAm21**. Comparisons of the two series revealed that the tricarboxylato amphiphiles were substantially more soluble in neutral phosphate buffer than the saturated FAs.

Table 2.3 Aqueous Solubility Comparisons of Fatty Acids and the **3CAmn** Series

Fatty group		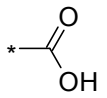 From ref. 20. pH 7.4	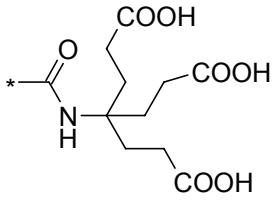 pH 7.2	
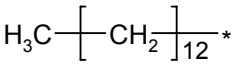	C_{14}	20–30 μM	**3CAm13**	6900 μM
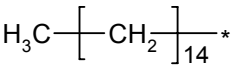	C_{16}	~1 μM (visibly clear)	**3CAm15**	3400 μM
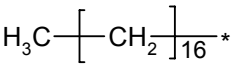	C_{18}	<<1 μM (visibly clear)	**3CAm17**	1700 μM
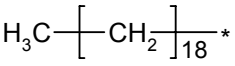	C_{20}	Not measured	**3CAm19**	140 μM
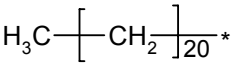	C_{22}	Not measured	**3CAm21**	79 μM

2.19 Cmc Measurements of the 3CAmn Series

Cmc (critical micelle concentration) values were attained by measurements done by Richard Macri (Table 2.4). As expected, the cmc decreased with chain length. The cmc for **3CAm13** was not measured because the cmc, if there was a cmc, would be too high. Amphiphile **3CAm13** might be too hydrophilic to form micelles. Initially, there were big declines in cmc as the chain length of the amphiphiles increased. The cmc dropped ≈35% from **3CAm15** to **3CAm17**. A dramatic drop (≈77%) in cmc was observed between **3CAm17** and **3CAm19**. A smallest drop in cmc (33%) was observed between **3CAm19** and **3CAm21**. The drops in cmc between amphiphiles appear to follow the trend observed for drops in aqueous solubility (Table 2.4).

Table 2.4 Cmcs (μM) of the **3CAmn** Series

Amphiphile	Cmc
3CAm13	>>17000
3CAm15	17000
3CAm17	11000
3CAm19	3000
3CAm21	2000

3CAm14 and **3CAm16** were not tested.

2.20 General Comments for Synthetic Work

Melting point data were obtained with a digital melting point apparatus. ^{1}H and ^{13}C NMR spectra were obtained at 500 and 125 MHz, respectively; TMS was used as the internal reference in ^{1}H spectra. IR spectra were obtained on neat samples with an FTIR equipped with a diamond ATR system. HRMS data were obtained on a dual-sector mass spectrometer in FAB mode with 2-nitrobenzylalcohol as the proton donor. Elemental analyses were performed by Atlantic Microlabs, Inc. in Norcross, GA. Solutions were concentrated by rotary evaporation unless specified otherwise. Unless specified, solvents and reagents were used as received. THF was dried with Na and benzophenone. Benzene was dried with molecular sieves. Tetradecanoyl, pentadecanoyl, heptadecanoyl, and octadecanoyl chloride were synthesized via a reaction of the corresponding carboxylic acid in refluxing thionyl chloride and a few drops of DMF for 48 h; the products were purified by bulb-to-bulb distillation until a clear, colorless liquid was obtained. Di-*tert*-butyl-4-amino-4-heptanedioate (Behera's Amine) was synthesized as previously described.[1]

2.21 General Procedure for the Synthesis of the 3EAmn Series: Procedure A

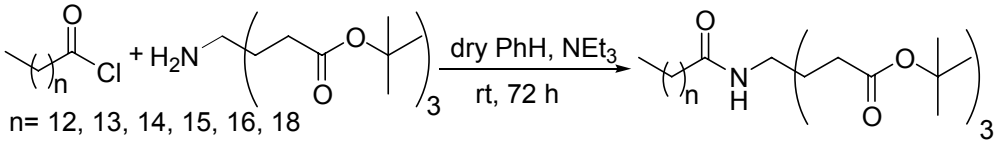

Scheme 2.14 Condensation of Behera's Amine with Long-Chain Acid Chlorides

Behera's amine (12.0 mmol) was dissolved in dry PhH (60 mL). Triethylamine (14.4 mmol) and the appropriate acid chloride (12.6 mmol) were added to the flask. The additions immediately resulted in a cloudy solution. The solution was stirred for 72 h at rt. The reaction mixture was washed with saturated aq. $NaHCO_3$, water, cold 10% aq. HCl, and brine. The solution was dried with Na_2SO_4. After filtration, the solution was concentrated yielding an off-white solid, which was recrystallized in $EtOH/H_2O$ to yield white needles or a white solid (61–84%).

2.22 Alternate Procedure for the Synthesis of the 3EAmn Series: Procedure B

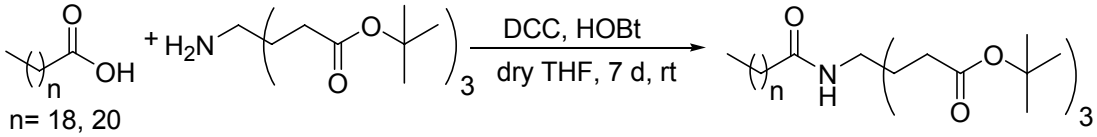

Scheme 2.15 Coupling of Behera's Amine with Long-Chain Carboxylic Acids

A mixture of the appropriate carboxylic acid (12.0 mmol), Behera's amine (12.6 mmol), DCC (12.0 mmol), and 1-hydroxybenzotriazole (12.03 mmol) was dissolved in dry THF (365 mL) and stirred at rt. A white precipitate crashed out of solution after approximately 1 h. The solution was stirred for 7 d. The precipitate was vacuum filtered; the filtrate was concentrated with a rotary evaporator. The slightly yellow solid was redissolved in CH_2Cl_2. The solution was placed in the freezer overnight. The resulting precipitate was again removed by vacuum filtration. The filtrate was washed with cold 10% aq HCl, water, saturated aq. $NaHCO_3$, and brine. The solution was dried with Na_2SO_4. After filtration, the solvent was concentrated yielding an off-white solid, which was recrystallized from with $EtOH/H_2O$ to yield a white solid (61–82%).

2.23 Experimental Procedures for the Formation of the 3EAmn Series

Di-*tert*-butyl 4-(2-(*tert*-butoxycarbonyl)ethyl)-4-(1-oxotetradecylamino)heptanedioate, 3EAm13

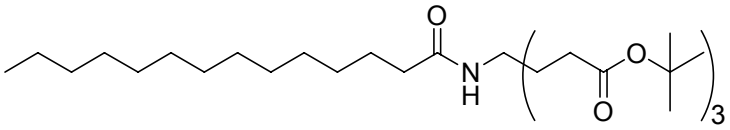

The general procedure (A) described above afforded a white solid (5.81 g, 77%); mp 72.8–73.7 °C; ^{1}H NMR ($CDCl_3$): δ 0.87 (t, 3H), 1.24–1.29 (bm, 20H), 1.42 (s, 27H), 1.57 (m, 2H), 1.95 (m, 6H), 2.08 (t, 2H), 2.21 (m, 6H), 5.78 (s, 1H); ^{13}C NMR ($CDCl_3$): δ 14.2, 22.8, 25.9, 28.1, 29.40, 29.43, 29.45, 29.6, 29.7, 29.9, 30.1, 32.0, 37.7, 57.3, 80.7, 172.7, 173.0; IR: 3358, 2918, 1719, 1709, 1676, 1536, 1147 cm^{-1}; HRMS: for $C_{36}H_{68}NO_7$ $(M + H)^+$ calcd 626.4996, found 626.4981. Anal. Calcd for $C_{36}H_{67}NO_7$: C, 69.08; H, 10.79; N, 2.24. Found: C, 69.22; H, 10.91; N, 2.34.

Di-*tert*-butyl-4-(2-(*tert*-butoxycarbonyl)ethyl)-4-(1-oxopentadecylamino)heptanedioate, 3EAm14

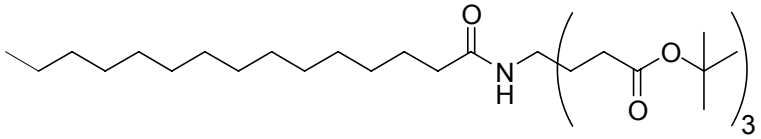

The general procedure described in the manuscript afforded a white solid (5.94 g, 76%); mp 66.4–67.2°C; ^{1}H NMR ($CDCl_3$): δ 0.87 (t, 3H), 1.24–1.30 (bm, 22H), 1.43 (s, 27H), 1.58 (bm, 2H), 1.96 (m, 6H), 2.08 (t, 2H), 2.21 (m, 6H), 5.77 (s, 1 H); ^{13}C NMR ($CDCl_3$) δ 14.2, 22.7, 25.9, 28.1, 29.39, 29.42, 29.44, 29.58, 29.71, 29.76, 29.89, 30.06, 37.7, 57.3, 80.7, 172.7, 173.0; IR 3362, 2918, 2851, 1718, 1708, 1676, 1536, 1149 cm^{-1}; HRMS: for $C_{37}H_{70}NO_7$ $(M + H)^+$ calcd

640.5152, found 640.5160. Anal. Calcd for $C_{37}H_{69}NO_7$: C, 69.44; H, 10.87; N, 2.19. Found: C, 69.42; H, 10.87; N, 2.21.

Di-*tert*-butyl 4-(2-(*tert*-butoxycarbonyl)ethyl)-4-(1-oxohexadecylamino)heptanedioate, 3EAm15

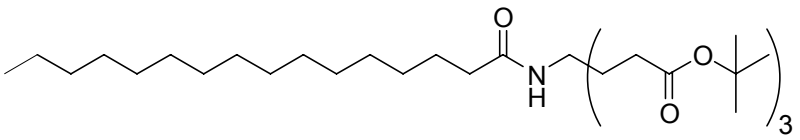

The general procedure (A) described above afforded a white solid (6.58 g, 84%); mp 62.6–63.3 °C; ^{1}H NMR ($CDCl_3$): δ 0.87 (t, 3H), 1.24–1.29 (bm, 24H), 1.42 (s, 27H), 1.56 (bm, 2H), 1.95 (m, 6H), 2.08 (t, 2H), 2.21 (m, 6H), 5.77 (s, 1H); ^{13}C NMR ($CDCl_3$): δ 14.2, 22.7, 25.9, 28.1, 29.37, 29.41, 29.43, 29.57, 29.71, 29.75, 29.88, 30.04, 30.18, 32.0, 37.7, 57.3, 80.7, 172.7, 173.0; IR: 3395, 2914, 1730, 1725, 1713, 1669, 1526, 1146 cm^{-1}; HRMS: for $C_{38}H_{72}NO_7$ $(M + H)^+$ calcd 654.5269, found 654.5309. Anal. Calcd for $C_{38}H_{71}NO_7$: C, 69.79; H, 10.94; N, 2.14; O, 17.12. Found: C, 69.76; H, 10.96; N, 2.21; O, 17.14.

X-ray analysis of 3EAm15

The analysis was done by Dr. Carla Slebodnick (Table 2.5). Long thin needles (~1.0 x 0.2 x 0.01 mm^3) were grown from slow cooling an ethanol/water solution. A needle was cut (~0.23 x 0.18 x 0.011 mm^3), mounted on a nylon CryoLoop™ (Hampton Research) with Krytox® Oil (DuPont) and centered on the goniometer of a Oxford Diffraction XCalibur2™ diffractometer equipped with a Sapphire™ CCD detector. The data collection routine, unit cell refinement, and data processing were all carried out with the program CrysAlis. Unit cell dimensions were consistent with the triclinic system and the space group $P\bar{1}$ was assigned. The structure was solved by direct methods and refined using the SHELXTL NT program package.

The final refinement involved an anisotropic model for all non-hydrogen atoms. Idealized hydrogen atom positions and thermal parameters were calculated. The program package SHELXTL NT was used for molecular graphics generation.

Table 2. 5 Crystal Data and Structure Refinement of **3EAm15**. Data obtained from Dr. Carla Slebodnick.

Category	Crystal Data and Structure Refinement	
Empirical formula	$C_{38}H_{71}NO$	
Formula weight	653.96	
Temperature	293(2) K	
Wavelength	0.71073 Å	
Crystal system	Triclinic	
Space group	P-1	
Unit cell dimensions	a = 5.6653(9) Å	α= 82.928(8)°
	b = 9.9138(10) Å	β= 89.815(10)°
	C = 35.868(3) Å	γ = 81.801(10)°
Volume	1978.6(4) $Å^3$	
Z	2	
Density (calculated)	1.098 Mg/m^3	
Absorption coefficient	0.074 mm^{-1}	
F(000)	724	
Crystal size	0.23 x 0.18 x 0.011 mm^3	
Theta range for data collection	2.86 to 25.05°	
Index ranges	$-6 \le h \le 4$, $-11 \le k \le 11$, $-42 \le l \le 42$	
Reflections collected	13578	
Independent reflections	7015 [R(int) = 0.0706]	
Completeness to theta = 30.07°	99.8 %	
Absorption correction	None	
Refinement method	Full-matrix least-squares on F^2	
Data / restraints / parameters	7015 / 0 / 425	
Goodness-of-fit on F^2	1.022	
Final R indices [I>2sigma(I)]	R1 = 0.0658, wR2 = 0.1215	
R indices (all data)	R1 = 0.1205, wR2 = 0.1396	
Largest diff. peak and hole	0.243 and -0.250 $e.Å^{-3}$	

Di-*tert*-butyl 4-(2-*tert*-butoxycarbonyl)ethyl)-4-(1-oxoheptadecylamino)heptanedioate, 3EAm16

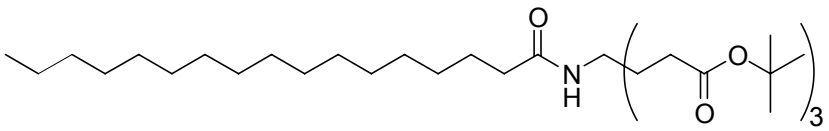

Procedure A afforded a yellow solid (7.47 g). During the recrystallization of the yellow solid in EtOH/water, a yellow solid formed. The clear, colorless liquid was decanted and left sitting at room temperature. The resulting white solid, 2.74 g, was removed via filtration. The filtrate was placed in a refrigerator overnight, which yielded a yellow solid (3.76 g). Additional material could possibly be attained from this filtrate. The ^{1}H NMR of the white solid was unsatisfactory; therefore, the solid was recrystallized again in EtOH/water, yielding white needles (2.02 g, 25%). This material was used in the subsequent formolysis reactions; mp 64.5–65.3 °C; ^{1}H NMR ($CDCl_3$) δ 0.87 (t, 3H), 1.25–1.28 (bm, 26H), 1.43 (s, 27H), 1.96 (m, 6H), 2.09 (m, 2H), 2.21 (m, 6H), 5.78 (s, 1H); ^{13}C NMR ($CDCl_3$) δ 14.2, 22.7, 25.9, 28,1, 29.37, 29.42, 29.57, 29.71, 29.75, 29.87, 30.0, 32.0, 37.7, 57.3, 80.7, 172.7, 173.0; IR 3381, 2915, 1729, 1727, 1712, 1671, 1529, 1146 cm^{-1}; HRMS: for $C_{39}H_{74}NO_7$ $(M + H)^+$ calcd 668.5465, found 668.5461. Anal. Calcd for $C_{39}H_{73}NO_7$: C, 70.12; H, 11.01; N, 2.10. Found: C, 69.77; H, 10.92; N, 2.09.

X-ray analysis of 3EAm16

The analysis was done by Dr. Carla Slebodnick (Table 2.6). Colorless needles (0.62 x 0.14 x 0.10 mm^3) were crystallized by slow cooling ethanol from 60 °C to room temperature. The chosen crystal was mounted on a nylon CryoLoop™ (Hampton Research) with Krytox® Oil (DuPont) and centered on the goniometer of an Oxford Diffraction Xcalibur2™ diffractometer equipped with a Sapphire 2™ CCD detector. The data collection routine, unit cell refinement, and data processing were carried out with the program CrysAlis. The unit cell parameters were consistent with the triclinic space group P-1. The structure was solved by direct methods and refined using the SHELXTL NT program package. The asymmetric unit of the structure comprises one crystallographically independent molecule. The final refinement model involved

anisotropic displacement parameters for non-hydrogen atoms and a riding model for all hydrogen atoms. The program package SHELXTL NT was used for molecular graphics generation.

Table 2.6 Crystal Data and Structure Refinement of **3EAm16**. Data obtained from Dr. Carla Slebodnick.

Category	Crystal Data and Structure Refinement
Empirical formula	$C_{39}H_{73}NO_7$
Formula weight	667.98
Temperature	100(2) K
Wavelength	0.71073 Å
Crystal system	Triclinic
Space group	P -1
Unit cell dimensions	a = 5.6690(17) Å α= 90.960(16)°. b = 9.918(2) Å β= 91.432(19)°. c = 36.317(6) Å γ = 98.21(2)°.
Volume	2020.0(8) $Å^3$
Z	2
Density (calculated)	1.098 Mg/m^3
Absorption coefficient	0.073 mm^{-1}
F(000)	740
Crystal size	0.62 x 0.14 x 0.10 mm^3
Theta range for data collection	3.09 to 25.05°.
Index ranges	-6≤=h≤=6, -11≤=k≤=11, -38≤=l≤=43
Reflections collected	9936
Independent reflections	7140 [R(int) = 0.0751]
Completeness to theta = 30.07°	99.7 %
Absorption correction	None
Refinement method	Full-matrix least-squares on F^2
Data / restraints / parameters	7140 / 0 / 434
Goodness-of-fit on F^2	1.065
Final R indices [I>2sigma(I)]	R1 = 0.0796, wR2 = 0.1999
R indices (all data)	R1 = 0.1238, wR2 = 0.2301
Largest diff. peak and hole	0.923 and -0.402 $e.Å^{-3}$

Di-*tert*-butyl 4-(2-*tert*-butoxycarbonyl)ethyl)-4-(1-oxooctadecylamino)heptanedioate, 3EAm17

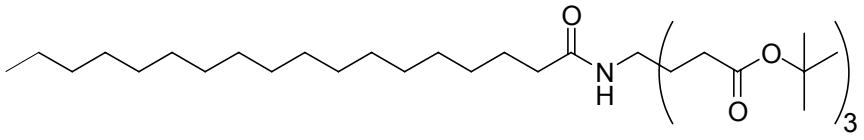

The general procedure (A) described above afforded a white solid (3.99 g, 82%); mp 66.6–67.2 °C; ^{1}H NMR ($CDCl_3$): δ 0.87 (t, 3H), 1.22–1.29 (bm, 28H), 1.42 (s, 27H), 1.57, (m, 2H), 1.95 (m, 6H), 2.08 (t, 2H), 2.21 (m, 6H), 5.77 (s, 1H); ^{13}C NMR ($CDCl_3$): δ 14.2, 22.7,

25.9, 28.1, 29.37, 29.41, 29.6, 29.71, 29.75, 29.87, 30.03, 32.0, 37.7, 57.3, 80.7, 172.7, 173.0; IR: 3397, 2915, 1730, 1725, 1714, 1670, 1528, 1148 cm^{-1}; HRMS: for $C_{40}H_{76}NO_7$ $(M + H)^+$ calcd 682.5622, found 682.5624. Anal. Calcd for $C_{40}H_{75}NO_7$: C, 70.44; H, 11.08; N, 2.05. Found: C, 70.56; H, 11.05; N, 2.07.

Di-*tert*-butyl 4-(2-*tert*-butoxycarbonyl)ethyl)-4-(1-oxoicosylamino)heptanedioate, 3EAm19

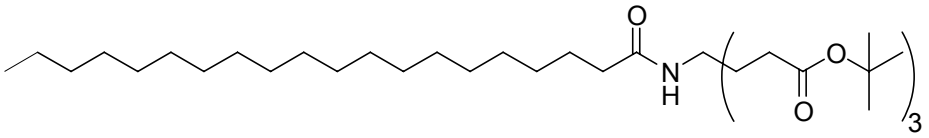

The general procedure (B) described above afforded a white solid (7.84 g, 82%); mp 70.6–71.3 °C; ^{1}H NMR ($CDCl_3$): δ 0.87 (t, 3H), 1.22-1.29 (bm, 32H), 1.42 (s, 27H), 1.57 (m, 2H), 1.95 (m, 6H), 2.08 (t, 2H), 2.21 (m, 6H), 5.77 (s, 1H); ^{13}C NMR ($CDCl_3$): δ 14.2, 22.7, 25.9, 28.1, 29.39, 29.43, 29.44, 29.6, 29.72, 29.76, 29.89, 30.1, 32.0, 37.7, 57.3, 80.71, 172.7, 173.0. IR: 3336, 2914, 1731, 1724, 1713, 1669, 1526, 1147 cm^{-1}; HRMS: for $C_{42}H_{80}NO_7$ $(M + H)^+$ calcd 710.5935, found 710.5923. Anal. Calcd for $C_{42}H_{79}NO_7$: C, 71.04; H, 11.21; N, 1.97. Found: C, 71.18; H, 11.17; N, 1.98.

Di-*tert*-butyl 4-(2-*tert*-butoxycarbonyl)ethyl)-4-(1-oxodocosylamino)heptanedioate, 3EAm21

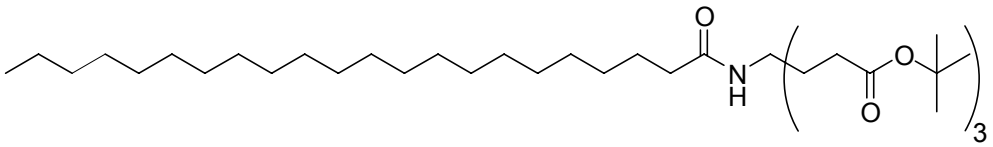

The general procedure (B) described above afforded a white solid (5.70 g, 61%); mp 74.7–75.0 °C; ^{1}H NMR ($CDCl_3$): δ 0.87 (t, 3H), 1.24–1.30 (bm, 36H), 1.42 (s, 27H), 1.57 (m, 2H), 1.95 (m, 6H), 2.08 (t, 2H), 2.21 (m, 6H), 5.77 (s, 1H); ^{13}C NMR ($CDCl_3$): δ 14.2, 22.8, 25.9, 28.2, 29.40, 29.43, 29.6, 29.8, 29.9, 30.1, 32.0, 37.7, 57.3, 80.7, 172.7, 173.0; IR: 3398,

2915, 1731, 1725, 1714, 1670, 1527, 1148; HRMS: for $C_{44}H_{84}NO_7$ $(M + H)^+$ calcd 738.6248, found 738.6212. Anal. Calcd for $C_{44}H_{83}NO_7$: C, 71.60; H, 11.33; N, 1.90. Found: C, 71.82; H, 11.33; N, 1.97.

2.24 General Synthesis of the 3CAmn Series

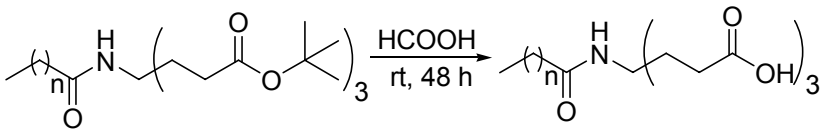

Scheme 2.16 General Synthesis of the **3CAmn** Series

Triesters **3EAm13**, **3EAm14,** and **3EAm16** were dissolved in a minimal amount of 98% or 99% HCOOH and stirred overnight at rt. Cosolvents, THF and acetone were added to get triesters **3EAm15**–**3EAm21** completely into solution; the reactions were stirred for 48 h at rt. The milky white solution was concentrated in vacuo. The white solid was recrystallized from glacial HOAc/hexane to yield a white solid (65–86%).

2.25 Experimental Procedures for the Formation of the 3CAmn Series

4-(2-Carboxyethyl)-4-(1-oxotetradecylamino)heptanedioic Acid, 3CAm13

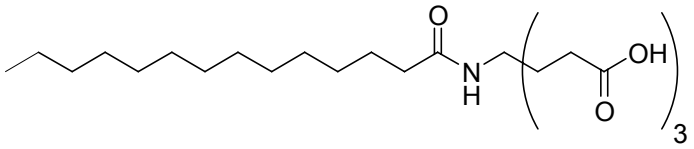

Following the general procedure described above, **3EAm13** (2.00 g, 3.195 mmol) was dissolved in HCOOH (21 mL). Most of the solid dissolved immediately. A small amount of solid remained but slowly went into solution as stirring continued. On work up, the reaction afforded a white solid (1.12 g, 77%); mp 162.7–163.1 °C; ^{1}H NMR (CD_3OD): δ 0.89 (t, 3H), 1.20–1.35 (bm, 20H), 1.58 (m, 2H), 2.00 (m, 6H), 2.16 (t, 2H), 2.26 (m, 6H); ^{13}C NMR (DMSO-d_6): δ 14.5, 22.7, 26.0, 28.6, 29.15, 29.27, 29.34, 29.53, 29.58, 31.9, 36.4, 56.8, 172.6, 175.0; IR:

3419, 3100, 2916, 1719, 1692, 1651, 1529, 1175 cm^{-1}; HRMS: for $C_{24}H_{44}NO_7$ $(M + H)^+$ calcd 458.3118, found 458.3080. Anal. Calcd for $C_{24}H_{43}NO_7$: C, 62.99; H, 9.47; N, 3.06. Found: C, 63.02; H, 9.53; N, 3.11.

X-ray analysis of 3CAm13

The analysis was done by Dr. Carla Slebodnick (Table 2.7). Colorless plates (0.33 x 0.27 x 0.01 mm^3) were crystallized from acetic acid/hexane at rt. The chosen crystal was mounted on a nylon CryoLoop™ (Hampton Research) with Krytox® Oil (DuPont) and centered on the goniometer of an Oxford Diffraction Xcalibur diffractometer equipped with a Sapphire 2 CCD detector. The data collection routine, unit cell refinement, and data processing were carried out with the program CrysAlis. The Laue symmetry was consistent with the triclinic space group P-1. Upon indexing the strongest reflections, it was clear that nonmerohedral twinning was present. Refinement of the UB matrices for the two twin domains showed the twin law to be a 180° rotation about the a-axis. The twinning option of CrysAlis was used to process the data for both orientations. The structure was solved by direct methods (SHELXTL NT) using the data from the major twin component. The final structure refinement was performed using an HKLF 5 format file for twin refinement (SHELXTL NT). The asymmetric unit of the structure comprises 2 crystallographically independent molecules. The final refinement model involved anisotropic displacement parameters for non-hydrogen atoms and a riding model for all hydrogen atoms. Bruker SHELXTL was used for molecular graphics generation. NT was used for molecular graphics generation.

Table 2.7 Crystal Data and Structure Refinement of **3CAm13**. Data obtained from Dr. Carla Slebodnick.

Category	Crystal Data and Structure Refinement	
Empirical formula	$C_{24}H_{43}NO_7$	
Formula weight	457.59	
Temperature	100(2) K	
Wavelength	0.71073 Å	
Crystal system	Triclinic	
Space group	P -1	
Unit cell dimensions	a = 5.4497(8) Å	α= 93.557(11)°.
	b = 15.755(2) Å	β= 91.632(11)°.
	C = 29.520(4) Å	γ = 91.894(12)°.
Volume	2527.2(6) $Å^3$	
Z	4	
Density (calculated)	1.203 Mg/m^3	
Absorption coefficient	0.087 mm^{-1}	
F(000)	1000	
Crystal size	0.33 x 0.27 x 0.01 mm^3	
Theta range for data collection	3.91 to 25.00°	
Index ranges	-6≤=h≤=6, -18≤=k≤=18, -35≤=l≤=35	
Reflections collected	18103	
Independent reflections	8931 [R(int) not calculated due to twin refinement]	
Completeness to theta = 30.07°	99.1 %	
Absorption correction	None	
Refinement method	Full-matrix least-squares on F^2	
Data / restraints / parameters	18103 / 0 / 588	
Goodness-of-fit on F^2	1.631	
Final R indices [I>2sigma(I)]	R1 = 0.1253, wR2 = 0.3922	
R indices (all data)	R1 = 0.1439, wR2 = 0.4168	
Largest diff. peak and hole	0.697 and -0.623 $e.Å^{-3}$	

4-(2-Carboxyethyl)-4-(1-oxopentadecylamino)heptanedioic Acid, 3CAm14

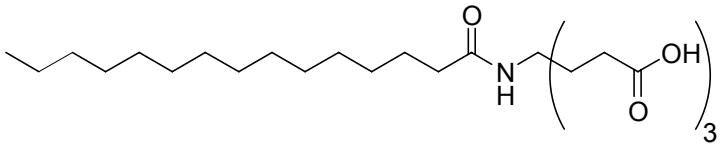

The general procedure described above afforded a white solid (0.42 g, 74%); mp 164.5–164.8 °C; ^{1}H NMR (CD_3OD) δ 0.89 (t, 3H), 1.28–1.32 (bm, 22H), 1.58 (bm, 2H), 2.02 (m, 6H), 2.16 (m, 2H), 2.26 (m, 6H); ^{13}C NMR (DMSO-d_6) δ 14.5, 22.7, 26.0, 28.6, 29.16, 29.28, 29.36, 29.54, 29.58, 29.61, 31.9, 36.4, 56.8, 172.6, 175.0; IR 3413, 3070, 2915, 2847, 1725, 1694,

1628, 1517, 1175 cm^{-1}; HRMS: for $C_{25}H_{46}NO_7$ $(M + H)^+$ calcd 472.3274, found 472.3247. Anal. Calcd for $C_{25}H_{45}NO_7$: C, 63.67; H, 9.62; N, 2.97. Found: C, 63.68; H, 9.67; N, 2.98

4-(2-Carboxyethyl)-4-(1-oxohexadecylamino)heptanedioic Acid, 3CAm15

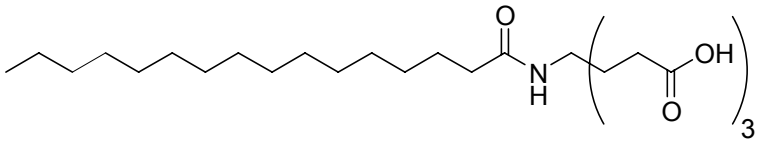

Following the general procedure described above, **3EAm15** (2.33 g, 3.56 mmol) was dissolved in HCOOH (100 mL), acetone (70 mL), and THF (50 mL); the solution was filtered to remove a trace amount of undissolved solids. On work up, the reaction afforded a white solid (1.14 g, 80%); mp 164.5–165.1 °C; ^{1}H NMR (CD_3OD) δ 0.89 (t, 3H), 1.28–1.31 (bm, 24H), 1.58 (bm, 2H), 2.00 (m, 6H), 2.16 (t, 2H), 2.26 (m, 6H); ^{13}C NMR (DMSO-d_6): δ 14.5, 22.7, 26.0, 28.6, 29.17, 29.27, 29.35, 29.6, 31.9, 36.4, 56.8, 172.6, 175.0; IR: 3417, 3100, 2915, 1723, 1694, 1636, 1520,1174 cm^{-1}; HRMS: calcd for $C_{26}H_{48}NO_7$ $(M + H)^+$ 486.3431, found 486.3423. Anal. Calcd for $C_{26}H_{47}NO_7$: C, 64.30; H, 9.75; N, 2.88. Found: C, 64.14; H, 9.74; N, 2.95.

4-(2-Carboxyethyl)-4-(1-oxoheptadecylamino)heptanedioic Acid, 3CAm16

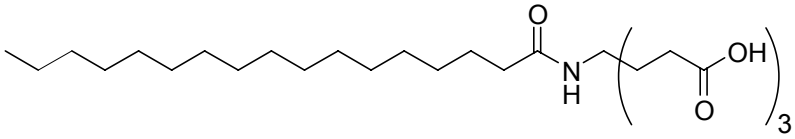

The general procedure described above afforded a white solid (0.57 g, 80%); mp 168.1–168.7 °C; ^{1}H NMR (CD_3OD) δ 0.89 (t, 3H), 1.28–1.32 (bm, 26H), 1.58 (bm, 2H), 2.01 (m, 6H), 2.16 (t, 2H), 2.26 (m, 6H); ^{13}C NMR (DMSO-d_6) δ 14.5, 22.7, 26.0, 28.59, 29.16, 29.27, 29.36, 29.54, 29.61, 31.9, 36.4, 56.8, 172.6, 175.0; IR 3412, 3103, 2915, 1724, 1694, 1628, 1518, 1175

cm^{-1}; HRMS: for $C_{27}H_{50}NO_7$ $(M + H)^+$ calcd 500.3587, found 500.3583. Anal. Calcd for $C_{27}H_{49}NO_7$: C, 64.90; H, 9.88; N, 2.80. Found: C, 64.65; H, 9.71; N, 2.80.

4-(2-Carboxyethyl)-4-(1-oxoicosylamino)heptanedioic Acid, 3CAm17

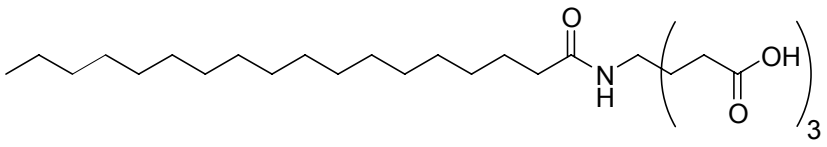

Following the general procedure described above, **3EAm17** (2.54 g, 2.93 mmol) was dissolved in HCOOH (80 mL) and THF (20 mL). On work up, the reaction afforded a white solid (1.40 g, 73%); mp 162.5–163.8 °C; ^{1}H NMR (CD_3OD): δ 0.89 (t, 3H), 1.24–1.31 (bm, 28H), 1.58 (m, 2H), 2.00 (m, 6H), 2.16 (t, 2H), 2.25 (m, 6H); ^{13}C NMR (DMSO-d_6): δ 14.5, 22.7, 26.0, 28.6, 29.17, 29.27, 29.36, 29.56, 29.60, 31.9, 36.4, 56.8, 172.6, 175.0; IR: 3418, 3100, 2916, 1720, 1694, 1652, 1521, 1175 cm^{-1}; HRMS: for $C_{28}H_{52}NO_7$ $(M + H)^+$ calcd 514.3744, found 514.3739. Anal. Calcd for $C_{28}H_{51}NO_7$: C, 64.47; H, 10.01; N, 2.73. Found: C, 64.38; H, 10.16; N, 2.80.

4-(2-Carboxyethyl)-4-(1-oxooctadecylamino)heptanedioic Acid, 3CAm19

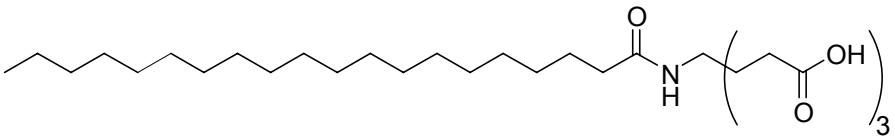

Following the general procedure described above, **3EAm19** (2.06 g, 2.90 mmol) was dissolved in HCOOH (125 mL), THF (40 mL), and acetone (30 mL); the solution was filtered to remove a trace amount of undissolved solids. On work up, the reaction afforded a white solid (1.02 g, 65%); mp 165.9–166.9 °C; ^{1}H NMR (CD_3OD): δ 0.89 (t, 3H), 1.28–1.31 (bm, 32H), 1.58 (m, 2H), 2.00 (m, 6H), 2.16 (t, 2H), 2.26 (m, 6H); ^{13}C NMR (DMSO-d_6): δ 14.5, 22.7, 26.0,

28.6, 29.17, 29.26, 29.36, 29.58, 31.9, 36.4, 56.8, 172.6, 175.0; IR: 3416, 3100, 2916, 1719, 1692, 1651, 1520, 1175; HRMS: for $C_{30}H_{56}NO_7$ $(M + H)^+$ calcd 542.4057, found 542.4052. Anal. Calcd for $C_{30}H_{55}NO_7$: C, 66.51; H, 10.23; N, 2.59. Found: C, 66.28; H, 10.37; N, 2.66.

4-(2-Carboxyethyl)-4-(1-oxodocosylamino)heptanedioic Acid, 3CAm21

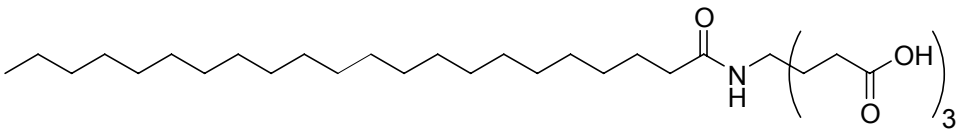

Following the general procedure described above, **3EAm21** (5.69 g, 7.72 mmol) was dissolved in HCOOH (350 mL), THF (40 mL), and acetone (60 mL). On work up, the reaction afforded a white solid (3.77 g, 86%); mp 165.0–165.9 °C; ^{1}H NMR (CD_3OD): δ 0.89 (t, 3H), 1.28–1.31 (bm, 36H), 1.58 (m, 2H), 2.00 (m, 6H), 2.16 (t, 2H), 2.26 (m, 6H); ^{13}C NMR (DMSO-d_6): δ 14.5, 22.7, 26.0, 28.6, 29.18, 29.27, 29.37, 29.56, 31.2, 31.9, 36.4, 56.8, 172.6, 175.0; IR: 3419, 3100, 2916, 1719, 1692, 1651, 1520, 1175 cm^{-1}; HRMS: for $C_{32}H_{60}NO_7$ calcd 570.4370, found 570.4354. Anal. Calcd for $C_{32}H_{59}NO_7$: C, 67.45; H, 10.44; N, 2.46. Found: C, 67.22; H, 10.60; N, 2.52.

2.26 Experimental Procedure for Aqueous Solubility Test of the 3CAmn Series

Solubility of 3CAmn (n = 13, 15, 17, 19, 21)

The solubilities of the odd members of **3CAmn** series were measured in 42 mM phosphate buffer (pH 7.2). Samples of **3CAmn** (n = 13, 15, 17, 19, 21) were placed in a vial and weighed. Buffer solution was added to the vial, which was then placed in a 37 °C water bath for 1 h and the appearance of the solution noted (i.e., clear vs. turbid, opalescent, or suspended particulates). This procedure was repeated by increasing the amount of an amphiphile (if clear) or the amount of buffer (if turbid, opalescent, or suspended particulates) until the appearance of a clear solution persisted for 48 h. Stock solutions (12,500 mg/L) for all homologues were easily

prepared by simply vortexing the tricarboxylic acid in the aqueous triethanolamine solution. Final stock concentrations ranged from 20,800 to 27,300 μM depending on the formula weight of the homologue.

2.27 References for Chapter 2

1. Newkome, G.R., Behera, R. K., Moorefield, C. N., Baker, G. R., *Chemistry of Micelles Series .18. Cascade Polymers - Syntheses and Characterization of One-Directional Arborols Based on Adamantane.* J. Org. Chem., 1991. **56**(25): p. 7162-7167.
2. Akpo, C., Weber, E., Reiche, U., *Synthesis, Langmuir and Langmuir-Blodgett film behaviour of new dendritic amphiphiles.* New J. Chem., 2006. **30**(12): p. 1820-1833.
3. Holden, D.A., H. Ringsdorf, and M. Haubs, *Photosensitive monolayers - photochemistry of long-chain diazo and azide compounds at the air water interface.* J. Am. Chem. Soc., 1984. **106**(16): p. 4531-4536.
4. Cardona, C.M., Wilkes, T., Ong, W., Kaifer, A. E., McCarley, T. D., Pandey, S., Baker, G. A., Kane, M. N., Baker, S. N., Bright, F. V., *Dendrimers functionalized with a single pyrene label: Synthesis, photophysics, and fluorescence quenching.* J. Phys. Chem. B, 2002. **106**(34): p. 8649-8656.
5. Ong, W., Grindstaff, J., Sobransingh, D., Toba, R., Quintela, J. M., Peinador, C., Kaifer, A. E., *Electrochemical and guest binding properties of Frechet- and Newkome-type dendrimers with a single viologen unit located at their apical positions.* J. Am. Chem. Soc., 2005. **127**(10): p. 3353-3361.
6. Adamczyk, M., Chen, Y. Y., Johnson, D. D., Mattingly, P. G., Moore, J. A., Pan, Y., Reddy, R. E., *Chemiluminescent acridinium-9-carboxamide boronic acid probes: Application to a homogenous glycated hemoglobin assay.* Bioorg. Med. Chem. Lett., 2006. **16**(5): p. 1324-1328.
7. Newkome, G.R., He, E. F., *Nanometric dendritic macromolecules: Stepwise assembly by double(2,2':6',2''-terpyridine)ruthenium(I) connectivity.* J. Mater. Chem., 1997. **7**(7): p. 1237-1244.
8. Newkome, G.R., Guther, R., Moorefield, C. N., Cardullo, F., Echegoyen, L., Perez-Cordero, E., Luftmann, H., *Routes to dendritic networks - bis-dendrimers by coupling of cascade macromolecules through metal centers.* Angew. Chem., Int. Ed. Engl., 1995. **34**(18): p. 2023-2026.
9. Safavy, A., Qin, H., Khazaeli, M. B., Buchsbaum *Design and synthesis of a new tripodal hydrazide bifunctional chelatig agent for radiometal labeling of antibodies* J. Labelled Compd. Radiopharm., 1997. **40**: p. 483.
10. Cardona, C.M., McCarley, T. D., Kaifer, A. E., *Synthesis, electrochemistry, and interactions with beta-cydodextrin of dendrimers containing a single ferrocene subunit located "off-center".* J. Org. Chem., 2000. **65**(6): p. 1857-1864.
11. Cardona, C.M., Alvarez, J., Kaifer, A. E., McCarley, T. D., Pandey, S., Baker, G. A., Bonzagni, N. J., Bright, F. V., *Dendrimers functionalized with a single fluorescent dansyl group attached "off center": Synthesis and photophysical studies.* J. Am. Chem. Soc., 2000. **122**(26): p. 6139-6144.

12. Newkome, G.R., Yoo, K. S., Moorefield, C. N., *Spirometallodendrimers: terpyridine-based intramacromolecular cyclization upon complexation.* Chem. Commun., 2002(18): p. 2164-2165.
13. Newkome, G.R., Weis, C. D., Moorefield, C. N., Fronczek, F. R., *Chemistry of micelles series .66. A useful dendritic building block: di-tert-butyl 4-[(2-tert-butoxycarbonyl)ethyl]-4-isocyanato-1,7-heptanedicarboxylate.* Tetrahedron Lett., 1997. **38**(40): p. 7053-7056.
14. Newkome, G.R., Weis, C. D., Childs, B. J., *Syntheses of 1 → 3 branched isocyanate monomers for dendritic construction.* Des. Monomers Polym., 1998. **1**: p. 3-14.
15. Newkome, G.R., Woosley, B. D., He, E., Moorefield, C. N., Guether, R., Baker, G. R., Escamilla, G. H., Merrill, J., Luftmann, H., *Supramolecular chemistry of flexible, dendritic-based structures employing molecular recognition.* Chem. Commun., 1996. **24**: p. 2737-2738.
16. Newkome, G.R., Childs, B. J., Rourk, M. J., Baker, G. R., Moorefield, C. N., *Dendrimer construction and macromolecular property modification via combinatorial methods.* Biotechnol. Bioeng., 1999. **61**(4): p. 243-253.
17. Newkome, G.R., *Heterocyclic loci within cascade dendritic macromolecules.* J. Heterocycl. Chem., 1996. **33**(5): p. 1445-1460.
18. Newkome, G.R., Godinez, L. A., Moorefield, C. N., *Molecular recognition using beta-cyclodextrin-modified dendrimers: novel building blocks for convergent self-assembly.* Chem. Commun., 1998. **17**: p. 1821-1822.
19. Moriyama, H., Hiramatsu, Y., Kiyoi, T., Achiha, T., Inoue, Y., Kondo, H., *Studies on selectin blocker. 9. SARs of non-sugar selectin blocker against E-, P-, L-selectin bindings.* Bioorg. Med. Chem., 2001. **9**(6): p. 1479-1491.
20. Hiramatsu, Y., Tsukida, T., Nakai, Y., Inoue, Y., Kondo, H., *Study on selectin blocker. 8. Lead discovery of a non-sugar antagonist using a 3D-pharmacophore model.* J. Med. Chem., 2000. **43**(8): p. 1476-1483.
21. Vorum, H., Brodersen, R., Kragh-Hansen, U., Pedersen, A. O., *Solubility of long-chain fatty acids in phosphate buffer at pH 7.4. .* Biochim. Biophyis. Acta., 1992. **1126**(2): p. 135-142.

Chapter 3. Synthesis of 3DMAUr18Me, 3MorUr18Me, 3DMAUrn and 3MorUrn Series

3.1 Overall Synthesis of 3DMAUr18Me, 3MorUr18Me, 3DMAUrn and 3MorUrn Series

Following the success of the **3CAmn** series, we attempted to synthesize a homologous series of tricationic amphiphiles (Scheme 3.1). Unlike the **3CAmn** series, which contained intermediates that were previously synthesized and published (**13** and **15**), all intermediates in the attempted synthesis of **3DMAUr18Me**, **3MorUr18Me**, and the **3DMAUrn** and **3MorUrn** series would be new compounds.

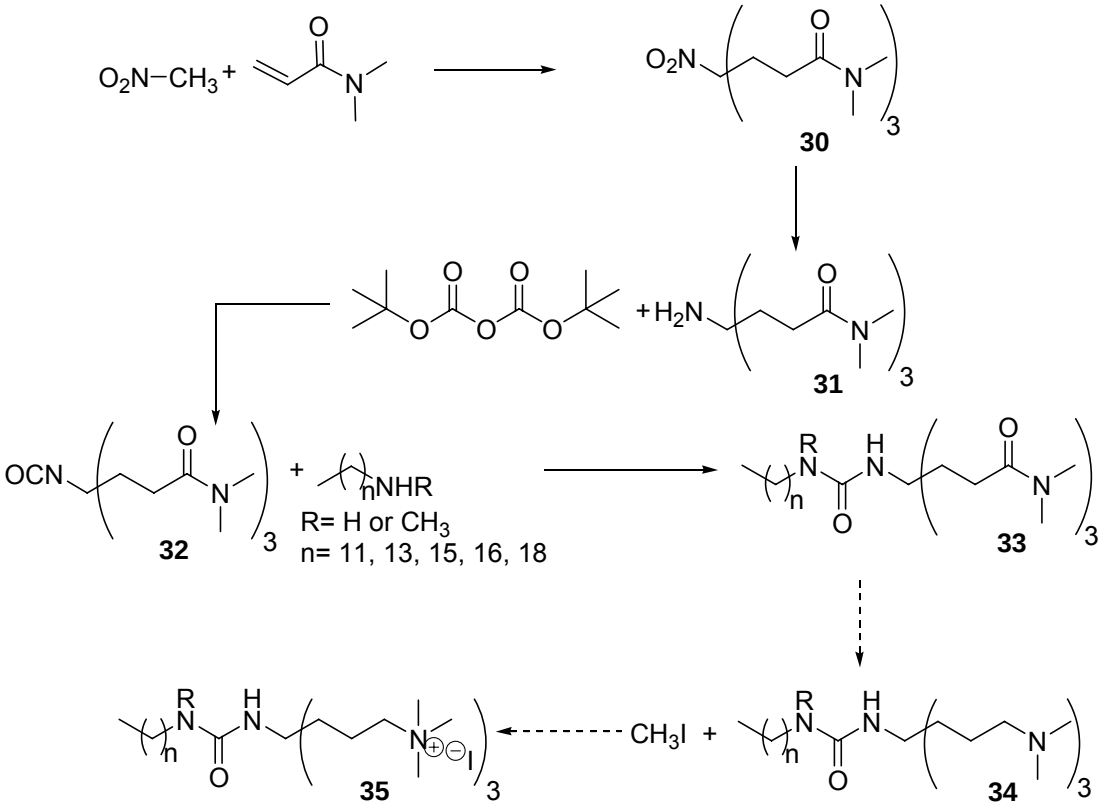

Scheme 3.1 Attempted Synthesis of Tricationic Amphiphiles

Along the synthetic route to **35**, we discovered that **33** was water soluble. To date, the attempted syntheses of the tricationic amphiphiles are unsuccessful; however, the observation

that the trisdimethylamide intermediates are water soluble prompted us to test these intermediates as antimicrobial agents. Following the successful synthesis of **33** (which represents the **3DMAUrn** series and **3DMAUr18Me**), we decided to synthesize the morpholino analogs of the **3DMAUrn** series and **3DMAUr18Me** (Scheme 3.2).

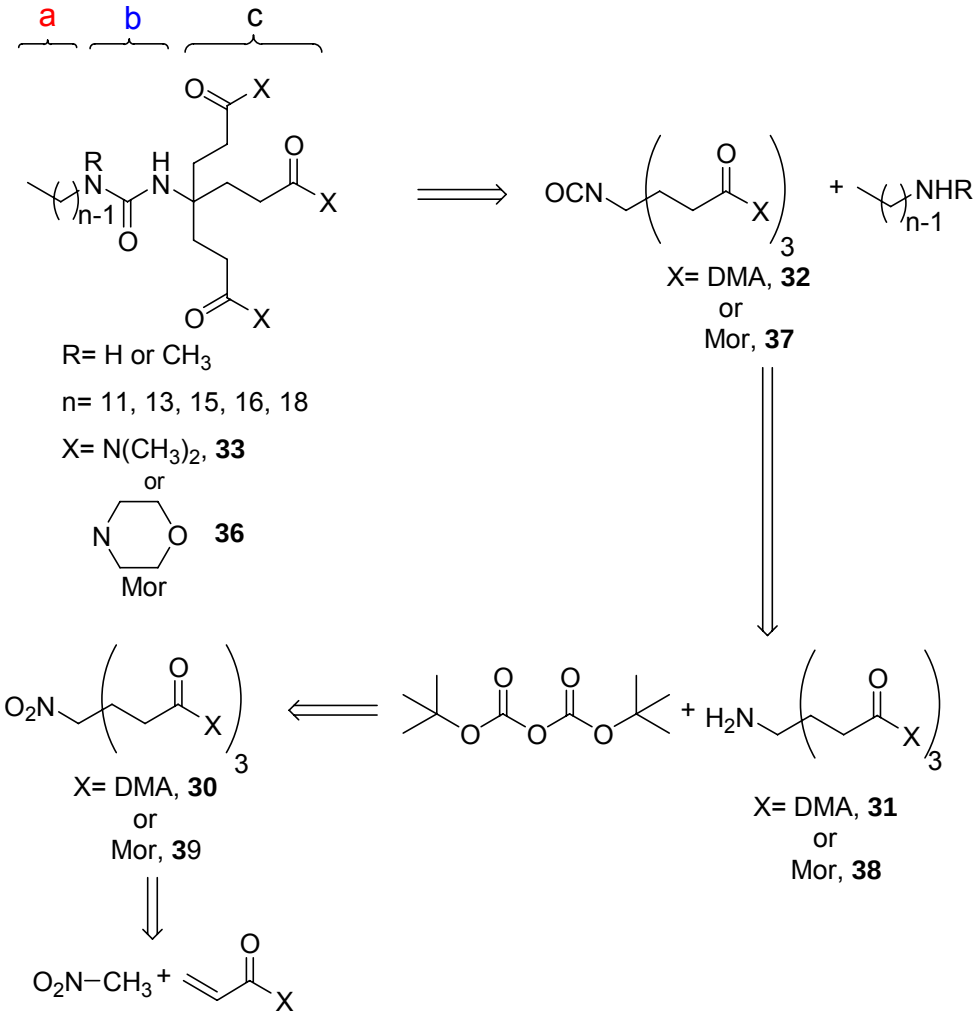

a. hydrophobic moiety; b. uriedo linker; c. *N,N*-dimethyl or morpholino amide headgroups

Scheme 3.2 Retrosynthesis of **3DMAUr18Me**, **3MorUr18Me**, and the **3DMAUrn** and **3MorUrn** Series

This homologous series is abbreviated **3DMAUrn**, where "**3DMA**" represents three dimethylamido headgroups, "**Ur**" represents the ureido linker, and "**n**" represents the number of

carbons in the hydrophobic carbon tail. The hydrophobic tail was attached to the hydrophilic **DMA** headgroup by combining the isocyanate with a variety of long-chain fatty amines. [1]

Similar to the **3DMAUrn** series, all intermediates and the final amphiphile products of the **3MorUrn** series are new compounds. This homologous series is abbreviated **3MorUrn**, where "**3Mor**" represents three morpholinoamide headgroups, "**Ur**" represents the ureido linker, and "**n**" represents the number of carbons in the hydrophobic tail. The hydrophobic tail was attached to the hydrophilic **Mor** headgroup by combining the isocyanate with a variety of long-chain fatty amines.[1]

3.2 Formation of Mono, Di, and Trinitroamides

Patterson and Barnes used KF for the formation of nitromono-, di-, and triamides (Scheme 3.3).[2] Unfortunately, an increase in the number of headgroups led to a decrease in percent yield. The triamide product was obtain in the lowest yield (30%), followed by the diamide (46%), and monoamide (75%).

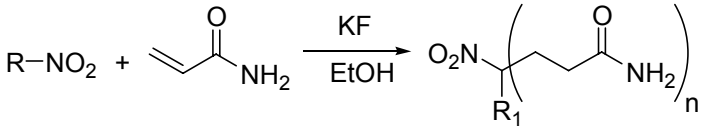

R= methyl
ethyl
isopropyl

n=3, R_1=H
n=2, R_1= CH_3
n=1, R_1= $(CH_3)_2$

Scheme 3.3 Formation of Mono-, Di-, and Triamides utilizing Potassium Fluoride

Other researchers reported the Michael addition of nitromethane with various acrylamides. Newkome et al. reported the Michael addition of nitromethane and *N*-{5-[4′-(2,2′:6′,2″)terpyridinyloxy]pentyl}acrylamide in 75% yield (Scheme 3.4).[3] This procedure led to the formation of a nitromonoamide.

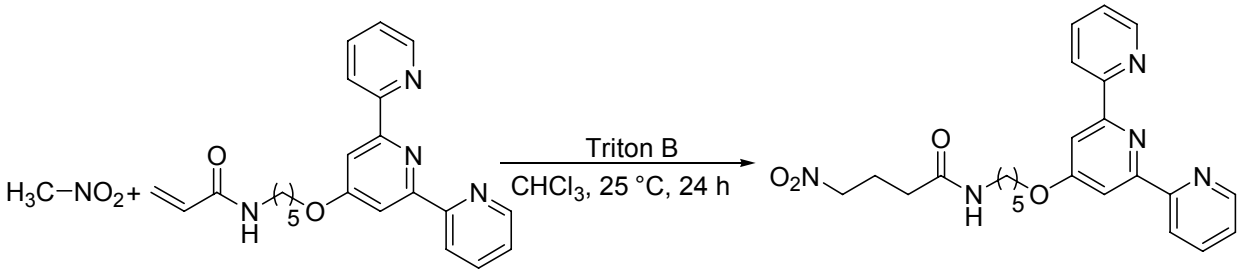

Scheme 3.4 Michael Addition Formation of a Nitromonoamide

Newkome et al. reported the Michael addition of nitromethane with the acrylamido analog of **13** in 95% yield (Scheme 3.5). Tetramethylguanidine (TMG) was used as the basic catalyst instead of the customary Triton B.[4]

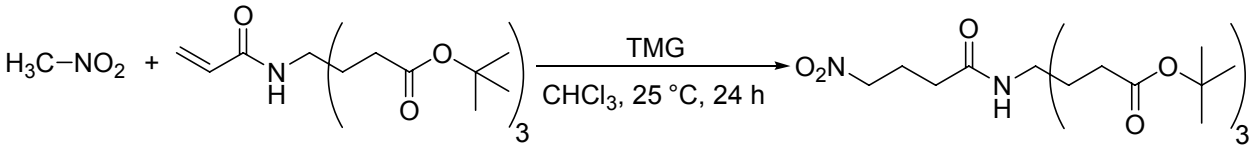

Scheme 3.5 Michael Addition Formation of a Nitromono-*tert*-amide

Newkome et al. reported the Michael addition took place when the product obtained (Scheme 3.5) reacted with an acrylamido analogue to give the corresponding nitrotriamide in 91% yield (Scheme 3.6).[4]

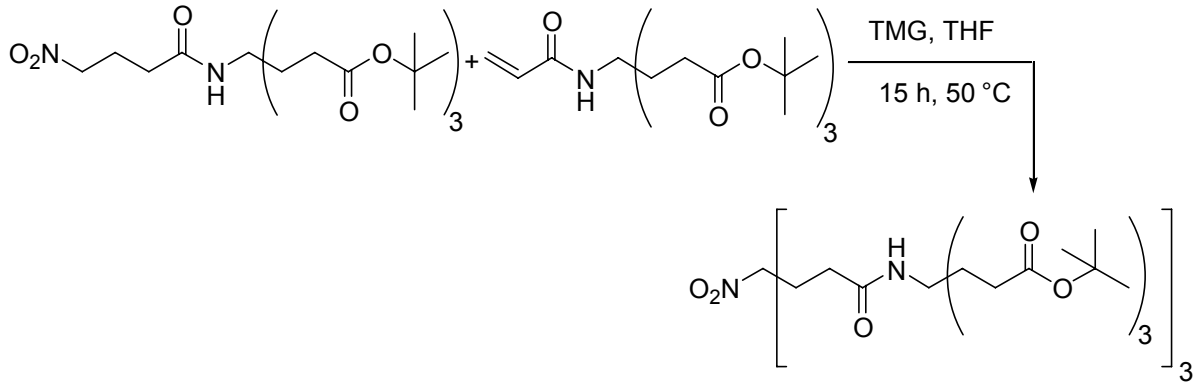

Scheme 3.6 Michael Addition Formation of a Nitrotriamide

3.3 Formation of Aminotriamides

Newkome et al. reported the Raney Ni reduction of a nitrotriamide to the corresponding aminotriamide in 95% yield (Scheme 3.7).[4] This procedure was similar, with minor changes in temperature and time, to the procedure used in the formation of Behera's amine.[5]

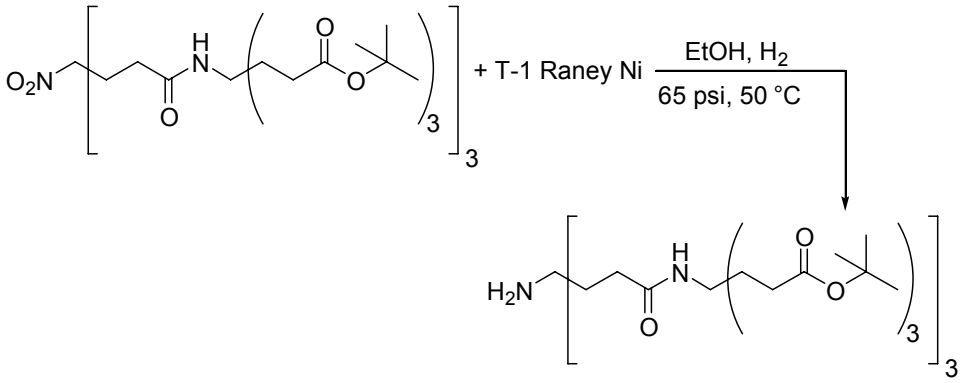

Scheme 3.7 Raney Ni Reduction of a Nitrotriamide

3.4 Formation of Triamidoisocyanate

Newkome et al. reported the conversion of a nitrotriamide into an isocyanotriamide using triphosgene, under an inert nitrogen atmosphere (Scheme 3.8).[4] The product was obtained in moderate yield (70%).

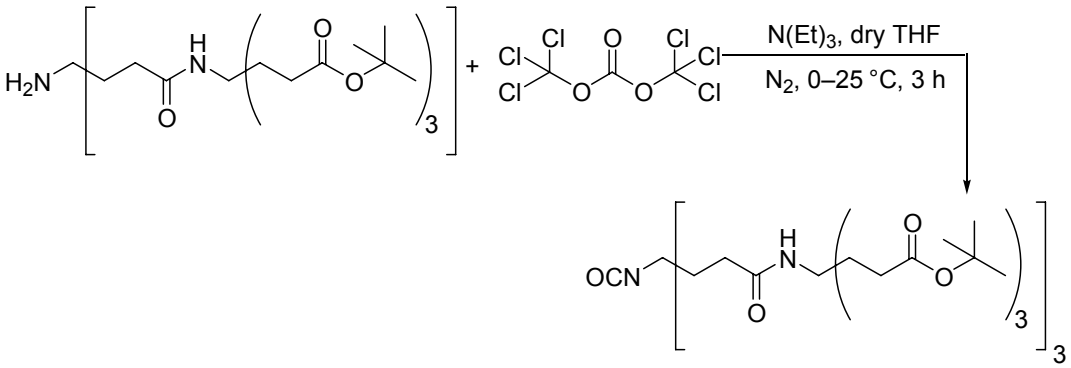

Scheme 3.8 Formation of a Triamidoisocyanate

3.5 Synthetic Strategy for the Formation of 3DMAUr18Me, 3MorUr18Me and the 3DMAUrn and 3MorUrn Series

The first three steps of the **3DMAUrn** synthesis are very similar to those of the reported[6] formation of **15** (Scheme 3.9). The first step is a Michael addition reaction involving nitromethane and *tert*-butyl acrylate. This step mirrors the formation of **30** and **39**. The next step is the Raney Ni reduction of the nitro-*tert*-butyl ester into **13**. This step mirrors the formation of **31** and **38**. The last step is the conversion of **13** into **15**. This step mirrors the formation of **32** and **37**.

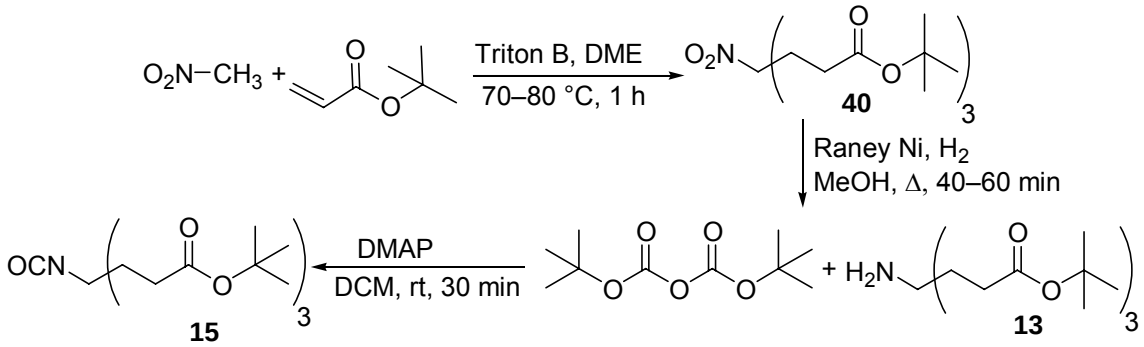

Scheme 3.9 Newkome et al. Synthesis of Weisocyanate™

3.6 Synthesis of 4-(2-Dimethylcarbamoyl-ethyl)-4-nitro-heptanedioic acid bis-dimethylamide (30) and 1,7-Di-morpholin-4-yl-4-(3-morpholin-4-yl-3-oxo-propyl)-4-nitro-heptane-1,7-dione (39)

The procedure (Scheme 3.10) used for the synthesis of both **DMA** and **Mor** triamides is directly based on the synthesis **40**. Adjustments were made for the differing solubilities and reactivity of the reagents involved.

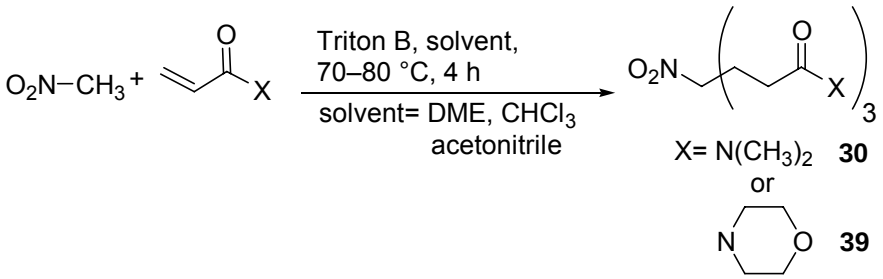

Scheme 3.10 Formation of **DMA-** and **Mor-** Headgroups

One major difference between our procedure and the Newkome et al. procedure[6] (first reaction of Scheme 3.9) was reaction time. In the cases of triamides, the reaction ran for 4 h instead of 1 h for the formation of **40**. Initially, the reaction involving *N*,*N*-dimethylacrylamide ran for 1 h, however, the yields were low. Consequently, after 4 h, the yields were better. The extended reaction time was probably due to *N*,*N*-dimethylacrylamide not being as electrophilic as *tert*-butyl acrylate. The decreased electrophilic character of *N*,*N*-dimethylacrylamide is probably due to amide resonance, which results in the terminal carbon of the alkene being less electrophilic. The reaction involving 4-acryloylmorpholine was initially run for 4 h because of belief that 4-acryloylmorpholine would have a similar reactivity to that of *N*,*N*-dimethylacrylamide.

While the formation of **30** proceeded without incident, the synthesis of **39** required major adjustments. The reason lies with the relative insolubility of **39** in many organic solvents. During the synthesis of **39**, 4-acryloylmorpholine was added in two portions. Following the first addition of 4-acryloylmorpholine in DME, precipitation occurred. It was not known if the precipitate was the final product, one-headed derivative, or two-headed derivative of the desired product. To ensure that the reaction went to completion, $CHCl_3$ was added to dissolve the precipitate, followed by the addition of the remaining 4-acryloylmorpholine. The reaction was

run overnight at 70–80 °C to ensure a complete reaction. Following workup, ^{1}H NMR shows that **39** was attained.

Following the initial reaction in DME, we observed that **39** was not soluble in DME. Subsequently, the reaction was run in acetonitrile. A solubility test confirmed that **39** was soluble in acetonitrile. The change in solvent seemed to help to a certain extent as precipitate appeared following the final addition. Once again, the precipitate was dissolved in $CHCl_3$ and the reaction was allowed to run overnight to guarantee a complete reaction. ^{1}H NMR confirmed **39** was attained. Precipitation also occurred went the amount of solvent was increased.

Following the attempts in DME and acetonitrile, the reaction was run in $CHCl_3$. In $CHCl_3$, the product stayed in solution and the reaction ran for 4 h instead of overnight. ^{1}H NMR shows **39** was attained.

3.7 X-ray Crystal Structure of 4-(2-Dimethylcarbamoyl-ethyl)-4-nitro-heptanedioic acid bis-dimethylamide (30)

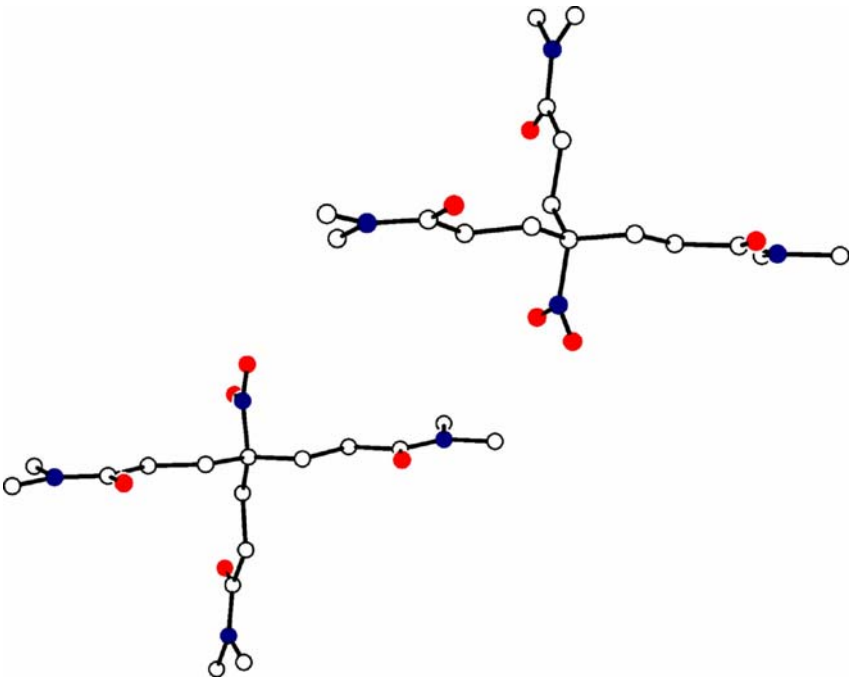

Figure 3.1 X-ray Crystal Structure of 4-(2-Dimethylcarbamoyl-ethyl)-4-nitro-heptanedioic acid bis-dimethylamide. Picture obtained from Dr. Carla Slebodnick.

The X-ray crystal structure of **30** does not contain any H-bonds or interaction with solvent molecules. The three amide components of **30** are extended and adopt a "T" orientation.

3.8 X-ray Crystal Structure of 1,7-Di-morpholin-4-yl-4-(3-morpholin-4-yl-3-oxo-propyl)-4-nitro-heptane-1,7-dione (39)

The X-ray structure of **39**, similar to **30**, does not contain any H-bonding However, a solvent molecule (CH_2Cl_2) is trapped in the crystal matrix. The morpholino headgroups form a channel, which the CH_2Cl_2 molecule occupies. The solvent molecule appears to be surrounded exclusively by morpholino amide groups, with the exclusion of the nitro group. The Cl atom is close to certain atoms of the morpholino group. The Cl atom is closest to O4 (3.402 Å), O6 (3.48 Å), C18 (3.55 Å) and N4 (3.59 Å).

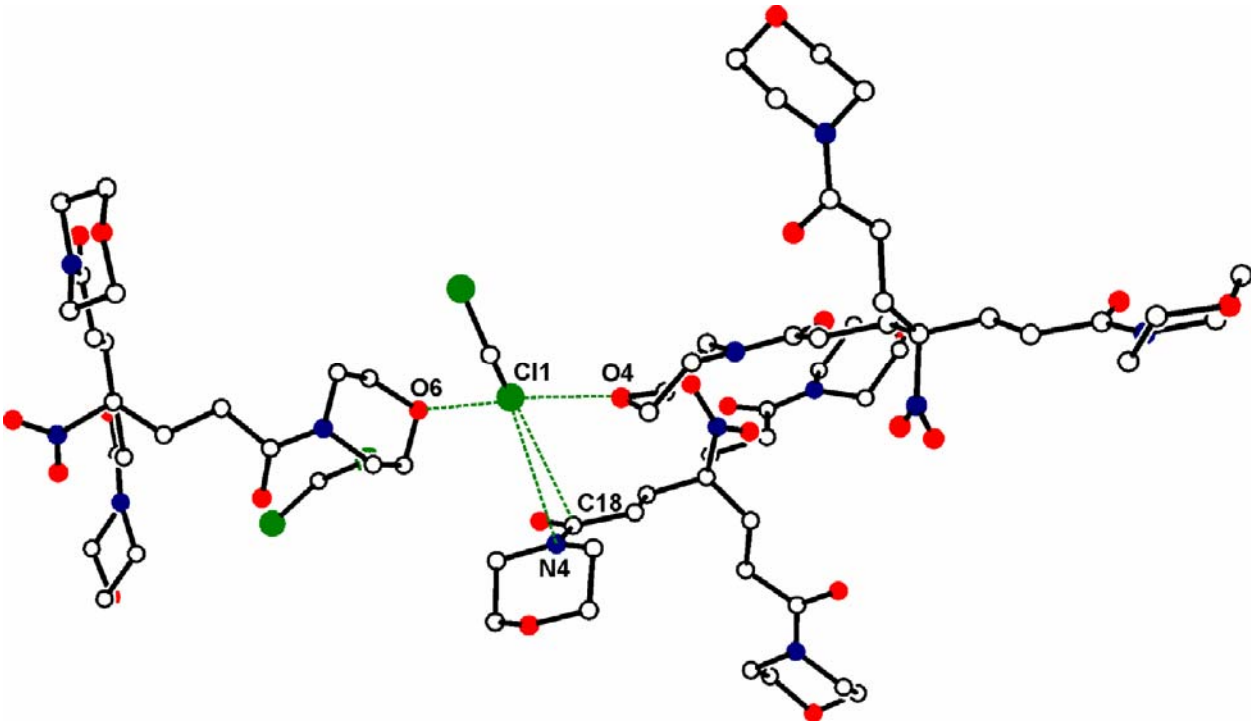

Figure 3.2 X-ray Crystal Structure of 1,7-Di-morpholin-4-yl-4-(3-morpholin-4-yl-3-oxo-propyl)-4-nitro-heptane-1,7-dione. Picture obtained from Dr. Carla Slebodnick.

3.9 Synthesis of 4-Amino-4-(2-dimethylcarbamoyl-ethyl)-heptanedioic acid bis-dimethylamide (31) and 4-Amino-1,7-di-morpholin-4-yl-4-(3-morpholin-4-yl-3-oxo-propyl)-heptane-1,7-dione (38)

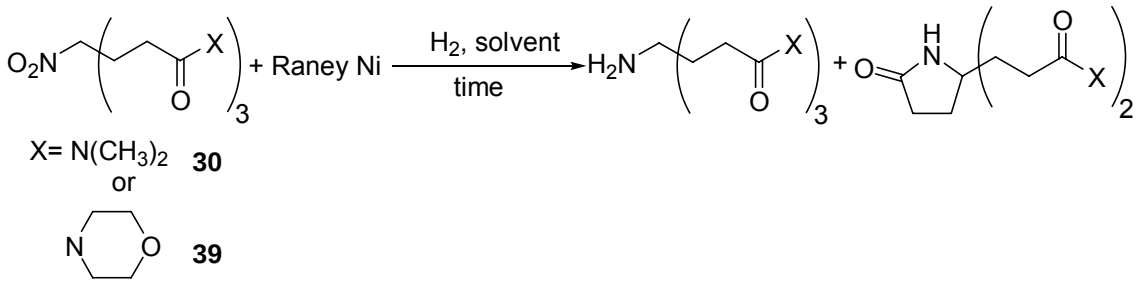

Scheme 3.11 Raney Ni Reduction of **DMA**- and **Mor**-Nitrotriamides

3.9.1 Synthesis of 4-Amino-4-(2-dimethylcarbamoyl-ethyl)-heptanedioic acid bis-dimethylamide (31)

The reduction of the nitro group to form **31** was accomplished with H_2 and Raney Ni (Scheme 3.11). The choice of solvent and reaction time was very important for the reduction reaction. Alcohols are typically used in the Raney Ni reduction of nitro groups. Similar to the Raney Ni reduction used in the formation of **13**, if the reaction was allowed to run too long, in this case 60 min, the reduction of the nitrotrisdimethylamide led to the formation of 3-[2-(2-dimethylcarbamoyl-ethyl)-5-oxo-pyrrolidin-2-yl]-*N*,*N*-dimethyl-propionamide (**41**). If protic solvents, such as methanol and ethanol, were used exclusively, **41** was observed in the ^{1}H NMR spectra of the reaction product. The lactam product was sometimes observed if the reaction was run for short (30 min) or long (60 min) periods of time.

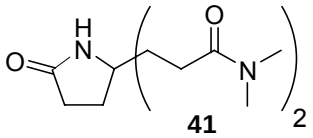

41

Figure 3.3 Lactam of Amino**DMA**

To prevent lactam formation, hexane, a nonpolar, nonprotic solvent was employed. When only hexane was used, the reaction does not go to completion in 30 min. The incomplete reactions were probably due to the low solubility of **30** in hexane. However, the reaction product did not contain **41**. If the reaction was allowed to run for an hour, in hexane, the reaction went to completion; however, **41** was formed. When an 80:20 hexane:methanol solvent mixture was employed, the reaction went to completion and no lactam product was observed in a 30 min reaction period.

3.9.2 X-ray Crystal Structure of 4-Amino-4-(2-dimethylcarbamoyl-ethyl)-heptanedioic acid bis-dimethylamide (31) without Solvent Participation

The X-ray crystal structure of **31** illustrates extensive H-bonding. The amino group N1 is simultaneously H-bonded to two carbonyl oxygens (O3 and O1) of an adjacent molecule. The bond distances of the N1…O1 and N1…O3 hydrogen bonds are 3.17 Å.

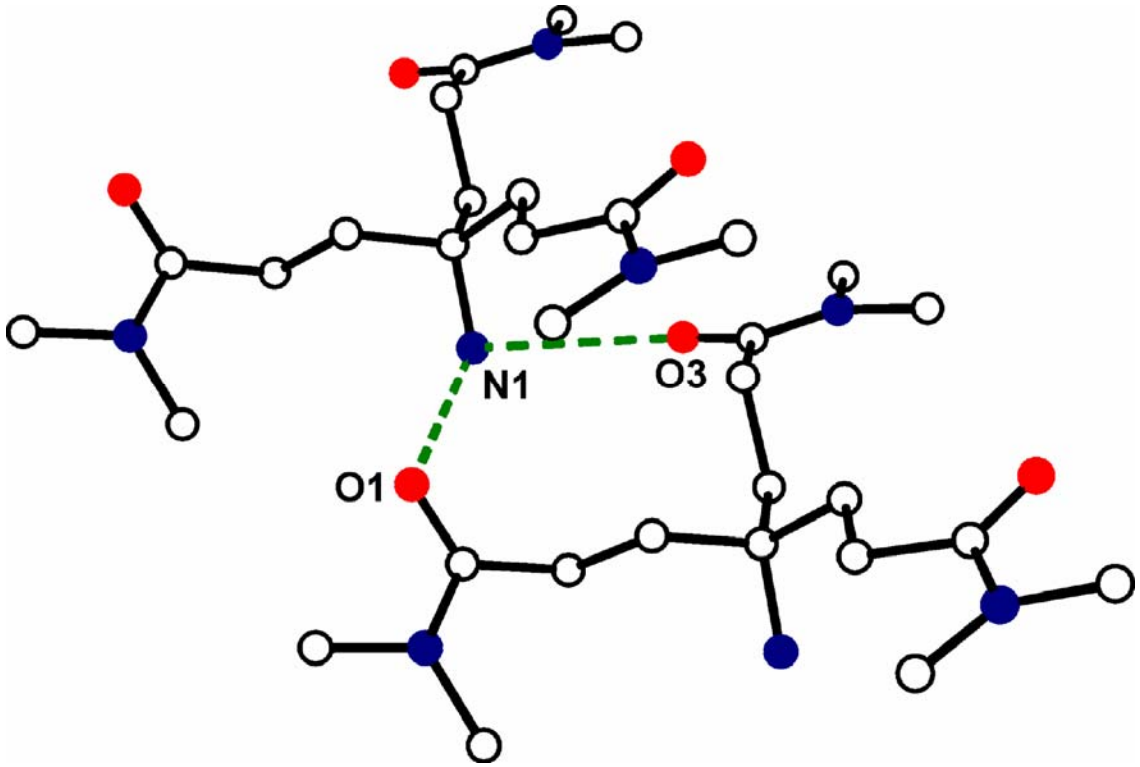

Figure 3.4 X-ray Crystal Structure of 4-Amino-4-(2-dimethylcarbamoyl-ethyl)-heptanedioic acid bis-dimethylamide without Solvent Participation. Picture obtained from Dr. Carla Slebodnick.

3.9.3 X-ray Crystal Structure of 4-Amino-4-(2-dimethylcarbamoyl-ethyl)-heptanedioic acid bis-dimethylamide (31) with Solvent Participation

The crystal matrix has an extensive H-bonding because of the inclusion of a water molecule in the crystal matrix. There are four distinct H-bonds. The amino group is simultaneously involved in three H-bonds. The amino group is hydrogen bonded to a water molecule that is trapped in the crystal matrix. The N1…O4 bond distance is 2.87 Å. Additionally, the amino group is also involved as an H-bond donor with two carbonyl groups of an adjacent molecule. The H-bonds between the amine group and the carbonyl groups are weaker than the amino-water H-bonds. The N1…O2 (3.14 Å) and N1…O3 (3.13 Å) are weaker

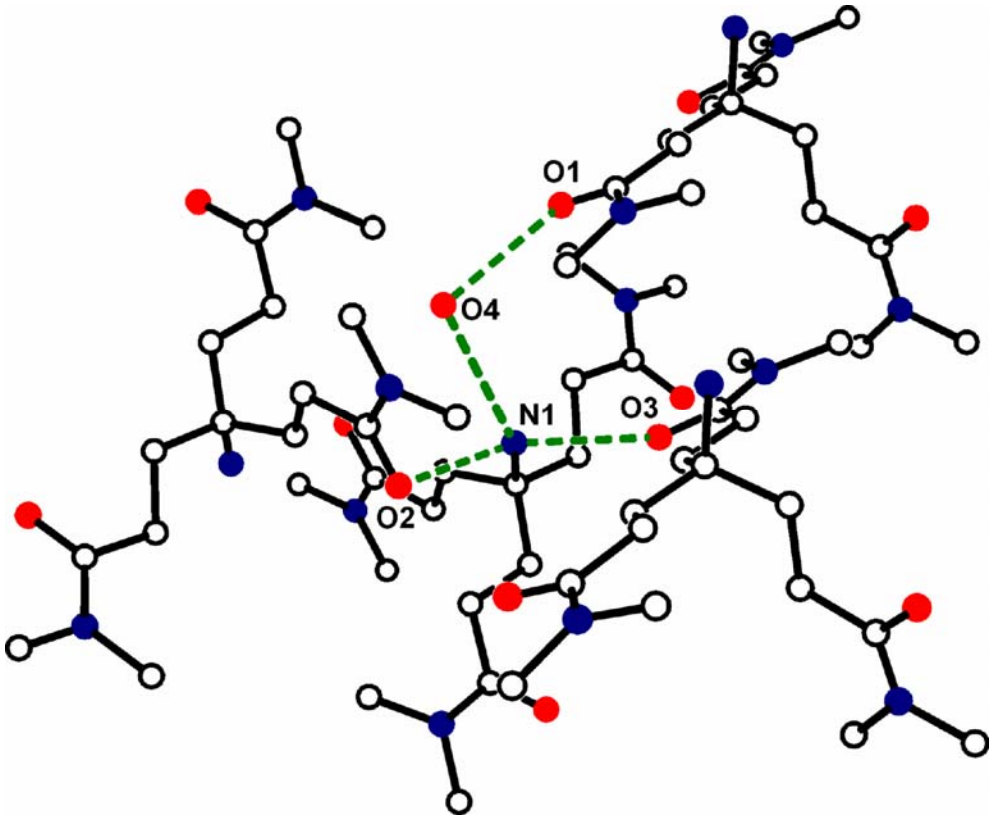

Figure 3.5 X-ray Crystal Structure of 4-Amino-4-(2-dimethylcarbamoyl-ethyl)-heptanedioic acid bis-dimethylamide with Solvent Participation. Picture obtained from Dr. Carla Slebodnick.

H-bonds. In addition to the N1…O4 H-bond, the water molecule is also H-bonded to an adjacent carbonyl group. The O4…O1 H-bond is 2.83 Å.

3.9.4 Synthesis of 4-Amino-1,7-di-morpholin-4-yl-4-(3-morpholin-4-yl-3-oxo-propyl)-heptane-1,7-dione (38)

Similar to the formation of the **31**, solvent choice and reaction time were essential to obtain a pure product (Table 3.1). Intermediate **39** was insoluble in a large number of solvents. Additionally, if the reaction was allowed to proceed too long, 5, 5-bis-(3-morpholin-4-yl-3-oxo-propyl)-pyrrolidin-2-one (**42**) was observed in the ^{1}H NMR spectrum of the reaction product.

Table 3.1 Effects of Solvent and Reaction Time on Raney Ni Reduction Reaction

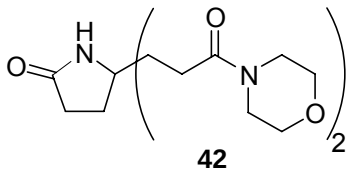

42

Solvent	Temp.	Duration	Product obtained	Lactam present
Acetone	rt	15 h	NR	N/A
Acetone	rt	5 h	Incomplete	Yes
Pyridine	Δ	5.23 h	Incomplete	No
Anisole	Δ	1 h	Incomplete	Yes
Anisole	Δ	34 min	Yes	Yes
Anisole	Δ	30 min	Yes	No
Anisole	Δ	11.4 h	Yes	Yes
Benzyl alcohol	Δ	19 h	N/A	N/A
$CHCl_3$/acetone	rt	3 h	NR	N/A
MeOH	Δ	18 h	Incomplete	Yes
Hexane	Δ	10.2 h	Incomplete	Yes
Hexane	Δ	2 h	Incomplete	Yes
Hexane	Δ	5 h	Incomplete	Yes
Water	Δ	2 h	Incomplete	Yes
$CHCl_3$	Δ	2 h	NR	N/A
MEOH/Water	Δ	2.5 h	Incomplete	Yes
Benzene	Δ	30 min	Incomplete	No
Benzene	Δ	45 min	Complete	Yes
THF	Δ	30 min	Incomplete	Yes

NR= no reaction, N/A= not applicable, Δ= ~45°C, rt= room temperature

While **39** was water soluble, it was not soluble in alcohols (MeOH, EtOH, *tert*-butylOH, and isopropanol) at rt. However, **39** it was soluble in benzyl alcohol but benzyl alcohol is not an

ideal solvent because of the high boiling point of benzyl alcohol (b.p. 205 °C). When the reaction was run in benzyl alcohol, the reaction product could not be isolated because of the high boiling point of the solvent. Similar to the formation of **31**, the choice of solvent and reaction time greatly affected the amount and quality of the product attained. The reaction was run in water; however, the reaction did not go to completion and **42** was formed. A wide variety of solvents and reaction times were tried for the reduction reaction with varying results (Table 3.1).

The results from Table 3.1 were not always consistent (i.e. acetone). Sometimes the reaction in benzene would go to completion in 30 min. and sometimes it would not. Solvents and reaction times had a profound effect not only on the completion of reaction, but also whether lactam was formed. Following multiple reactions, the ideal solvents were determined to be anisole and benzene. The ideal reaction time was determined to be 30–35 min.

3.9.5 X-ray Crystal Structure of 4-Amino-1,7-di-morpholin-4-yl-4-(3-morpholin-4-yl-3-oxo-propyl)-heptane-1,7-dione (38)

The X-ray crystal structure of **38** shows the amino group is simultaneously involved in two H-bonds with adjacent molecules. In both cases, the amino group acts as an H-bond donor. In one H-bond, N1 is bonded to a carbonyl oxygen (O3) of adjacent molecule (3.19 Å), while in another case, N1 is bonded to an oxygen atom (O5) of the morpholino ring (3.11 Å).

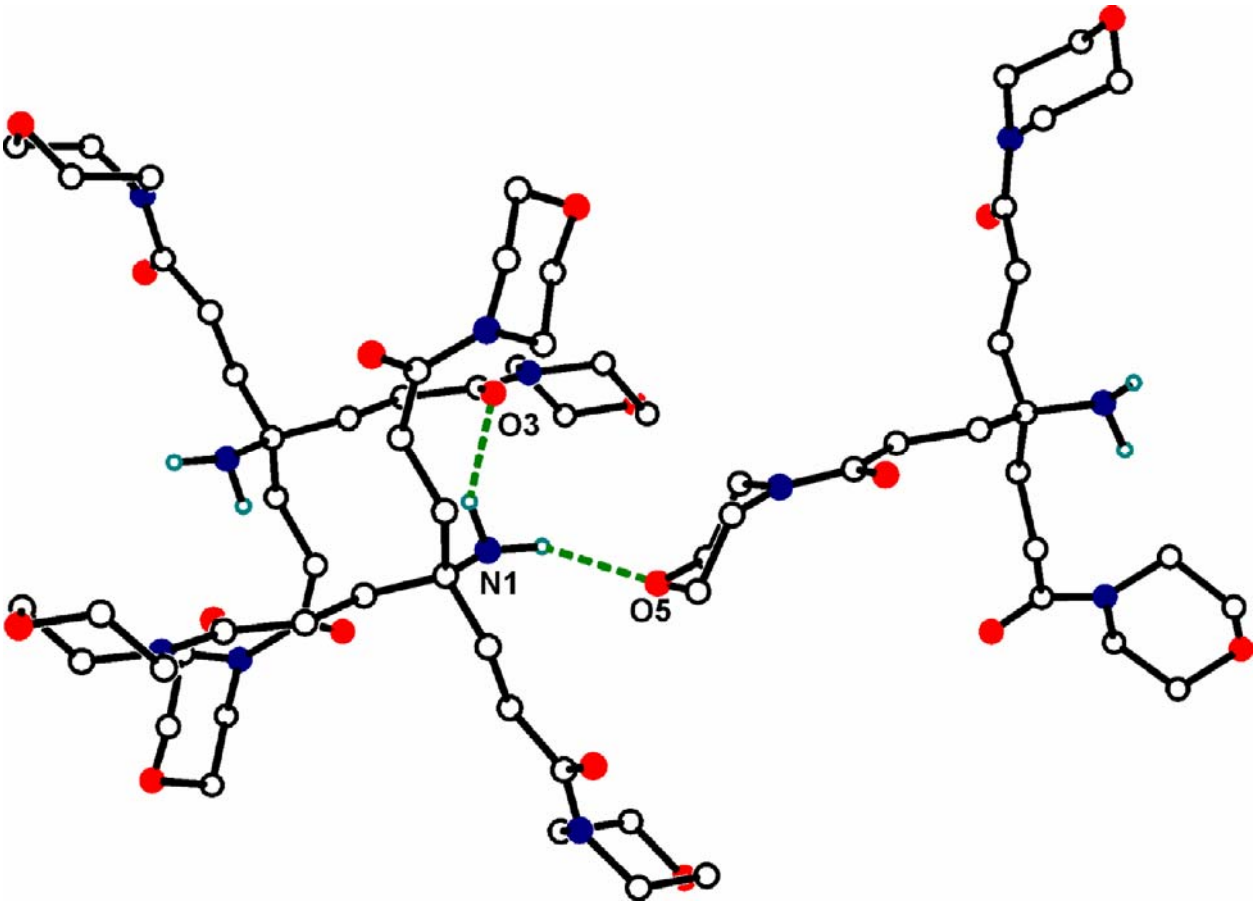

Figure 3. 6 X-ray Crystal Structure of 4-Amino-1,7-di-morpholin-4-yl-4-(3-morpholin-4-yl-3-oxo-propyl)-heptane-1,7-dione. Picture obtained from Dr. Carla Slebodnick.

3.10 Synthesis of 4-(2-Dimethylcarbamoyl-ethyl)-4-isocyanato-heptanedioic acid bis-dimethylamide (32) and 4-Isocyanato-1,7-di-morpholin-4-yl-4-(3-morpholin-4-yl-3-oxo-propyl)-heptane-1,7-dione (37)

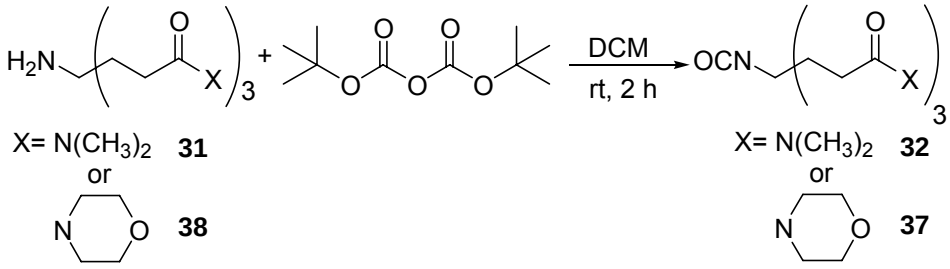

Scheme 3.12 Formation of Triamidoisocyanate Intermediates

Initially, for the synthesis of **32**, the reaction was run for 1 h. However, unreacted starting material (**31**) was observed in the ^{1}H NMR spectrum of the reaction product. Consequently, the reaction was run for 2 h, resulting in a complete reaction.

Following consultation with my lab mate (Shauntrece Hardrict), an attempt was made to run the reaction in 20 min, with a different addition procedure. Instead of adding the di-*tert*-butyldicarbonate solution all at once, the solution was added dropwise over a 20 min period. The product was obtained with no starting material following workup.

The formation of the isocyanate-morpholino intermediate **37** followed the same experimental procedure used in the formation of **32**. The reaction was allowed to run for 2 h because we expected the reactivity of **38** to be similar to that of **31**; consequently, we never attempted to run the reaction for 1 h. The formation of **32** was never attempted with the 20 min. procedure.

3.11 Crystal Structure of 2,2-Bis-(2-dimethylcarbamoyl-ethyl)-5-oxo-pyrrolidine-1-carboxylic acid *tert*-butyl ester

After an attempt to synthesize **32**, a crystalline solid was obtained. The solid was submitted for X-ray crystal analysis. We expected an X-ray crystal structure of **32**; instead, an X-ray crystal structure of **43** was obtained. This X-ray crystal structure confirms the formation of **41**. The formation of **41** probably occurred during the reduction of **30**. The NH group was then acylated with di-*tert*-butyldicarbonate.

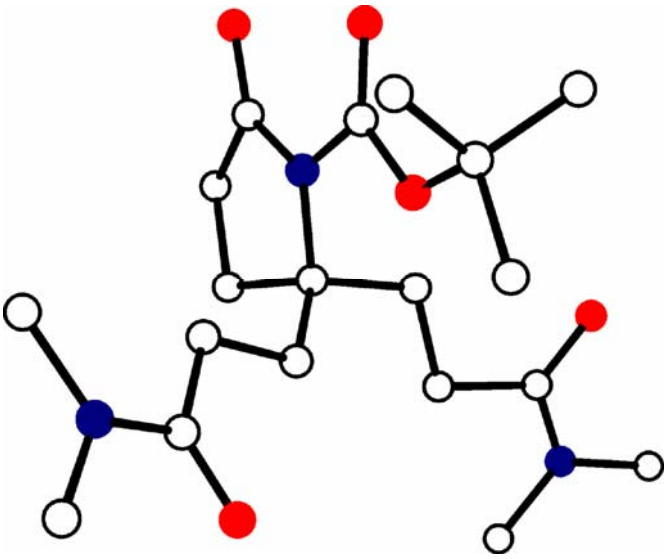

43

Figure 3.7 X-ray Crystal Structure of 2,2-Bis-(2-dimethylcarbamoyl-ethyl)-5-oxo-pyrrolidine-1-carboxylic acid *tert*-butyl ester. Picture obtained from Dr. Carla Slebodnick.

3.12 X-ray Crystal Structure of 4-Isocyanato-1,7-di-morpholin-4-yl-4-(3-morpholin-4-yl-3-oxo-propyl)-heptane-1,7-dione (37)

The crystal structure of **37** has solvent molecules (THF) trapped in the crystal matrix. The crystal structure contains a disorder and only one of the disordered structures is shown in Figure 3.7. Disorder is when an atom or group does not adopt the same position in all unit cells. The disorder involves one of the three morpholino amide group and THF. A disorder can be dynamic, static, or a combination of the two. A dynamic disorder means that an atom or group is in motion. A static disorder means that two thermodynamic minima are obtained (random from unit cell to unit cell). The shown crystal structure is an average. The THF molecule is surrounded by both the isocyanate group as well as the morpholino amide groups. Atom O8 is 3.39 Å from C2 and 3.39 Å from the carbon of the morpholino amide (not shown). Both of these interactions could be due to dipole-dipole interactions.

In addition to the disorder, the bond angle of the N=C=O group (170°) is different from the expected bond angle of 180°. However, the bond angle is similar to that of Weisocyanate™ (173.9°).

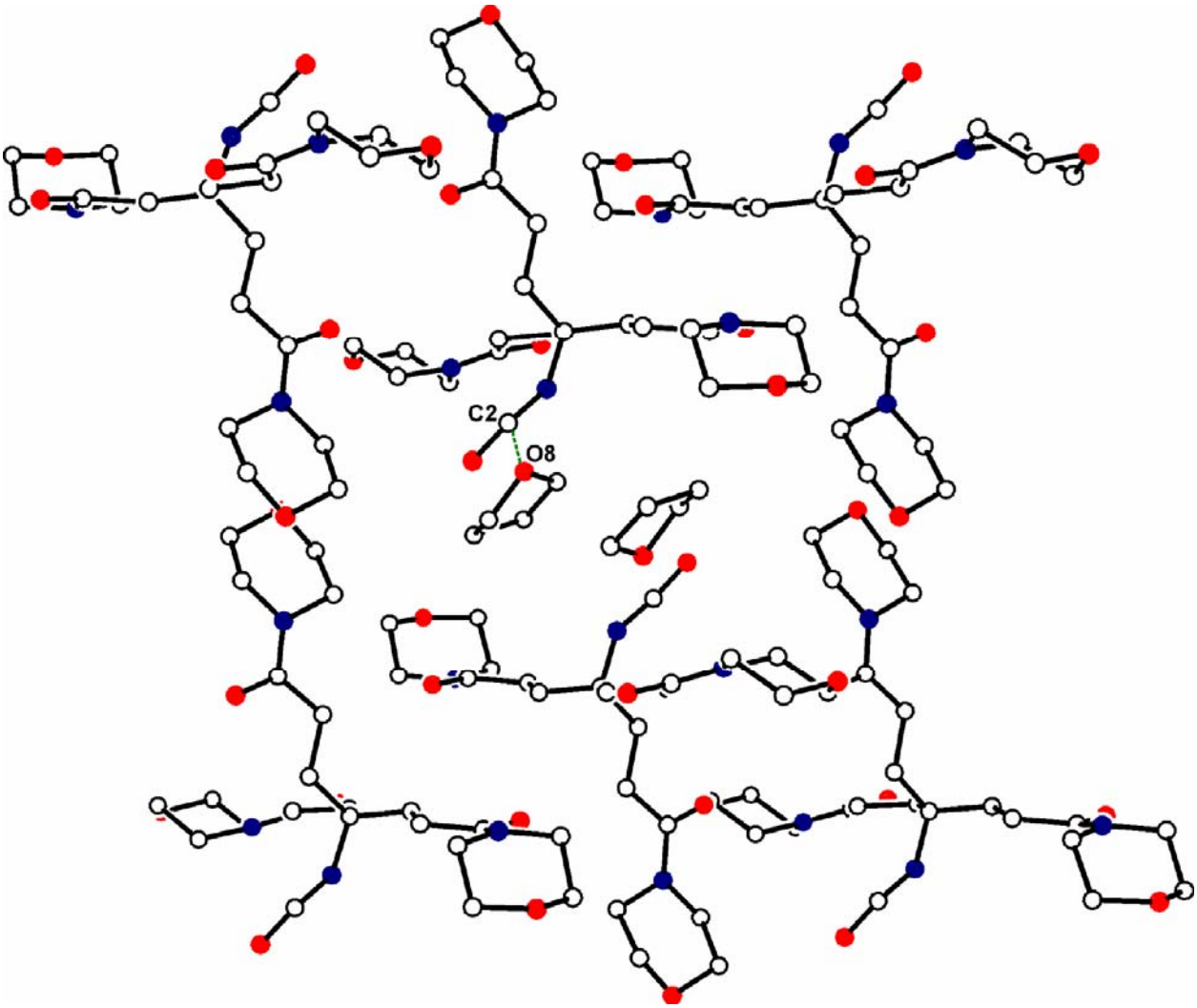

Figure 3.8 X-ray Crystal Structure of 4-Isocyanato-1,7-di-morpholin-4-yl-4-(3-morpholin-4-yl-3-oxo-propyl)-heptane-1,7-dione. Picture obtained from Dr. Carla Slebodnick.

3.13 Synthesis of 3DMAUr18Me and the 3DMAUrn Series

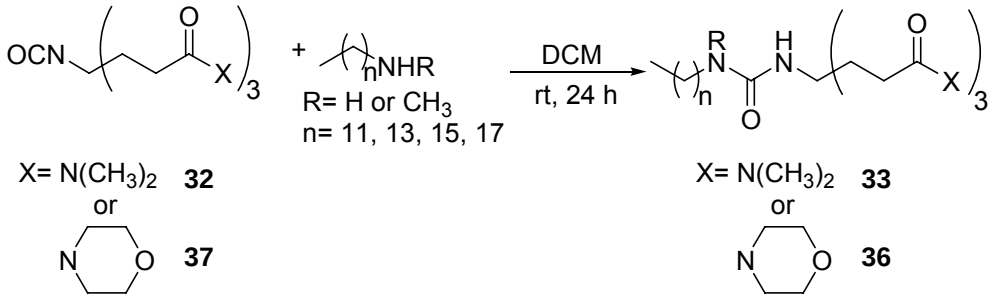

Scheme 3.13 Condensation of Fatty Amines with Triamidoisocyanates

The final step in the synthesis of **3DMAUr18Me**, **3MorUr18Me**, and the **3DMAUrn** and **3MorUrn** series is the condensation of **32** and **37** with commercially available fatty amines.[1] During the synthesis of the **DMA** and **Mor** amphiphiles, it was observed that some amphiphiles were water soluble. Unfortunately, not all amphiphiles are water soluble. With regard to the **DMA** headgroup, amphiphiles **3DMAUr16** and **3DMAUr18** are not water soluble due to the length of the hydrophobic chain. Unexpectedly, **3DMAUr18Me** is water soluble. **3DMAUr18Me** is not as water soluble as **3DMAUr12** and **3DMAUr14**.

We propose that **3DMAUr18Me** is water soluble because of the loss of H-bonding. The difference in structure of **3DMAUr18** and **3DMAUr18Me** is due to the replacement of the N–H bond of **3DMAUr18** with an N–CH_3 bond of **3DMAUr18Me**. Due to the loss of a potential hydrogen bonding group, the crystal matrix of **3DMAUr18Me** can be broken up more readily than the crystal matrix of **3DMAUr18**.

This hypothesis is supported by the melting point data. The melting point of a compound gives an indication of inter- and intramolecular attractive forces within the crystal matrix. If the melting point increases within a series that is an indication that attractive forces within the series are also increasing. With respect to the **3DMAUr**n series, the melting point increases with increasing tail length from **3DMAUr12** (119.3–119.6 °C) to **3DMAUr18** (127.0–127.8 °C).

However, the melting point of **3DMAUr18Me** (91.4–92.4 °C) is dramatically lower than the melting point of **3DMAUr12**. The relatively lower melting point of **3DMAUr18Me** indicates that this compound has fewer attractive forces than that of **3DMAUrn** series.

Our hypothesis is further supported by a crystal structure obtain by my colleague Dr. Winny Sugandhi. Dr. Winny Sugandhi obtained a crystal structure for **3EUr16** (Figurre 3.9).[1] In this crystal structure, the N–H of the ureido group is involved in a intermolecular hydrogen bond with a neighboring ureido oxygen. Hypothetically, the **3DMAUrn** series could have a similar packing arrangement with involves hydrogen bonding between the carbonyl oxygen and NH of the ureido group. If this is the case, **3DMAUr18Me** would lack the ability to hydrogen bond in a similar fashion, which would result in fewer attractive forces and explain the lower melting point and possibly greater aqueous solubility.

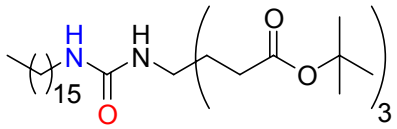

Figure 3.9 Structure of **3EUr16**

With regard to the **Mor** headgroup, amphiphiles **3MorUr12** and **3MorUr18Me** are not water soluble. However, **3MorUr14** is water soluble. The aqueous insolubility of **3MorUr12** is unexplainable and unexpected. Based on hydrophobicity, **3MorUr12** should be more water soluble than **3MorUr14**. The aqueous insolubility of **3MorUr18Me** can be rationalized based on the hydrophobicity of the C_{18} alkyl chain. Based on the aqueous solubility of **3DMAUr18Me** versus **3MorUr18Me**, we concluded that the **DMA** headgroup is more hydrophilic than the **Mor** headgroup.

3.14 Experimental of the 3DMAUrn and 3MorUrn Series, 3DMAUr18Me, and 3MorUr18Me

3.14.1 Synthesis of 4-(2-Dimethylcarbamoyl-ethyl)-4-nitro-heptanedioic acid bis-dimethylamide (30)

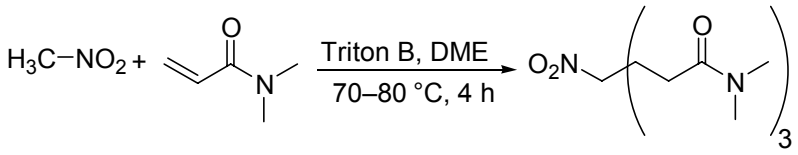

Scheme 3.14 Formation of the Nitrotri**DMA** Headgroup

A solution nitromethane (3.05 g, 49.0 mmol), Triton B (benyltrimethylammonium hydroxide, 0.5 mL), and DME (dimethoxyethane, 10 mL) was heated to 65 °C. Approximately half of the *N*,*N*-dimethylacrylamide (15.4 g, 155 mmol) was added dropwise to the solution, maintaining the temperature between 70–80 °C. Additional Triton B (0.5 mL) was added dropwise to the solution. The remaining *N*,*N*-dimethylacrylamide was then added dropwise. Triton B (0.5 mL) was added dropwise to the solution. The reaction mixture was stirred at 70–80 °C for 4 h. The reaction mixture was concentrated in vacuo, yielding an orange solid. The solid was redissolved in $CHCl_3$, washed with 10% aq. HCl, brine, and dried $MgSO_4$. Concentration in vacuo yielded a bright yellow solid, which was recrystallized with CH_2Cl_2/hexane, then $CHCl_3$/hexane to yield a white powder (65.9%), mp 128.0–129.0 °C. ^{1}H NMR ($CDCl_3$): δ 2.26-2.30 (bm, 12H), 2.90 (s, 9H), 2.95 (s, 9H); ^{13}C NMR ($CDCl_3$): δ 27.5, 30.9, 35.7, 37.2, 93.2, 170.9; IR 2924, 1636, 1527 cm^{-1}. HRMS: for $C_{16}H_{31}N_4O_5$ $(M + H)^+$ calcd 359.2294, found 359.2292 Anal. Calcd for $C_{16}H_{30}N_4O_5$: C, 53.62; H, 8.44; N, 15.63. Found: C, 53.51; H, 8.49; N, 15.48.

X-ray analysis of 4-(2-Dimethylcarbamoyl-ethyl)-4-nitro-heptanedioic acid bis-dimethylamide

Analysis done by Dr. Carla Slebodnick (Table 3.2). Flat needles (~4 x 1 x 0.3 mm^3) were crystallized from a mixture of ethanol, ether, and hexane by slow cooling at 40-60 °C. The chosen crystal was cut (0.36 x 0.17 x 0.09 mm^3) and mounted on a nylon CryoLoop™ (Hampton Research) with Krytox® Oil (DuPont) and centered on the goniometer of a Oxford Diffraction XCalibur2™ diffractometer equipped with a Sapphire 2™ CCD detector. The data collection routine, unit cell refinement, and data processing were carried out with the program CrysAlis. The Laue symmetry and systematic absences were consistent with the monoclinc space groups $P2_1/c$. The structure was solved by direct methods and refined using the SHELXTL NT program package. The asymmetric unit of the structure comprises two crystallographically independent molecules. The final refinement model involved anisotropic displacement parameters for non-hydrogen atoms and a riding model for all hydrogen atoms. The program package SHELXTL NT was used for molecular graphics generation.

Table 3.2 Crystal Data and Structure Refinement of 4-(2-Dimethylcarbamoyl-ethyl)-4-nitro-heptanedioic acid bis-dimethylamide. Data obtained from Dr. Carla Slebodnick.

Category	Crystal Data and Structure Refinement	
Empirical formula	$C_{16}H_{30}N_4O_5$	
Formula weight	358.44	
Temperature	100(1) K	
Wavelength	0.71073 Å	
Crystal system	Monoclinic	
Space group	P 2_1/c	
Unit cell dimensions	a = 17.762(2) Å	α= 90°
	b = 18.933(3) Å	β= 91.586(13)°
	c = 11.274(2) Å	γ = 90°
Volume	3789.9(10) $Å^3$	
Z	8	
Density (calculated)	1.256 Mg/m^3	
Absorption coefficient	0.094 mm^{-1}	
F(000)	1552	
Crystal size	36 x 0.17 x 0.09 mm^3	
Theta range for data collection	3.05 to 25.06°	
Index ranges	-21<=h<=21, -22<=k<=21, -13<=l<=13	
Reflections collected	20913	
Independent reflections	6707 [R(int) = 0.0266]	
Completeness to theta = 30.07°	99.8%	
Absorption correction	None	
Refinement method	Full-matrix least-squares on F^2	
Data / restraints / parameters	6707 / 0 / 463	
Goodness-of-fit on F^2	1.120	
Final R indices [I>2sigma(I)]	R1 = 0.0468, wR2 = 0.1311	
R indices (all data)	R1 = 0.0624, wR2 = 0.1415	
Largest diff. peak and hole	0.439 and -0.275 e.$Å^{-3}$	

3.14.2 Synthesis of 1,7-Di-morpholin-4-yl-4-(3-morpholin-4-yl-3-oxo-propyl)-4-nitro-heptane-1,7-dione (39)

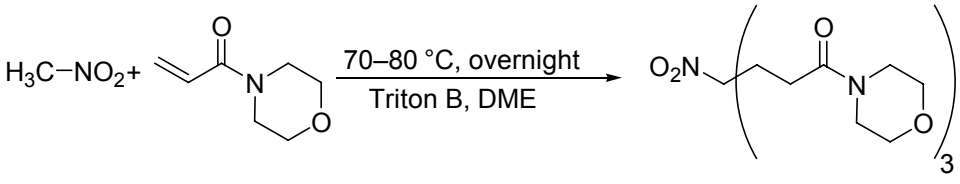

Scheme 3.15 Formation of the Nitrotri**Mor** Headgroup

Nitromethane (3.02 g, 49.2 mmol) was added to a 3-neck RBF followed by the addition of acetonitrile (19.9 mL). Triton B (0.5 mL) was added to the RBF via a syringe. Upon the

mixture of Triton B, the reaction solution changed from colorless to yellow. The solution was then heated to 65 ºC. Half of the 4-acryloylmorpholine (11.4 g, 80.8 mmol) was then added dropwise to the solution via an addition funnel while maintaining the temperature between 70–80 °C. A second portion of Triton B (0.5 mL) was added to the solution. The remaining 4-acryloylmorpholine was added dropwise to the RBF. The last portion of Triton B (0.5 mL) was added dropwise to the RBF. The solution was then allowed to react for 4 h. The reaction mixture solidified into a dark yellow solid. The solid was dissolved by stirring it with $CHCl_3$ overnight at 60–70 °C and then concentrated. The resulting brown solid was placed under vacuum overnight. The brown solid was dissolved in $CHCl_3$ and added to a separatory funnel. The organic layer was washed with 10% aq. HCl (3 × 20 mL) and brine (3 × 20 mL). The organic color changed from red to orange following the acid wash, but remained unchanged following the brine wash. $MgSO_4$ was used to remove any H_2O from the organic layer. The $MgSO_4$ was removed by gravity filtration; the resulting yellow solid was placed under vacuum overnight. Approximately 150 mL of ethanol was added to the RBF. The flask was heated at 45 °C for approximately 2 h. Vacuum filtration was used to isolate the solid. Following an ethanol wash, an off-white, slightly yellow solid was obtained (61%). The filtrate was discarded. The solid was recrystallized in CH_2Cl_2/hexane or THF with a heat gun, m.p. 171.5–171.4 °C. ^{1}H NMR ($CDCl_3$): δ 2.28–2.32 (m, 12H), 3.42 (m, 6H), 3.58 (m, 6H), 3.65 (m 12H); ^{13}C NMR ($CDCl_3$): δ 27.1, 30.8, 42.2, 45.8, 66.6, 66.8, 92.9, 169.6; IR 2968, 2853, 1634, 1532, 1439, 1111 cm^{-1}; HRMS: for $C_{22}H_{37}N_4O_8$ $(M + H)^+$ calcd 485.2611, found 485.2603. Anal. Calcd for $C_{22}H_{36}N_4O_8$: C, 54.53; H, 7.49; N, 11.56. Found: C, 54.72; H, 7.39; N, 11.61.

The above procedure can be repeated in $CHCl_3$. The use of $CHCl_3$ avoids the solubility issues observed when DME or acetonitrile is used as the solvent. Chloroform is the ideal solvent for this reaction.

X-ray analysis of 1,7-Di-morpholin-4-yl-4-(3-morpholin-4-yl-3-oxo-propyl)-4-nitro-heptane-1,7-dione

Analysis done by Dr. Carla Slebodnick (Table 3.3). Colorless plates (~3 x 3 x 0.3 mm^3) were crystallized from CH_2Cl_2/hexanes at -40 °C. The chosen crystal was cut (0.24 x 0.36 x 0.44 mm^3) and mounted on a nylon CryoLoop™ (Hampton Research) with Krytox® Oil (DuPont) and centered on the goniometer of an Oxford Diffraction Xcalibur™ diffractometer equipped with a Sapphire 3™ CCD detector. The data collection routine, unit cell refinement, and data processing were carried out with the program CrysAlis. The Laue symmetry and systematic absences were consistent with the orthorhombic space groups *Iba*2 and *Ibam*. The accentric space group *Iba*2 was chosen based on the $|E^2-1|$ value (0.784) and the Z value. The ADDSYMM subroutine of the PLATON program package indicated the absence of any higher symmetry in the final model. The structure was solved by direct methods and refined using SHELXTL NT. The asymmetric unit of the structure comprises one crystallographically independent molecules and two half-CH_2Cl_2 molecules that each lie on a 2-fold axis. The final refinement model involved anisotropic displacement parameters for non-hydrogen atoms and a riding model for all hydrogen atoms. SHELXTL NT was used for molecular graphics generation.

Table 3.3 Crystal Data and Structure Refinement of 1,7-Di-morpholin-4-yl-4-(3-morpholin-4-yl-3-oxo-propyl)-4-nitro-heptane-1,7-dione. Data obtained from Dr. Carla Slebodnick.

Category	Crystal Data and Structure Refinement
Empirical formula	$C_{22}H_{36}N_4O_8$•2[0.5(CH_2Cl_2)]
Formula weight	569.47
Temperature	100(2) K
Wavelength	0.71073 Å
Crystal system	Orthorhombic
Space group	I b a 2
Unit cell dimensions	*a* = 25.8052(13) Å *α*= 90° *b* = 12.7527(8) Å *α*= 90° *c* = 16.967(7) Å *α*= 90°
Volume	5584(2) $Å^3$
Z	8
Density (calculated)	1.355 Mg/m^3
Absorption coefficient	0.284 mm^{-1}
F(000)	2416
Crystal size	0.44 x 0.36 x 0.24 mm^3
Theta range for data collection	3.73 to 27.50°
Index ranges	-31≤=h≤=33, -13≤=k≤=16, -22≤=l≤=22
Reflections collected	16578
Independent reflections	6394 [R(int) = 0.0344]
Completeness to theta = 30.07°	99.7 %
Absorption correction	None
Refinement method	Full-matrix least-squares on F^2
Data / restraints / parameters	6394 / 1 / 335
Goodness-of-fit on F^2	0.985
Final R indices [I>2sigma(I)]	R1 = 0.0545, wR2 = 0.1479
R indices (all data)	R1 = 0.0704, wR2 = 0.1533
Absolute structure parameter	-0.02(8)
Largest diff. peak and hole	1.047 and -0.741 e.$Å^{-3}$

3.14.3 Synthesis of 4-Amino-4-(2-dimethylcarbamoyl-ethyl)-heptanedioic acid bis-dimethylamide (31)

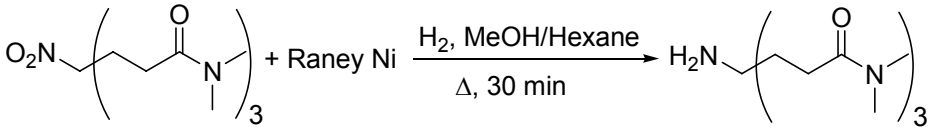

Scheme 3.16 Raney Ni Reduction of Nitrotri**DMA** Headgroup

A solution of **30** (3.88 g, 10.8 mmol) was dissolved with hexane (131 mL) and methanol (21 mL). Raney Ni (7.51 g) was added to the solution. Hydrogen was introduced to the solution via a hydrogenator. A heating pad was used to heat the solution. With the starting temperature

at low, the mixture was shaken on the hydrogenator for 31 min; a drop in the psi was noted (58.9–56 psi). At this point, the solution yielded a clear liquid with Raney Ni at the bottom of the hydrogenator vessel. Raney Ni was removed via filtration through Celite® and the filtrate was concentrated, which yielded an off-white solid. The solid was then placed under vacuum overnight to remove any remaining solvent. The solid was used without further purification (86%). If a purified sample is needed, a DCM/hexane recrystallization can be done; mp 105–106 °C; ^{1}H NMR ($CDCl_3$): δ 1.71 (m, 6H), 2.32 (m, 6H), 2.91 (s, 9H) 2.97 (s, 9H); ^{13}C NMR ($CDCl_3$ MHz): 27.5, 34.7, 35.6, 37.4, 52.6, 173.0; IR 3336, 2930, 1649, 1615, 1495, 1395 cm^{-1}; HRMS: for $C_{16}H_{33}N_4O_3$ $(M + H)^+$ calcd 329.2553, found 329.2565. Anal. Calcd for $C_{16}H_{32}N_4O_3$: C, 58.51; H, 9.82; N, 17.06. Found: C, 58.51; H, 9.79; N, 16.95.

X-ray analysis of 4-Amino-4-(2-dimethylcarbamoyl-ethyl)-heptanedioic acid bis-dimethylamide without solvent participation

Analysis done by Dr. Carla Slebodnick (Table 3.4). Colorless plates (0.31 x 0.14 x 0.03 mm^3) were crystallized from CH_2Cl_2/hexanes by slow evaporation at room temperature. The chosen crystal was mounted on a nylon CryoLoop™ (Hampton Research) with Krytox® Oil (DuPont) and centered on the goniometer of a Oxford Diffraction XCalibur2™ diffractometer equipped with a Sapphire 2™ CCD detector. The data collection routine, unit cell refinement, and data processing were carried out with the program CrysAlis. The Laue symmetry and systematic absences were consistent with the monoclinic space group $P2_1/c$. The structure was solved by direct methods and refined using the SHELXTL NT program package. The asymmetric unit of the structure comprises one crystallographically independent molecule. The final refinement model involved anisotropic displacement parameters for non-hydrogen atoms and a riding model for all hydrogen atoms except the two hydrogen atoms on the primary amine.

These hydrogen atoms were located from the electron density map and their positions and isotropic thermal parameters were refined independently. The program package SHELXTL NT was used for molecular graphics generation.

Table 3.4 Crystal Data and Structure Refinement of 4-Amino-4-(2-dimethylcarbamoyl-ethyl)-heptanedioic acid bis-dimethylamide without Solvent Participation. Data obtained from Dr. Carla Slebodnick.

Category	Crystal Data and Structure Refinement	
Empirical formula	$C_{16}H_{32}N_4O_3$	
Formula weight	328.46	
Temperature	100(2) K	
Wavelength	0.71073 Å	
Crystal system	Monoclinic	
Space group	$P2_1/c$	
Unit cell dimensions	a = 18.770(4) Å	α= 90°
	b = 6.1742(12) Å	β= 116.70(2)°
	c = 17.088(3) Å	γ= 90°
Volume	1769.2(6) $Å^3$	
Z	4	
Density (calculated)	1.233 Mg/m^3	
Absorption coefficient	0.086 mm^{-1}	
F(000)	720	
Crystal size	0.31 x 0.14 x 0.03 mm^3	
Theta range for data collection	3.42 to 27.57°	
Index ranges	-24<=h<=24, -5<=k<=8, -22<=l<=22	
Reflections collected	10040	
Independent reflections	4078 [R(int) = 0.0281]	
Completeness to theta = 30.07°	99.8%	
Absorption correction	None	
Refinement method	Full-matrix least-squares on F^2	
Data / restraints / parameters	4078 / 0 / 222	
Goodness-of-fit on F^2	1.045	
Final R indices [I>2sigma(I)]	R1 = 0.0442, wR2 = 0.1041	
R indices (all data)	R1 = 0.0658, wR2 = 0.1130	
Largest diff. peak and hole	0.300 and -0.198 $e.Å^{-3}$	

X-ray analysis of 4-Amino-4-(2-dimethylcarbamoyl-ethyl)-heptanedioic acid bis-dimethylamide with solvent participation

Analysis done by Dr. Carla Slebodnick (Table 3.5). Colorless parallelepipeds were crystallized from $CHCl_3$/hexane at room temperature. The chosen crystal was cut (0.26 x 0.28 x 0.30 mm^3) and mounted on a nylon CryoLoop™ (Hampton Research) with Krytox® Oil

(DuPont) and centered on the goniometer of an Oxford Diffraction Xcalibur™ diffractometer equipped with a Sapphire 3™ CCD detector. The data collection routine, unit cell refinement, and data processing were carried out with the program CrysAlis. The Laue symmetry and systematic absences were consistent with the monoclinic space group $P2_1/n$. The structure was solved by direct methods and refined using SHELXTL NT. The asymmetric unit of the structure comprises one crystallographically independent molecule and a water solvate. The final refinement model involved anisotropic displacement parameters for all non-hydrogen atoms and a riding model for the hydrogen atoms of **31**. The hydrogen atoms of the water molecule were located from the residual electron density map and the O–H distances restrained to 0.84(1) Å. The program SHELXTL NT was used for molecular graphics generation.

Table 3. 5 Crystal Data and Structure Refinement of 4-Amino-4-(2-dimethylcarbamoyl-ethyl)-heptanedioic acid bis-dimethylamide with Solvent Participation. Data obtained from Dr. Carla Slebodnick.

Category	Crystal Data and Structure Refinement
Empirical formula	$C_{16}H_{32}N_4O_3 \cdot H_2O$
Formula weight	346.47
Temperature	100(2) K
Wavelength	0.71073 Å
Crystal system	Monoclinic
Space group	$P2_1/n$
Unit cell dimensions	a = 10.2734(14) Å α = 90° b = 10.3293(12) Å β = 95.371(11)° c = 17.858(2) Å γ = 90°
Volume	1886.7(4) Å^3
Z	4
Density (calculated)	1.220 Mg/m^3
Absorption coefficient	0.088 mm^{-1}
F(000)	760
Crystal size	0.301 x 0.281 x 0.259 mm^3
Theta range for data collection	4.42 to 30.07°.
Index ranges	-14≤h≤14, -14≤k≤11, -22≤l≤25
Reflections collected	13891
Independent reflections	5529 [R(int) = 0.0266
Completeness to theta = 30.07°	99.6 %
Absorption correction	None
Refinement method	Full-matrix least-squares on F^2
Data / restraints / parameters	5529 / 4 / 237
Goodness-of-fit on F^2	1.091
Final R indices [I>2sigma(I)]	R1 = 0.0499, wR2 = 0.1425
R indices (all data)	R1 = 0.0676, wR2 = 0.1539
Largest diff. peak and hole	0.376 and -0.247 e.Å^{-3}

3.14.4 Synthesis of 4-Amino-1,7-di-morpholin-4-yl-4-(3-morpholin-4-yl-3-oxo-propyl)-heptane-1,7-dione (38)

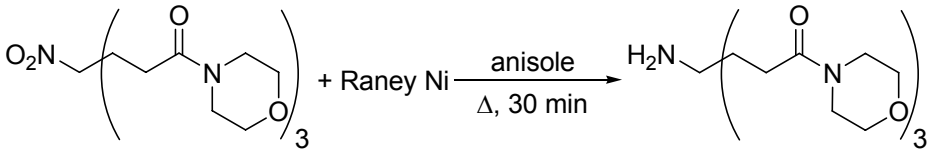

Scheme 3.17 Raney Ni Reduction of Nitrotri**Mor** Headgroup

Intermediate **39** (1.00 g) was added to a hydrogenation vessel. Anisole or benzene (40 mL) can be used as solvents in the reaction. Some of **39** dissolved in anisole but did not dissolve in benzene. Raney Ni (2.00 g) was added to vessel. The vessel was shaken on the hydrogenator for 30 min at approximately 45 °C. MeOH was used to wash the Raney Ni from the sides of the vessel. Raney Ni was removed via filtration through Celite®. The filtrate was concentrated to a yellow/orange oil. The oil was triterated overnight in hexane. If benzene is used as the solvent, the oil must be placed under vacuum before triteration is performed. If not, a solid will not form. Following triteration a white solid resulted. The white solid was recrystallized in CH_2Cl_2/hexane to give a crystalline solid, (77%); mp 117.7–118.4 °C. Sometimes, recrystallization of **38** led to increased formation of **42**. ^{1}H NMR ($CDCl_3$): δ 1.69 (m, 6H), 2.33 (m, 6H), 3.46 (m, 6H), 3.58–3.64 (m, 18H); ^{13}C NMR ($CDCl_3$): δ 27.1, 34.6, 42.1, 46.0, 52.5, 66.7, 66.9, 171.6; IR 2968, 2853, 1634, 1535, 1439 cm^{-1}; HRMS: for $C_{22}H_{39}N_4O_6$ $(M + H)^+$ calcd 455.2870, found 455.2838. Anal. Calcd for $C_{22}H_{38}N_4O_6$: C, 58.13; H, 8.43; N, 12.33. Found: C, 58.21; H, 8.51; N, 12.22.

X-ray analysis of 4-Amino-1,7-di-morpholin-4-yl-4-(3-morpholin-4-yl-3-oxo-propyl)-heptane-1,7-dione

Analysis done by Dr. Carla Slebodnick (Table 3.6). Clusters of colorless rods were crystallized from ethyl acetate by slow cooling from 60°C to room temperature. The chosen

crystal was cut (0.092 x 0.167 x 0.293 mm^3) and mounted on a nylon CryoLoop™ (Hampton Research) with Krytox® Oil (DuPont) and centered on the goniometer of an Oxford Diffraction Xcalibur™ diffractometer equipped with a Sapphire 3™ CCD detector. The data collection routine, unit cell refinement, and data processing were carried out with the program CrysAlis. The Laue symmetry and systematic absences were consistent with the monoclinic space group $P2_1/c$. The structure was solved by direct methods and refined using SHELXTL NT. The asymmetric unit of the structure comprises one crystallographically independent molecule. The final refinement model involved anisotropic displacement parameters for non-hydrogen atoms and a riding model for all hydrogen atoms. SHELXTL NT was used for molecular graphics generation.

Table 3. 6 Crystal Data and Structure Refinement of 4-Amino-1,7-di-morpholin-4-yl-4-(3-morpholin-4-yl-3-oxo-propyl)-heptane-1,7-dione. Data obtained from Dr. Carla Slebodnick.

Category	Crystal Data and Structure Refinement
Empirical formula	$C_{22}H_{38}N_4O_6$
Formula weight	454.56
Temperature	100(2) K
Wavelength	0.71073 Å
Crystal system	Monoclinic
Space group	$P2_1/c$
Unit cell dimensions	a = 9.0673(3) Å α= 90°. b = 22.2409(6) Å β= 99.368(3)°. C = 11.3489(4) Å γ = 90°
Volume	2258.15(13) $Å^3$
Z	4
Density (calculated)	1.337 Mg/m^3
Absorption coefficient	0.097 mm^{-1}
F(000)	984
Crystal size	0.29 x 0.17 x 0.092 mm^3
Theta range for data collection	3.75 to 25.16°
Index ranges	-10<=h<=10, -26<=k<=26, -9<=l<=13
Reflections collected	11015
Independent reflections	4025 [R(int) = 0.0292]
Completeness to theta = 30.07°	99.4 %
Absorption correction	None
Refinement method	Full-matrix least-squares on F^2
Data / restraints / parameters	4025 / 0 / 297
Goodness-of-fit on F^2	0.976
Final R indices [I>2sigma(I)]	R1 = 0.0348, wR2 = 0.0811
R indices (all data)	R1 = 0.0584, wR2 = 0.0861
Largest diff. peak and hole	0.192 and -0.203 $e.Å^{-3}$

3.14.5 Synthesis of 4-(2-Dimethylcarbamoyl-ethyl)-4-isocyanato-heptanedioic acid bis-dimethylamide (32)

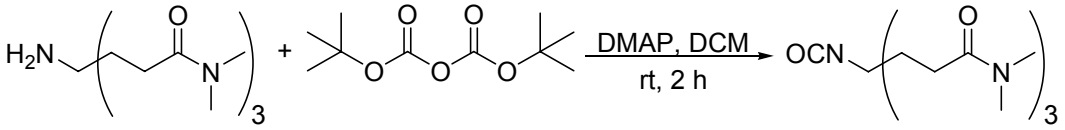

Scheme 3.18 Formation of 4-(2-Dimethylcarbamoyl-ethyl)-4-isocyanato-heptanedioic acid bis-dimethylamide

To a stirred solution of **31** (3.38 g, 10.3 mmol) and DMAP (1.25, 10.3 mmol) in DCM (34 mL), the entire solution of di-*tert*-butyldicarbonate (3.14 g, 14.4 mmol) in DCM (51 mL) was added at rt. After stirring for 2 h, the solution was washed with aq. HCl (3 × 60 mL), followed by water (3 × 30 mL), and dried with Na_2SO_4. The solution was concentrated to give a slightly tan solid, which was recrystallized in ethyl acetate/hexane to yield a white powder (1.79 g, 49%); mp 102.2–103.0 °C; ^{1}H NMR ($CDCl_3$): δ 1.96 (m, 6H), 2.40 (m, 6H), 2.94 (s, 9H), 3.02 (s, 9H); ^{13}C NMR ($CDCl_3$): δ 27.7, 34.5, 35.6, 37.3, 62.7, 122.5, 171.7; IR 2969, 2246, 1649, 1633, 1494, 1396 cm^{-1}; HRMS: for $C_{17}H_{31}N_4O_4$ $(M + H)^+$ calcd 355.2345, found 355.2357. Anal. Calcd for $C_{17}H_{30}N_4O_4$: C, 57.61; H, 8.53; N, 15.81. Found: C, 57.70; H, 8.60; N, 15.66.

In a slightly different procedure, a stirred solution of **31** (3.38 g, 10.3 mmol) and DMAP (1.25, 10.3 mmol) in DCM (34 mL), a solution of di-*tert*-butyldicarbonate (3.14 g, 14.4 mmol) in DCM (51 mL) was added dropwise over 20 min. Any remaining di-*tert*-butyldicarbonate/DCM solution was added at once. The reaction mixture was immediately was washed with aq. HCl (3 × 60 mL), followed by water (3 × 30 mL), and dried with Na_2SO_4. The solution was concentrated to give a slightly tan or white solid, which was recrystallized in ethyl acetate/hexane to yield a white powder (64%).

X-ray analysis of 2,2-Bis-(2-dimethylcarbamoyl-ethyl)-5-oxo-pyrrolidine-1-carboxylic acid *tert*-butyl ester

Analysis done by Dr. Carla Slebodnick (Table 3.7). Colorless rods (1 x 1 x 5 mm^3) were crystallized from $CHCl_3$/hexane at room temperature. The chosen crystal was cut (0.18 x 0.21 x 0.22 mm^3) and mounted on a nylon CryoLoop™ (Hampton Research) with Krytox® Oil (DuPont) and centered on the goniometer of an Oxford Diffraction Xcalibur™ diffractometer equipped with a Sapphire 3™ CCD detector. The data collection routine, unit cell refinement, and data processing were carried out with the program CrysAlis. The Laue symmetry and systematic absences were consistent with the orthorhombic space group $P2_12_12_1$. The structure was solved by direct methods and refined using SHELXTL NT. As there were no heavy atoms, the absolute configuration could not be determined from the Friedel pairs; the Friedel pairs were therefore merged for the final refinement. The asymmetric unit of the structure comprises one crystallographically independent molecule. The final refinement model involved anisotropic displacement parameters for non-hydrogen atoms and a riding model for all hydrogen atoms. SHELXTL NT was used for molecular graphics generation.

Table 3. 7 Crystal Data and Structure Refinement of 2,2-Bis-(2-dimethylcarbamoyl-ethyl)-5-oxo-pyrrolidine-1-carboxylic acid *tert*-butyl ester. Data obtained from Dr. Carla Slebodnick.

Category	Crystal Data and Structure Refinement
Empirical formula	$C_{19}H_{33}N_3O_5$
Formula weight	383.48
Temperature	100(2) K
Wavelength	0.71073 Å
Crystal system	Orthorhombic
Space group	$P2_12_12_1$
Unit cell dimensions	a = 11.1150(19) Å α= 90° b = 11.3874(16) Å β= 90° c = 16.665(2) Å γ = 90°
Volume	2109.4(6) $Å^3$
Z	4
Density (calculated)	1.208 Mg/m^3
Absorption coefficient	0.087 mm^{-1}
F(000)	832
Crystal size	0.22 x 0.21 x 0.18 mm^3
Theta range for data collection	4.08 to 27.57°
Index ranges	-14<=h<=14, -14<=k<=14, -21<=l<=14
Reflections collected	13107
Independent reflections	2748 [R(int) = 0.0468]
Completeness to theta = 30.07°	99.4%
Absorption correction	None
Refinement method	Full-matrix least-squares on F^2
Data / restraints / parameters	2748 / 0 / 251
Goodness-of-fit on F^2	1.048
Final R indices [I>2sigma(I)]	R1 = 0.0469, wR2 = 0.1199
R indices (all data)	R1 = 0.0592, wR2 = 0.1269
Largest diff. peak and hole	0.293 and -0.199 e.$Å^{-3}$

3.14.6 Synthesis of 4-Isocyanato-1,7-di-morpholin-4-yl-4-(3-morpholin-4-yl-3-oxo-propyl)-heptane-1,7-dione (37)

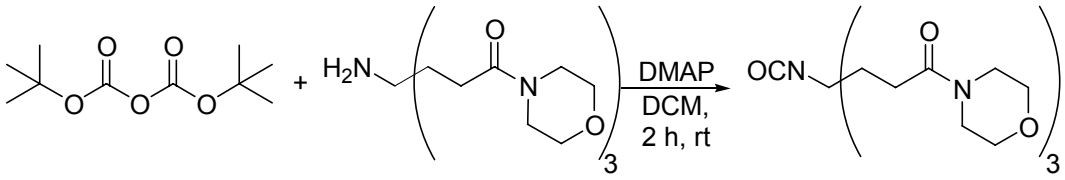

Scheme 3.19 Formation of 4-Isocyanato-1,7-di-morpholin-4-yl-4-(3-morpholin-4-yl-3-oxo-propyl)-heptane-1,7-dione

To a stirred solution of **38** (0.70 g, 1.54 mmol) and DMAP (0.17 g, 1.54 mmol) in DCM (14 mL), the entire solution of di-*tert*-butyldicarbonate (0.47 g, 2.16 mmol) in DCM (51 mL)

was added at rt. After stirring for 2 h, the solution was washed with aq. HCl (3 × 10 mL), followed by water (3 × 10 mL), and dried with Na_2SO_4. The solution was filtered, and then concentrated to leave a white solid. The solid was recrystallized in THF, resulting in a white powder or crystals (0.343 g, 43%), mp 147.7–148.1 °C; ^{1}H NMR ($CDCl_3$): δ 1.96 (m, 6H), 2.40 (m, 6H), 3.46 (m, 6H), 3.47 (m, 6H), 3.61-3.68 (bm, 18H); ^{13}C NMR ($CDCl_3$): δ 27.3, 34.4, 42.2, 45.9, 62.6, 66.6, 66.9, 122.6, 170.3; IR 2971, 2860, 2265, 1629, 1436, 1416 cm^{-1}. HRMS: for $C_{23}H_{37}N_4O_7$ $(M + H)^+$ calcd 481.2662, found 481.2665. Anal. Calcd for $C_{23}H_{36}N_4O_7$: C, 57.49; H, 7.55; N, 11.66. Found: C, 57.43; H, 7.69; N, 11.50.

X-ray analysis of 4-Isocyanato-1,7-di-morpholin-4-yl-4-(3-morpholin-4-yl-3-oxo-propyl)-heptane-1,7-dione

Analysis done by Dr. Carla Slebodnick (Table 3.8). Colorless plates (0.11 x 0.25 x 0.27 mm^3) were crystallized from THF by slow cooling from ~60 °C. The chosen crystal was mounted on a nylon CryoLoop™ (Hampton Research) with Krytox® Oil (DuPont) and centered on the goniometer of an Oxford Diffraction Xcalibur™ diffractometer equipped with a Sapphire 3™ CCD detector. The data collection routine, unit cell refinement, and data processing were carried out with the program CrysAlis. The Laue symmetry was consistent with the triclinc space group P-1. The structure was solved by direct methods and refined using SHELXTL NT. The asymmetric unit of the structure comprises one crystallographically independent molecule and one THF solvate. The final refinement model involved anisotropic displacement parameters for non-hydrogen atoms and a riding model for all hydrogen atoms. One of the morpholine groups of the title compound was modeled as having 2-position disorder with relative occupancies that refined to 0.578(4) and 0.422(4). The entire THF molecule was also modeled

as having 2-position disorder with relative occupancies that refined to 0.611(9) and 0.389(9). SHELXTL NT was used for molecular graphics generation.

Table 3. 8 Crystal Data and Structure Refinement of 4-Isocyanato-1,7-di-morpholin-4-yl-4-(3-morpholin-4-yl-3-oxo-propyl)-heptane-1,7-dione. Data obtained from Dr. Carla Slebodnick.

Category	Crystal Data and Structure Refinement
Empirical formula	$C_{23}H_{36}N_4O_7 \bullet C_4H_8O$
Formula weight	552.66
Temperature	100(2) K
Wavelength	0.71073 Å
Crystal system	Triclinic
Space group	P -1
Unit cell dimensions	a = 8.7158(14) Å α= 112.163(17)°. b = 12.822(2) Å β= 95.296(14)°. c = 14.002(3) Å γ = 102.828(14)°
Volume	1385.9(4) $Å^3$
Z	2
Density (calculated)	1.324 Mg/m^3
Absorption coefficient	0.098 mm^{-1}
F(000)	596
Crystal size	0.27 x 0.25 x 0.11 mm^3
Theta range for data collection	3.73 to 25.17°
Index ranges	-8<=h<=10, -15<=k<=13, -16<=l<=16
Reflections collected	6823
Independent reflections	4914 [R(int) = 0.0217]
Completeness to theta = 30.07°	98.7 %
Absorption correction	None
Refinement method	Full-matrix least-squares on F^2
Data / restraints / parameters	4914 / 20 / 444
Goodness-of-fit on F^2	0.917
Final R indices [I>2sigma(I)]	R1 = 0.0353, wR2 = 0.0817
R indices (all data)	R1 = 0.0582, wR2 = 0.0859
Largest diff. peak and hole	0.154 and -0.185 $e.Å^{-3}$

3.14.7 General Procedure for Synthesis of 3DMAUr18Me and the 3DMAUrn Series

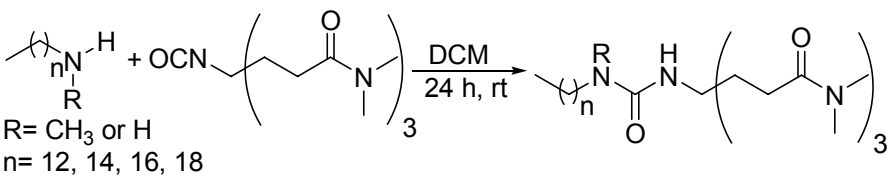

Scheme 3.20 Synthesis of **3DMAUr18Me** and the **3DMAUrn** Series

To a solution or mixture of the appropriate long chain amine (0.564 mmol) in DCM (14 mL), **32** or **36** (0.564 mmol) was added at rt. After stirring for 24 h, the solution was concentrated to yield a white solid. For **3DMAUr18Me** and the **3DMAUrn** series, the solid was recrystallized in ethyl acetate, which yielded a white powder. For **3MorUr18Me** and the **3MorUrn** series, the solid was recrystallized in ethyl acetate/hexane or hexane (**3MorUr18Me**), which yielded a white powder.

4-(2-Dimethylcarbamoyl-ethyl)-4-(3-dodecyl-ureido)-heptanedioic acid bis-dimethylamide (3DMAUr12)

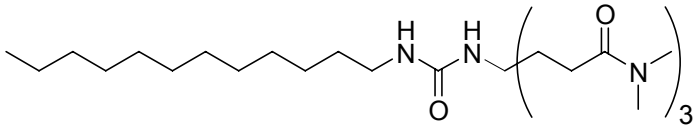

The general procedure described above afforded a white solid (42%); mp 119.3–119.6 °C; ^{1}H NMR ($CDCl_3$): δ 0.87 (t, 3H), 1.24 (m, 18H), 1.42 (m, 2H), 2.06 (m, 6H), 2.39 (m, 6H), 2.92 (s, 9H), 3.02–3.06 (m, 11H), 4.14 (t, 1H), 6.18 (s, 1H); ^{13}C NMR ($CDCl_3$): δ 14.2, 22.8, 27.0, 28.2, 29.42, 29.49, 29.7, 30.6, 31.6, 32.0, 35.7, 37.7, 40.4, 56.5, 157.6, 173.6; IR 3430, 3372, 2917, 2849, 1640, 1627, 1532 cm^{-1}; HRMS: for $C_{29}H_{58}N_5O_4$ $(M + H)^+$ calcd 540.4489, found 540.4492. Anal. Calcd for $C_{29}H_{57}N_5O_4$: C, 64.53; H, 10.64; N, 12.97. Found: C, 64.76; H, 10.57; N, 12.85.

4-(2-Dimethylcarbamoyl-ethyl)-4-(3-tetradecyl-ureido)-heptanedioic acid bis-dimethylamide (3DMAUr14)

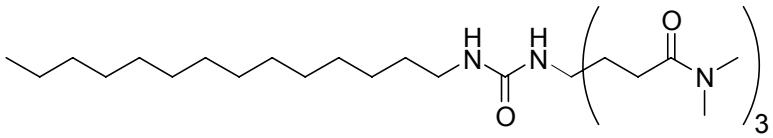

The general procedure described above afforded a white solid (83%); mp 127.3–127.5 °C; ^{1}H NMR ($CDCl_3$): δ 0.87 (t, 3H), 1.24 (m, 22H), 1.42 (m, 2H), 2.05 (m, 6H), 2.38 (m, 6H), 2.92 (s, 9H), 3.02–3.05 (m, 11H), 4.21 (t, 1H), 6.16 (s, 1H); ^{13}C NMR ($CDCl_3$): δ 14.1, 22.7, 27.0, 28.1, 29.4, 29.5, 29.69, 29.73, 30.7, 31.3, 32.0, 35.6, 37.6, 40.2, 56.4, 157.8, 173.5; IR 3431, 3372, 2916, 2849, 1640, 1628, 1533 cm^{-1}; HRMS: for $C_{31}H_{62}N_5O_4$ $(M + H)^+$ calcd 568.4802, found 568.4787. Anal. Calcd for $C_{31}H_{61}N_5O_4$: C, 65.57; H, 10.83; N, 12.33. Found: C, 65.61; H, 10.87; N, 12.21.

4-(2-Dimethylcarbamoyl-ethyl)-4-(3-hexadecyl-ureido)-heptanedioic acid bis-dimethylamide (3DMAUr16)

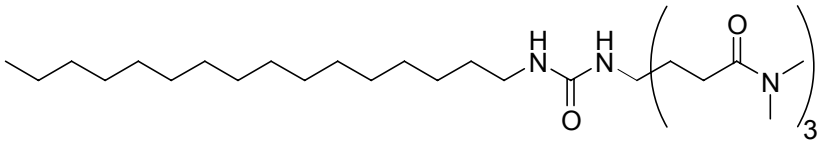

The general procedure described above afforded a white solid (82%); mp 122.2–122.9 °C; ^{1}H NMR ($CDCl_3$): δ 0.87 (t, 3 H), 1.24 (m, 26H), 1.42 (m, 2 H), 2.05 (m, 6 H), 2.39 (m, 6H), 2.92 (s, 9H), 3.02–3.06 (m, 11H), 4.19 (t, 1H), 6.17 (s, 1H); ^{13}C NMR ($CDCl_3$): δ 14.2, 22.8, 27.0, 28.2, 29.4, 29.5, 29.7, 29.77, 29.81, 30.6, 31.5, 32.0, 35.6, 37.7, 40.3, 56.5, 157.7, 173.6; IR 3431, 3372, 2916, 2849, 1641, 1628, 1533 cm^{-1}; HRMS: for $C_{33}H_{66}N_5O_4$ $(M + H)^+$ calcd 596.5115, found 596.5096. Anal. Calcd for $C_{33}H_{65}N_5O_4$: C, 66.51; H, 10.99; N, 11.75. Found: C, 66.64; H, 10.99; N, 11.66.

4-(2-Dimethylcarbamoyl-ethyl)-4-(3-octadecyl-ureido)-heptanedioic acid bis-dimethylamide (3DMAUr18)

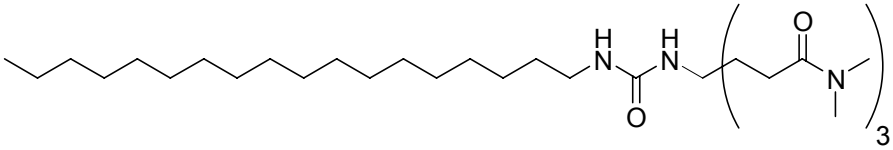

The general procedure described above afforded a white solid (88%); mp 127.0–127.8 °C; ^{1}H NMR ($CDCl_3$): δ 0.87 (t, 3H), 1.25 (m, 30H), 1.42 (m, 2H), 2.05 (m, 6H), 2.39 (m, 6H), 2.91 (s, 9H), 3.04–3.06 (m, 11H), 4.25 (t, 1H), 6.15 (1H); ^{13}C NMR ($CDCl_3$, 500 MHz): δ 14.2, 22.8, 27.0, 28.2, 29.4, 29.5, 29.73, 29.78, 30.6, 31.5, 32.0, 35.7, 37.7, 40.4, 56.5, 157.7, 173.5; IR 3431, 3372, 2916, 2849, 1641, 1625, 1534 cm^{-1}; HRMS: for $C_{35}H_{70}N_5O_4$ $(M + H)^+$ calcd 625.5428, found 624.5417. Anal. Calcd for $C_{35}H_{69}N_5O_4$: C, 67.37; H, 11.15; N, 11.22. Found: C, 67.08; H, 11.09; N, 11.20.

4-(2-Dimethylcarbamoyl-ethyl)-4-(3-methyl-3-octadecyl-ureido)-heptanedioic acid bis-dimethylamide (3DMAUrMe18)

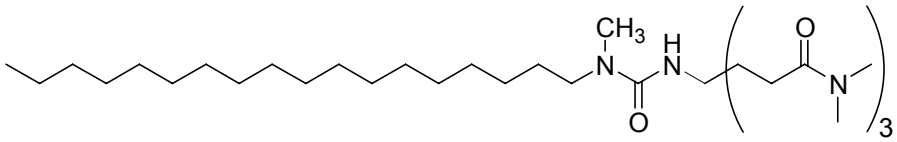

The general procedure described above afforded a white solid (55%); mp 91.4–92.4 °C; ^{1}H NMR ($CDCl_3$): δ 0.87 (t, 3H), 1.24 (m, 30H), 1.44 (m, 2H), 2.09 (m, 6H), 2.37 (m, 6H), 2.81 (s, 3H), 2.91 (s, 9H), 3.01 (s, 9H), 3.15 (m, 2H), 6.02 (s, 1H); ^{13}C NMR ($CDCl_3$): δ 14.2, 22.8, 27.0, 28.3, 29.4, 29.68, 29.73, 29.78, 29.81, 31.5, 32.0, 34.6, 35.6, 37.6, 48.8, 56.9, 157.4, 173.5; IR 2915, 2848, 1634, 1512 cm^{-1}; HRMS: for $C_{36}H_{72}N_5O_4$ $(M + H)^+$ calcd 638.5584, found 638.5548. Anal. Calcd for $C_{36}H_{71}N_5O_4$: C, 67.77; H, 11.22; N, 10.98. Found: C, 67.74; H, 11.25; N, 11.01.

3.14.8 General Procedure for the Synthesis of 3MorUr18Me and the 3MorUrn Series

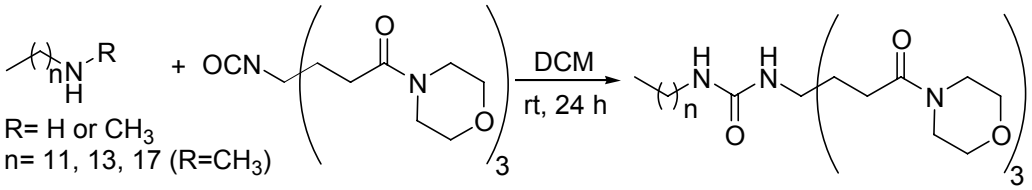

Scheme 3.21 Synthesis of **3MorUr18Me** and the **3MorUrn** Series

To a solution or mixture of the appropriate long-chain amine (0.208 mmol) in DCM (8 mL), the isocyanate (0.208 mmol) was added at rt. After stirring for 24 h, the solution was concentrated to yield a white solid. The solid was recrystallized with ethyl acetate/hexane and hexane (**3MorUr18Me**), which yielded a white powder.

Synthesis of 1-Dodecyl-3-[4-morpholin-4-yl-1,1-bis-(3-morpholin-4-yl-3-oxo-propyl)-4-oxo-butyl]-urea, 3MorUr12

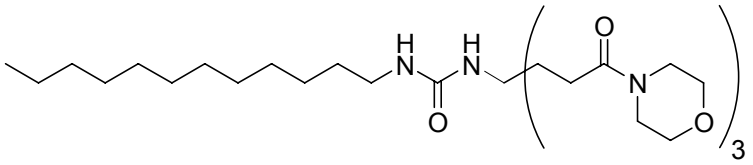

The general procedure described above afforded a white solid (44%); mp 156.2–157.1 °C; ^{1}H NMR ($CDCl_3$): δ 0.87 (t, 3H), 1.24 (m, 18H), 1.41 (m, 2H), 2.02 (m, 6H), 2.37 (m, 6H), 3.03 (m, 2H), 3.48 (m, 6H), 3.58 (m, 6H), 3.66 (m, 12), 4.24 (m, 1H), 5.82 (1H); ^{13}C NMR ($CDCl_3$): δ 14.2, 22.8, 27.0, 27.9, 29.4, 29.7, 30.5, 31.8, 40.6, 42.1, 46.2, 56.5, 66.8, 66.9, 157.4, 172.0; IR 3392, 3365, 2923, 2849, 1681, 1640, 1622, 1553 cm^{-1}; HRMS: for $C_{35}H_{64}N_5O_7$ $(M + H)^+$ calcd 666.4806, found 666.4783. Anal. Calcd for $C_{35}H_{63}N_5O_7$: C, 63.13; H, 9.54; N, 10.52. Found: C, 62.85; H, 9.54; N, 10.44.

Synthesis of 1-[4-Morpholin-4-yl-1,1-bis-(3-morpholin-4-yl-3-oxo-propyl)-4-oxo-butyl]-3-tetradecyl-urea, 3MorUr14

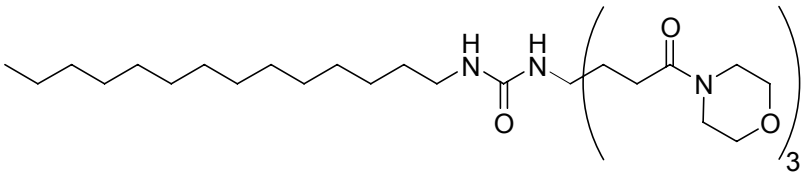

The general procedure described above afforded a white solid (73%); mp 158.8–159.8 °C; ^{1}H NMR ($CDCl_3$): δ 0.87 (t, 3H), 1.24 (m, 22H), 1.41 (m, 2H), 2.02 (m, 6H), 2.37 (m, 6H),

3.02 (m, 2H), 3.48 (m, 6H), 3.58 (m, 6H), 3.65 (m, 12H), 4.29 (m, 1H), 5.81 (1H); ^{13}C NMR ($CDCl_3$): δ 14.2, 22.8, 27.0, 27.9, 29.4, 29.5, 29.72, 29.75, 30.6, 31.8, 32.0, 40.5, 42.1, 46.3, 56.5, 66.81, 66.87, 157.5, 172.1; IR 3389, 3363, 2919, 2849, 1681, 1640, 1621, 1547, 1432 cm^{-1}; HRMS: for $C_{37}H_{68}N_5O_7$ $(M + H)^+$ calcd 694.5119, found 694.5118. Anal. Calcd for $C_{37}H_{67}N_5O_7$: C, 64.04; H, 9.73; N, 10.09. Found: C, 63.79; H, 9.60; N, 9.86.

Synthesis of 1-Methyl-3-[4-morpholin-4-yl-1,1-bis-(3-morpholin-4-yl-3-oxo-propyl)-4 -oxo-butyl]-1-octadecyl-urea, 3MorUr18Me

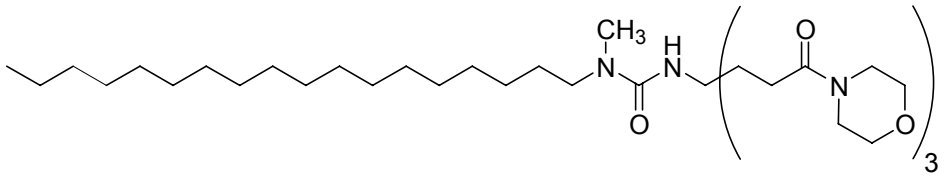

The general procedure described above afforded a white solid (57%); mp 102.0–102.8 °C. ^{1}H NMR ($CDCl_3$): δ 0.87 (t, 3H), 1.25–1.29 (bm, 30H), 1.44 (bm, 2H), 2.08 (m, 6H), 2.37 (m, 6H), 2.80 (s, 3H), 3.15 (m, 3H), 3.48 (m, 6H), 3.58 (m, 6H), 3.64-3.67 (bm, 12H), 5.81 (s, 1H); ^{13}C NMR ($CDCl_3$): δ 14.2, 22.8, 27.0, 28.0, 28.3, 29.4, 29.74, 29.78, 31.8, 32.0, 34.6, 42.1, 46.2, 48.9, 56.8, 66.82, 66.89, 157.3, 172.1; IR 3395, 2918, 2850, 1645, 1634, 1524, 1429 cm^{-1}; HRMS: for $C_{42}H_{78}N_5O_7$ $(M + H)^+$ calcd 764.5901, found 764.5932. Anal. Calcd for $C_{42}H_{77}N_5O_7$: C, 66.02; H, 10.16; N, 9.17. Found: C, 66.10; H, 10.15; N, 9.02.

3.15 References for Chapter 3

1. Sugandhi, E.W., Macri, R. V., Williams, A. A., Kite, B. L., Slebodnick, C., Falkinham, J. O., Esker, A. R., Gandour, R. D., *Synthesis, critical micelle concentrations, and antimycobacterial properties of homologous, dendritic amphiphiles. Probing intrinsic activity and the "cutoff" effect.* J. Med. Chem., 2007. **50**(7): p. 1645-1650.
2. Patterson, J.M., Barnes, M. W., *Potassium fluoride-catalyzed Michael addition of nitro alkanes.* Bull. Chem. Soc. Jpn., 1967. **40**: p. 2715-2716.
3. Newkome, G.R., Yoo, K. S., Kim, H. J., Moorefield, C. N., *Routes to metallodendrimers: Synthesis of isomeric neutral metallomacro-molecules based on Bis(2,2 ': 6 ',2 ''-terpyridine)ruthenium(II) connectivity.* Chem.–Eur. J., 2003. **9**(14): p. 3367-3374.

4. Newkome, G.R., Kotta, K. K., Moorefield, C. N., *Convenient synthesis of 1 -> 3 C-branched dendrons.* J. Org. Chem., 2005. **70**(12): p. 4893-4896.
5. Newkome, G.R., Behera, R. K., Moorefield, C. N., Baker, G. R., *Chemistry of Micelles Series .18. Cascade Polymers - Syntheses and Characterization of One-Directional Arborols Based on Adamantane.* J. Org. Chem., 1991. **56**(25): p. 7162-7167.
6. Newkome, G.R., Weis, C. D., Childs, B. J., *Syntheses of 1 → 3 branched isocyanate monomers for dendritic construction.* Des. Monomers Polym., 1998. **1**: p. 3-14.

Chapter 4: Results and Discussion of MIC Measurements for the 3CAmn Series

4.1 Introduction to Antimicrobial Testing

The Gandour group is a synthetic organic chemistry group; consequently, our labs are not equipped for microbiological experiments. Dr. Joseph Falkinham III, of the Biology Department at VA Tech, graciously provided lab space, microorganisms, equipment, and supervision. Thomas Wall, a former VA Tech undergraduate student, taught me how to do microbial assays.

4.2 General Antimicrobial Activity of the 3CAmn Series

Typically, FAs are active against Gram-positive bacteria,[1] mycobacteria,[2] and fungi.[3] In general, FAs are not active against Gram-negative bacteria. The **3CAmn** series displayed the best antimicrobial activities against yeasts and *M. smegmatis* (a mycobacterium), and modest to minimal activity against Gram-negative and Gram-positive bacteria.

4.3 Antimicrobial Activity of the 3CAmn Series against Gram-negative Bacteria

In this chapter, chain length effects will be discussed and comparisons will be made between the chain lengths of FAs and those of the **3CAmn** series. Some members of the **3CAmn** series (**3CAm19** and **3CAm21**) were synthesized directly from FAs (Chapter 2). Due to the presence of the amide linker and how we chose to name the series, direct comparisons between FAs and the **3CAmn** series can be tricky. For example, **3CAm21** is synthesized directly from C_{22} acid (Figure 4.1). Both the FA and the amphiphile have C_{22} carbon chains; however, because the carbonyl carbon is included in the linker, the amphiphile is named **3CAm21** instead of **3CAm22**. In this chapter, I will refer to the "true" chain length of the **3CAmn** series. For example, I will state that **3CAm19** has a C_{20} carbon chain. This issue is present for all members of the **3CAmn** series.

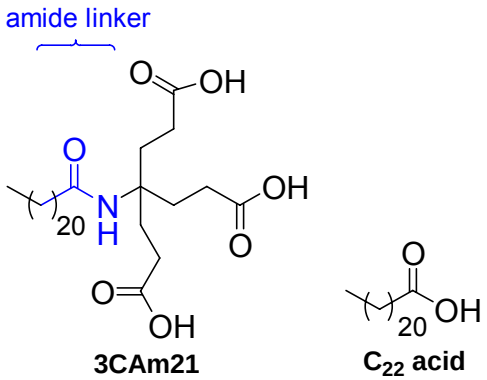

Figure 4.1 Nomenclature of the **3CAmn** Series

Similar to long-chain FAs, the **3CAmn** series displayed modest activity against Gram-negative bacteria (Table 4.1). Both **3CAm19** and **3CAm21** displayed the best activity against *E. coli*. The activity increased with chain length up to **3CAm21**. Even though the activity against *E. coli* was unimpressive, the activities displayed by the **3CAmn** (0.61–0.13 mM) series were better than those shown by the best FAs [(complete inhibition C_{18}, 1300 µg/mL, 4.4 mM)[4] and (incomplete inhibition C_8, 450 µg/mL, 3.1 mM)] reported in the literature.[5] The results also indicated that a longer chain might result in better activity. As the activity increased with chain length, it is possible that the optimum chain length for activity against *E. coli* has not been established.

Table 4.1 Antimicrobial Activities of the **3CAmn** Series against Gram-negative Bacteria

	MIC (µg/mL)		
Compound	**Microorganisms**		
	E. coli	***K. pneumoniae***	***N. gonorrhoeae***
3CAm13	280	570–280[a]	570
3CAm14	160	570–280[a]	570
3CAm15	140–280	570–140[a]	570
3CAm16	280	570–140[a]	570
3CAm17	140	570–280[a]	140
3CAm19	71	570–280[a]	71
3CAm21	71	280	71

Superscript "a" indicates incomplete inhibition

The **3CAmn** series displayed less antimicrobial activity against *K. pneumoniae* than *E. coli* and exhibited both incompletely and complete inhibition of *K. pneumoniae*. With respect to incomplete inhibition, **3CAm15** (0.29 mM) and **3CAm16** (0.28 mM) displayed the best activity. Following **3CAm16**, the activity decreased with chain length. With respect to complete inhibition, the activity stayed constant with increasing chain length up to **3CAm19**, then increased (**3CAm21**, 0.52 mM). Due to such an observation, the specific chain length that gives optimum activity against *K. pneumoniae* has not been discovered. Even though the activities against *K. pneumoniae* were unimpressive, the activity displayed by **3CAm21** (0.52 mM) was better than the best FA (C_{18}, 4.40 mM).[4]

Unlike most Gram-negative bacteria, *N. gonorrhoeae* showed susceptibility to long chain FAs.[6] Similar to FAs, the longest members of the **3CAmn** series, **3CAm19** (0.14 mM) and **3CAm21** (0.13 mM), exhibited good activities against *N. gonorrhoeae*. From **3CAm13** to **3CAm16**, the MICs remained constant. Then, there is a large increase in activity for **3CAm16**, followed by another increase in activity for **3CAm19**; however, the activity remains the same for **3CAm21**. Although the activity against *N. gonorrhoeae* had leveled off, a longer chain could have better activity. Thus, the optimum chain length against *N. gonorrhoeae* might not have been established. The **3CAmn** series was not as active as the most active FA (C_{16}, 1.5 μg/mL, 0.006 mM);[6] however, we believe our compounds could be considered more active because the reported value[6] is an IC_{50} (concentration required to inhibited 50% growth of organism) value. The **3CAmn** series completely inhibited the growth of *N. gonorrhoeae*. Bergsson et al. studied the susceptibilities of five strains of *N. gonorrhoeae* to FAs (C_8–C_{14}).[7] The C_{12} acid was the most active FA tested and completely inhibited the growth of *N. gonorrhoeae* at 2.5 mM.

4.4 Antifungal Activity of the 3CAmn Series against Yeasts and *A. niger*

The **3CAmn** series displayed the best activity against fungi, specifically, yeast (Table 4.2). Among the microorganisms tested, *S. cerevisiae* was most susceptible to the **3CAmn** series. **3CAm21** completely inhibited the growth of S. *cerevisiae* at concentrations of 4.4 μg/mL. The antifungal activity of homologues containing odd numbered chains increased with chain length. The activity did not decrease or plateau, meaning that the activity was still increasing. This indicated that a longer chain could lead to better activity. The activity displayed by **3CAm21** (0.008 mM) was better than that displayed by the most active FA (C_{11}, 500 μg/mL, 2.7 mM).[8]

Table 4.2 Antimicrobial Activities of the **3CAmn** Series against Fungi

	MIC (μg/mL)			
Compound	**Microorganisms**			
	S. cerevisiae	***C. albicans***	***C. neoformans***	***A. niger***
3CAm13	570	280[a]	140[a]	6300
3CAm14	570	280[a]	140[a]	6300
3CAm15	280	140[a]	140[a]	3100
3CAm16	280	140[a]	140[a]	280
3CAm17	140	140[a]	71[a]–140[a]	140
3CAm19	36	8.9[a]	18[a]–36[a]	71
3CAm21	4.4	4.4[a]	140[a]	71

Superscript "a" indicates incomplete inhibition

The **3CAmn** series also showed very good activity against *C. albicans*. Similar to *S. cerevisiae*, **3CAm21** also inhibited *C. albicans* at a concentration of (4.4 μg/mL, 0.008 mM). However, unlike *S. cerevisiae*, the **3CAmn** series incompletely inhibited the growth of *C. albicans*. There was not a strict, direct relationship between chain length and antimicrobial activity. Initially, the activity was constant for **3CAm13** and **3CAm14**. The activity increased and leveled off between **3CAm15** and **3CAm17**. Then, there was a very sharp increase in activity between **3CAm17** and **3CAm19**, followed by the increased activity of **3CAm21.** The

longest chain amphiphile, **3CAm21**, was more active than the best FA (C_{10}, 100 μg/mL, 0.58 mM)[8] although the reported value pertains to complete inhibition.

Similar to the activity observed against *N. gonorrhoeae*, there seems to be a large preference for the longer chain homologues versus the shorter chain homologues. Similar to the activity of *S. cerevisiae*, the activity against *C. albicans* was still increasing and had not leveled off. Thus, an optimum chain length has not been established and it is possible that a longer chain could lead to increased activity and possibly complete inhibition.

Within the yeasts—*S. cerevisiae*, *C. albicans*, and *C. neoformans*— the **3CAmn** series showed the least activity against *C. neoformans*. Similar to *C. albicans*, the **3CAmn** series incompletely inhibited *C. neoformans*. The activity increased with chain length, until a decrease in activity was observed for **3CAm21**. Because the activity decreased, the optimum chain length for *C. neoformans* was C_{20} (**3CAm19**, 0.035 mM). Although the activities were not impressive, the activities were better than that reported for FAs (C_{14}, >5.0 mM)[9] although the reported value pertains to complete inhibition.

Unlike the yeast, *A. niger* (a fungus) was more resistant to the **3CAmn** series. With the exception of **3CAm14**, the activity increased with chain length until it leveled off between **3CAm19** and **3CAm21**. Although the activity leveled off, it is possible that a longer chain length could lead to increased activity. The activities displayed by **3CAm19** (0.14 mM) and **3CAm21** (0.13 mM) were better than the best activity reported in the literature (C_{14}, 2.7 mM).[9]

4.5 Antimicrobial Activity of the 3CAmn Series against Gram-positive Bacteria and *M. smegmatis*

Unlike Gram-negative bacteria, Gram-positive bacteria are typically susceptible to FAs.[8, 10, 11] This trend was also observed in the **3CAmn** series except in the case of *M.*

luteus (Table 4.3). *M. luteus* was not inhibited (incompletely or completely) by any member of the **3CAmn** series at the maximum concentration tested (6300 μg/mL). This was the only microorganism tested that was totally resistant to the **3CAmn** series. We could not find any studies in the literature that reported the MIC of FAs against *M. luteus*.

Table 4.3 Antimicrobial Activities of the **3CAmn** Series against Gram-positive Bacteria and *M. smegmatis*

MIC (μg/mL)

Compound	Microorganisms				
	M. luteus	***L. plantarum***	***S. aureus***	***MRSA***	***M. smegmatis***
3CAm13	>6300	280[a]	6300[a]	570[a]	280
3CAm14	>6300	570[a]	6300[a]	570[a]	140
3CAm15	>6300	280[a]	6300[a]	570[a]	140
3CAm16	>6300	570[a]	6300[a]	570[a]	140
3CAm17	>6300	280[a]	6300[a]	570[a]	36
3CAm19	>6300	280[a]	780[a]	36	18
3CAm21	>6300	280[a]	391[a]	71	36

Superscript "a" indicates incomplete inhibition

The **3CAmn** series displayed modest activities against *L. plantarum*, which is advantageous because *L. plantarum* is a beneficial bacterium. The fact that the **3CAmn** series has low-incomplete activity against a beneficial bacterium but relatively higher activities against pathogens, such as *N. gonorrhoeae* and *C. albicans*, was promising.

Based on the results, it appears that chain length did not have any affect on antimicrobial activity. This is true except in the case of **3CAm14** and **3CAm16**. Interestingly, these odd chain homologues exhibit better activities than their even-chain counterparts. However, with only two data points, we cannot convincingly conclude that even chain homologues are less active than odd chain homologues. We cannot find any antimicrobial FA studies against *L. plantarum* to compare to the **3CAmn** series.

The **3CAmn** series displayed modest activity against *S. aureus*. Increasing chain length did not affect activity until a dramatic increase for **3CAm19** (1.5 mM) and **3CAm21** (0.72 mM)

was observed. The **3CAmn** series only incompletely inhibited *S. aureus*. The optimum chain length for *S. aureus* was not established because the activity was still increasing. Due to the increasing activity, a longer chain length could possibly lead to increased activity, complete inhibition of growth, or both. Although the **3CAmn** series does not display impressive activity against *S. aureus*, the activity displayed was better than the best reported MIC values for FAs (C_{12}, 2.5 mM).[12]

Surprisingly, the **3CAmn** series displayed much better activity against MRSA than *S. aureus*. Similar to *S. aureus*, MRSA was incompletely inhibited by the shorter homologues (**3CAm13**–**3CAm17**). Higher homologues, **3CAm19** (0.07 mM) and **3CAm21** (0.13 mM), completely inhibited the growth of MRSA. The optimum chain length for inhibiting MRSA was C_{20} because the activity begins to decrease for **3CAm21**.

The differences in antimicrobial properties of the **3CAmn** series against *S. aureus* and MRSA is surprising because MRSA is a more resilient strain of *S. aureus* and is resistant to an increasing number of antibiotics.[13] Although the **3CAmn** series is not very active against MRSA, the series was more active than the best FA (C_{12}, 2.0 mM).[13]

Mycobacteria are susceptible to FAs.[14, 15] We decided to test the **3CAmn** series against *M. smegmatis* as a test case to see if the series would be active against other mycobacteria. The optimum chain length for *M. smegmatis* was C_{20} (**3CAm19**, 0.035 mM). The activity initially increased (**3CAm13**–**3CAm14**), leveled off (**3CAm14**–**3CAm16**), increased (**3CAm16**–**3CAm19**), and then decreased (**3CAm21**). Although the activity was not as good as that seen in yeast (4.4 μg/mL), the result was still encouraging. The **3CAmn** series displayed good enough activity to warrant further testing against more pathogenic bacteria, such as *M. tuberculosis.*

Saito et al. studied the antimicrobial properties of even numbered FAs ranging from C_8–C_{20}.[2] Only C_{10} acid inhibited the growth of *M. smegmatis* at 40% and 80% (0.58 mM) (100 μg/mL). *M. smegmatis* was resistant to all other FAs that were tested at the maximum concentration of 400 μg/mL.

4.6 Conclusions

Overall, the **3CAmn** series inhibited *M. smegmatis*, fungi and exhibited comparable activity against Gram-positive and Gram-negative bacteria. Overall, the **3CAmn** series was most active against fungi. Antimicrobial activity was still increasing with chain length against *C. albicans*, *S. cerevisiae*, and *K. pneumoniae*. Additionally, activities against *A. niger*, *N. gonorrhoeae*, *E. coli*, *L. plantarum*, and *S. aureus* has level off, but not decreased. Based on these observations, longer chains (e. g. C_{23}) might lead to enhanced activity.

4.7 MIC Procedure for Antimicrobial Testing

4.7.1 Microbial Strains, Culture Conditions, and Preparations of Inocula for Susceptibility Testing

Strains of *E. coli* strain C (ATCC # 13706), *K. pneumoniae* (ATCC # 4352), *L. plantarum* (ATCC # 14917), *S. aureus* (ATCC # 6538), and *M. smegmatis* (ATCC # 607) were obtained from the American Type Culture Collection. A methicillin-resistant isolate of *S. aureus* (MRSA) was obtained from the Microbiology Laboratory, Danville Community Hospital (Virginia) and *S. cerevisiae*, *C. albicans, C. neoformans*, *A. niger,* and *M. luteus* strains were obtained from the Virginia Tech Microbiology teaching culture collection. Colonies of *E. coli*, *K. pneumoniae*, *S. aureus*, MRSA, *M. luteus*, *S. cerevisiae*, *C. albicans*, and *C. neoformans* were grown on 1/10-strength Brain Heart Infusion Broth containing 0.2% (wt/vol) sucrose (BHIB+S) and 1.5% (wt/vol) agar. *L. plantarum* was grown on ¼-strength Tryptic Soy Broth containing

0.2% glucose (TSB+G) and 1.5% (wt/vol) agar. *N. gonorrhoeae* was grown on Chocolate agar medium (BBL Microbiology Systems, Sparks, MD) containing hemoglobin. *M. smegmatis* was grown on Middlebrook 7H10 agar and *A. niger* on Potato Dextrose Agar. Streaked plates were incubated at 37 °C for 3–7 days, except for that of *A. niger*, which was incubated in the dark at 30 °C. A single colony for each microbe except *A. niger* was used to inoculate 5 mL of 1/10-strength BHIB+S (*E. coli*, *K. pneumoniae*, *M. luteus*, *S. aureus*, and MRSA), TSB (*L. plantarum*), Middlebrook 7H9 broth (*M. smegmatis*), Yeast Extract Peptone Maltose broth (*S. cerevisiae*, *C. albicans* and *C. neoformans*), or GC broth medium (*N. gonorrhoeae*) and incubated at 37 °C (*S. cerevisiae* and *M. luteus* at 30 °C) for 4–7 days. After growth, the resulting broth cultures were diluted with buffered saline gelatin to equal the turbidity of a No. 1 McFarland Standard. *N. gonorrhoeae* was grown at 37 °C in an anaerobic jar containing a CO_2 gas generator. After 4 days incubation, 5 mL of buffered saline gelatin (BSG) was added to each culture and vortexed at the highest speed. The brown insoluble contents of the GC medium were allowed to settle to the bottom of the tube at room temperature. The supernatant cell suspension was transferred to a fresh sterile tube with collecting the insoluble contents and the turbidity of the suspension diluted with BSG to equal a McFarland No. 1 standard.

To check for viability and contamination, broth cultures were streaked on Plate Count Agar or Chocolate agar (*N. gonorrhoeae*); the plates were incubated at 37 °C for 3–4 days. Plates for *M. luteus* and *S. cerevisiae* were grown at 30 °C. Plates for *N. gonorrhoeae* were incubated at 37 °C in an anaerobic jar containing a CO_2 gas generator. Spores of *A. niger* were scraped from the surface of PDA and suspended in 5 mL of 1/10-strength BHIB+S and that suspension transferred to a sterile test tube. The turbidity was adjusted to a No. 1 McFarland

Standard by dilution with BSG. To check for viability and contamination, those spore suspensions were streaked on PDA and incubated at 37 °C for 3–4 days.

4.7.2 Quality Assurance

For the work reported here, all cultures and suspensions that were used as inocula were uncontaminated and the colonies had the expected morphologies. All viable, uncontaminated inocula were stored up to 14 days at 4 °C until used without any differences in susceptibility to antimicrobial compounds.

4.7.3 Measurement of MIC

MICs of compounds dissolved in aqueous triethanolamine were measured by broth microdilution in 96-well microtiter plates. Preliminary experiments demonstrated that 4% (wt/vol) triethanolamine/water did not inhibit the growth of any microorganism tested. A two-fold dilution series of the compounds was prepared in 96-well microtiter plates in a 50 μL volume of 1/10-strength BHIB+S and the dilution series was inoculated with 50 μL of each cell suspension. For *E. coli* and *K. pneumoniae*, the volume of the medium and the inoculum were doubled. The resulting inoculated dilution series were incubated at 30 °C and growth, as turbidity, scored visually and recorded on the fourth day. For *E. coli* and *K. pneumoniae*, the incubation temperature was 37 °C and the duration was 7 days. The MIC of each compound was measured in triplicate and was defined as the lowest concentration of drug resulting in a prominent visible decrease in turbidity (incomplete; i.e., ≥ 50%) or a complete absence of visible turbidity compared to the drug-free control. In many cases ("a" in Tables 1–3), inhibition was incomplete.

4.8 References for Chapter 4

1. Kabara, J.J., Vrable, R., Liekenjie, M. S. F., *Antimicrobial lipids-natural and synthetic fatty-acids and monoglycerides.* Lipids, 1977. **12**(9): p. 753-759.

2. Saito, H., Tomioka, H., Yoneyama, T., *Growth of Group-IV mycobacteria on medium containing various saturated and unsaturated fatty-acids.* Antimicrob. Agents Chemother., 1984. **26**(2): p. 164-169.
3. Kabara, J.J., *Structure-function-relationships of surfactants as anti-microbial agents.* J. Soc. Cosmet. Chem., 1978. **29**(11): p. 733-741.
4. Jossifova, L.T., Manolov, I., Golovinsky, E. V., *Antibacterial action of some saturated and unsaturated long-chain carboxylic acids and their bis(2-chloroethyl)aminoethyl esters in vitro.* Die Pharmazie 1989. **44**(12): p. 854-856.
5. Marounek, M., Skrivanova, E., Rada, V., *Susceptibility of Escherichia coli to C_2-C_{18} fatty acids.* Folia Microbiol., 2003. **48**(6): p. 731-735.
6. Miller, R.D., Brown, K. E., Morse, S. A., *Inhibitory action of fatty-acids on growth of Neisseria-gonorrhoeae.* Infect. Immun., 1977. **17**(2): p. 303-312.
7. Bergsson, G., O. Steingrimsson, and H. Thormar, *In vitro susceptibilities of Neisseria gonorrhoeae to fatty acids and monoglycerides.* Antimicrob. Agents Chemother., 1999. **43**(11): p. 2790-2792.
8. Kabara, J.J., Vrable, R., Liekenjie, M. S. F., *Antimicrobial lipids -natural and synthetic fatty-acids and monoglycerides.* Lipids, 1977. **12**(9): p. 753-759.
9. Parang, K., Knaus, E. E., Wiebe, L. I., Sardari, S., Daneshtalab, M., Csizmadia, F., *Synthesis and antifungal activities of myristic acid analogs.* Arch. Pharm., 1996. **329**(11): p. 475-482.
10. Bergsson, G., Arnfinnsson, J., Steingrimsson, O., Thormar, H., *Killing of Gram-positive cocci by fatty acids and monoglycerides.* Apmis, 2001. **109**(10): p. 670-678.
11. Kabara, J.J., Conley, A. J., Truant, J. P., *Relationship of chemical structure and antimicrobial activity of alkyl amides and amines.* Antimicrob. Agents Chemother., 1972. **2**(6): p. 492-498.
12. Kabara, J.J., *Structure-function-relationships of surfactants as antimicrobial agents.* J. Soc. Cosmet. Chem., 1978. **29**(11): p. 733-741.
13. Kitahara, T., Koyama, N., Matsuda, J., Aoyama, Y., Hirakata, Y., Kamihira, S., Kohno, S., Nakashima, M., Sasaki, H., *Antimicrobial activity of saturated fatty acids and fatty amines against Methicillin-Resistant Staphylococcus aureus.* Biol. Pharm. Bull., 2004. **27**(9): p. 1321-1326.
14. Kondo, E. and K. Kanai, *Lethal effect of long-chain fatty acids on mycobacteria.* Jpn. J. Med. Sci. Biol., 1972. **25**(1): p. 1-13.
15. Kondo, E., Kanai, K., *Further-studies on lethal effect of long-chain fatty-acids on mycobacteria.* Japan. J. Med. Sci. Biol., 1976. **29**(1): p. 25-37.

Chapter 5: Results and Discussion: Antimicrobial Activity of 3DMAUr18Me, 3MorUr18Me and the 3DMAUrn and 3MorUrn Series

5.1 Introduction to MIC Measurements

The **3CAmn** series exhibited the best activity against *M. smegmatis* and yeasts. The **3CAmn** series inhibited the growth of Gram-negative bacteria and Gram-positive bacteria equally, albeit modestly. As the nonionic series (**3DMAUr18Me**, **3DMAUr12**, **3DMAUr14**, and **3MorUr14)** are drastically different (nonionic vs. ionic headgroups) from the **3CAmn** series, would these series show similar antimicrobial activity? The results were mixed. Both ionic and nonionic amphiphiles inhibited the growth of Gram-positive bacteria, *M. smegmatis*, yeasts, and *A. niger*. However, there were some important differences between the **3CAmn** series and the nonionic amphiphiles. Unlike the **3CAmn** series, the nonionic amphiphiles were mostly inactive against Gram-negative bacteria (except *N. gonorrhoeae*) and inhibited the growth of all Gram-positive microorganisms. Compared to the **3CAmn** series, the nonionic amphiphiles were far less active against yeasts and *A. niger*.

Unfortunately, some nonionic amphiphiles were not tested due to the low aqueous solubility. While **3DMAUr12**, **3DMAUr14**, **3DMAUr18Me** and **3MorUr14** were water soluble and tested; **3DMAUr16**, **3DMAUr18**, **3MorUr18Me,** and **3MorUr12** were not water soluble and not tested. The case of **3MorUr12** was puzzling because, based on hydrophobicity, **3MorUr12** should be more water soluble than **3MorUr14**, but was not. The sample of **3MorUr12** had a good melting range (≤ 1°) and passed elemental analysis, therefore, purity should not be a concern. The aqueous solubility of these amphiphiles was not solely based on the length of the hydrocarbon chain (hydrophobicity). Aqueous solubility is also based on a mixture of polarity and melting point. For example, **3DMAUr16** (122.2–122.9 °C) has a C_{16}

alkyl chain and is not water soluble but **3DMAUr18Me** (91.4–92.4 °C) has a C_{18} alkyl chain and is water soluble. A lower melting point corresponds to fewer attractive forces holding the individual molecules together, which could explain why **3DMAUr18Me** dissolves more readily than **3DMAUr16**.

5.2 Antimicrobial Activity of 3DMAUr18Me, 3DMAUr12, 3DMAUr14, and 3MorUr14 against Gram-negative Bacteria

Similar to FAs, the nonionic amphiphiles exhibited minimal activity against Gram-negative bacteria (Table 5.1). *N. gonorrhoeae* was the only exception. Against *E. coli* and *K. pneumoniae*, **3DMAUr12**, **3DMAUr14**, and **3DMAUr18Me** were equally active. Amphiphiles **3DMAUr12** (5000 μg/mL, 9.5 mM), **3DMAUr14** (5000 μg/mL, 9.0 mM), and **3DMAUr18Me** (5000 μg/mL, 8.0 mM) were far less inhibitory against *E. coli* than the best FA, (complete inhibition C_{18}, 1300 μg/mL, 4.4 mM)[1] and incomplete inhibition C_8, (450 μg/mL, 3.1 mM) [2], reported in the literature. Ōmura et al. reported that C_{12}-*N*,*N*-dimethylamide (31 μg/mL, 0.14 mM) inhibited the growth of *E. coli*.[3] In contrast, Kabara et al. reported that C_{12}-*N*,*N*-dimethylamide did not inhibit the growth of *E. coli*.[4]

Table 5.1 Antimicrobial Activity of **3DMAUr12**, **3DMAUr14**, **3DMAUr18Me**, and **3MorUr14** against Gram-negative Bacteria

Microorganisms	MIC (μg/mL) Amphiphiles			
	3DMAUr12	**3DMAUr14**	**3DMAUr18Me**	**3MorUr14**
E. coli	2500[a]–5000	2500[a]–5000	5000	NT
K. pneumoniae	2500[a]–5000	2500[a]–5000	1400[a]–5000	2500[a]–5000
N. gonorrhoeae	39	9.8	NT	20[a]–630

E. coli and *K. pneumoniae* was allowed to grow for 7 d, while *N. gonorrhoeae* was grown for 4 d. Superscript "a" indicates incomplete inhibition

The nonionic amphiphiles had the same activity against *K. pneumoniae* as they did against *E. coli*. Amphiphiles **3DMAUr12** (5000 μg/mL, 9.5 mM), **3DMAUr14** (5000 μg/mL, 9.0 mM), **3DMAUr18Me** (5000 μg/mL, 8.0 mM) and **3MorUr14** (5000 μg/mL, 7.2 mM) were

far less active against *K. pneumoniae* than the best FA (C_{18}, 4.4 mM).[1] Additionally, the nonionic amphiphiles were less active than the **3CAmn** series (1.3–0.52 mM) against *K. pneumoniae*.

Against *N. gonorrhoeae*, **3DMAUr12**, **3DMAUr14**, and **3DMAUr18Me** were much more active than **3MorUr14**. Amphiphile **3DMAUr14** (9.8 μg/mL, 0.018 mM) was more active than any member of the **3CAmn** series (**3CAm19** and **3CAm21,** 71 μg/mL, 0.14–0.13 mM) but **3MorUr14** (630 μg/mL, 0.90 mM) was not as active compared to **3CAm19** and **3CAm21**. Amphiphile **3DMAUr14** (9.8 μg/mL, 0.018 mM) was not as active as the most active FA (C_{16}, 1.5 μg/mL, 0.006 mM)[5]. We believe our amphiphiles were more active because the reported value[2] is an IC_{50} (concentration required to inhibited 50% growth of organism) value while the nonionic amphiphiles completely inhibited *N. gonorrhoeae*. Bergsson et al. reported that 2.5 mM of the C_{12} acid inhibited the growth of *N. gonorrhoeae*.[6] Lower concentrations (e.g. 0.31 mM) led to the loss of almost all activity.

5.3 Antimicrobial Activity of 3DMAUr18Me, 3DMAUr12, 3DMAUr14, and 3MorUr14 against Gram-positive Bacteria and *M. smegmatis*

Kabara et al. and Ōmura et al. reported that long-chain amides inhibited the growth of Gram-positive bacteria.[3, 7] Consequently, we expected the nonionic amphiphiles to inhibit the growth of Gram-positive bacteria. While the activities of long-chain amides have been reported against *S. aureus*, this author could find no evidence of reported activity against MRSA, *M. luteus*, and *L. plantarum*. Unlike the **3CAmn** series, all nonionic amphiphiles were active against all Gram-positive bacteria that were tested (Table 5.2).

Table 5.2 Antimicrobial Activity of the **3DMAUrn** and **3MorUrn** Series against Gram-positive Bacteria and *M. smegmatis*

Microorganisms	MIC (μg/mL)			
	Amphiphiles			
	3DMAUr12	**3DMAUr14**	**3DMAUr18Me**	**3MorUr14**
S. aureus	39–78	20[a]–39	22[a]–45	20[a]–78
MRSA	78[a]–5000	39[a]–1300	22[a]–89	39[a], 78–630
M. luteus	39	20	89	20[a]–39
L. plantarum	5000	156[a]–5000	179	156[a]–5000
M. smegmatis	20[a]–39	39	22	20

Superscript "a" indicates incomplete inhibition

Unlike the **3CAmn** series, which exhibited modest incomplete inhibition against *S. aureus*, the nonionic amphiphiles completely inhibited growth at relatively low concentrations. All nonionic amphiphiles (78–20.0 μg/mL, 0.15 mM–0.040 mM) exhibited greater activity than the best activity displayed by the **3CAmn** series (**3CAm21**, 390 μg/mL, 0.72 mM). Amphiphiles **3DMAUr12** (78 μg/mL, 0.15 mM), **3DMAUr14** (39 μg/mL, 0.071 mM), and **3DMAUr18Me** (45 μg/mL, 0.071 mM) inhibited *S. aureus* to a greater extent than the best FA (C_{14}, 400 μg/mL, 1.8 mM) reported in the literature. Amphiphiles **3DMAUr14**, and **3DMAUr18Me** completely inhibited growth at lower concentrations than **3MorUr14** (78 μg/mL, 0.11 mM). Although **3MorUr14** was more active than the **3CAmn** series and the most active FA, it was less inhibitory against *S. aureus* than **3DMAUr14**, **3DMAUr18Me** and C_{12}-*N*,*N*-dimethylamide (16 μg/mL, 0.069 mM) as reported by Ōmura et al.[3] Amphiphiles **3DMAUr14** and **3DMAUr18Me** were equally as active as C_{12}-*N*,*N*-dimethylamide. Kabara et al. reported that C_{12}-*N*,*N*-dimethylamide inhibited the growth of *S. aureus* at 0.11 mM[7] and 0.2 mM[4] in a later study.

While the **3CAmn** series was more active against MRSA than *S. aureus*, the opposite was true for the nonionic amphiphiles. In fact, the activity was greatly reduced. While the complete-inhibition MIC values were greatly reduced, the incomplete-inhibition MIC values

against MRSA were similar to the complete inhibition values against *S. aureus*. While the activity of **3DMAUr12** (0.15 mM to 9.5 mM) and **3DMAUr14** (0.071 mM to 2.3 mM) decreased by 64-and 32-fold, respectively, the activity of **3DMAUr18Me** (0.071 mM to 0.14 mM) only decreased by two-fold. Despite the drop in activity against MRSA, **3DMAUr18Me** was still more active than the best FA (C_{12}, 400 μg/mL, 2.0 mM)[8] and the best member of the **3CAmn** series (**3CAm21**, 390 μg/mL, 0.72 mM). The optimal chain length also switched for maximum activity against MRSA (C_{18}) versus *S. aureus* (C_{14}).

The **3CAmn** series did not inhibit the growth of *M. luteus* at the highest concentration tested (6300 μg/mL). The only FA (C_{18}) tested against *M. luteus* was inactive.[9] Sivasamy et al. reported that two C_{18} diacid derivates did inhibit the growth of *M. luteus* to different degrees.[9] However, as a zone of inhibition study was employed in the experiment, no MIC values were reported. Amphiphile **3DMAUr14** (0.035 mM) was the most active nonionic amphiphile but **3DMAUr12** (0.074 mM), **3DMAUrn18Me** (0.14 mM), and **3MorUr14** (0.056 mM) also exhibited good activities.

The **3CAmn** series exhibited minimal, mostly incomplete inhibition, against *L. plantarum* [complete inhibition, **3CAm14** (1.2 mM) and **3CAm16** (1.1 mM)]. We did not find any antimicrobial studies of FAs or long-chain amides against *L. plantarum*. *L. plantarum* is a beneficial bacterium; therefore, we would prefer our amphiphiles not inhibit the growth of *L. plantarum*. Unfortunately, **3DMAUr18Me** (180 μg/mL, 0.29 mM) completely inhibited the growth of *L. plantarum* and was more inhibitory than the **3CAmn** series. The other nonionic amphiphiles, **3DMAUr12**, **3DMAUr14**, and **3MorUr14** completely inhibited the growth of *L. plantarum* at very high concentrations (5000 μg/mL, 7.2–9.5 mM). With respect to incomplete inhibition, **3DMAUr14** (0.28 mM) and **3MorUr14** (0.23 mM) inhibited the growth of *L.*

plantarum at 160 μg/mL, but were more active than the incomplete inhibition exhibited by the **3CAmn** amphiphiles (0.61–0.52 mM).

Neither **3DMAUr12** (39 μg/mL, 0.074 mM) nor **3DMAUr14** (39 μg/mL, 0.071 mM) was as effective as the most active member of the **3CAmn** series (**3CAm19**, 18 μg/mL, 0.035 mM) against *M. smegmatis*. However, **3DMAUr18Me** (22 μg/mL, 0.036 mM), and **3MorUrn** (20 μg/mL, 0.028 mM) were just as active as or more active than **3CAm19.** Amphiphile **3MorUr14** was more active than any other nonionic amphiphile. The activity of the nonionic amides was more active than the best FAs reported in the literature FA (C_{12} and C_{14}, 0.10 mM and 0.088 mM, respectively).[10] The activity was also better than the best long-chain amide reported in the literature (C_{12}-*N*,*N*-dimethylamide, 31 μg/mL, 0.14 mM).[3]

5.4 Antimicrobial Activity of 3DMAUr18Me, 3DMAUr12, 3DMAUr14, and 3MorUr14 against Yeasts and *A. niger*

Unlike the **3CAmn** series, **3MorUr14**, **3DMAUr18Me**, **3DMAUr12,** and **3DMAUr14** were relatively inactive against yeasts and *A. niger* (Table 5.3). The only advantage that nonionic amphiphiles had over the **3CAmn** series was the complete inhibition against *C. albicans* and *C. neoformans*, while the **3CAmn** series led to incomplete inhibition. All nonionic amphiphiles minimally inhibited *C. albicans* (7.2–9.0 mM), which was somewhat surprising as Ōmura et al. reported that C_{12}-*N*,*N*-dimethylamide inhibited the growth of *C. albicans* at 63 μg/mL (0.28 mM).[3] Similarly, Kabara et al. reported than C_{12}-*N*,*N*-dimethylamide inhibited the growth of *C. albicans* at 0.11 mM.[7] All nonionic amphiphiles were also less inhibitory that the most active FA (C_{10}, 100 μg/mL, 0.58 mM).[11]

Table 5.3 Antimicrobial Activity of the **3DMAUrn** and **3MorUrn** Series against Fungi and Yeasts

Microorganisms	MIC (μg/mL)			
	Amphiphiles			
	3DMAUr12	**3DMAUr14**	**3DMAUr18Me**	**3MorUr14**
S. cerevisiae	625	625	NT	625
C. albicans	5000	2500[a]–5000	NT	5000[a]
C. neoformans	5000	≤5000	NT	NA
A. niger	625[a]–1250	625	1429[a]–2857	2500

NT= not tested, NA= not active. Superscript "a" indicates incomplete inhibition

The antifungal activities of the **3DMAUr12**, **3DMAUr14** and **3MorUr14** against *C. neoformans* and *A. niger* were extremely low. Against *C. neoformans*, amphiphile **3MorUr14** was inactive, while the most active nonionic amphiphile was **3DMAUr12** (5000 μg/mL, 9.5 mM)**.** The nonionic amphiphiles were 278–139 fold less active against *C. neoformans* than the most active **3CAmn** compound (**3CAm19**, 18–36 μg/mL, 0.035–0.070 mM).

The nonionic amphiphiles also exhibited decreased activity, relative to the **3CAmn** series, against *A. niger*. Both **3CAm19** (71 μg/mL, 0.14 mM) and **3CAm21** (71 μg/mL, 0.13 mM) inhibited the growth of *A. niger*, which were approximately 8-fold more active than the most effective nonionic amphiphile (**3DMAUr14**, 630 μg/mL, 1.1 mM). The nonionic amphiphiles were also less inhibitory than the most active FA (C_{14}, 620 μg/mL, 2.7 mM).[12]

The **3CAmn** series and the nonionic amphiphiles inhibited the growth of *S. cerevisiae*; however, the most active compound of the **3CAmn** series (**3CAm21**, 4.4 μg/mL, 0.008 mM) was 142-fold more active than the most active nonionic amphiphile (**3MorUr14,** 630 μg/mL, 0.90 mM). However, the nonionic amphiphiles were more active than the best FA (C_{11}, 500 μg/mL, 2.7 mM).[11]

5.5 Conclusions

Overall, **3MorUr14**, **3DMAUr18Me**, **3DMAUr12**, and **3DMAUr14** selectively inhibited Gram-positive bacteria and mycobacteria. The nonionic amphiphiles were generally

inactive against Gram-negative bacteria (except for *N. gonorrhoeae*), yeasts, and fungi. Another downside of the nonionic amphiphiles was the limited water solubility of some compounds. Due to poor aqueous solubility, we believed the maximum activity might not be observed for amphiphiles **3DMAUr16**, **3DMAUr18**, **3MorUr12,** and **3MorUr18Me**. In a couple of cases, **3DMAUr14** was more active than **3DMAUr18Me**. It is possible that the water-insoluble members of the series (**3DMAUr16** and **3DMAUr18**) could be more active than **3DMAUr18Me**. Another drawback to the insolubility of **3DMAUr18** was the missed opportunity to test if the *N*-methyl group of **3DMAUr18Me** offers any enhancements in activity over **3DMAUr18.**

5.6 MIC Procedure for Antimicrobial Testing

5.6.1 Microbial Strains, Culture Conditions, and Preparations of Inocula for Susceptibility Testing

Strains of *E. coli* strain C (ATCC # 13706), *K. pneumoniae* (ATCC # 4352), *L. plantarum* (ATCC # 14917), *S. aureus* (ATCC # 6538), and *M. smegmatis* (ATCC # 607) were obtained from the American Type Culture Collection. A MRSA strain or isolate was obtained from the Microbiology Laboratory, Danville Community Hospital (Virginia) and *S. cerevisiae*, *C. albicans, C. neoformans*, *A. niger*, and *M. luteus* strains were obtained from the Virginia Tech Microbiology teaching culture collection. Colonies of *E. coli*, *K. pneumoniae*, *S. aureus*, MRSA, *M. luteus*, *S. cerevisiae*, *C. albicans*, and *C. neoformans* were grown on 1/10-strength Brain Heart Infusion Broth containing 0.2% (wt/vol) sucrose (BHIB+S) and 1.5% (wt/vol) agar. *L. plantarum* was grown on ¼-strength Tryptic Soy Broth containing 0.2% glucose (TSB+G) and 1.5% (wt/vol) agar. *N. gonorrhoeae* was grown on Chocolate agar medium (BBL Microbiology Systems, Sparks, MD) containing hemoglobin.*M. smegmatis* was grown on Middlebrook 7H10

agar and *A. niger* on Potato Dextrose Agar. Streaked plates were incubated at 37 °C for 3–7 days, except for that of *A. niger*, which was incubated in the dark at 30 °C. A single colony for each microbe except *A. niger* was used to inoculate 5 mL of 1/10-strength BHIB+S (*E. coli*, *K. pneumoniae*, *M. luteus*, *S. aureus*, and MRSA), TSB (*L. plantarum*), Middlebrook 7H9 broth (*M. smegmatis*), Yeast Extract Peptone Maltose broth (*S. cerevisiae*, *C. albicans* and *C. neoformans*), or GC broth medium (*N. gonorrhoeae*) and incubated at 37 °C (*S. cerevisiae* and *M. luteus* at 30 °C) for 4–7 days. After growth, the resulting broth cultures were diluted with buffered saline gelatin to equal the turbidity of a No. 1 McFarland Standard. *N. gonorrhoeae* was grown at 37 °C in an anaerobic jar containing a CO_2 gas generator. After 4 days incubation, 5 mL of buffered saline gelatin (BSG) was added to each culture and vortexed at the highest speed. The brown insoluble contents of the GC medium were allowed to settle to the bottom of the tube at room temperature. The supernatant cell suspension was transferred to a fresh sterile tube with collecting the insoluble contents and the turbidity of the suspension diluted with BSG to equal a McFarland No. 1 standard.

To check for viability and contamination, broth cultures were streaked on Plate Count Agar or Chocolate agar (*N. gonorrhoeae*); the plates were incubated at 37 °C for 3–4 days. Plates for *M. luteus* and *S. cerevisiae* were grown at 30 °C. Plates for *N. gonorrhoeae* were incubated at 37 °C in an anaerobic jar containing a CO_2 gas generator. Spores of *A. niger* were scraped from the surface of PDA and suspended in 5 mL of 1/10-strength BHIB+S and that suspension transferred to a sterile test tube. The turbidity was adjusted to a No. 1 McFarland Standard by dilution with BSG. To check for viability and contamination, those spore suspensions were streaked on PDA and incubated at 37 °C for 3–4 days.

5.6.2 Quality Assurance

For the work reported here, all cultures and suspensions that were used as inocula were uncontaminated and the colonies had the expected morphologies. All viable, uncontaminated inocula were stored up to 14 days at 4 °C until used without any differences in susceptibility to antimicrobial compounds.

5.6.3 Measurement of MIC

MICs of compounds dissolved in aqueous triethanolamine were measured by broth microdilution in 96-well microtiter plates. Preliminary experiments demonstrated that 4% (wt/vol) triethanolamine/water did not inhibit the growth of any microorganism tested. A two-fold dilution series of the compounds was prepared in 96-well microtiter plates in a 50 μL volume of 1/10-strength BHIB+S and the dilution series was inoculated with 50 μL of each cell suspension. For *E. coli* and *K. pneumoniae*, the volume of the medium and the inoculum were doubled. The resulting inoculated dilution series were incubated at 30 °C and growth, as turbidity, scored visually and recorded on the fourth day. For *E. coli* and *K. pneumoniae*, the incubation temperature was 37 °C and the duration was 7 d. The MIC of each compound was measured in triplicate and was defined as the lowest concentration of drug resulting in a prominent visible decrease in turbidity (incomplete; i.e., ≥ 50%) or a complete absence of visible turbidity compared to the drug-free control. In many cases ("a" for Tables 1-3), inhibition was incomplete.

5.7 References for Chapter 5

1. Jossifova, L.T., Manolov, I., Golovinsky, E. V., *Antibacterial action of some saturated and unsaturated long-chain carboxylic acids and their bis(2-chloroethyl)aminoethyl esters in vitro.* Die Pharmazie 1989. **44**(12): p. 854-856.
2. Marounek, M., Skrivanova, E., Rada, V., *Susceptibility of Escherichia coli to C_2-C_{18} fatty acids.* Folia Microbiol., 2003. **48**(6): p. 731-735.

3. Omura, S., Katagiri, M., Awaya, J., Furukawa, T., Umezawa, I., Oi, N., Mizoguchi, M., Aoki, B., Shindo, M., *Relation between the structures of fatty acid amide derivatives and their antimicrobial activities.* Antimicrob. Agents Chemother., 1974. **6**(2): p. 207-215.
4. Kabara, J.J., Conley, A. J., Truant, J. P., *Relationship of chemical structure and antimicrobial activity of alkyl amides and amines.* Antimicrob. Agents Chemother., 1972. **2**(6): p. 492-498.
5. Miller, R.D., Brown, K. E., Morse, S. A., *Inhibitory action of fatty-acids on growth of Neisseria-gonorrhoeae.* Infect. Immun., 1977. **17**(2): p. 303-312.
6. Bergsson, G., Steingrimsson, O., Thormar, H., *In vitro susceptibilities of Neisseria gonorrhoeae to fatty acids and monoglycerides.* Antimicrob. Agents Chemother., 1999. **43**(11): p. 2790-2792.
7. Kabara, J.J., Swieczkowski, D. M., Conley, A. J., Truant, J. P., *Fatty acids and derivatives as antimicrobial agents.* Antimicrob. Agents Chemother., 1972. **2**(1): p. 23-28.
8. Kitahara, T., Koyama, N., Matsuda, J., Aoyama, Y., Hirakata, Y., Kamihira, S., Kohno, S., Nakashima, M., Sasaki, H., *Antimicrobial activity of saturated fatty acids and fatty amines against Methicillin-Resistant Staphylococcus aureus.* Biol. Pharm. Bull., 2004. **27**(9): p. 1321-1326.
9. Sivasamy, A., Krishnaveni, M., Rao, P. G., *Preparation, characterization, and surface and biological properties of N-stearoyl amino acids.* J. Am. Oil Chem. Soc., 2001. **78**(9): p. 897-902.
10. Kondo, E. and K. Kanai, *Lethal effect of long-chain fatty acids on mycobacteria.* Jpn. J. Med. Sci. Biol., 1972. **25**(1): p. 1-13.
11. Kabara, J.J., Vrable, R., Liekenjie, M. S. F., *Antimicrobial lipids -natural and synthetic fatty-acids and monoglycerides.* Lipids, 1977. **12**(9): p. 753-759.
12. Parang, K., Knaus, E. E., Wiebe, L. I., Sardari, S., Daneshtalab, M., Csizmadia, F., *Synthesis and antifungal activities of myristic acid analogs.* Archiv Der Pharmazie, 1996. **329**(11): p. 475-482.

Chapter 6: Spermicidal and Anti-HIV Activity of Anionic and Nonionic Amphiphiles

6.1 Introduction to Antiviral and Spermicidal Activity

The UN estimates, in 2005, that 38.7 million people have HIV infections.[1] There are some good signs, in some parts of southern Africa, the HIV epidemic seems to have leveled off—however, at an extraordinary high level.[1] Unfortunately, HIV continues to be a health concern in both industrialized and developing countries.

The rapid rise of HIV infections around the world—an estimated 4.1 million new HIV infections in 2006[1]—especially in developing countries, have increased demands for antimicrobial agents that will rapidly kill pathogenic viruses and bacteria, and will prevent infections of the skin and mucosa.[2] These agents must be able to kill pathogenic bacteria such as *N. gonorrhoeae* and sexually transmitted viruses (HIV and HSV). These agents would be used in sensitive areas of the body (i.e. genitals), therefore, these agents must be nontoxic to the users. FAs have a long history of inhibiting the growth of pathogenic bacteria, such as *N. gonorrhoeae*,[3] and inhibiting the growth of enveloped viruses[4], such as HSV.

The ultimate goal of this project is the development of microbicides that can be used to prevent and treat infections of viruses, bacteria, and other pathogens. To prevent infections, the microbicide will have to create a chemical barrier that prevents infections during sexual intercourse.[2] Specifically, the microbicide would be used as a topical microbicide (e.g., hydrogel or cream), which can be applied to the vagina. This hydrogel or cream must be used in quantities that would be undetectable by her partner, in cases where she did not want her partner to know. Additionally, the microbicide must be nonirritating. A vaginal microbicide would be ideal because it would protect both members during sexual intercourse. The genital area commonly serves as points of entry for pathogens. It would protect the female against various

infectious pathogens transmitted through both physical contact and semen.[2] It would likewise protect the male from pathogens transmitted through physical contact and vaginal secretions.[2] Additionally, these microbicides should be spermicidal.

Lipids have been shown to kill sexually transmitted viruses, bacteria, and other pathogens that infect mucosa and skin.[3, 5] Nucleoside analogues have long been used against viruses; however, viruses are becoming increasingly resistance to these drugs. This resistance necessitates the development of new drugs.[2] FAs have long been known to possess antiviral and antibacterial properties, due to their ability to disrupt the membranes of both viruses and bacteria.[2]

Amphiphile **3DMAUr18Me**, the **3DMAUrn** and **3CAmn** series were tested and found to be antimicrobial (Chapters 4 and 5). The antimicrobial properties of **3DMAUr18Me**, the **3DMAUrn** and **3CAmn** series are important because sexually transmitted diseases (STDs) and microbial infections have been noted to increase HIV-1 transmissions.[6-8]

From the antimicrobial data in the previous chapter, the **3CAmn** series exhibited good activity against *C. albicans* and moderate activity against *N. gonorrhoeae*. The data also showed that the **3CAmn** series was weakly active against the beneficial bacterium *L. plantarum*. Due to the series' selectivity, the **3CAmn** series contained several prime candidates to be considered as possible topical microbicides.

Conversely, the **3DMAUrn** series lacked antifungal activity against *C. albicans*. However, the series was active against *N. gonorrhoeae* but mostly lacked activity against *L. plantarum*. Consequently, **3DMAUr18Me** and the **3DMAUrn** series were also candidates as possible topical microbicides.

The ideal microbicide should also protect against HIV as well as other pathogens, such as *C. albicans* and *N. gonorrhoeae*. Although sperm is not a microbe, a dual-acting microbicide should be able to inhibit sperm to prevent unplanned pregnancies.[9] To probe the antiviral property and vaginal irritation, **3DMAUr18Me**, the **3CAmn** and **3DMAUrn** series were tested against HIV and human vaginal cells. In this study, **3DMAUr18Me** and the two series, namely **3CAmn** and **3DMAUrn**, were compared to the commercially available Nonoxynol-9 or N-9 (Figure 6.1).

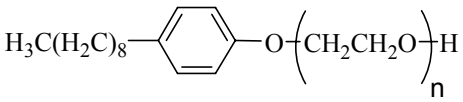

Figure 6.1 Structure of N-9

The microbicidal effectiveness of N-9 has yielded mixed results.[10, 11] N-9 has shown spermicidal, antimicrobial, and antiviral properties.[12, 13] There are contradictions to the reported antimicrobial activity of N-9.[10] Roddy et al. has reported that both gonorrheal and chlamydial infections increased when N-9 was used.[11] However, an additional study reported that N-9 did not inhibit gonorrheal or chlamydial infections, nor did N-9 inhibit the growth of HIV.[11, 14]

In addition to the antimicrobial concerns of N-9, there are also cytotoxicity concerns.[15, 16] Van Damme et al. reported that multiple daily use of N-9 led to lesions with epithelial disruption.[17] Epithelial disruption can lead to enhanced HIV transmission.[17] A single product that is antiviral, antibacterial, spermicidal, and less irritable to mucosal membranes than N-9, would be ideal. In order to determine antiviral and contraceptive properties, **3DMAUr18Me** and both series, **3DMAUrn** and **3CAmn**, were assayed against HIV[18] and

sperm[18, 19] by Dr. Gustavo Doncel of the Eastern Virginia Medical College. Dr. Doncel also measured the cytotoxicity[18] of our amphiphiles as well as the release of cytokines.[18]

Unlike the case with antimicrobial activity, we cannot directly compare the antiviral and spermicidal activities of **3DMAUr18Me**, the **3CAmn** and **3DMAUrn** series to FAs and amides because there are no documented studies. However, there are studies of FAs and amides against other enveloped viruses, such as HSV[4, 20] and Influenza[21].

6.2 Anti-HIV and Spermicidal Activity of the 3CAmn Series

Table 6.1 Cytotoxicities and Anti-HIV Properties of the **3CAmn** Series

Compound	Solvent (aq.)	Cytotoxicity EC_{50} (μg/mL)	Antiviral Activity EC_{50} (μg/mL)	Selectivity Index
3CAm13	$N(EtOH)_3$	138.5	340.3	0.4
3CAm15	$N(EtOH)_3$	458.6	113.8	4.0
3CAm19	$N(EtOH)_3$	183.7	90.6	2
3CAm21	$N(EtOH)_3$	143.8	74.3	1.9
3CAm23	$N(EtOH)_3$	104.0	72.6	1.4
N-9	$N(EtOH)_3$	69.6	79.6	0.9
$N(EtOH)_3$		643.3	>1000	<0.6

The antiviral and cell (vaginal tissue) toxicity of the **3CAmn** series were assayed (Table 6.1). Ideally, a compound should have a selectivity index (cytotoxicity/antiviral activity) of at least 50; therefore, the compound would inhibit the HIV at a much lower concentration than it would kill human cells. It is desirable for any drug to be active at low concentrations because that lowers the chance of possible side effects being expressed. Both **3CAm21** and **3CAm23** were slightly more active against the HIV than N-9 (72.6 and 74.3 μg/mL vs. 79.6 μg/mL). Additionally, they all have better selectivity indices than N-9 due to their lower cytotoxicity. Both **3CAm15** and **3CAm19** were not as active against HIV; however, these compounds had

selectivity indices of four to two times that of N-9. If a compound that is not as active as N-9, but had a larger selectivity index (i.e., ≥ 50), this would also be acceptable.

There was a direct correlation between chain length and anti-HIV activity. Excluding **3CAm13**, anti-HIV activity increased with chain length. Unfortunately, this also applied to cytotoxicity. As the chain length increased, the **3CAmn** series became more cytotoxic. Due to the increasing cytotoxicity, the selective index decreased with increasing chain length. Although the **3CAmn** series did not have a selectivity index close to 50, **3CAm21** and **3CAm23** were as active as and less toxic than the commercial product (N-9).

The proinflammatory potential was measured by the release of IL-1α. IL-1α is a potent proinflammatory cytokine.[18] Cytokines are peptides that are the primary mediators of the inflammatory response, such as tissue damage.[7, 18] A large release of proinflammatory cytokines can amplify the penetration and replication of viral pathogens.[18] The measurement of the amount of IL-1α that was released will determine if the **3CAmn** series could cause irritation and inflammation. Because the **3CAmn** series was designed to be used on female genitals, if these compounds caused a large release of IL-1α, they likely would be unsuitable as topical microbicides.[7, 18] These experiments will determine whether the **3CAmn** series would be suitable topical microbicides.

Table 6.2 Cytotoxicities and Irritation Caused by the **3CAmn** Series

Compound	Cytotoxicity (CC_{50} ± SD) (μg/mL)	IL-1α (AUC)
3CAm13	>2000.0 ± 0.0	58.7 ± 5.7
3CAm15	262 ± 20	69.2 ± 3.8
3CAm19	165 ± 4	98.8 ± 3.0
3CAm21	86 ± 12	448.7 ± 12.3
3CAm23	54 ± 5	766.9 ± 16.1
N-9	44 ±3	692.8 ± 9.8
$N(EtOH)_3$	>1000:10000	58.7 ± 5.7

AUC: area under the curve, a measure of the amount of cytokine released

All compounds in the **3CAmn** series were less toxic (> ± 54 μg/mL) than N-9 (Table 6.2). The cytotoxicity of the **3CAmn** series increased with chain length. Amphiphile **3CAm23**, which had the best virucidal activity, caused the largest release of proinflammatory IL-1α. The release of proinflammatory IL-1α by **3CAm23** is even higher than that of N-9. The amount of cytokine released by **3CAm23** and N-9 were 766.9 ± 16.1 and 692.8 ± 9.8, respectively. The other members of the series produced considerably less IL-1α than N-9. However, there was a considerable increase in cytotoxicity and proinflammatory response from a C_{20} to a C_{22} alkyl chain. Compounds with an alkyl chain greater than C_{22} triggered a large increase in cytotoxicity and IL-1α release that was too detrimental to be considered as topical microbicides. As a whole, these results show that most members of the **3CAmn** series were less inflammatory than N-9.

Unfortunately, the **3CAmn** series displayed no spermicidal activity. Therefore, these compounds could not be used to prevent pregnancies. The result indicated that if the **3CAmn** series were to be used as a topical microbicide, an additional compound would be needed to inhibit sperm.

Taken as a whole, the data for the **3CAmn** series were mixed. While the data in Table 1 suggest the series would be good antiviral agents, there are cytotoxicity concerns with the more active antiviral members of the series. Additionally, while the antiviral activities of some members of the **3CAmn** series were better than N-9, statistically, there was not much difference. The lack of spermicidal activity was a drawback for the series.

6.3 Anti-HIV and Spermicidal Activity of 3DMAUr18Me and the 3DMAUrn Series

Amphiphile **3DMAUr18Me** and the **3DMAUrn** series were better anti-HIV agents than the **3CAmn** series (Table 6.3). Except for **3DMAUr18**, all compounds exhibited better anti-HIV activity than the **3CAmn** series. In fact, the most active compound, **3DMAUr18Me**, was approximately 40% more active than the most active in the **3CAmn** series (**3CAm23**). Additionally, **3DMAUr18Me** was almost 50% more active than N-9. On the downside, **3DMAUr18Me** and the **3DMAUrn** series (except for **3DMAUr18**) were more cytotoxic than both N-9 and the **3CAmn** series. However, because **3DMAUr18Me** and the **3DMAUrn** series were more active than N-9, the selectivity indices were equal to that of N-9 (approximately 1). The selectivity indices of amphiphile **3DMAUr18Me** (1.3) and the **3DMAUrn** series (**≈**1) were less than those of the most active **3CAmn** series [**3CAm23** (1.9) and **3CAm21** (1.4)]. Although the anti-HIV activities of the nonionic amphiphiles were greater than the **3CAmn** series and N-9, the increased cytotoxicities were disconcerting. Cyctotoxicity and antiviral activity remained relatively constant for the shorter chain lengths (**3DMAUr12–3DMAUr16**). Excluding **3DMAUr18**, which had solubility problems, there was a large increase in cytotoxicity and anti-HIV activity between **3DMAUr16** and **3DMAUr18Me**.

Table 6.3 Anti-HIV Activities and Cytotoxicities of the **3DMAUr18Me** and **3DMAUrn** Series

Compound	Solvent (aq.)	Cytotoxicity EC_{50} (μg/mL)	Antiviral Activity EC_{50} (μg/mL)	Selectivity Index
3DMAUr12	$N(EtOH)_3$	65.4	67.2	1.0
3DMAUr14	$N(EtOH)_3$	66.7	65.7	1.0
3DMAUr16	$N(EtOH)_3$	62.2	64.5	1.0
3DMAUr18	$N(EtOH)_3$	93	>1000	<0.1
3DMAUr18Me	$N(EtOH)_3$	55.9	43.6	1.3
$N(EtOH)_3$		643.3	>1000	<0.6
N-9	$N(EtOH)_3$	69.6	79.6	0.9

Looking at the antiviral activity, it might be easy to dismiss **3DMAUr18**; however, a closer look is warranted. Amphiphile **3DMAUr18** has the same tail length of as **3DMAUr18Me** (C_{18}). However, the antiviral activities are drastically different. The differences in antiviral activity were due to solubility because the C_{18} chain length seemed ideal for anti-HIV activity. Amphiphile **3DMAUr18** was not water soluble, while **3DMAUr18Me** was water soluble. Additionally, **3DMAUr16** also had solubility concerns. Perhaps if **3DMAUr18** and **3DMAUr16** were more water soluble, these compounds could possibly have equal or better anti-HIV activities than **3DMAUr18Me**. This leads to an interesting question. Is the antiviral activity due to the C_{18} chain of **3DMAUr18Me** or due to the N-CH_3 subsituent? Because **3DMAUr18** was insoluble, this question cannot be answered. However, based on the activities of **3DMAUr16** (64.5 μg/mL) and **3DMAUr18Me** (43.6 μg/mL), the antiviral activities are probably due to the chain length. A perfect example of the cutoff effect is clearly shown to be due to aqueous solubility (Table 6.4). Amphiphile **3DMAUr18** is the least cytotoxic and antiviral because it is the least water soluble of the series. If an amphiphile is not soluble, then the antiviral activity or cytotoxicity of the amphiphile will not be exhibited. (The poor water solubility of **3DMAUr18** led to a poor selectivity index.)

Table 6.4 Spermicidal Activity of the **3DMAUrn** Series

Compound	Solvent (aq.)	M.E.C. EC_{50} (μg/mL)	Solubility
3DMAUr12	$N(EtOH)_3$	352±36	OK
3DMAUr14	$N(EtOH)_3$	226±23	OK
3DMAUr16	$N(EtOH)_3$	11700±1600	ppt
3DMAUr18	$N(EtOH)_3$	N.A.	ppt
3DMAUr18Me	$N(EtOH)_3$	2000±500	OK
$N(EtOH)_3$	dH_2O	>1000	OK
N-9	dH_2O	281±43	OK

Unlike the **3CAmn** series, **3DMAUr18Me** and the **3DMAUrn** series (except **3DMAUr18**) were spermicidal (Table 6.4). Amphiphile **3DMAUr18** was not spermicidal due to poor aqueous solubility. Amphiphile **3DMAUr14** was the best spermicide of the group (226 ± 23 μg/mL). Unlike cyctoxicity, there was not a direct correlation between chain length and spermicidal activity. The two amphiphiles with the shortest alkyl chains, **3DMAUr12** and **3DMAUr14**, were the most active. In fact, the spermicidal activity drastically dropped off following **3DMAUr14**. The C_{14} chain was the optimal chain length for spermicidal activity for the **3DMAUrn** series. Contrary to the tricarboxylate headgroup of the **3CAmn** series, the trisdimethylamide headgroup exhibited good spermicidal activity. The drastic differences in spermicidal activity between **3DMAUr18Me** and both series (**3CAmn** and **3DMAUrn**) were probably indicative of different mechanisms of action. The anionic headgroups of the **3CAmn** series seemed to be a deterrent for spermicidal activity, while the nonionic dimethylamide headgroup seemed beneficial.

The potential irritancy of the nonionic amphiphiles was measured with **3DMAUr14** (Table 6.5). Amphiphile **3DMAUr18Me** was by far the best antiviral agent. However, the spermicidal activity of **3DMAUr18Me** was much lower than that of N-9, (2000 ± 500 and 281 ±

43, respectively). Amphiphile **3DMAUr14** was the only member of the **3DMAUrn** series that had better antiviral and spermicidal activities than N-9. Additionally, it had good aqueous solubility. Unfortunately, there was a major drawback with **3DMAUr14**. It released a large amount of the proinflammatory cytokine IL-1α and was more cytotoxic than N-9 (Table 6.5). Amphiphile **3DMAUr14** releases approximately 16% more IL-1α and was 1.4 fold more cytotoxic than N-9. Because **3DMAUr14** released a large amount of proinflammatory cytokine, it would probably be too irritating to be used as a topical microbicide in the genital area.

Table 6.5 Cytotoxicity and Irritation of the **3DMAUrn** Series

Compound	Cytotoxicity (CC_{50} ± SD) (μg/mL)	IL-1α (AUC)
3DMAUr14	32 ± 1	808.5 ± 7.1
N-9	44 ± 3	692.8 ± 9.8
$N(EtOH)_3$	>1000:10000 ± 0.0	119.0 ± 5.8

6.4 Conclusions

Although the **3DMAUrn** series are good leads that possess good anti-HIV and spermicidal activities, the cytotoxicity and cytokine releases prevent this series from being considered as topical microbicides. The **3DMAUrn** series is a better lead than the **3CAmn** series. Unlike the **3CAmn** series, the nonionic amphiphiles have a complete package (anti-HIV and spermicidal activity). The only drawbacks are cytotoxicity and irritation.

The *N*–CH_3 issue that arose between **3DMAUr18** and **3DMAUr18Me** begs for further investigation. It could be the case that **3DMAUr18** is the best antiviral agent due to its chain length (C_{18}). However, there is the possibility that the N–CH_3 group could introduce some additional anti-HIV activity. To determine if *N*-methylation introduces additional antiviral activity, *N*-methyl derivates of **3DMAUr12, 3DMAUr14**, and **3DMAUr16** need to be synthesized and assayed. Further alterations in the structure of the **3DMAUrn** series could reduce the series' cytotoxicity and irritation concerns. If both concerns are remedied, this series

could be considered as viable microbicides. Despite the cytotoxicity and irritation concerns, the observation that *N*-methylation improved the aqueous solubility of long chains could be beneficial in future studies.

6.5 References for Chapter 6

1. *UNAIDS. 2006 report on the global AIDS epidemic : Executive summary / UNAIDS.*, http://data.unaids.org/pub/GlobalReport/2006/2006_GR-ExecutiveSummary_en.pdf, Accessed July 16, 2007
2. Thormar, H., Bergsson, G., *Antimicrobial effects of lipids.* Recent Dev. Antiviral Res., 2001. **1**: p. 157-173.
3. Miller, R.D., Brown, K. E., Morse, S. A., *Inhibitory action of fatty-acids on growth of Neisseria-gonorrhoeae.* Infect. Immun., 1977. **17**(2): p. 303-312.
4. Thormar, H., Isaacs, C. E., Brown, H. R., Barshatzky, M. R., Pessolano, T., *Inactivation of enveloped viruses and killing of cells by fatty-acids and monoglycerides.* Antimicrob. Agents Chemother., 1987. **31**(1): p. 27-31.
5. Hilmarsson, H., Kristmundsdottir, T., Thormar, H., *Virucidal activities of medium- and long-chain fatty alcohols, fatty acids and monoglycerides against herpes simplex virus types 1 and 2: comparison at different pH levels.* Apmis, 2005. **113**(1): p. 58-65.
6. Cohen, M.S., *Sexually transmitted diseases enhance HIV transmission: no longer a hypothesis.* Lancet, 1998. **351**: p. 5-7.
7. Doncel, G.F., N. Chandra, and R.N. Fichorova, *Preclinical assessment of the proinflammatory potential of microbicide candidates.* Jaids-J. Acquir. Immune Defic. Syndr., 2004. **37**: p. S174-S180.
8. Mayaud, P. and D. McCormick, *Interventions against sexually transmitted infections (STI) to prevent HIV infection.* Br. Med. Bull., 2001. **58**: p. 129-153.
9. Doncel, G.F., *Exploiting common targets in human fertilization and HIV infection: development of novel contraceptive microbicides.* Hum. Reprod. Update, 2006. **12**(2): p. 103-117.
10. Roddy, R.E., *Up-date on microbicide clinical trials for the Microbicide 2000 Conference.* Aids, 2001. **15**: p. S12-S13.
11. Roddy, R.E., Zekeng, L., Ryan, K. A., Tamoufe, U., Tweedy, K. G., *Effect of Nonoxynol-9 gel on urogenital gonorrhea and chlamydial infection - A randomized controlled trial.* JAMA, J. Am. Med. Assoc., 2002. **287**(9): p. 1117-1122.
12. Harrison, C., Chantler, E., *The effect of nonoxynol-9 and chlorhexidine on HIV and sperm in vitro.* Int. J. of Std Aids, 1998. **9**(2): p. 92-97.
13. Malkovsky, M., Newell, A., Dalgleish, A. G., *Inactivation of HIV by Nonoxynol-9.* Lancet, 1988. **1**(8586): p. 645-645.
14. Roddy, R.E., Zekeng, L., Ryan, K. A., Tamoufe, U., Weir, S. S., Wong, E. L., *A controlled trial of Nonoxynol 9 film to reduce male-to-female transmission of sexually transmitted diseases.* New. England J. Med., 1998. **339**(8): p. 504-510.
15. Van Damme, L., Niruthisard, S., Atisook, R., Boer, K., Dally, L., Laga, M., Lange, J. M. A., Karam, M., Perriens, J. H., *Safety evaluation of Nonoxynol-9 gel in women at low risk of HIV infection.* Aids, 1998. **12**(4): p. 433-437.

16. Niruthisard, S., Roddy, R. E., Chutivongse, S., *Use of Nonoxynol-9 and reduction in rate of Gonococcal and Chlamydial Cervical infections.* Lancet, 1992. **339**(8806): p. 1371-1375.
17. Van Damme, L., Chandeying, V., Ramjee, G., Rees, H., Sirivongrangson, P., Laga, M., Perriens, J., COL-1492 Phase II Study Grp., *Safety of multiple daily applications of COL-1492, a Nonoxynol-9 vaginal gel, among female sex workers.* Aids, 2000. **14**(1): p. 85-88.
18. Fichorova, R.N., et al., *Interleukin IL-1, IL-6, and IL-8 predict mucosal toxicity of vaginal microbicidal contraceptives.* Biol. Reprod., 2004. **71**(3): p. 761-769.
19. Savle, P.S., Doncel, G. F., Bryant, S. D., Hubieki, M. P., Robinette, R. G., Gandour, R. D., *Acylcarnitine analogues as topical, microbicidal spermicides.* Bioorg. Med. Chem. Lett., 1999. **9**(17): p. 2545-2548.
20. Asculai, S.S., Weis, M. T., Rancourt, M. W., Kupferberg, A. B., *Inactivation of Herpes-Simplex Viruses by non-ionic surfactants.* Antimicrob. Agents Chemother., 1978. **13**(4): p. 686-690.
21. Stock, C.C., Francis, T., *Inactivation of the virus of epidemic influenza by soaps.* J. Exp. Med., 1940. **71**: p. 661-681.

Chapter 7: Surface Chemistry

7.1 Introduction to Surface Chemistry

We wanted to determine whether the **3CAmn** series could be utilized as anti-corrosion agents or ore flotation enhancers. With respect to anti-corrosion, we enlisted the help of Dr. John Morris's group at VA Tech to study the adsorption of the **3CAmn** series on metal oxide surfaces. Dr. Morris's graduate studetss, Dr. Scott Day prepared the **3CAmn**-silver oxide surfaces and Dr. Melinda McPherson did the IR analysis. With respect to ore flotation, we collaborated with Dr. Roe–Hoan Yoon's group of the Mining and Engineering Department at VA Tech. Dr. Yoon's graduate student, Ruijia Wang measured the ability of the **3CAmn** series to complex calcite and apatite. Calcite ($CaCO_3$) and apatite [$(Ca_{10}(PO_4)_6X_2$ (X= F, OH, or Cl)] are common semisoluble salt minerals that are typically used in industry for a variety of applications, such as fillers, fertilizers, cements, etc.[1] Fatty acids are typically used to hydrophobize the hydrophilic minerals so the minerals can be separated and collected by flotation.[1] The carboxylate group of FAs chemisorp with lattice cations on mineral surfaces.[1]

7.2 Results and Discussion: 3CAmn Series on Ag–oxide Surfaces

FAs form dense, highly-ordered SAMs on silver oxide surfaces.[2] Based on the successes of FA–SAMs on silver oxide, our study measured how well the **3CAmn** series adsorb on silver oxide. Our attempts to form **3CAmn–**SAMs were unsuccessful; however, the **3CAmn** series did form thin films on the silver oxide surface.[3] We did not consider these thin films to be SAMs because they lacked the highly ordered structure that FAs typically form on silver oxide.

We concluded that the **3CAmn** series did not form SAMs based on an analysis of the methylene stretches in the IR spectra. While Figure 7.1 shows narrow, intense peaks for CH_2 symmetrical and asymmetric stretches at 2856 cm^{-1} and 2928 cm^{-1}, respectively, the reflection

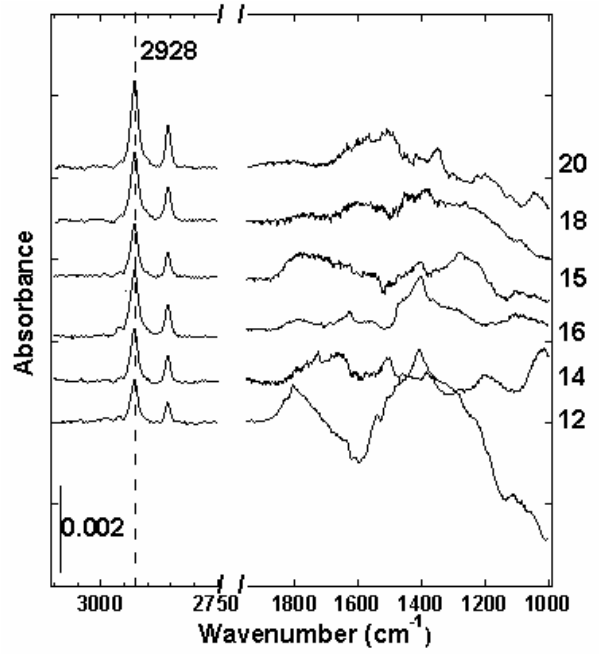

Figure 7.1 RAIRS Spectrum of the **3CAmn** Series. **3CAm15** not tested.

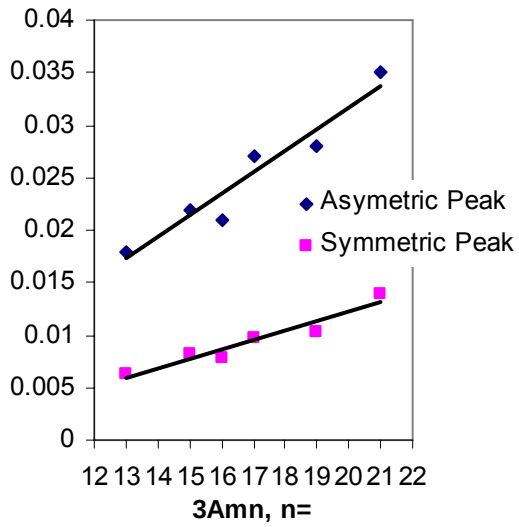

Figure 7.2 Integrated Intensities of Two Methylene Signals Versus the Number of Methylenes

absorption infrared spectra (RAIRS) lack the red-shifted methylene asymmetric stretch below 2920 cm^{-1} and clearly resolved methyl stretches at 2965 cm^{-1} and 2885 cm^{-1} associated with SAM formation. The spectrum has no uniformity from 1000–1900 cm^{-1} probably because of the multiple binding states that each carboxyl group can have with the surface. For example, each molecule can have one, two, or three headgroups attached to the surface. Furthermore, each headgroup can be bound to the Ag–oxide surface in a bidentate or monodendate orientation.

The lack of a highly ordered film was probably due to the dendritic headgroup of the **3CAmn** series. The three carboxylate groups would probably leave a large "footprint" (space that the molecule occupies on a metal surface) on the metal surface due to intramolecular ionic

repulsion among the carboxylate groups. Relative to FAs, the "footprint" of the headgroup could have led to fewer molecules on the metal surface. This would lead to poor coverage (low density) of molecules on the metal surface. Also, intermolecular ionic repulsion and the dendritic nature of the headgroup could have led to individual molecules being farther away from each other. This would lead to decreased van der Waals interactions among the alkyl chains, which is vital for SAM formation. Another potential reason for non-SAM formation is the competition of the carboxylate group between the surface and other carboxylate groups. Studies by Allara et al., [4] as well as Zhang and Imae,[5] have shown that multi-carboxylate molecules sometimes are bound to the metal surface via one carboxylate group, while the other carboxylate group is involved in intermolecular hydrogen bonding or was physisorbed on the metal surface.

7.3 Conclusions

Despite non-SAM formation, the results are encouraging. The **3CAmn** series did form thin films that were resistant to extensive ethanol rinsing. This suggests that the films were stable. Another encouraging sign is that the methylene stretching intensity was directly proportional to the number of methylenes in the triacid used to make the film (Figure 7.2). The linear relationship suggests that the overall coverage and density of the acids adsorbed on the metal surface was consistent and uniform. Further analysis is needed to (1) determine if the thin films that were formed were monolayers, bilayers, or multilayer thin films, (2) determine if the headgroups were bound to the surface in a bidentate or monodentate orientation, and (3) determine if the carboxylate groups are chemisorbed or physisorbed to the metal surface.

7.4 Results and Discussion: Contact Angles of the 3CAmn Series on Mineral Surfaces

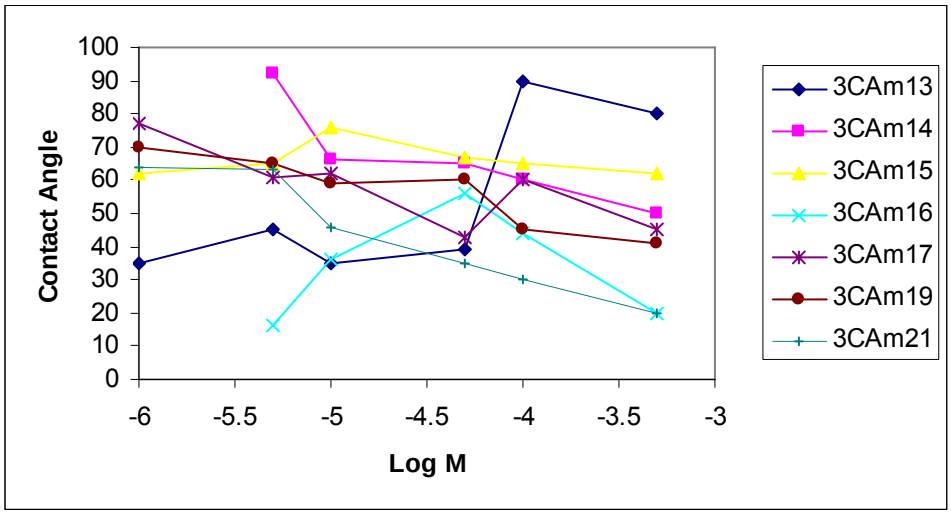

Figure 7.3 Contact Angles of the **3CAmn** Series on Calcite

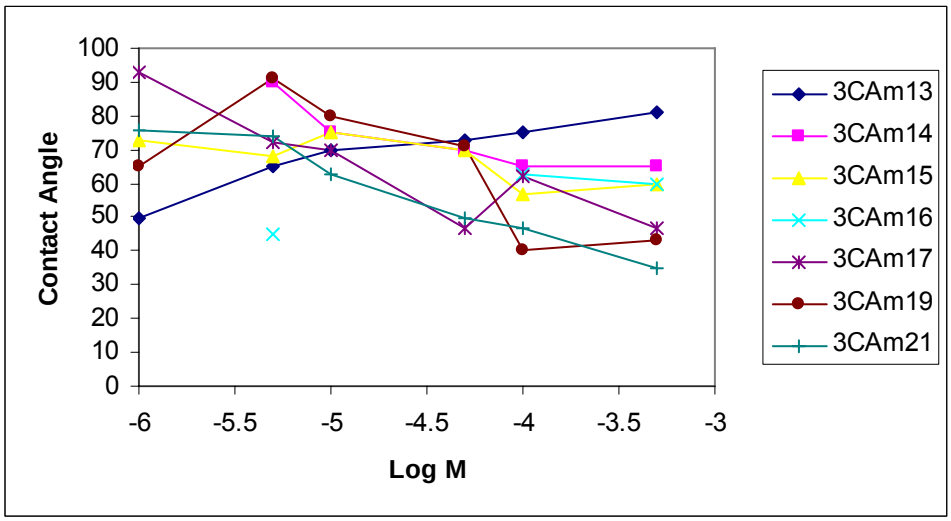

Figure 7.4 Contact Angles of the **3CAmn** Series on Apatite

The contact angle data clearly shows a distinction between calcite and apatite (Figures 7.3 and 7.4). The type of mineral, chain length, and concentration of the amphiphile were factors that affected contact angles. Good maximum contact angles (>90°) were obtained on both surfaces. Unfortunately, the data was sometimes inconsistent and definite trends can be difficult to identify.

The type of mineral affected the quality of the contact angles. Each amphiphile of the **3CAmn** series had higher average contact angles on apatite (65°) than those on calcite (53°). This indicates that the amphiphiles bind preferably to apatite over calcite. Not all amphiphiles preferred apatite binding over calcite binding as **3CAm13** gave a higher contact angle on calcite (90°) than that on apatite (81°). In some cases, there was no major preference in mineral surfaces for some amphiphiles. On apatite, while the longer chain amphiphiles had higher contact angles over a wider concentration range, the maximum contact angles on apatite were not drastically different from those on calcite. Although **3CAm14** had a higher average contact angle on apatite (71°) than that on calcite (61°), **3CAm14** had a better maximum contact angle on calcite (92°) than on apatite (90°). The average and/or maximum contact on both surfaces were similar for **3CAm14** and **3CAm15**. Amphiphile **3CAm15** had nearly identical average contact angles on calcite (66°) and apatite (67°) and nearly identical maximum contact angles of 76° and 75°, respectively.

Unlike the shorter chains, long-chain amphiphiles (**3CAm16**, **3CAm17**, **3CAm19**, **3CAm21**) had a stronger preference for apatite binding versus calcite binding. The long-chain amphiphiles had greater differences in average and maximum contact angles than short-chain amphiphiles (**3CAm13**, **3CAm14**, and **3CAm15**). Amphiphiles with longer chains did not always give higher contact angles. For example, on apatite, the maximum contact angle for **3CAm14** (90°) was almost identical to that of **3CAm19** (91°).

After observing that contact angles were sometimes inversely proportional to concentration, additional measurements were done at lower concentrations. Following the initial results **3CAm21** was tested at lower concentrations (5×10^{-8} to 5×10^{-7} M). The other amphiphiles were tested at 1×10^{-6} to 5×10^{-4} M.

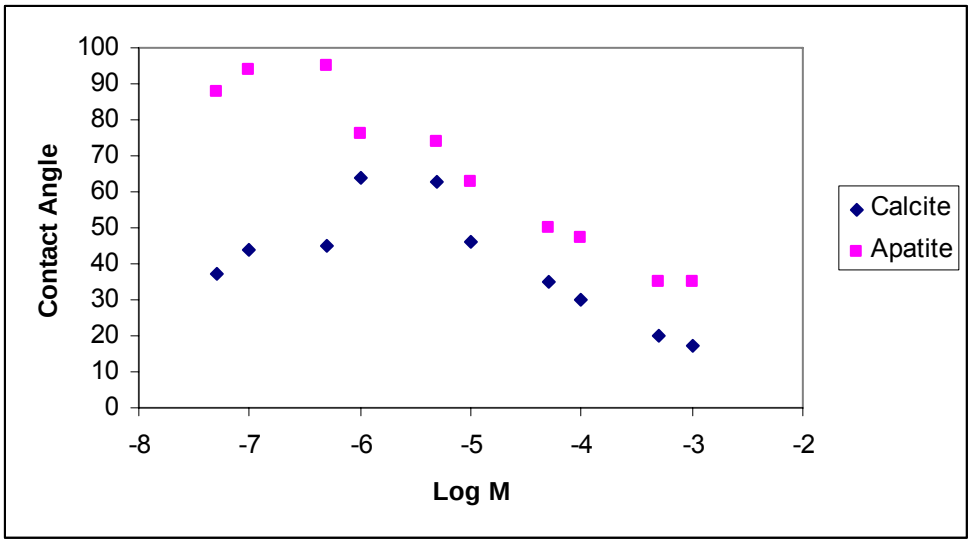

Figure 7.5 Water Contact Angles of **3CAm21** on Calcite and Apatite Surfaces

Amphiphile **3CAm21** can hydrophobize apatite at a low concentration (Figure 7.5), which is important as it suggests that hydrophobization is achieved with a small amount of amphiphile. There was also a contact angle-concentration dependency. For apatite, contact angles initially increased with concentration, then decreased with concentration. The best contact angles (88 to 95°) were obtained at the lowest concentrations (5×10^{-7} to5×10^{-6} M). Following an apparent leveling off between 1×10^{-6} and 5×10^{-6} M, contact angles decreased with concentration. The results with apatite are encouraging because the measurements were done at concentration (5×10^{-8} to 5×10^{-7} M) that were not done for the other amphiphiles. The minimum concentration used for the other amphiphiles was 1×10^{-6} M. As the maximum contact angles obtained for **3CAm21** were obtained at concentrations that were not measured for the other amphiphiles, there is the possibility that the other amphiphiles could give higher contact angles on apatite at lower concentrations.

For calcite, Figure 7.5 tells a different story. There is also a contact angle-concentration dependency; however, unlike apatite, the lower concentration also gives lower contact angles.

Contact angles increase with concentration, level off at 1×10^{-6} and 5×10^{-6} M, then decreases as the concentration increases. At every concentration, **3CAm21** gave lower contact angles on calcite than on apatite. Based on these results, the other amphiphiles probably would not benefit from additional measurements at lower concentrations on calcite.

The observation that contact angles were sometimes inversely proportional to concentration is expected. Typically, low concentrations of FAs ($<1 \times 10^{-5}$ M) are used to collect semisoluble salt minerals.[1] Higher concentrations of FAs can lead to surface precipitation or colloid adsorption due to reactions of the FA and lattice-released cations.[1]

7.5 Conclusions

The **3CAmn** series gave good maximum contact angles on calcite and apatite. However, the measurements should be repeated due to inconsistent data (Figure 7.3 and 7.4). For example **3CAm13** and **3CAm19** gave contact angles that increased and decreased over a wide concentration range. The remaining members of the **3CAmn** series should be tested at lower concentrations on an apatite surface as **3CAm21** gave a high contact angle (95°) at a low concentration (5×10^{-7}).

7.6 References for Chapter 7

1. Jang, W.-H., Drelich, J., Miller, J. D., *Wetting characteristics and stability of Langmuir-Blodgett carboxylate monolayers at the surfaces of calcite and fluorite.* Langmuir, 1995. **11**: p. 3491-3499.
2. Tao, Y.T., *Structural comparison of self-assembled monolayers of N-alkanoic acids on the surfaces of silver, copper, and aluminum.* J. Am. Chem. Soc., 1993. **115**(10): p. 4350-4358.
3. Williams, A.A., Day, B. S., Kite, B. L., McPherson, M. K., Slebodnick, C., Morris, J. R., Gandour, R. D., *Homologous, long-chain alkyl dendrons form homologous thin films on silver oxide surfaces.* Chem. Commun., 2005(40): p. 5053-5055.
4. Allara, D.L., Atre, S. V., Elliger, C. A., Snyder, R. G., *Formation of a crystalline monolayer of folded molecules by solution self-assembly of alpha,omega-alkanedioic acids on silver.* J. Am. Chem. Soc., 1991. **113**(5): p. 1852-1854.

5. Zhang, Z.J., Imae, T., *Hydrogen-bonding stabilized self-assembled monolayer film of a functionalized diacid, protoporphyrin IX zinc(II), onto a gold surface.* Nano Lett., 2001. **1**(5): p. 241-243.

Chapter 8: Summary and Future Work

8.1 Summary of the 3CAmn Series

The synthesis of the **3CAmn** series was successful. Except for **3EAm23** and **3CAm23**, all members of the **3CAmn** series, and precursors (**3EAmn** series), have been fully characterized. Fourteen compounds have been synthesized and fully characterized. [1, 2] Additionally, three X-ray structures (**3EAm15**, **3EAm16**, and **3CAm13**) were obtained for the series.

The **3CAmn** series exhibited selective antimicrobial activity. The series was equally active against both Gram-positive and Gram-negative bacteria.[2] The amphiphiles exhibited the best activity against *M. smegmatis* and yeasts.

The **3CAmn** series was also tested as possible spermicidal and anti-HIV agents. The **3CAmn** series was not spermicidal but inhibited HIV. The **3CAmn** series had similar or slightly better activity than that of N-9. Most of the series was less irritating, less cytotoxic, and had better selectivity indices than that of N-9. However, as currently constituted, due to similar activities and cytotoxicity, this series did not offer any substantial improvements over N-9.

With regard to surface chemistry, we demonstrated that the **3CAmn** series will form stable thin films on Ag oxide surfaces.[1] Unfortunately, the **3CAmn** series did not form SAMs, which was probably due to the headgroup's large "footprint". Although the **3CAmn** series did not form SAMs on Ag, this does not mean the **3CAmn** series could not be used to prevent corrosion by providing a hydrophobic barrier. Water contact angles were never measured on the **3CAmn**–Ag thin films. If good contact angles (>90°) were obtained, the **3CAmn** series could still be used as anti-corrosive agents because the **3CAmn** series formed stable thin films on Ag that were resistant to ethanol washing. We also demonstrated that the **3CAmn** series binds to

calcite and apatite surfaces. The **3CAmn** series hydrophobized these surfaces and produced modest contact angles (63 to 92°). While the water contact angles on calcite and apatite were encouraging, the data was sporadic and the experiments need to be repeated.

8.2 Possible Antimicrobial and Antiviral Mechanisms of Action

One of the main questions that arise from this project is how these amphiphiles inhibit the growth of microorganisms. While determining the mechanism of action is not a goal of this project, we can speculate what the mechanism of action might be. Using the cmc data, we began to put the pieces of the puzzle together and at the very least exclude one possibility. Judging from Figure 8.1, we can speculate that micelles are probably not the active species that inhibit the growth of microorganisms. As the MIC is lower than the cmc, the active species is more likely to be a monomer (single amphiphile) than a micelle. Micellar activity cannot be dismissed in all cases. The activity displayed by **3CAm13** and **3CAm15** against *N. gonorrhoeae* is mostly likely due to micelles. Against *S. aureus*, the activities displayed by **3CAm13**, **3CAm15,** and **3CAm17** are probably due to micelles. Against *S. aureus* and *N. gonorrhoeae*, it appears that the shorter chain amphiphiles are active as micelles while the longer chain amphiphiles are active as monomers. Against *M. smegmatis* and *C. albicans*, all amphiphile activities are well below the cmc and are probably active as monomers.

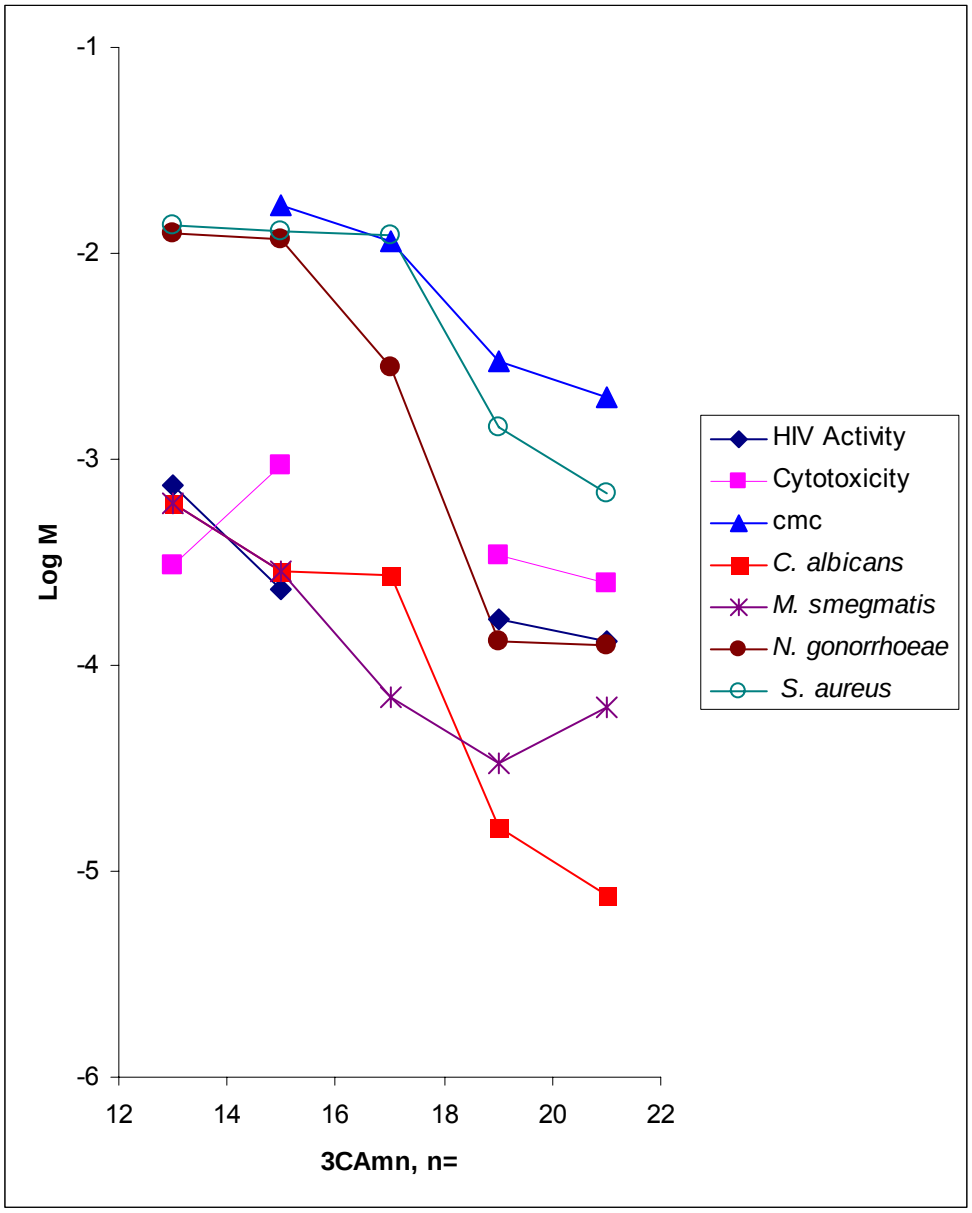

Figure 8.1 Biological and Physical Properties of the **3CAmn** Series. The cytotoxicity for **3CAm17** was not measured.

Based on our interpretation of the cmc and cytotoxicity data, we can remove micelles as the cause of cytotoxicity. The most active amphiphiles (**3CAm19** and **3CAm21**) inhibited most microorganisms and HIV below the cytotoxic concentrations. The only exceptions were *K. pneumoniae* (data not shown), *L. plantarum* (data not shown), and *S. aureus*. Due to these

results we believe that cell toxicity occurs well below the cmc. This suggests micelles are not the cause of cytotoxicity. These results support our intention of using these amphiphiles as topical microbicides, in which the amphiphiles can be safely applied to sensitive areas (e.g. genitals and skin) because they do not cause any irritation, sores, bleeding, etc.

8.3 Summary of 3DMAUr18Me, 3MorUr18Me, and the 3DMAUrn and 3MorUrn Series

The synthesis of **3DMAUr18Me**, **3MorUr18Me**, and the **3DMAUrn** and **3MorUrn** series was successful. Fourteen compounds have been synthesized and fully characterized. Unlike the **3CAmn** series, all nonionic amphiphiles and all intermediates are new compounds. The precursors in the **3EAmn** and **3CAmn** series, Behera's amine and nitrotriester, have already been reported in the literature.[3] Five X-ray crystal structures of the **3DMAUrn** and **3MorUrn** series were obtained. X-ray crystal structures for all intermediates of the **3MorUrn** series were obtained.

Similar to the **3CAmn** series, the nonionic amphiphiles exhibited selective antimicrobial activity. The nonionic amphiphiles exhibited much better activities against Gram-positive bacteria than Gram-negative bacteria (except for *N. gonorrhoeae*). The nonionic amphiphiles displayed better activities against Gram-positive bacteria than the **3CAmn** series but substantially less activity against Gram-negative bacteria and fungi. Both nonionic and anionic amphiphiles exhibited similar activities against *M. smegmatis*.

The nonionic amphiphiles exhibited good anti-viral and spermicidal activity. Amphiphile **3DMAUr18Me** and all members of the **3DMAUrn** series were spermicidal and displayed anti-HIV activity (except for **3DMAUr18**). Amphiphile **3DMAUr18Me** and the **3DMAUrn** series were better spermicidal and anti-HIV agents than the **3CAmn** series. Only **3DMAUr14** exhibited better spermicidal activity than N-9. All nonionic amphiphiles (except for

3DMAUr18) exhibited enhanced HIV activity relative to the **3CAmn** series. Except for **3DMAUr18Me** and **3DMAUr18**, all nonionic amphiphiles were more antiviral than N-9. Against HIV, amphiphile **3DMAUr16** was the most active member of the **3DMAUrn** series, while **3DMAUr18Me** was the most active compound (anionic and nonionic) tested.

Unfortunately, unlike the "**3C**" headgroup, the "**3DMA**" headgroup presented cytotoxicity concerns. Only **3DMAUr18** was less cytotoxic than N-9, while **3DMAUr18Me** was the most cytotoxic compound (anionic and nonionic) tested. Furthermore, an additional major drawback to the nonionic compounds was potential irritancy. Amphiphile **3DMAUr14** caused the release of the proinflammatory cytokine to a larger extent than N-9. Amphiphile **3DMAUr14** was the only nonionic amphiphile tested, so we can only assume that the other amphiphiles would give similar results. Unfortunately, measurements for cytotoxicity, spermicidal and anti-HIV activity for the **3MorUrn** series and **3MorUr18Me** have not yet been performed.

8.4 Future Work for the 3CAmn Series

All amphiphiles (nonionic and anionic) are the first series of compounds in this project. For a first attempt, these initial series have been very successful. The series are antibacterial and antifungal (**3CAmn**, **3DMAUr18Me**, **3DMAUrn**, **3MorUr14**), antiviral (**3CAmn**, **3DMAUr18Me, 3DMAUrn**), and spermicidal (**3DMAUr18Me** and **3DMAUrn**). Amphiphile **3MorUr18Me** and the **3MorUrn** series have not been tested for possible antiviral or spermicidal activity. Currently, we have identified some good leads; consequently, additional synthesis and antimicrobial experiments must be performed to advance this project.

In the case of the **3CAmn** series, antibacterial and antifungal experiments indicated that longer chain lengths could lead to enhanced antimicrobial activity. Specifically, the

antimicrobial activity against *C. albicans* and *S. cerevisiae* was still increasing with chain length. Against both microorganisms, **3CAm21** was the most active compound.

In addition to longer saturated chains, unsaturated analogs (Figure 8.2) of the **3CAmn** series should be synthesized and tested for antibacterial, antifungal, spermicidal, and antiviral activities. Multiple studies reported that unsaturated FAs were more active than saturated FAs against various microorganisms, such as *A. niger*, *S. aureus*, and *MRSA*. For example, unsaturated FAs have exhibited enhanced antimicrobial activity, relative to saturated FAs, against *A. niger*, [4] *M. smegmatis*, [5, 6] *S. aureus*, [4, 7-10] *E. coli*, [11] *C. albicans*,[7, 8] and MRSA.[10] Additionally, FAs with multiple double bonds in the alkyl tails are sometimes more active than monounsaturated FAs against certain microorganisms[5, 6, 10, 12] or components of microbial cell walls.[13]

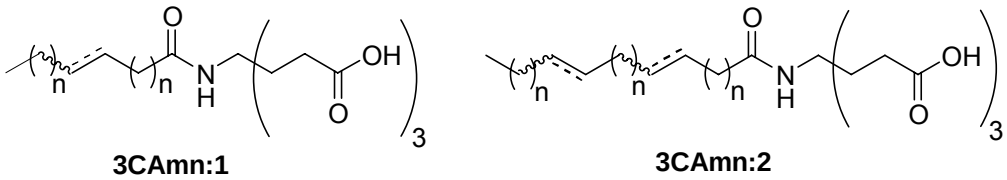

Figure 8.2 Possible Unsaturated Derivatives of the **3CAmn** Series

Niwano et al. reported that unsaturated FA inhibited the growth of vital components of bacterial (peptidoglycan) and fungal (β-1,3-glucan and chitin) cell walls.[13] Unlike unsaturated FAs, saturated FAs were inactive against β-1,3-glucan and chitin. Unsaturated FAs $C_{18:1}$ (6 μg/mL), $C_{18:2}$ (200 μg/mL), $C_{18:3}$ (66 μg/mL) inhibited the growth of β-1,3-glucan. Against chitin, the unsaturated FAs ($C_{18:1}$, $C_{18:2}$, $C_{18:3}$) were less active at concentrations of 90, 400, and 360 μg/mL, respectively. Against peptidoglycan, C_{12} (1200 μg/mL), C_{18} (450 μg/mL), and C_{20} (1500 μg/mL) exhibited relatively minimal activity, while $C_{18:1}$ (6 μg/mL), $C_{18:2}$ (200 μg/mL), and $C_{18:1}$ (66 μg/mL) exhibited much better activity.

If we make the assumption that these amphiphiles exhibit their antimicrobial activity through the insertion of their alkyl tails into the cytoplasmic membrane, which results in the subsequent destabilization of the cytoplasmic membrane, the incorporation of double bond(s) could be beneficial. The inclusion of a double bond in the tail can bring about a conformational change in the tail of the molecule.[14] The change will lead to the tail occupying a greater area within the cytoplasmic membrane. If individual molecules occupy a greater area, then fewer molecules will be required to occupy the cytoplasmic membrane, leading to increased activity.[14]

In addition to enhanced antibacterial and antifungal activity, unsaturated FAs have exhibited enhanced antiviral activity relative to saturated FAs. For example, unsaturated FAs have exhibited enhanced antiviral activity against enveloped viruses, such as Influenza A_1, Sindis, Sendai, vesicular stomatitis virus (VSV), HIV, HSV, and Visna virus.[15-17] Thomar et al. reported that $C_{18:2}$ acid caused leakage of VSV's viral envelope as well as the partial or complete disintegration of the VSV's cell membrane, which led to cell lysis.[17] Kohn et al. reported that $C_{18:2}$ acid damaged or destroyed the viral envelope of Sendai and Sindbis viruses.[15]

8.5 Future Work for 3DMAUr18Me, 3MorUr18Me, the 3DMAUrn and 3MorUrn Series

The **3DMAUrn** and **3MorUrn** series, more so than the **3CAmn** series, would really benefit from the synthesis of additional analogs. The **3DMAUrn** and **3MorUrn** series, as well as **3MorUr18Me**, are limited due to poor aqueous solubility. Amphiphiles **3DMAUr16**, **3DMAUr18**, **3MorUr12** and **3MorUr18Me** were all insoluble in water and the antiviral, spermicidal, and antimicrobial activity could not be measured. With respect to antiviral, spermicidal, and antimicrobial activity, **3DMAUr14** was always as active as or more active than

3DMAUr12. In some cases, **3DMAUr14** was more active than **3DMAUr18Me**. It would be beneficial to measure the activity of **3DMAUr16** to determine if **3DMAUr16** exhibits greater antiviral, antibacterial, antifungal, and spermicidal activities relative to **3DMAUr14** and **3DMAUr18Me**.

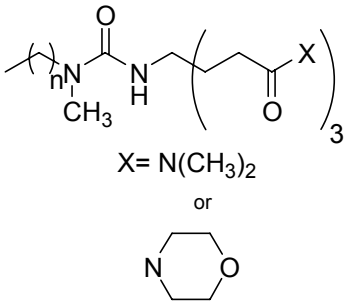

Figure 8.3 Possible *N*-methyl Derivatives of the **3DMAUrn** and **3MorUrn** Series

Three synthetic strategies should be undertaken. First, *N*-methyl derivatives of the **3DMAUrn** and **3MorUrn** series should be synthesized (Figure 8.3). As illustrated by Leydet et al., *N*-methylation of an amide nitrogen improved aqueous solubility.[18] This result was further illustrated in our antimicrobial and antiviral experiments. In both cases, we observed greater aqueous solubility for **3DMAUr18Me** versus **3DMAUr18**.

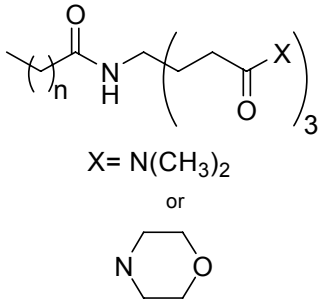

Figure 8.4 Possible Amide Derivative: **3DMAAmn**

The second synthetic strategy would be to make a series with an amide linker (**3DMAAmn**) instead of an ureido linker (**3DMAUrn**) (Figure 8.4). Measurements have shown that the **3CAmn** series has higher cmcs than the **3CUrn** and **3CCbn** isosteres (Figure 8.5). The

isosteres differ in the linker (amido, ureido, and carbamato). For example, **3CAm19** (3 mM) has a slightly higher cmc than **3CUr18** (2.2 mM) and **3CCb18** (2.7 mM) even though **3CAm19** has a longer hydrophobic tail. Additionally, **3CAm19** has a slightly lower cmc than **3CUr16** (3.5 mM) but a much lower cmc than **3CCb16** (6.8 mM). While cmc is not a direct measure of aqueous solubility, the cmc data indicates that the amide derivates aggregate at a much higher concentration than both **3CCbn** and **3CUrn** series. The cmc data shows that the linker has a noticeable effect on cmc; therefore, an amide linker could enhance the aqueous solubility relative to the current **3DMAUrn** series.

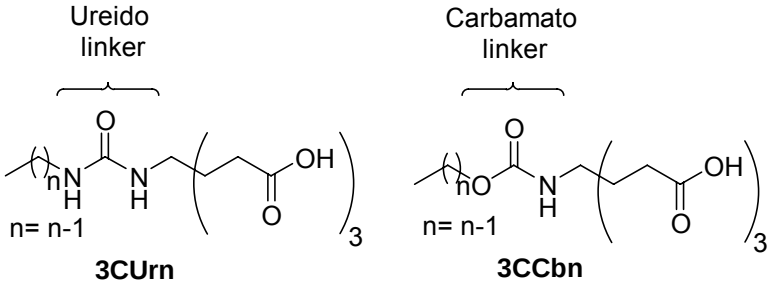

Figure 8.5 Structures of the **3CUrn** and **3CCbn** Series

The third synthetic strategy would be the synthesis of unsaturated analogs of the **3DMAUrn** and **3MorUrn** series (Figure 8.6). Unsaturation in the alkyl tail might lead to enhanced aqueous solubility. For example, in FAs, unsaturation in the alkyl tail leads to a more liquid-like compound. FAs $C_{18:1}$ and $C_{20:4}$ are liquids at room temperature while the corresponding saturated FAs are solids at room temperature. Similarly, $C_{18:1}$ amine is a liquid at room temperature, while C_{18} amine is a solid at room temperature. Due to inclusion of double bonds, fewer van der Waals interactions among the alkyl tails is probably the reason why unsaturated FAs and amines are mostly liquids at room temperature. An additional benefit of unsaturated derivatives could be enhanced antimicrobial and antiviral activity. Like FAs, in

some cases, unsaturated amides exhibit greater antimicrobial activity against some microorganisms than the corresponding saturated counterparts.[19-21]

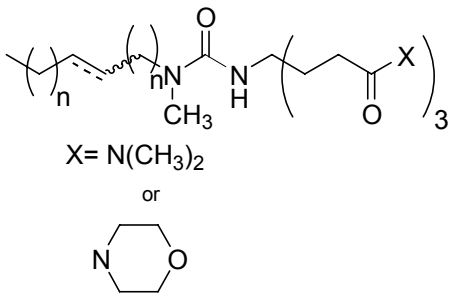

Figure 8.6 Possible Unsaturated Derivatives of the **3DMAUrn** and **3MorUrn** Series

8.6 Conclusions

Overall, the **3CAmn**, **3DMAUrn**, and **3MorUrn** series would really benefit from additional synthesis. As a group, these series have shown good antibacterial, antifungal, antiviral, and spermicidal activities. With the additional analogs suggested above, we believe the overall goal of this project can be realized.

8.7 References for Chapter 8

1. Williams, A.A., Day, B. S., Kite, B. L., McPherson, M. K., Slebodnick, C., Morris, J. R., Gandour, R. D., *Homologous, long-chain alkyl dendrons form homologous thin films on silver oxide surfaces.* Chem. Commun., 2005(40): p. 5053-5055.
2. Williams, A.A., Sugandhi, E. W., Macri, R. V., Falkinham, J. O., Gandour, R. D., *Antimicrobial activity of long-chain, water-soluble, dendritic tricarboxylato amphiphiles.* J. Antimicrob. Chemother., 2007. **59**(3): p. 451-458.
3. Newkome, G.R., Behera, R. K., Moorefield, C. N., Baker, G. R., *Chemistry of Micelles Series .18. Cascade Polymers - Syntheses and Characterization of One-Directional Arborols Based on Adamantane.* J. Org. Chem., 1991. **56**(25): p. 7162-7167.
4. Wyss, O., Ludwig, B. J., Joiner, R. R., *The fungistatic and fungicidal action of fatty acids and related compounds.* Arch. Biochem., 1945. **7**: p. 415-425.
5. Saito, H., Tomioka, H., Yoneyama, T., *Growth of Group-IV mycobacteria on medium containing various saturated and unsaturated fatty-acids.* Antimicrob. Agents Chemother., 1984. **26**(2): p. 164-169.
6. Kondo, E. and K. Kanai, *Lethal effect of long-chain fatty acids on mycobacteria.* Jpn. J. Med. Sci. Biol., 1972. **25**(1): p. 1-13.
7. Kabara, J.J., *Structure-function-relationships of surfactants as antimicrobial agents.* J. Soc. Cosmet. Chem., 1978. **29**(11): p. 733-741.

8. Kabara, J.J., *Lipids as host-resistance factors of human-milk.* Nutr. Rev., 1980. **38**(2): p. 65-73.
9. Perez Gutierrez, R.M., *Antimicrobial activity of fatty acids isolated from Tubifex tubifex.* Rev. Mex. Cienc. Farmaceut., 2005. **36**(1): p. 5-10.
10. Ohta, S., Shiomi, Y., Kawashima, A., Aozasa, O., Nakao, T., Nagate, T., Kitamura, K., Miyata, H., *Antibiotic effect of linolenic acid from chlorococcum Strain Hs-101 and Dunaliella-Primolecta on Methicillin-Resistant Staphylococcus-Aureus.* J. Appl. Phycol., 1995. **7**(2): p. 121-127.
11. Kilic, T., Dirmenci, T., Satil, F., Bilsel, G., Kocagoz, T., Altun, M., Goren, A. C., *Fatty acid compositions of seed oils of three Turkish salvia species and biological activities.* Chem. Nat. Compd., 2005. **41**(3): p. 276-279.
12. Nieman, C., *Influence of trace amounts of fatty acids on the growth of microorganisms.* Bacteriol. Rev., 1954. **18**: p. 147-63.
13. Niwano, M., Mirumachi, E., Uramoto, M., Isono, K., *Fatty-acids as inhibitors of microbial cell-wall synthesis.* Agric. Biol. Chem. Tokyo, 1984. **48**(5): p. 1359-1360.
14. Kanai, K., Kondo, E., *Antibacterial and cytotoxic aspects of long-chain fatty-acids as cell-surface events-selected topics.* Jpn. J. Med. Sci. Biol., 1979. **32**(3): p. 135-174.
15. Kohn, A., Gitelman, J., Inbar, M., *Interaction of polyunsaturated fatty acids with animal cells and enveloped viruses.* Antimicrob. Agents and Chemother., 1980. **18**: p. 962-968.
16. Horowitz, B., Piet, M. P. J., Prince, A. M., Edwards, C. A., Lippin, A., Walakovits, L. A., *Inactivation of lipid-enveloped viruses in labile blood derivatives by unsaturated fatty-acids.* Vox Sanguinis, 1988. **54**(1): p. 14-20.
17. Thormar, H., Isaacs, C. E., Brown, H. R., Barshatzky, M. R., Pessolano, T., *Inactivation of enveloped viruses and killing of cells by fatty-acids and monoglycerides.* Antimicrob. Agents Chemother., 1987. **31**(1): p. 27-31.
18. Leydet, A., Barthelemy, P., Boyer, B., Lamaty, G., Roque, J. P., Bousseau, A., Evers, M., Henin, Y., Snoeck, R., Andrei, G., Ikeda, S., Reymen, D., Declercq, E., *Polyanion inhibitors of Human-Immunodeficiency-Virus and other viruses .1. Polymerized anionic surfactants.* J. Med. Chem., 1995. **38**(13): p. 2433-2440.
19. Omura, S., Katagiri, M., Awaya, J., Furukawa, T., Umezawa, I., Oi, N., Mizoguchi, M., Aoki, B., Shindo, M., *Relation between the structures of fatty acid amide derivatives and their antimicrobial activities.* Antimicrob. Agents Chemother., 1974. **6**(2): p. 207-215.
20. Kabara, J.J., Conley, A. J., Truant, J. P., *Relationship of chemical structure and antimicrobial activity of alkyl amides and amines.* Antimicrob. Agents Chemother., 1972. **2**(6): p. 492-498.
21. Novak, A.F., Clark, G. C., Dupuy, H. P., Fisher, M. J., Fore, S. P., Dupuy, H. P., *Antimycotic activity of some fatty acid derivatives.* J. Am. Oil Chem. Soc., 1964. **41**(7): p. 503-505.